THE PHYSIOLOGY OF AMMONIA TRANSPORT IN THE DISEASE VECTOR MOSQUITO *AEDES AEGYPTI:* AMMONIA TRANSPORTER LOCALIZATION, FUNCTION, AND CHARACTERIZATION

Andrea Claire Durant

A DISSERTATION SUBMITTED TO THE FACULTY OF GRADUATE STUDIES IN PARTIAL FULFILLMENT OF THE REQUIREMENTS FOR THE DEGREE OF DOCTOR OF PHILOSOPHY

GRADUATE PROGRAM IN BIOLOGY

YORK UNIVERSITY

TORONTO, ONTARIO, CANADA

MARCH 2021

Abstract

The formation of ammonia (NH_3/NH_4^+) through protein metabolism is ubiquitous in animals. However, ammonia is typically destined for conversion and/or elimination from the body because the toxicological consequences of systemic ammonia accumulation are grave. Specialized ammonia transporters regulate excretion of ammonia by moving it across biological membranes. The yellow fever mosquito, *Aedes aegypti*, possess four ammonia transporters: two Rhesus glycoproteins (Rh proteins, *AeRh50-1* and *AeRh50-2*) and two ammonium transporters (Amt proteins, *AeAmt1* and *AeAmt2*), but functionally they are poorly understood in this medically important disease vector. This presents a serious gap in knowledge, in particular because aquatic larvae of *A. aegypti* can inhabit ammonia-rich sewage, intensifying the possibility of vector success in regions where poorly maintained septic systems are used for sewage treatment. My studies sought to advance our understanding of Rh and Amt proteins in *A. aegypti* by examining their function in (1) larvae residing in high environmental ammonia (HEA) and (2) hematophagous adult females that are naturally loaded with high ammonia while handling a blood meal. In larvae, all four ammonia transporters are expressed in the anal papillae (AP), structures that are in direct contact with the external environment. Rh proteins and AeAmt2 are involved in ammonia excretion across the AP but decrease in abundance upon HEA exposure. The AP are still critical sites of ammonia excretion when larvae are in HEA, evidenced by enhanced NH_4^+ efflux. Rh proteins may also play a role in acid-base balance as protein levels of Rh significantly increase in conditions that challenge blood pH regulation. Of particular importance was that laboratory observations of ammonia transport physiology of larvae in HEA reconciled with observations of wild *A. aegypti* larvae collected from ammonia-rich septic tanks. In adult *A. aegypti*, Rh proteins are expressed in the excretory organs and facilitate NH_4^+ secretion via the urine. Novel observations of AeAmt1 being almost exclusively expressed in the spermatozoa of males revealed a vital role for this protein in sperm survival and successful egg fertilization. Collectively, my studies significantly

advance our mechanistic understanding of ammonia transport proteins in *A. aegypti* by revealing their broad and critical roles.

Acknowledgements

I would not be in research today, let alone having completed this degree, without the encouragement and support of Dr. Andrew Donini, Dr. Scott Kelly, and Dr. Jean Paul Paluzzi. Andrew, it was an honor to be your student and if I am one day a fraction of the mentor to others that you have been to me, then I have accomplished my goals and dreams. My professional and personal growth is largely owed to the fact that you provided the freedom for me to pursue my research wherever it took me, and to take advantage of any opportunity that came my way. I have never seen you bat an eyelash at some of my more questionable ideas, and your words of encouragement during times of serious self-doubt (imposter syndrome, some may say) will stick with me always. While your support in everything research-related was immense, this is only minor compared to the ways in which you have supported me and all of your members outside of the lab. I will never forget the kindness of you and Natasha when my computer and other valuables were destroyed in Hurricane Irma, nor will I forget the financial assistance that you provided to many of us during the never-ending union strikes, as well as during the pandemic. If not for these extremely thoughtful actions, I would have definitely not accomplished a sliver of what I have and I (and Coco and Keone) would probably be homeless (only slightly kidding). I am eternally grateful that you had faith in me to undertake this degree with minimal to no research experience prior to my PhD work, and I will always seek out your advice and guidance regardless of where I end up in this world (and also, because I have all of my pet critters in the lab that I am entrusting you with). Scott, if it were not for your inspiration and endless motivation, I would have never climbed into septic tanks or pivoted my research interests to the deepest depths of the ocean. In writing that sentence, it sounds like you are trying to get rid of me, but of course that is never going to happen. I owe so much gratitude to Jean Paul, whose support is the only reason I committed to teaching a 3rd year course remotely during a global pandemic, who *patiently* trained me to use many techniques that were out of my comfort zone, and who I can always count on for the latest happenings in research and the world, in general. I am forever grateful for each of you for your immense kindness, never-ending support, and friendship.

I would also like to thank my past and present lab friends (whom are also colleagues, I guess). Sima, if it was not for a knock on the door to my master's lab 7 years ago inviting me to the Animal Physiology meetings, I may not be writing this today! Your friendship, guidance, and all of our travels (past and future!) have meant the world to me. Some of the best memories of my life come from my time spent with Dennis, Chun, Julia, Fargol, Lidiya, Gil, Anna, and David. Each of you have tolerated

(encouraged, even) my antics and have continually supported me while also enduring the late nights and often demanding workloads. Nobody has been as keen as you, Britney, to deplete their benefits on all day massage and spa treatments, and that, in short, is why we will be lifelong friends. Elia and Sydney, thank you for the stimulating discussions and never judging me for my daily coffee naps. To the fashion-forward brainiacs of the Paluzzi lab (Farwa, Aryan, Aziza, and Andreea), I am grateful to you for keeping me "current" and caffeinated.

I would require another dissertation to put into words how grateful I am to have the parents that I do, who always encouraged me to pursue whatever passions I may have. Mom, thank you for teaching me anatomy and physiology at the age of 12, for regularly bringing me home dissection equipment (scalpels, gloves, formalin) at a questionably young age, and for the monthly trips to the abattoir to collect eyeballs, hearts, and other animal organs. I am sure you are relieved that I ended up an animal physiologist, and not a serial killer. Dad, you are the only person in the world that can listen to me ramble about my research for hours while maintaining eye contact, showing interest, and not falling asleep. Thank you for driving me around the entire island in search of the prized septic tanks, and for being my greatest support system (and lifelong cheerleader). To my wonderful siblings, while I know that you have no idea what it is that I do, your support, very useful connections, and never-ending entertainment have been instrumental to my professional and personal wellbeing. Alex, I promise that I will pay you back one day for all of the money I have pilfered from you over the years.

To my little family, Keone and my beloved Coco (yes, Coco is my cat and must be acknowledged). Your unwavering love and understanding have been my primary inspiration these last 5 ½ years. You have kept me company (and kept me sane) during my self-imposed all-nighters and long days. I can always rely on Coco to paw me awake in the middle of the night (for treats) when I have a looming deadline. Keone, you are always in earshot for me to vent or ramble, whether you wanted to be or not, and you are my ultimate voice of reason. I am also grateful that there is always a Hershey's white chocolate bar close by when I need it the most. You have always encouraged me to shoot for the stars, and I hope you know that your immeasurable support really makes it easier to get up in the mornings (okay…*some* mornings).

Contents

Table of Figures

Table of Tables

List of Abbreviations

ADB — antibody dilution buffer

ADP — adenosine diphosphate

AeAmt1 — *Aedes aegypti* ammonium transporter 1

AeAmt2 — *Aedes aegypti* ammonium transporter 2

AeRh50-1 — *Aedes aegypti* Rh protein 1

AeRh50-2 — *Aedes aegypti* Rh protein 2

AgAmt — *Anopheles gambiae* ammonium transporter

AMG — anterior midgut

AMT — ammonium transporter

AmtB — *Escherichia coli* ammonium transporter B

ANOVA — analysis of variance

AP — anal papillae

ASET — automated scanning electrode technique

AT — antennae

BF — brightfield

BLAST — Basic Local Alignment Search Tool

BSA — bovine serum albumin

B.V.I. — British Virgin Islands

CA — carbonic anhydrase

CAM — cell adhesion molecule

CAR — carcass

CCC —cation-chloride (Cl^-) co-transporter

cDNA — complementary deoxyribonucleic acid

CDS — coding sequence

cRNA — capped RNA

Cy-2 — cyanine-2

DAPI — 4',6-diamidino-2-phenylindole

ddH_2O — double distilled water

deH_2O — dechlorinated tap water

DMSO — dimethyl sulfoxide

DNA — deoxyribonucleic acid

dNTP — deoxynucleotide triphosphate

dsRNA — double stranded RNA

DTT — dithiothreitol

ECL — enhanced chemiluminescence

EDTA — ethylenediaminetetraacetic acid

FB — fat body

FITC —fluorescein isothiocyanate

FW — freshwater

GAPDH — glyceraldehyde 3-phosphate dehydrogenase

GC — gastric caeca

GDH — glutamine dehydrogenase

GS/GOGAT — glutamine synthetase/glutamate synthase

HD — head

HEA — high environmental ammonia

HEPES — 4-(2-hydroxyethyl)-1-piperazineethanesulfonic acid

HG — hindgut

IL — Ileum

ISH — *in situ* hybridization

ISME — ion-selective microelectrode

kDa — kilodalton

Kir — inwardly rectifying K^+ channel

MEP — methylammonium permease

MG — midgut

mRNA — messenger RNA

MT — Malpighian tubules

MW — molecular weight

N — nitrogen

N_2 — dinitrogen

NADH — reduced nicotinamide adenine dinucleotide

NBF — neutral buffered formalin

NCBI — National Center for Biotechnology Information

ND — not detected

NH_3 — gaseous ammonia

NH_4^+ — cationic ammonia, ammonium

NHE — Na^+/H^+ exchanger 3

NKA — Na^+-K^+-ATPase

NKCC — Na^+-K^+-$2Cl^-$ cotransporter

NO — nitric oxide

NTC — no template control

ORF — open reading frame

OV— ovary

PBM — post blood meal

PBS — phosphate-buffered saline

PCR — polymerase chain reaction

PMG— posterior midgut

PMSF — phenylmethylsulfonyl fluoride

Pt — peptide

qRT-PCR — quantitative real-time PCR

Rh — Rhesus glycoprotein

RM — rectum

RNA — ribonucleic acid

RNAi — RNA interference

RO — reverse osmosis

RP — rectal pads or reproductive organs (as specified)

Rp49 — ribosomal protein 49

RpL8 — ribosomal protein L8

RpS18— 60s ribosomal protein S18

RT — room temperature

RT-PCR — reverse transcriptase PCR

SDS-PAGE — sodium dodecyl sulfate polyacrylamide gel electrophoresis

SEI — homogenization buffer containing sucrose, EDTA and imidazole

SEID — SEI with sodium deoxycholate

SEM — standard error of the mean

SIET — scanning ion-selective electrode technique

TBS-T — TBS with Tween-20

TEVC — two-electrode voltage clamping

TPM — transcripts per million

VA — V-type H^+-ATPase

VectorBase — Bioinformatics Resource for Invertebrate Vectors of Human Pathogens

WG — whole gut

18S rRNA — 18S ribosomal RNA

βLac — β-lactamase

ΔP_{NH3}— partial pressure gradient, gaseous ammonia

Statement of Contributions

Chapter Two

This chapter was written by A. Durant with valuable guidance and significant editorial support from Dr. A. Donini, Dr. Helen Chasiotis, and Lidiya Misyura. This chapter was conceptualized by Dr. A. Donini, Dr. Helen Chasiotis, and A. Durant. Data collection and formal analyses executed by A. Durant, with the exception of Fig. 2-2 which was completed by A. Durant, Dr. Helen Chasiotis, and Lidiya Misyura. dsRNA experiments were executed by A. Durant with valuable assistance from Dr. Sima Jonusaite and Dr. Helen Chasiotis.

Chapter Three

This chapter was written by A. Durant with valuable guidance and editorial support from Dr. A. Donini. A. Durant performed the experiments, data collection and data analysis.

Chapter Four

This chapter was written by A. Durant with valuable guidance and editorial support from Dr. A. Donini. A. Durant performed the experiments, data collection and data analysis. Activity assay experiments were executed by A. Durant with valuable assistance from Dr. Sima Jonusaite.

Chapter Five

This chapter was written by A. Durant with valuable guidance and significant editorial support from Dr. A. Donini. A. Durant performed the experiments, data collection and data analysis with valuable assistance from BugOut B.V.I. vector control officer James Alexander in mosquito collection. Dr. A. Donini secured import permits (Canadian Food Inspection Agency, Canada) and substantial resources for this study.

Chapter Six

This chapter was written by A. Durant with valuable guidance and editorial support from Dr. A. Donini. RNAseq analyses were completed with the valuable assistance and guidance of Dr. Dennis Kolosov. A. Durant performed all other experiments, data collection and data analysis.

Chapter Seven

This chapter was written by A. Durant with valuable guidance and editorial support from Dr. A. Donini. A. Durant performed the experiments, data collection and data analysis. Dr. Jean Paul Paluzzi and Dr. David Rocco provided rearing/mating assay containers and valuable advice on egg-laying assays.

Appendix A1

All supplementary experiments and analyses described in this section were executed by A. Durant with significant guidance and support from Dr. Jean Paul Paluzzi (cloning, cRNA synthesis), Dr. Peter Piermarini (two-electrode voltage clamping) and Dr. Dirk Weihrauch and Haonan Zhouyao (Xenopus oocyte harvesting and injection protocols, pGEMHE plasmid), and Dr. A Donini.

_____

Andrea Claire Durant (PhD Candidate)

_____

Andrew Donini (PhD Supervisor)

Chapter One

Overview

1.1 Nitrogen regulation is a vital element of all life

Nitrogen (N) is an essential component of nucleic acids, amino acids, and proteins that constitute living matter. An intricate network of nitrogen flow exists between the atmosphere and the biosphere, from nitrogen atoms in the air (e.g. dinitrogen, N_2) through to nitrogen-containing compounds found in living organisms (Delwiche, 1970). Consequently, strategies of nitrogen control have been described in all domains of life. Bacteria and Archaea possess ancient and highly conserved nitrogen regulatory mechanisms to assimilate inorganic nitrogen (e.g. N_2) from the environment or to produce nitrogen-containing compounds intracellularly for cell growth (Leigh and Dodsworth, 2007; Merrick and Edwards, 1995). Among Eukarya, the multitude of nitrogen regulatory strategies identified to date reflects the diversity of physiological functions in these life forms. Unicellular eukaryotes (Fernandez and Galvan, 2007; Sanz-Luque et al., 2015; Terrado et al., 2015), fungi (Morton and Macmillan, 1954), and plants (Lea and Miflin, 1974; Miflin and Lea, 1976; Pate, 1973) fulfill nutritional nitrogen requirements through a variety of nitrogen assimilation pathways from the external environment. On the other hand, virtually all metabolically active animal cells produce nitrogen-containing compounds as metabolites which are destined for excretion or nitrogen recycling pathways (Ballantyne, 2001; Bucking, 2017; Weihrauch et al., 2004; Weihrauch et al., 2012a; Wright, 1995a). A unifying feature among the majority of organisms is the eventual production of ammonia (gaseous ammonia, NH_3, and cationic ammonium, NH_4^+). The production of intracellular ammonia from a wide range of nitrogen-containing compounds (e.g. dinitrogen, nitrate, ammonium salts, and amino acids) occurs through various cellular biosynthetic pathways, or ammonia can be obtained from the extracellular environment (Leigh and Dodsworth, 2007; Merrick and Edwards, 1995). Therefore, the majority of organisms, and animals, in particular, are tasked with either excreting ammonia and other nitrogenous compounds or incorporating ammonia into molecules that can be stored and later utilized. In fact, in virtually all living organisms ammonia plays a crucial role in the maintenance of nitrogen homeostasis, and ammonia formation is considered to be the most primitive system for nitrogenous waste excretion (Cooper and Plum, 1987;

Regnault, 1987). Therefore, the importance of understanding the mechanisms underlying ammonia regulation and excretion in different life forms is evidenced by the ubiquity of these processes across all domains of life.

1.2 Ammonia formation in animals

Much of the ammonia (NH_3/NH_4^+) produced in cells come from amino acids during the metabolism of dietary and metabolic protein, in which amino acids ultimately undergo oxidative degradation through the process of amino acid catabolism (Regnault, 1987). Nucleic acid catabolism also yields similar nitrogenous end products as amino acid catabolism, albeit to a lesser extent. Ammonia production in organisms is continual due to a variety of metabolic circumstances including routine protein turnover in cells, ingestion of protein-rich foods, or the metabolism of body proteins during periods of starvation (Bender, 2012a; Campbell, 1997; Campbell and Smith Jr., 1992). Unlike lipids and carbohydrates which when in excess can be stored as triglycerides and glycogen, respectively, amino acids cannot be stored in animals and are instead preferentially degraded (Campbell, 1991).

In the majority of organisms, the process of amino acid deamination (or oxidation) generates ammonia during the removal of an amino group (Bucking, 2017; Bursell, 1967; Ip and Chew, 2010; Leigh and Dodsworth, 2007; Merrick and Edwards, 1995; Weihrauch et al., 2012a). Amino acid deamination also yields α-keto acids that are directly oxidized to carbon dioxide (CO_2) and water to produce energy via the citric acid cycle. Alternatively, some α-keto acids that arise from amino acid deamination are a significant source of substrate for metabolic fuel generation, whereby the carbon skeletons of specific amino acids are diverted to gluconeogenesis or ketogenesis pathways (Bender, 2012b; Campbell, 1991). Transamination reactions are a common first step preceding ammonia production during amino acid catabolism and entail the transfer of an amino group from an amino acid to a ketoacid, catalyzed by an aminotransferase (or transaminase) enzyme. The most common acceptor of this amino group in organisms is the ketoacid α-ketoglutarate, which together form L-glutamate

(Bender, 2012b). Transamination reactions confer the advantage that there is no net loss of amino groups (i.e. ammonia production) but instead the collection of amino groups into only one amino acid form, namely L-glutamate (Ballantyne, 2001). Transamination reactions typically occur in the cytosol of cells and glutamate is subsequently shuttled into the mitochondria. Within the mitochondria, glutamate is deaminated producing ammonia in the form of NH_4^+. Together, the transamination and deamination steps constitute the process termed transdeamination, the primary pathway of ammonia production resulting from amino acid catabolism. Alternatively, glutamate can be further aminated to produce the non-toxic, neutrally charged amino acid glutamine, a process that requires ATP but is ideal for ammonia transport in bodily fluids and across plasma membranes of cells (Ballantyne, 2001). Both glutamate and glutamine are critical for ammonia sequestration in organisms and virtually all cells possess at least one of two pathways, glutamine synthetase/glutamate synthase (GS/GOGAT) and/or glutamate dehydrogenase/glutamine synthetase (GDH/GS), for incorporating or removing amino groups within these two amino acids (Ballantyne, 2001; Campbell, 1991; Leigh and Dodsworth, 2007; Merrick and Edwards, 1995). Following the deamination of glutamate or glutamine which liberates NH_4^+, a biochemical fork in the road occurs whereby ammonia can either be recycled for the synthesis of other amino acids and nucleic acids or ammonia can be channeled into a single nitrogenous waste product to be excreted. Ultimately, the metabolic fate of ammonia that is destined for excretion depends on the organism and/or the habitat; excess ammonia can be directly excreted as NH_3/NH_4^+ or converted to less toxic urea and uric acid forms before being excreted (see Section 1.3).

1.3 Nitrogenous waste excretion in animals

Nitrogenous waste excretion in animals predominantly occurs via organs having a function in osmoregulation and/or gas exchange. For example, digestive and excretory organs (Browne and O'Donnell, 2013; Weihrauch, 2006; Weiner and Hamm, 2007; Wilson et al., 2013), the integument (Adlimoghaddam et al., 2015; Cruz et al., 2013; Glover et al., 2013; Shih et al., 2013), and gills (Donini

and O'Donnell, 2005; Weihrauch et al., 2002; Wood et al., 1995a) in various animal groups have been shown to facilitate nitrogenous waste excretion. With some exceptions, water availability is a key determinant in the form of nitrogenous waste that an animal excretes. The main nitrogenous waste compounds, in order of increasing water solubility, are uric acid, urea, and ammonia (Wright, 1995a). While ammonia is the most soluble of the nitrogenous wastes, it is also the most toxic form (see Section 1.4) and, therefore, its excretion demands significant water availability to maintain non-toxic levels internally. Accordingly, aquatic animals generally excrete the majority of nitrogenous wastes in the form of ammonia. This phenomenon has been widely documented in many invertebrate and vertebrate animal groups including crustacea (Weihrauch and O'Donnell, 2015; Weihrauch et al., 1999; Weihrauch et al., 2004), mollusks (Boucher-Rodoni and Mangold, 1995; Hu and Tseng, 2017; Hu et al., 2014; Regnault, 1987), insects (O'Donnell and Donini, 2017; Weihrauch and O'Donnell, 2015; Weihrauch et al., 2012a), annelids (Quijada-Rodriguez et al., 2015; Tillinghast, 1967), teleost fish (Bucking, 2017; Ip and Chew, 2010; Wilkie, 1997; Wood et al., 1995b) and mammals (Good et al., 1984; Weiner and Hamm, 2007; Weiner and Verlander, 2014). On the other hand, water retention is paramount for terrestrial and semi-terrestrial animals, thus these animals typically convert ammonia to less soluble urea or uric acid forms which can be concentrated in the body with minimal toxic effects (Baldwin and Needham, 1934; Needham, 1935). One caveat is that urea and uric acid production are more costly than ammonia in regards to energy expenditure, as many enzymes are required for the conversion of purine nucleic acids (adenine and guanine) to uric acid (Alexander, 1965; Maiuolo et al., 2016) and the formation of urea via the ornithine-urea cycle or uric acid degradation (McDonald et al., 2006; Regnault, 1987; Wright, 1995a).

It is also worth noting that some animals have evolved more peculiar strategies in the handling of nitrogenous waste products irrespective of water availability, often the result of specialized adaptations to environmental challenges. Elasmobranch fishes, for instance, retain a significant proportion of

metabolically produced urea which is utilized as an osmolyte to mitigate challenges in water retention and urine formation that is often faced in teleost fishes (McDonald et al., 2006; Smith, 1936; Wilkie, 2002). The majority of squid families, particularly those that are pelagic deep-sea squid, retain ammonia in specialized compartments as a means of buoyancy (Clarke et al., 1979; Seibel et al., 2004). Remarkably, some terrestrial and amphibious animals excrete nitrogenous wastes in the form of ammonia through gaseous NH_3 volatilization (De Vries and Wolcott, 1993; De Vries et al., 1994; Ip et al., 2004; Randall and Ip, 2006; Speeg and Campbell, 1968). No matter the means of nitrogenous waste excretion, nitrogen retention in specialized compartments, or conversion to non-toxic nitrogen-containing forms, animals face the collective challenge of preventing ammonia toxicity by utilizing efficient detoxification and excretory pathways.

1.4 Ammonia toxicity in animal cells

Perhaps the greatest necessity of rapid and efficient ammonia detoxification and excretory mechanisms in animals is the toxicity of ammonia at relatively low quantities in cells and bodily fluids. In aqueous solutions, gaseous ammonia (NH_3) and the protonated form ammonium (NH_4^+) are in equilibrium. The unprotonated form, NH_3, is a strong base in solution while NH_4^+ is a weak acid (Jacobs, 1940). The relative ratio of NH_3 and NH_4^+ is directly dependent on the pH, and the pKa of this equilibrium reaction is 9.24 at 25°C (Cooper and Plum, 1987; Ip and Chew, 2010; Wright, 1995a). Because the pH of bodily fluids is typically 1-2 units below the pKa, the majority of ammonia (> 98%) in physiological solutions exists as NH_4^+ (Campbell, 1991; Marcaggi and Coles, 2001). The same is also true of most environments in the biosphere where near-neutral pH prevails, such that NH_4^+ dominates relative to NH_3. While amino acid catabolism produces NH_4^+ in the mitochondria (see Section 1.2), the deamination of purines produces NH_3/NH_4^+ in the cytosol of cells (Bogusky et al., 1976; Lowenstein, 1972). Consequently, NH_4^+ toxicity arises through a variety of possible mechanisms at the cytosolic or intraorganelle level (Cooper and Plum, 1987). For example, hydrated ammonium ions,

NH_4^+, have an identical hydrodynamic (and ionic) radius as hydrated potassium ions (K^+) (Martinelle and Häggström, 1993; Mudry et al., 2006), and can therefore perturb electrochemical gradients (Glacken, 1988) and neuronal activity (Cooper and Plum, 1987) by directly competing with K^+ ions for passage through K^+ channels and transporters (Marcaggi and Coles, 2001).

While the catabolic production of ammonia primarily yields NH_4^+, a few metabolic reactions (e.g. purine nucleotide cycle) produce NH_3 (Bogusky et al., 1976). NH_3 is mainly responsible for the pathological consequences of altered ammonia metabolism in animals as it is moderately lipid-soluble and can readily cross biological membranes via simple diffusion (Marcaggi and Coles, 2001; Martinelle and Häggström, 1993), albeit to a much lesser extent than NO, CO_2, and O_2 (Ip and Chew, 2010). Nonetheless, the diffusion (simple and/or facilitated) rates of NH_3 across cell membranes are 10^3-10^4 fold greater than NH_4^+ (Marcaggi and Coles, 2001; Martinelle and Häggström, 1993), emphasizing the critical nature of the ratio of NH_3/NH_4^+ in animals as a means of minimizing ammonia toxicity. The molecular basis for NH_3 toxicity is extensive, from changes in cellular and organelle pH to the depletion of intermediates for both the citric acid cycle (e.g. α-ketoglutarate) and the electron transport chain (e.g. NADH) when sequestering NH_3 during situations of altered ammonia metabolism (Campbell, 1991; Marcaggi and Coles, 2001; Martinelle and Häggström, 1993). NH_3 can also act as an uncoupler of oxidative phosphorylation through the dissipation of proton gradients in the mitochondria, by binding with H^+ and forming NH_4^+ in the inner mitochondrial membrane space (Brierley and Stoner, 1970; Campbell, 1997).

1.5 Transport of NH_3 and NH_4^+ across plasma membranes

NH_4^+ transport through a "leaky", cation-selective paracellular pathway has been suggested in some vertebrate animals (Good et al., 1984; Wilkie, 1997), with some support from a study demonstrating that a tight junction protein (claudin-8) modulates NH_4^+ paracellular permeability in a cell culture system (Angelow et al., 2006). On the other hand, considerable evidence exists demonstrating

that the rapid diffusion of gaseous ammonia (NH_3) occurs across plasma membranes of cells (Kleiner, 1981). The cell membrane permeability to neutral NH_3 is much less than its larger, more hydrophobic counterparts, methylamine and trimethylamine (Ritchie and Gibson, 1987). However, simple NH_3 diffusion can still be quite rapid owing to the thinness of cell membranes (Ip and Chew, 2010). A key argument for NH_3 diffusion across biological membranes lies in the findings that (1) ammonia equilibrates across membranes as NH_3 becomes "trapped" by NH_4^+ formation on the more acidic side of the membrane, and (2) the rate of ammonia transport across membranes increases in a pH-dependent manner (Jacobs, 1940; Kleiner, 1981). Later, it was demonstrated that the ammonia transport system within the internal membrane of mitochondria in animal cells relied primarily on the movement of NH_4^+ with minimal effects by changes in pH (Gutiérrez et al., 1987). Many examples of biological membranes in animals with low permeability to NH_3 now exist, for instance, the plasma membranes of epithelial cells lining gastric and urinary tracts (Kikeri et al., 1989; Singh et al., 1995). It is now broadly acknowledged that the majority of ammonia transport across biological membranes in animal systems is tightly regulated and that this regulation is achieved through the action of ion channel and transport proteins (Wright and Wood, 2009).

1.5.1 Passage of NH_4^+ on ATP-dependent membrane transporters in animal cells

The enzyme Na^+/K^+-ATPase (NKA) is present in the membrane of essentially all cells where it plays a principal role in establishing electrochemical gradients that power ion transport (Towle and Holleland, 1987). NKA is a key energizer in the epithelia of organ systems that regulate ion and water homeostasis, and it has long been known that NH_4^+ can replace K^+ as a substrate to be actively transported from the body fluids into the cytoplasm of cells (Post and Jolly, 1957; Skou, 1965; Towle and Holleland, 1987). So, in addition to its importance in osmoregulation, substantial evidence exists showing that NKA is highly involved in active ammonia transport processes in many species from various phyla (Ip and Chew, 2010; O'Donnell and Donini, 2017; Weihrauch et al., 2004; Weiner and Hamm,

2007). The V-type H^+-ATPase (VA) is another primary ion-motive pump generally shown to be associated with endosomal membranes but is now found in increasing examples on the plasma membrane of cells (Beyenbach, 2006; Wieczorek et al., 2009). VA actively transports protons (H^+) across biological membranes, and in turn, the transmembrane electrochemical potential difference of H^+ is used to power an array of secondary active and channel-mediated transport systems. For example, members of the cation/proton exchanger (NHE) family of integral membrane proteins have been shown to play an indirect role in transmembrane ammonia transport (Benos, 1982; Weihrauch et al., 2004; Weihrauch et al., 2012a). While predominantly facilitating the electroneutral exchange of Na^+ or K^+ for H^+ down their respective NKA- and VA-derived concentration gradients, NH_4^+ can substitute for Na^+ or K^+ which occurs in a manner consistent with ammonia secretion across the apical membrane of cells, albeit NH_4^+ transport by NHEs occurs at slower velocities (Orlowski and Grinstein, 2004; Zachos et al., 2005). Another secondary-active transport mechanism involving NH_4^+ is the Na^+-K^+-$2Cl^-$ (NKCC) cotransport system located in ion-motive epithelia of osmoregulatory organs in some animals, where NH_4^+ is transported in lieu of K^+ (Beyenbach et al., 2010; Good, 1987; Good et al., 1985).

1.5.2 Ammonia transporters of the AMT/MEP/Rh families

Studies over the last two decades have revealed that organisms from all kingdoms of life possess membrane-spanning proteins that are highly specific for the movement of NH_3 and NH_4^+ across biological membranes (Neuhäuser et al., 2014). The ammonium transporter gene family consists of three main clades, all of which share high sequence similarity and a very similar trimeric overall structure across all life domains (McDonald and Ward, 2016a; McDonald et al., 2012). Methylammonium/ammonium permeases (MEP) in fungi (Marini et al., 1994; Marini et al., 1997a), ammonium transporters (AMT) in bacteria and plants (Ninnemann et al., 1994; Soupene et al., 1998), and the vertebrate Rhesus glycoproteins (Rh proteins) (Marini et al., 1997b; Marini et al., 2000) were demonstrated to have ammonia transport capabilities. AMT proteins are considered to be of ancient origin as

they are ubiquitous in bacteria and dispersed in archaea, in contrast to Rh proteins which occur in some microbial eukarya (e.g. algae) and widespread in vertebrates, with increased prominence in mammals, in particular (Huang and Peng, 2005; Kitano and Saitou, 2000; Kustu and Inwood, 2006; Peng and Huang, 2006). While the distribution of AMT proteins is largely complementary to that of Rh proteins in organisms, invertebrate animals are unique in that they possess both AMT and Rh proteins (Chasiotis et al., 2016; Lecompte et al., 2019; Menuz et al., 2014; Pitts et al., 2014; Weihrauch et al., 2012a).

1.6 The challenge of nitrogen regulation imposed on mosquitoes, *Aedes aegypti* by environmental factors and life history.

The *Aedes aegypti* (Diptera: Culicidae) mosquito is an urban-dwelling, tropical and subtropical species which undergoes larval and pupal development in natural freshwater followed by complete metamorphosis, involving dramatic changes in body shape and function, into the terrestrial adult forms (Clements, 1992). As with most holometabolous insects, the entirely aquatic larval stage is a period of feeding and growth whereas the adult stage is the reproductive stage (Nelson, 1986). The latter stage is of great medical and economical importance because adult females feed on human blood to meet nutrient demands for reproduction, and in turn transmit serious human arboviral diseases including the Dengue, Chikungunya, and Zika viruses (Bhatt et al., 2013; Leta et al., 2018). However, despite the negative connotations associated with mosquitoes, they are also of great ecological importance. The primary food of all adult mosquitoes is floral nectar and in this regard, mosquitoes are effective pollinators of some plant species (Dexter, 1913; Lahondère et al., 2020). Of the 3,500 named species of mosquito, only a couple hundred actually bite humans and most species provide important ecosystem services. For example, the larvae constitute a substantial biomass in aquatic ecosystems globally where they process detritus materials and are a primary food source for many insect, amphibian, bird, and fish species (Fang, 2010). The specialized adaptations of larvae to cope with osmoregulatory challenges in aquatic life, coupled with drastic morphological changes involving significant remodeling of

organs as the mosquito transitions to the adult, offers many comparative and integrative approaches in the study of ammonia transport physiology within a single animal species. This, in addition to the fact that *A. aegypti* are one of only a few animals that have been shown to possess both AMT and Rh proteins within a single species [see Section 1.5.2; (Chasiotis et al., 2016; Pitts et al., 2014; Weihrauch et al., 2012a)]. *A. aegypti* express two AMT transporter genes, *AeAmt1* and *AeAmt2*, as well as two Rh transporter genes, *AeRh50-1* and *AeRh50-2*. A readily accessible and well-annotated genome assembly for *A. aegypti* also offers the additional prospect of comprehensive genetic studies with the use of powerful molecular tools such as next generation sequencing techniques (i.e. RNA sequencing) (Matthews et al., 2018).

1.6.1 Environmental challenges and strategies of ammonia excretion in *A. aegypti* larvae

Historically considered to be a freshwater (FW) species (Clements, 1992), *A. aegypti* larvae are osmo- and iono-regulators. Therefore, they maintain relatively constant haemolymph (i.e. blood) ion concentrations and an overall haemolymph osmotic concentration at levels much higher than the freshwater habitats occupied by these larvae (Bradley, 1987; Edwards, 1982; Patrick et al., 2002a). In fact, *A. aegypti* larvae spend their lives in intimate contact with an aqueous milieu that almost always differs in ionic composition and pH from the internal fluids. This has two important consequences for ammonia regulation and excretion in larvae: First, the larvae can excrete ammonia (NH_3 and NH_4^+) directly into the aquatic environment via copious amounts of water. Second, the larvae face the added challenge of passive ammonia absorption across ion permeant epithelia as water and food are ingested in aquatic environments. *A. aegypti* larvae exhibit some of the highest drinking rates among mosquitoes (Aly and Dadd, 1989). In line with most aquatic animals (see Section 1.3), the larvae were shown to excrete significant quantities of cationic ammonia, NH_4^+ (Donini and O'Donnell, 2005). *A. aegypti* larvae are also some of the most capable acid-base regulators among animals, maintaining their haemolymph pH within 0.1 units while observed developing in FW habitats ranging in pH 4 to 11 (Clark,

2004; Clark et al., 2007). Of course, the pH regulatory strategies of larvae and the pH of the external media they inhabit is intertwined with ammonia regulation and excretory mechanisms because pH heavily influences the ratio of NH_3 and NH_4^+ in solution (see Section 1.4) of which NH_3 is the more toxic form. Adding to the value in understanding the mechanisms underlying ammonia regulation and excretion in *A. aegypti* are the decades of reports demonstrating that the larvae routinely inhabit ammonia-rich sewage collections around the globe (Barrera et al., 2008; Burke et al., 2010; Chitolina et al., 2016; Irving-Bell et al., 1987; Lam and Dharmaraj, 1982; Mackay et al., 2009; Somers et al., 2011).

1.6.2 Physiological challenges related to blood-feeding and reproduction in adult female *A. aegypti*

In anautogenous mosquitoes, such as *Aedes aegypti*, the adult female periodically requires a vertebrate blood meal to undergo a cycle of egg maturation. The blood meal provides a significant source of proteins required for this process and the female is capable of ingesting more blood than is often needed for oogenesis (Briegel, 1985; Briegel, 1986). Nonetheless, all blood protein is catabolized and excess nitrogen that is not utilized to produce proteins, lipids, and carbohydrates, the latter two of which are both lacking in the blood meal, is excreted (Pennington et al., 2003). *A. aegypti* females have evolved efficient mechanisms to detoxify large ammonia loads during the digestion of a blood meal (Scaraffia et al., 2005), and they are an exception to most terrestrial animals in that they excrete ammonia in the faeces as their primary nitrogenous waste (Scaraffia et al., 2006).

1.6.3 Ammonia transporting mechanisms in larvae and adult *A. aegypti*

The key organs associated with ion and water homeostasis in *A. aegypti* larvae are the midgut, Malpighian tubules, rectum, and anal papillae (Figure 1-1). Digestion of food and absorption of nutrients and ions into the haemolymph occur via the midgut (MG) (Bradley, 1987). The Malpighian tubules (MT) and hindgut (HG) are the organs responsible for excretion, with the primary urine produced in the MT by the active secretion of ions (principally Na^+, K^+, and Cl^-) and the osmotically-obliged influx of water into the tubule lumen (Ramsay, 1951). In many insects, the MT are also the site of

nitrogenous waste excretion (Weihrauch et al., 2012a). The primary urine is then directed via the ileum (IL) towards the rectum (RM), and both of the structures are located posteriorly to the midgut and comprise the hindgut (HG). The cells of the rectal segment possess highly infolded apical and basolateral membranes in keeping with their role in the selective reabsorption of ions from the primary urine, producing a dilute urine that is eliminated (Bradley, 1987; Meredith and Phillips, 1973). The larvae also possess extra-renal structures associated with ion and water homeostasis in the form of the externally protruding anal papillae (AP; Figure 1-1). The four AP surrounding the anal opening are primary sites of ion exchange with the environment (Sohal and Copeland, 1966; Wigglesworth, 1932), and it is within these structures that the most comprehensive mechanism of ammonia transport and excretion exists in *A. aegypti* larvae. A significant amount of ammonia is directly excreted from the AP lumen (i.e. haemolymph) into the external aquatic environment (Donini and O'Donnell, 2005). It was also demonstrated that the AP express three ammonia transporters: *AeAmt1*, *AeRh50-1*, and *AeRh50-2* (see Section 1.6; Chasiotis et al., 2016). Loss of function (i.e. RNA interference or RNAi) studies combined with pharmacological characterization of ammonia transport mechanisms implicated AeAmt1, ion-motive pumps NKA and VA, and an NHE protein (NHE3) in facilitating ammonia excretion within the AP. At the beginning of the current studies, another Amt transporter in *A. aegypti*, *AeAmt2*, was recently identified through a BLAST search of the *A. aegypti* genome but had not yet been characterized to any degree (unpublished findings by Dr. Dirk Weihrauch).

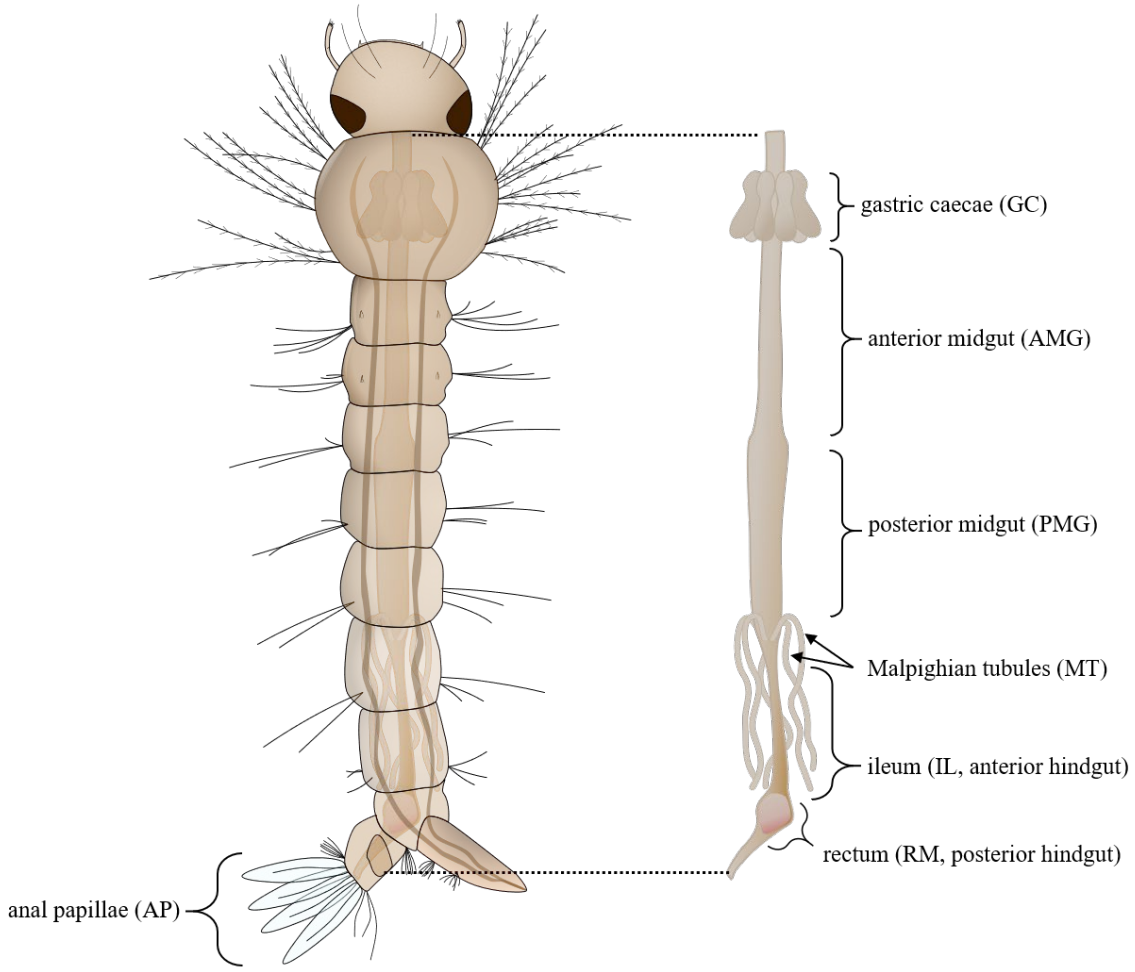

Figure 1- 1. Organs associated with ion and water transport in *Aedes aegypti* larvae. The midgut (MG) is the site of digestion and subsequent ion and nutrient absorption. The primary urine is formed in the Malpighian tubules (MT), which actively secrete ions (Na^+, K^+, Cl^-) from the haemolymph to the tubule lumen which causes the osmotic influx of water into the lumen. The rectum (RM) segment of the hindgut (HG) forms a dilute urine by reabsorbing ions from the primary urine back into the haemolymph. The externally protruding anal papillae (AP) are the sites of ion uptake from the external media and ammonia excretion from the haemolymph. Illustrations created by Dr. Chun Chih Chen.

Osmoregulatory organs are modified during metamorphosis to become well suited for a terrestrial lifestyle and ingestion of a blood meal by adult females. The design of the female alimentary canal is reflective of its feeding habits, possessing a large distensible midgut which is the site of storage and digestion of blood meals (Figure 1-2; Bradley, 1987). The hindgut consists of an anterior ileum and a posterior rectum similarly to the larvae, but the rectum in adults contains six pear-shaped rectal papillae which are the site of ion resorption from the primary urine produced by the MT (Figure 1-2; Ramsay, 1950; Ramsay, 1951). The fat body plays functionally analogous roles to the vertebrate liver (Clements, 1992) and is the primary site of ammonia detoxification in female *A. aegypti* (Scaraffia et al., 2005; Scaraffia et al., 2006). However, nothing is known regarding specific ammonia transport or excretory mechanisms, nor the expression and possible roles of ammonia transporters in these processes in adult *A. aegypti*. Expression of an Rh transporter gene (*AalRh50*) in another mosquito species, *Aedes albopictus*, was significantly upregulated in the midgut, fat body, and MT of females up to 24 hours following a blood meal (Wu et al., 2010a). *AalRh50* transcript was also detected in the ovary of *A. albopictus*, suggesting a potential role for Rh proteins in processes related to egg development (Wu et al., 2010a). In the malaria vector mosquito, *Anopheles gambiae*, transcripts of ammonia transporters *AgAmt* and *AgRh50* are enriched in the antennae where it is postulated that they have an important function in ammonia sensing pertaining to host-seeking behaviors (Pitts et al., 2014).

1.7 Research aims and objectives

Nitrogen regulation and, in particular, the regulation of ammonia (NH_3/NH_4^+) transport and excretion is a fundamental feature in all animals (see Section 1.1). However, comparatively little is known about the mechanisms underlying these processes in mosquitoes relative to their invertebrate (Adlimoghaddam et al., 2015; Hu and Tseng, 2017; Quijada-Rodriguez et al., 2015; Weihrauch, 2006; Weihrauch et al., 2004; Weihrauch et al., 2009; Weihrauch et al., 2012b) and vertebrate (Bucking,

2017; Hung et al., 2007; Ip and Chew, 2010; Ip et al., 2004; Lee et al., 2013; Weiner and Verlander, 2014; Wilkie, 1997; Wright and Wood, 2009) counterparts.

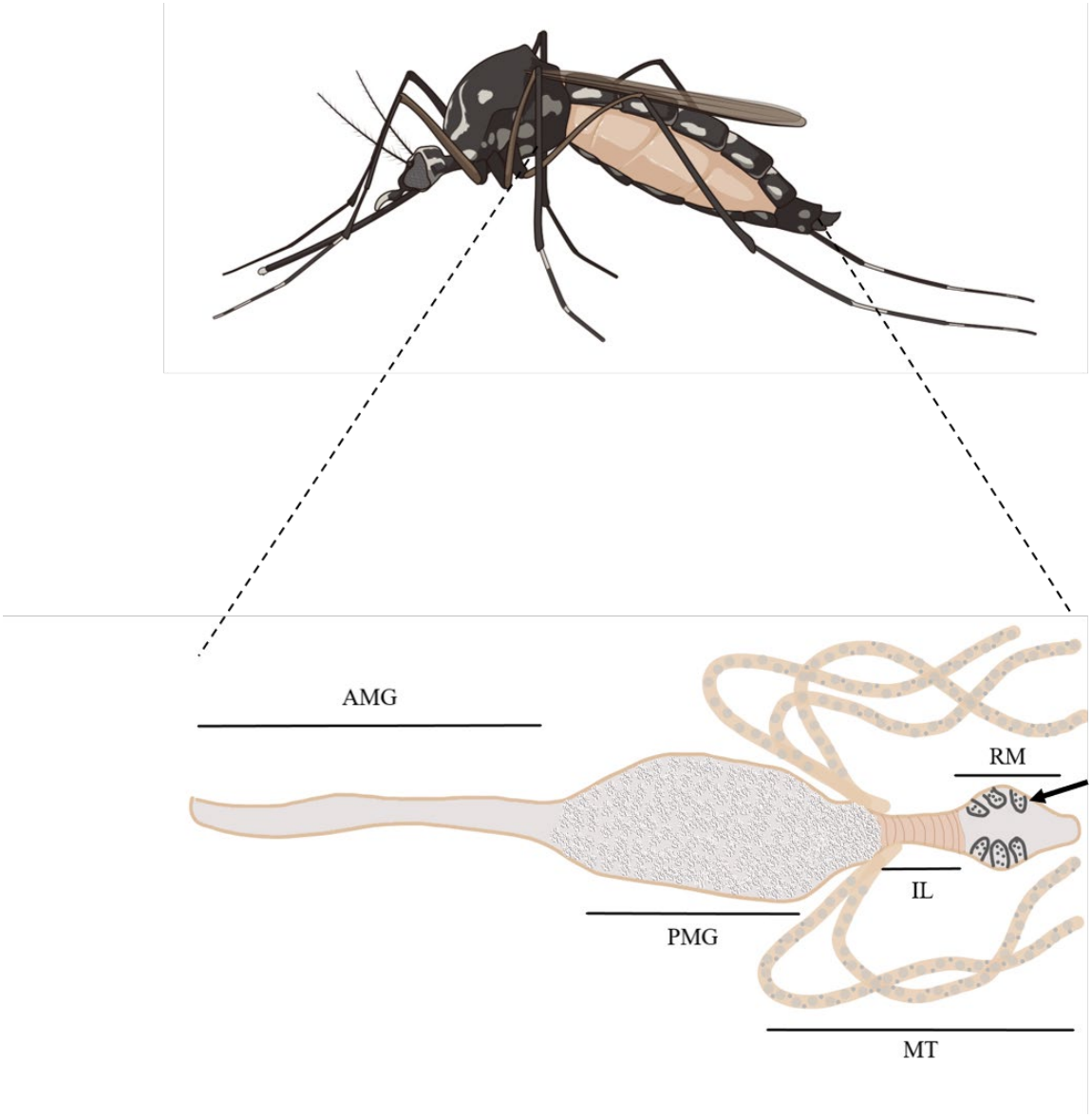

Figure 1- 2. Organs associated with ion and water transport, and blood meal digestion in adult female *Aedes aegypti*. The midgut (MG), divided into the anterior (AMG) and posterior (PMG), is the site of blood meal digestion and subsequent ion and nutrient absorption. The primary urine is formed in the Malpighian tubules (MT). Within the hindgut, the highly contractile ileum (IL) facilitates the forward movement of gut contents, and the rectum (RM) including the six rectal pads that are not present in larvae (black arrow), forms a dilute urine by reabsorbing ions from the primary urine back into the haemolymph. Adult female illustration created by BioRender (BioRender.com).

1.7.1 Aim 1: Characterize the mechanisms underlying ammonia transport and excretion in osmoregulatory organs of *A. aegypti* larvae

A prior study demonstrated that larvae utilize specialized organs (the anal papillae, see Section 1.6.3) for the direct excretion of ammonia into the external medium (Donini and O'Donnell, 2005) and that these organs express ammonia transporters *AeAmt1*, *AeRh50-1*, and *AeRh50-2* at the messenger RNA (mRNA) level (Chasiotis et al., 2016). The protein of one of these transporters, AeAmt1, was localized to the anal papillae epithelium where it was shown to be involved in ammonia excretion. These initial findings provide a framework that allows for a more profound understanding of ammonia transport and excretory processes in *A. aegypti* larvae. Of course, these findings also have major implications for the documented expansion in the habitats of larvae to high ammonia sewage water and other high environmental ammonia (HEA) habitats. Based on this information, it was hypothesized that all of the AMT and Rh ammonia transporters have integral roles in ammonia transporting mechanisms in the anal papillae and other organs associated with ion and water homeostasis which are important for the larvae to develop in HEA habitats. The objectives of this research aim were four-fold:

(1) Characterize the specific localizations and the contributions of Rh proteins, AeRh50-1 and AeRh50-2, to ammonia excretion within the anal papillae;
(2) Explore the expression and spatial distribution of the recently identified AMT protein, AeAmt2, and investigate potential roles for this transporter in the anal papillae of larvae;
(3) Determine the involvement of AMT and Rh proteins in ammonia regulation and excretion upon exposure of larvae to HEA conditions reflective of natural sewage water habitats;
(4) Survey other osmoregulatory organs using, in part, next-generation sequencing to identify other potential ammonia-transporting mechanisms and establish a more complete, systems-level model of ammonia regulation and excretion in *A. aegypti* larvae.

1.7.2 Aim 2: Examine the expression and a potential role of AMT and Rh proteins during blood meal digestion in adult *A. aegypti*

Broadly, there are many unanswered questions in adult *A. aegypti* pertaining to the specific ammonia excretory mechanisms that allow for the tolerance of females to remarkably high ammonia loads that arise after blood-feeding (Scaraffia et al., 2005). Further, nothing is known regarding the expression nor the potential function of ammonia transporters in *A. aegypti* adults. There is only limited information from the adult females of other mosquito species regarding the presence of Amt and Rh genes and their contribution to ammonia-related processes, such as host-seeking, blood meal digestion, and egg development (see Section 1.6.3). Interestingly, the uncharacterized *AeAmt2* in *A. aegy*pti exhibits high sequence similarity with the antennal-expressed *AgAmt* in *A. gambiae*. Therefore, the working hypothesis was that the tissue- and organ-specific expression and alterations in the abundance of AMT and Rh proteins are indicative of their importance in ammonia transport and excretion during blood meal digestion and within ammonia-sensing structures in adult female *A. aegypti*. The objectives of this research aim were two-fold:

(1) Identify AMT and Rh proteins in chemosensory and osmoregulatory organs
(2) Establish a potential role for these proteins in the regulation of ammonia detoxification and excretion during the entirety of the female gonotrophic cycle (i.e. blood-feeding, egg development, egg-laying) using RNAi

1.8 References

Adlimoghaddam, A., Boeckstaens, M., Marini, A.-M., Treberg, J. R., Brassinga, A.-K. C. and Weihrauch, D. (2015). Ammonia excretion in Caenorhabditis elegans: mechanism and evidence of ammonia transport of the Rhesus protein CeRhr-1. *J. Exp. Biol.* **218**, 675–683.

Alexander, B. (1965). Significance of Uric Acid as a Nitrogenous Waste in Vertebrate Evolution *. **8**, 614–626.

Aly, C. and Dadd, R. H. (1989). Drinking rate regulation in some fresh-water mosquito larvae. *Physiol. Entomol.* **14**, 241–256.

Angelow, S., Kim, K.-J. and Yu, A. S. L. (2006). Claudin-8 modulates paracellular permeability to acidic and basic ions in MDCK II cells. *J. Physiol.* **571**, 15–26.

Baldwin, E. and Needham, J. (1934). Problems of nitrogen catabolism in invertebrates. *Biochem. J.* **28**, 1372–1392.

Ballantyne, J. S. (2001). Amino acid metabolism. In *Nitrogen Excretion*, pp. 77–107. Academic Press.

Barrera, R., Amador, M., Diaz, A., Smith, J., Munoz-Jordan, J. L. and Rosario, Y. (2008). Unusual productivity of *Aedes aegypti* in septic tanks and its implications for dengue control. *Med. Vet. Entomol.* **22**, 62–69.

Bender, D. A. (2012a). *Amino acid metabolism* . 3rd ed. Chichester, West Sussex: John Wiley & Sons.

Bender, D. A. (2012b). The metabolism of "surplus" amino acids. *Br. J. Nutr.* **108**, S113–S121.

Benos, D. J. (1982). Amiloride: a molecular probe of sodium transport in tissues and cells. *Am. J. Physiol.* **242**, C131–C144.

Beyenbach, K. W. (2006). The V-type H^+ ATPase: molecular structure and function, physiological roles and regulation. *J. Exp. Biol.* **209**, 577–589.

Beyenbach, K. W., Skaer, H. and Dow, J. A. T. (2010). The Developmental , Molecular , and Transport Biology of Malpighian Tubules. *Annu. Rev. Entomol.* **55**, 351–374.

Bhatt, S., Gething, P. W., Brady, O. J., Messina, J. P., Farlow, A. W., Moyes, C. L., Drake, J. M., Brownstein, J. S., Hoen, A. G., Sankoh, O., et al. (2013). The global distribution and burden of dengue. *Nature* **496**, 504–507.

Bogusky, R. T., Lowenstein, L. M. and Lowenstein, J. M. (1976). The purine nucleotide cycle. A pathway for ammonia production in the rat kidney. *J. Clin. Invest.* **58**, 326–335.

Boucher-Rodoni, R. and Mangold, K. (1995). Ammonia production in cephalopods, physiological and evolutionary aspects. *Mar. Freshw. Behav. Physiol.* **25**, 53–60.

Bradley, T. J. (1987). Physiology of osmoregulation in mosquitoes. *Annu. Rev. Entomol.* **32**, 439–462.

Briegel, H. (1985). Mosquito reproduction: Incomplete utilization of the blood meal protein for oogenesis. *J Insect Physiol* **31**, 15–21.

Briegel, H. (1986). Protein catabolism and nitrogen partitioning during oogenesis in the mosquito *Aedes aegypti*. *J. Insect Physiol.* **32**, 455–462.

Brierley, G. P. and Stoner, C. D. (1970). Ion transport by heart mitochondria. XVIII. Swelling and contraction of heart mitochondria suspended in ammonium chloride. *Biochemistry* **9**, 708–713.

Browne, A. and O'Donnell, M. J. (2013). Ammonium secretion by Malpighian tubules of *Drosophila melanogaster*: Application of a novel ammonium-selective microelectrode. *J. Exp. Biol.* **216**, 3818–3827.

Bucking, C. (2017). A broader look at ammonia production, excretion, and transport in fish: a review of impacts of feeding and the environment. *J. Comp. Physiol. B* **187**, 1–18.

Burke, R. L., Barrera, R., Lewis, M., Kluchinsky, T. and Claborn, D. (2010). Septic tanks as larval habitats for the mosquitoes *Aedes aegypti* and *Culex quinquefasciatus* in Playa-Playita, Puerto Rico. *Med. Vet. Entomol.* **24**, 117–123.

Bursell, E. (1967). The Excretion of Nitrogen in Insects. In (ed. Beament, J. W. L.), Treherne, J. E.), and Wigglesworth, V. B. B. T.-A. in I. P.), pp. 33–67. Academic Press.

Campbell, J. W. (1991). Excretory Nitrogen Metabolism. In: Experimental and Metabolic Animal Physiology. In *Comparative Animal Physiology* (ed. Prosser, C. L.), pp. 277–324. New York: Wiley-Interscience.

Campbell, J. W. (1997). Mitochondrial ammonia metabolism and the proton-neutral theory of hepatic ammonia detoxication. *J. Exp. Zool.* **278**, 308–321.

Campbell, J. W. and Smith Jr., D. D. (1992). Metabolic compartmentation of vertebrate glutamine synthetase: putative mitochondrial targeting signal in avian liver glutamine synthetase. *Mol. Biol. Evol.* **9**, 787–805.

Chasiotis, H., Ionescu, A., Misyura, L., Bui, P., Fazio, K., Wang, J., Patrick, M., Weihrauch, D. and Donini, A. (2016). An animal homolog of plant Mep/Amt transporters promotes ammonia excretion by the anal papillae of the disease vector mosquito *Aedes aegypti*. *J. Exp. Biol.* **219**, 1346–55.

Chitolina, R. F., Anjos, F. A., Lima, T. S., Castro, E. A. and Costa-Ribeiro, M. C. V. (2016). Raw sewage as breeding site to *Aedes (Stegomyia) aegypti* (Diptera, culicidae). *Acta Trop.* **164**, 290–296.

Clark, T. M. (2004). pH tolerances and regulatory abilities of freshwater and euryhaline Aedine mosquito larvae. *J. Exp. Biol.* **207**, 2297–2304.

Clark, T. M., Vieira, M. A. L., Huegel, K. L., Flury, D. and Carper, M. (2007). Strategies for regulation of haemolymph pH in acidic and alkaline water by the larval mosquito *Aedes aegypti* (L.) (Diptera; Culicidae). *J. Exp. Biol.* **210**, 4359–4367.

Clarke, M. R., Denton, E. J. and Gilpin-Brown, J. B. (1979). On the use of ammonium for buoyancy in squids. *J. Mar. Biol. Assoc. United Kingdom* **59**, 259–276.

Clements, A. N. (1992). *The biology of mosquitoes, Vol. I; Development, nutrition and reproduction*. London: Elsevier.

Cooper, A. J. L. and Plum, F. (1987). Biochemistry and Physiology of Brain Ammonia. *Physiol. Rev.*

67, 440–519.

Cruz, M. J., Sourial, M. M., Treberg, J. R., Fehsenfeld, S., Adlimoghaddam, A. and Weihrauch, D. (2013). Cutaneous nitrogen excretion in the African clawed frog *Xenopus laevis*: Effects of high environmental ammonia (HEA). *Aquat. Toxicol.* **136**–**137**, 1–12.

De Vries, M. C. and Wolcott, D. L. (1993). Gaseous ammonia evolution is coupled to reprocessing of urine at the gills of ghost crabs. *J. Exp. Zool.* **267**, 97–103.

De Vries, M. C., Wolcott, D. L. and Holliday, C. W. (1994). High ammonia and low pH in the urine of the ghost crab, *Ocypode quadrata*. *Biol. Bull.* **186**, 342–348.

Delwiche, C. C. (1970). The Nitrogen Cycle. *Sci. Am.* **223**, 136–147.

Dexter, J. S. (1913). Mosquitoes pollinating orchids. *Science (80-.).* **37**, 867.

Donini, A. and O'Donnell, M. J. (2005). Analysis of Na^+, Cl^-, K^+, H^+ and NH_4^+ concentration gradients adjacent to the surface of anal papillae of the mosquito *Aedes aegypti*: application of self-referencing ion-selective mi. *J. Exp. Biol.* **208**, 603–10.

Edwards, H. a (1982). Ion concentration and activity in the haemolymph of *Aedes aegypti* larvae. *J. Exp. Biol.* **101**, 143–151.

Fang, J. (2010). Ecology: A world without mosquitoes. *Nature* **466**, 432–434.

Fernandez, E. and Galvan, A. (2007). Inorganic nitrogen assimilation in Chlamydomonas. *J. Exp. Bot.* **58**, 2279–2287.

Glacken, M. W. (1988). Catabolic control of mammalian cell culture. *Nat. Biotechnol.* **6**, 1041–1050.

Glover, C. N., Bucking, C. and Wood, C. M. (2013). The skin of fish as a transport epithelium: A review. *J. Comp. Physiol. B Biochem. Syst. Environ. Physiol.* **183**, 877–891.

Good, D. W. (1987). Effects of potassium on ammonia transport by medullary thick ascending limb of the rat. *J. Clin. Invest.* **80**, 1358–1365.

Good, D. W., Knepper, M. A. and Burg, M. B. (1984). Ammonia and bicarbonate transport by thick ascending limb of rat kidney. *Am. J. Physiol.* **247**, F35–F44.

Good, D. W., Knepper, M. A. and Burg, M. B. (1985). Ammonia absorption by the thick ascending limb of henle's Loop. In *Contributions to Nephrology*, pp. 110–115.

Gruswitz, F., Chaudhary, S., Ho, J. D., Schlessinger, A., Pezeshki, B., Ho, C.-M., Sali, A., Westhoff, C. M. and Stroud, R. M. (2010). Function of human Rh based on structure of RhCG at 2.1 A. *Proc. Natl. Acad. Sci.* **107**, 9638–9643.

Gutiérrez, C., Beaty, G., López-Vancell, R. and Estrada, S. (1987). Mechanism of ammonium translocation in rat liver mitochondria. Finger-printing of the translocator. *Acta Physiol. Pharmacol. Latinoam.* **37**, 257–275.

Hu, M. and Tseng, Y.-C. (2017). Acid--base regulation and ammonia excretion in cephalopods: An Ontogenetic Overview. In *Acid-Base Balance and Nitrogen Excretion in Invertebrates: Mechanisms and Strategies in Various Invertebrate Groups with Considerations of Challenges Caused by Ocean Acidification* (ed. Weihrauch, D.) and O'Donnell, M.), pp. 275–298. Cham: Springer International Publishing.

Hu, M. Y., Guh, Y. J., Stumpp, M., Lee, J. R., Chen, R. D., Sung, P. H., Chen, Y. C., Hwang, P. P. and Tseng, Y. C. (2014). Branchial NH_4^+-dependent acid-base transport mechanisms and energy metabolism of squid (*Sepioteuthis lessoniana*) affected by seawater acidification. *Front. Zool.* **11**, 1–17.

Huang, C.-H. and Peng, J. (2005). Evolutionary conservation and diversification of Rh family genes and proteins. *Proc. Natl. Acad. Sci.* **102**, 15512–15517.

Hung, C. Y. C., Tsui, K. N. T., Wilson, J. M., Nawata, C. M., Wood, C. M. and Wright, P. a (2007). Rhesus glycoprotein gene expression in the mangrove killifish *Kryptolebias marmoratus* exposed to elevated environmental ammonia levels and air. *J. Exp. Biol.* **210**, 2419–2429.

Ip, Y. K. and Chew, S. F. (2010). Ammonia production, excretion, toxicity, and defense in fish: A review. *Front. Physiol.* **1 OCT**, 1–20.

Ip, Y. K., Chew, S. F. and Randall, D. J. (2004). Five tropical air-breathing fishes, six different

strategies to defend against ammonia toxicity on land. *Physiol. Biochem. Zool.* **77**, 768–782.

Irving-Bell, R. J., Okoli, E. I., Diyelong, D. Y., Lyimo, E. O. and Onyia, O. C. (1987). Septic tank mosquitoes: competition between species in central Nigeria. *Med. Vet. Entomol.* **1**, 243–250.

Jacobs, M. H. (1940). Some aspects of cell permeability to weak electrolytes. *Cold Spring Harb. Symp. Quant. Biol.* **8**, 30–39.

Khademi, S., O'Connell III, J., Remis, J., Robles-Colmenares, Y., Miercke, L. J. W. and Stroud, R. M. (2004). Mechanism of ammonia transport by Amt/MEP/Rh: Structure of AmtB at 1.35 angstroms. *Science (80-.).* **305**, 1587–1594.

Kikeri, D., Sun, A., Zeidel, M. L. and Hebert, S. C. (1989). Cell membranes impermeable to NH_3. *Nature* **339**, 478–480.

Kitano, T. and Saitou, N. (2000). Evolutionary history of the Rh blood group-related genes in vertebrates. *Immunogenetics* **51**, 856–862.

Kleiner, D. (1981). The transport of NH_3 and NH_4^+ across biological membranes. *Biochim. Biophys. Acta* **639**, 41–52.

Kustu, S. and Inwood, W. (2006). Biological gas channels for NH_3 and CO_2: evidence that Rh (Rhesus) proteins are CO_2 channels. *Transfus. Clin. Biol.* **13**, 103–110.

Lahondère, C., Vinauger, C., Okubo, R. P., Wolff, G. H., Chan, J. K., Akbari, O. S. and Riffell, J. A. (2020). The olfactory basis of orchid pollination by mosquitoes. *Proc. Natl. Acad. Sci.* **117**, 708–716.

Lam, W. K. and Dharmaraj, D. (1982). A survey on mosquitoes breeding in septic tanks in several residential areas around Ipoh municipality. *Med. J. Malaysia* **37**, 114–123.

Lea, P. J. and Miflin, B. J. (1974). Alternative route for nitrogen assimilation in higher plants. *Nature* **251**, 614–616.

Lecompte, M., Cattaert, D., Vincent, A., Birman, S. and Chérif-Zahar, B. (2019). Drosophila ammonium transporter Rh50 is required for integrity of larval muscles and neuromuscular system

. *J. Comp. Neurol.* 1–14.

Lee, H.-W., Verlander, J. W., Handlogten, M. E., Han, K.-H., Cooke, P. S. and Weiner, I. D. (2013). Expression of the rhesus glycoproteins, ammonia transporter family members, RHCG and RHBG in male reproductive organs. *Reproduction* **146**, 283–296.

Leigh, J. A. and Dodsworth, J. A. (2007). Nitrogen Regulation in Bacteria and Archaea. *Annu. Rev. Microbiol.* **61**, 349–377.

Leta, S., Beyene, T. J., De Clercq, E. M., Amenu, K., Kraemer, M. U. G. and Revie, C. W. (2018). Global risk mapping for major diseases transmitted by *Aedes aegypti* and *Aedes albopictus*. *Int. J. Infect. Dis.* **67**, 25–35.

Li, X., Jayachandran, S., Nguyen, H.-H. T. and Chan, M. K. (2007). Structure of the *Nitrosomonas europaea* Rh protein. *Proc. Natl. Acad. Sci. U. S. A.* **104**, 19279–84.

Loqué, D., Mora, S. I., Andrade, S. L. A., Pantoja, O. and Frommer, W. B. (2009). Pore mutations in ammonium transporter AMT1 with increased electrogenic ammonium transport activity. *J. Biol. Chem.* **284**, 24988–24995.

Lowenstein, J. M. (1972). Ammonia production in muscle and other tissues: the purine nucleotide cycle. *Physiol. Rev.* **52**, 382–414.

Ludewig, U., Von Wiren, N. and Frommer, W. B. (2002). Uniport of NH_4^+ by the root hair plasma membrane ammonium transporter LeAMT1;1. *J. Biol. Chem.* **277**, 13548–13555.

Lupo, D., Li, X.-D., Durand, A., Tomizaki, T., Cherif-Zahar, B., Matassi, G., Merrick, M. and Winkler, F. K. (2007). The 1.3-A resolution structure of *Nitrosomonas europaea* Rh50 and mechanistic implications for NH_3 transport by Rhesus family proteins. *Proc. Natl. Acad. Sci. U. S. A.* **104**, 19303–19308.

Mackay, A. J., Amador, M., Diaz, A., Smith, J. and Barrera, R. (2009). Dynamics of *Aedes aegypti* and *Culex quinquefasciatus* in Septic Tanks. *J. Am. Mosq. Control Assoc.* **25**, 409–416.

Maiuolo, J., Oppedisano, F., Gratteri, S., Muscoli, C. and Mollace, V. (2016). Regulation of uric

acid metabolism and excretion. *Int. J. Cardiol.* **213**, 8–14.

Marcaggi, P. and Coles, J. A. (2001). Ammonium in nervous tissue: transport across cell membranes, fluxes from neurons to glial cells, and role in signalling. *Prog. Neurobiol.* **64**, 157–183.

Marini, A. M., Vissers, S., Urrestarazu, A. and Andre, B. (1994). Cloning and expression of the MEP1 gene encoding an ammonium transporter in *Saccharomyces cerevisiae*. *Embo J* **13**, 3456–3463.

Marini, A. M., Soussi-Boudekou, S., Vissers, S. and Andre, B. (1997a). A family of ammonium transporters in *Saccharomyces cerevisiae*. *Mol. Cell. Biol.* **17**, 4282–93.

Marini, A.-M., Urrestarazu, A., Beauwens, R. and André, B. (1997b). The Rh (Rhesus) blood group polypeptides are related to NH_4^+ transporters. *Trends Biochem. Sci.* **22**, 460–461.

Marini, a M., Matassi, G., Raynal, V., André, B., Cartron, J. P. and Chérif-Zahar, B. (2000). The human Rhesus-associated RhAG protein and a kidney homologue promote ammonium transport in yeast. *Nat. Genet.* **26**, 341–344.

Martinelle, K. and Häggström, L. (1993). Mechanisms of ammonia and ammonium ion toxicity in animal cells: Transport across cell membranes. *J. Biotechnol.* **30**, 339–350.

Matthews, B. J., Dudchenko, O., Kingan, S. B., Koren, S., Antoshechkin, I., Crawford, J. E., Glassford, W. J., Herre, M., Redmond, S. N., Rose, N. H., et al. (2018). Improved reference genome of *Aedes aegypti* informs arbovirus vector control. *Nature* **563**, 501–507.

McDonald, T. R. and Ward, J. M. (2016). Evolution of electrogenic ammonium transporters (AMTs). *Front. Plant Sci.* **7**, 1–9.

McDonald, M. D., Smith, C. P. and Walsh, P. J. (2006). The physiology and evolution of urea transport in fishes. *J. Membr. Biol.* **212**, 93–107.

McDonald, T. R., Dietrich, F. S. and Lutzoni, F. (2012). Multiple horizontal gene transfers of ammonium transporters/ammonia permeases from prokaryotes to eukaryotes: Toward a new functional and evolutionary classification. *Mol. Biol. Evol.* **29**, 51–60.

Menuz, K., Larter, N. K., Park, J. and Carlson, J. R. (2014). An RNA-Seq screen of the *Drosophila* antenna identifies a transporter necessary for ammonia detection. *PLoS Genet.* **10**,.

Meredith, J. and Phillips, J. E. (1973). Rectal ultrastructure in salt- and freshwater mosquito larvae in relation to physiological state. *Zeitschrift fur Zellforsch. und mikroskopische Anat.* **138**, 1–22.

Merrick, M. J. and Edwards, R. A. (1995). Nitrogen control in bacteria. *Microbiol. Rev.* **59**, 604–622.

Miflin, B. J. and Lea, P. J. (1976). The pathway of nitrogen assimilation in plants. *Phytochemistry* **15**, 873–885.

Morton, A. G. and Macmillan, A. (1954). The assimilation of nitrogen from ammonium salts and nitrate by fungi. *J. Exp. Bot.* **5**, 232–252.

Mudry, B., Guy, R. H. and Delgado-Charro, M. B. (2006). Transport numbers in transdermal iontophoresis. *Biophys. J.* **90**, 2822–2830.

Needham, J. (1935). Problems of nitrogen catabolism in invertebrates. *Biochem. J.* **29**, 238–251.

Nelson, M. J. (1986). *Aedes aegypti*: biology and ecology. *Pan Am. Heal. Organ.* 1–56.

Neuhäuser, B. and Ludewig, U. (2014). Uncoupling of ionic currents from substrate transport in the plant ammonium transporter AtAMT1;2. *J. Biol. Chem.* **289**, 11650–11655.

Neuhäuser, B., Dynowski, M. and Ludewig, U. (2014). Switching substrate specificity of AMT/MEP/ Rh proteins. *Channels* **8**, 496–502.

Ninnemann, O., Jauniaux, J. C. and Frommer, W. B. (1994). Identification of a high affinity NH_4^+ transporter from plants. *EMBO J.* **13**, 3464–3471.

O'Donnell, M. J. and Donini, A. (2017). Nitrogen excretion and metabolism in insects. In *Acid-Base Balance and Nitrogen Excretion in Invertebrates* (ed. Weihrauch, D.) and O'Donnell, M. J.), pp. 109–126. Springer International Publishing Switzerland.

Orlowski, J. and Grinstein, S. (2004). Diversity of the mammalian sodium/proton exchanger SLC9 gene family. *Pflugers Arch. Eur. J. Physiol.* **447**, 549–565.

Pate, J. S. (1973). Uptake, assimilation and transport of nitrogen compounds by plants. *Soil Biol. Biochem.* **5**, 109–119.

Patrick, M. L., Gonzalez, R. J., Wood, C. M., Wilson, R. W., Bradley, T. J. and Val, A. L. (2002). The characterization of ion regulation in amazonian mosquito larvae: Evidence of phenotypic plasticity, population-based disparity, and novel mechanisms of ion uptake. *Physiol. Biochem. Zool.* **75**, 223–236.

Peng, J. and Huang, C. H. (2006). Rh proteins vs Amt proteins: an organismal and phylogenetic perspective on CO_2 and NH_3 gas channels. *Transfus. Clin. Biol.* **13**, 85–94.

Pennington, J. E., Goldstrohm, D. A. and Wells, M. A. (2003). The role of haemolymph proline as a nitrogen sink during blood meal digestion by the mosquito *Aedes aegypti*. *J. Insect Physiol.* **49**, 115–121.

Pitts, R. J., Derryberry, S. L., Pulous, F. E. and Zwiebel, L. J. (2014). Antennal-expressed ammonium transporters in the malaria vector mosquito *Anopheles gambiae*. *PLoS One* **9**,.

Post, R. L. and Jolly, P. C. (1957). The linkage of sodium, potassium, and ammonium active transport across the human erythrocyte membrane. *Biochim. Biophys. Acta* **25**, 118–128.

Quijada-Rodriguez, A. R., Treberg, J. R. and Weihrauch, D. (2015). Mechanism of ammonia excretion in the freshwater leech *Nephelopsis obscura*: characterization of a primitive Rh protein and effects of high environmental ammonia. *Am. J. Physiol. Regul. Integr. Comp. Physiol.* ajpregu.00482.2014.

Ramsay, J. A. (1950). Osmotic regulation in mosquito larvae. *J. Exp. Biol.* **27**, 145.

Ramsay, J. A. (1951). Osmotic regulation in mosquito larvae: the role of the Malpighian tubules. *J. Exp. Biol.* **28**, 62–73.

Randall, D. J. and Ip, Y. K. (2006). Ammonia as a respiratory gas in water and air-breathing fishes. *Respir. Physiol. Neurobiol.* **154**, 216–225.

Regnault, M. (1987). Nitrogen excretion in marine and fresh-water crustacea. *Biol. Rev.* **62**, 1–24.

Ritchie, R. J. and Gibson, J. (1987). Permeability of ammonia and amines in *Rhodobacter sphaeroides* and *Bacillus firmus*. *Arch. Biochem. Biophys.* **258**, 332–341.

Sanz-Luque, E., Chamizo-Ampudia, A., Llamas, A., Galvan, A. and Fernandez, E. (2015). Understanding nitrate assimilation and its regulation in microalgae. *Front. Plant Sci.* **6**,.

Scaraffia, P. Y., Isoe, J., Murillo, A. and Wells, M. A. (2005). Ammonia metabolism in *Aedes aegypti*. *Insect Biochem. Mol. Biol.* **35**, 491–503.

Scaraffia, P. Y., Zhang, Q., Wysocki, V. H., Isoe, J. and Wells, M. A. (2006). Analysis of whole body ammonia metabolism in *Aedes aegypti* using [15N]-labeled compounds and mass spectrometry. *Insect Biochem. Mol. Biol.* **36**, 614–622.

Seibel, B. A., Goffredi, S. K., Thuesen, E. V., Childress, J. J. and Robison, B. H. (2004). Ammonium content and buoyancy in midwater cephalopods. *J. Exp. Mar. Bio. Ecol.* **313**, 375–387.

Shih, T.-H., Horng, J.-L., Lai, Y.-T. and Lin, L.-Y. (2013). Rhcg1 and Rhbg mediate ammonia excretion by ionocytes and keratinocytes in the skin of zebrafish larvae: H^+-ATPase-linked active ammonia excretion by ionocytes. *Am. J. Physiol. Integr. Comp. Physiol.* **304**, R1130–R1138.

Singh, S. K., Binder, H. J., Geibel, J. P. and Boron, W. F. (1995). An apical permeability barrier to NH_3/NH_4^+ in isolated, perfused colonic crypts. *Proc. Natl. Acad. Sci.* **92**, 11573–11577.

Skou, J. C. (1965). Enzymatic Basis for Active Transport of Na^+ and K^+ Across Cell Membrane. *Physiol. Rev.* **45**, 596–618.

Smith, H. W. (1936). The retention and physiological role of urea in the Elasmobranchii. *Biol. Rev.* **11**, 49–82.

Sohal, R. S. and Copeland, E. (1966). Ultrastructural variations in the anal papillae of *Aedes aegypti* (L.) at different environment salinities. *J Insect Physiol* **12**, 429–434.

Somers, G., Brown, J. E., Barrera, R. and Powell, J. R. (2011). Genetics and morphology of *Aedes*

aegypti (Diptera: Culicidae) in septic tanks in Puerto Rico. *J. Med. Entomol.* **48**, 1095–1102.

Soupene, E., He, L., Yan, D. and Kustu, S. (1998). Ammonia acquisition in enteric bacteria: physiological role of the ammonium/methylammonium transport B (AmtB) protein. *Proc. Natl. Acad. Sci. U. S. A.* **95**, 7030–4.

Soupene, E., Chu, T., Corbin, R. W., Hunt, D. F. and Kustu, S. (2002). Gas channels for NH_3: Proteins from hyperthermophiles complement an *Escherichia coli* mutant. *J. Bacteriol.* **184**, 3396–3400.

Speeg, K. V and Campbell, J. W. (1968). Formation and volatilization of ammonia gas by terrestrial snails. *Am. J. Physiol.* **214**, 1392–1402.

Terrado, R., Monier, A., Edgar, R. and Lovejoy, C. (2015). Diversity of nitrogen assimilation pathways among microbial photosynthetic eukaryotes. *J. Phycol.* **51**, 490–506.

Tillinghast, E. K. (1967). Excretory pathways of ammonia and urea in the earthworm *Lumbricus terrestris* L. *J. Exp. Zool.* **166**, 295–300.

Towle, D. W. and Holleland, T. (1987). Ammonium ion substitutes for K^+ in ATP-dependent Na^+ transport by basolateral membrane vesicles. *Am. J. Physiol. Integr. Comp. Physiol.* **252**, R479–R489.

Weihrauch, D. (2006). Active ammonia absorption in the midgut of the Tobacco hornworm *Manduca sexta* L.: Transport studies and mRNA expression analysis of a Rhesus-like ammonia transporter. *Insect Biochem. Mol. Biol.* **36**, 808–821.

Weihrauch, D. and O'Donnell, M. J. (2015). Links between osmoregulation and nitrogen-excretion in insects and crustaceans. *Integr. Comp. Biol.* **55**, 816–829.

Weihrauch, D., Becker, W., Postel, U., Luck-Kopp, S. and Siebers, D. (1999). Potential of active excretion of ammonia in three different haline species of crabs. *J. Comp. Physiol. B* **169**, 25–37.

Weihrauch, D., Ziegler, A., Siebers, D. and Towle, D. W. (2002). Active ammonia excretion across the gills of the green shore crab *Carcinus maenas*: participation of Na(+)/K(+)-ATPase, V-type

H(+)-ATPase and functional microtubules. *J. Exp. Biol.* **205**, 2765–2775.

Weihrauch, D., Morris, S. and Towle, D. W. (2004). Ammonia excretion in aquatic and terrestrial crabs. *J. Exp. Biol.* **207**, 4491–4504.

Weihrauch, D., Wilkie, M. P. and Walsh, P. J. (2009). Ammonia and urea transporters in gills of fish and aquatic crustaceans. *J. Exp. Biol.* **212**, 1716–1730.

Weihrauch, D., Donini, A. and O'Donnell, M. J. (2012a). Ammonia transport by terrestrial and aquatic insects. *J. Insect Physiol.* **58**, 473–487.

Weihrauch, D., Chan, a. C., Meyer, H., Doring, C., Sourial, M. and O'Donnell, M. J. (2012b). Ammonia excretion in the freshwater planarian *Schmidtea mediterranea*. *J. Exp. Biol.* **215**, 3242–3253.

Weiner, I. D. and Hamm, L. L. (2007). Molecular mechanisms of renal ammonia transport. *Annu. Rev. Physiol.* **69**, 317–340.

Weiner, I. D. and Verlander, J. W. (2014). Ammonia transport in the kidney by Rhesus glycoproteins. *Am. J. Physiol. Renal Physiol.* **306**, F1107–F1120.

Wieczorek, H., Beyenbach, K. W., Huss, M. and Vitavska, O. (2009). Vacuolar-type proton pumps in insect epithelia. *J. Exp. Biol.* **212**, 1611–1619.

Wigglesworth, V. B. (1932). The function of the anal gills of the mosquito larva. *J. Exp. Biol.* **10**, 16–26.

Wilkie, M. P. (1997). Mechanisms of ammonia excretion across fish gills. *Comp. Biochem. Physiol. Part A Physiol.* **118**, 39–50.

Wilkie, M. P. (2002). Ammonia excretion and urea handling by fish gills: Present understanding and future research challenges. *J. Exp. Zool.* **293**, 284–301.

Wilson, J. M., Moreira-Silva, J., Delgado, I. L. S., Ebanks, S. C., Vijayan, M. M., Coimbra, J. and Grosell, M. (2013). Mechanisms of transepithelial ammonia excretion and luminal alkalinization in the gut of an intestinal air-breathing fish, *Misgurnus anguilliacaudatus*. *J. Exp.*

Biol. **216**, 623–632.

Wood, C., Part, P. and Wright, P. (1995a). Ammonia and urea metabolism in relation to gill function and acid-base balance in a marine elasmobranch, the spiny dogfish (*Squalus acanthias*). *J. Exp. Biol.* **198**, 1545–58.

Wood, C. F., Part, P. and Wright, P. A. (1995b). Ammonia and urea metabolism in relation to gill function and acid-base balance in a marine elasmobranch, the spiny dogfish (Squalus acanthias). *J. Exp. Biol.* **198**, 1545–1558.

Wright, P. (1995). Nitrogen excretion : Three end products , many physiological roles. *J. Exp. Biol.* **281**, 273–281.

Wright, P. A. and Wood, C. M. (2009). A new paradigm for ammonia excretion in aquatic animals: role of Rhesus (Rh) glycoproteins. *J. Exp. Biol.* **212**, 2303–12.

Wu, Y., Zheng, X., Zhang, M., He, A., Li, Z. and Zhan, X. (2010). Cloning and functional expression of Rh50-like glycoprotein, a putative ammonia channel, in *Aedes albopictus* mosquitoes. *J. Insect Physiol.* **56**, 1599–1610.

Zachos, N. C., Tse, M. and Donowitz, M. (2005). Molecular physiology of intestinal Na^+/H^+ exchange. *Annu. Rev. Physiol.*

Zheng, L., Kostrewa, D., Bernèche, S., Winkler, F. K. and Li, X.-D. (2004). The mechanism of ammonia transport based on the crystal structure of AmtB of *Escherichia coli*. *Proc. Natl. Acad. Sci. U. S. A.* **101**, 17090–5.

Chapter Two

Aedes aegypti Rhesus glycoproteins contribute to ammonia excretion by larval anal papillae

This chapter has been published and reproduced with permission:

Durant A.C., Chasiotis H., Misyura L., Donini A. (2017) *Aedes aegypti* Rhesus glycoproteins contribute to ammonia excretion by larval anal papillae. *Journal of Experimental Biology* 220:588-596.

2.1 Summary

In larval *Aedes aegypti*, transcripts of the Rhesus-like glycoproteins *AeRh50-1* and *AeRh50-2* have been detected in the anal papillae, sites of ammonia (NH_3/NH_4^+) excretion; however, these putative ammonia transporters have not been previously localized or functionally characterized. In this study we show that the AeRh50s co-immunolocalize with apical V-type H^+ ATPase as well as with basal Na^+/K^+ ATPase in the epithelium of anal papillae. The double-stranded RNA mediated knockdown of *AeRh50-1* and *AeRh50-2* resulted in a significant reduction in AeRh50 protein abundance in the anal papillae and this was coupled to decreased ammonia excretion. The knockdown of *AeRh50-1* resulted in decreased haemolymph [NH_4^+] and pH whereas knockdown of *AeRh50-2* had no effect on these parameters. We conclude that the AeRh50s are important contributors to ammonia excretion at the anal papillae of larval *Aedes aegypti*, which may be the basis for their ability to inhabit areas with high ammonia levels.

2.2 Introduction

In animals, ammonia (NH_3/NH_4^+) as a byproduct of protein metabolism is toxic when concentrated in cells and tissues and must be readily excreted. For microorganisms and plants, ammonia is an important nutrient that serves as a source of nitrogen for synthesis of various metabolites, such as amino acids. Ammonia is present in physiological solutions predominantly in the ionic form, NH_4^+ (pKa of ~9.5), but a certain portion of the gaseous form, NH_3, is always present and can readily diffuse across plasma membranes (Weihrauch et al., 2012a). As a consequence, ammonia levels in animals must be tightly regulated and this regulation is achieved by various ammonia transporting proteins and mechanisms.

Almost all prokaryotes and eukaryotes possess ammonia transporting mechanisms. The ammonia transporters (Amt) family in plants and bacteria and the methylammonium/ammonia permeases (MEP) in yeast function to facilitate the uptake of ammonia. Analogs of the Mep/Amt family are present in vertebrates, the Rhesus-like glycoproteins (Rh proteins), and these transporters function in the movement of ammonia across cell membranes and its excretion from the body. The Rh proteins are glycosylated, comprising a group of Rh-50 proteins (having a molecular weight of ~50 kDa). The crystallographic structure of the trimeric mammalian RhCG predicts the transport of NH_3 over NH_4^+ (Gruswitz et al., 2010), presumably owing to the presence of two highly conserved histidine residues that were shown to be important for function similar to that of bacterial AmtB (see below; Conroy et al., 2005). Furthermore, Rh proteins are proposed to be CO_2 gas channels in addition to transporting ammonia (Li *et al*., 2007; Lupo *et al.,* 2007). Evidence of CO_2 transport by Rh proteins has been shown in human erythrocytes (Endeward et al., 2006), zebrafish (Perry et al., 2010), and green algae (Soupene et al., 2002; Soupene et al., 2004).

The crystal structure of AmtB in *Escherichia coli* indicates that the trimeric structure has a hydrophobic pore located at the center of each monomer, with an NH_4^+ binding site at the entry of each pore (Zheng *et al.,* 2004). Two highly conserved histidine residues bridged by a hydrogen bond within the pore were thought to facilitate the deprotonation of ammonium as it enters the hydrophobic pore followed by protonation on the cytoplasmic side, indicating that these transporters function as ammonia gas channels but transport net NH_4^+. This assures selectivity for ammonia transport against all other ions (i.e. similarly sized K^+ ions), and also eliminates any leak of proton motive force during conduction through the pore (Khademi et al., 2004). The Rh-50 proteins also recruit NH_4^+; however, after deprotonation, it is suggested that the proton is recycled back to the extracellular side resulting in net NH_3 transport (Baday et al., 2015). Much remains to be resolved regarding the substrate specificity of Rh-50 proteins and ammonia transporters, as well as tissue specific regulation of each.

Invertebrates possess both Amt and Rh-50 proteins, whereas vertebrate animals possess only Rh-50 proteins (Kutsu and Inwood, 2006). In the mosquito *Aedes aegypti*, three putative ammonia transporters, *AeRh50-1*, *AeRh50-2*, and *AeAmt1*, were identified *in silico* (Weihrauch et al., 2012b) and the *AeAmt1* was characterized *in vivo* (Chasiotis et al., 2016). The *AeRh50-1* and *AeRh50-2* genes share sequence similarity with other invertebrate and vertebrate Rh-50s, and the Amt/Mep-like *AeAmt1* is most similar to the bacterial *AmtB* (Chasiotis et al., 2016). The transcripts of *AeRh50-1*, *AeRh50-2*, and *AeAmt1* were detected in the anal papillae of *A. aegypti* larvae, and a mechanism for ammonia excretion from the anal papillae involving the AeAmt1 was investigated (Chasiotis et al., 2016). The anal papillae are finger-like structures composed of a single layered syncytial epithelium which is externally covered by a thin cuticle (Credland, 1976). The lumen of the anal papillae is continuous with the hemocoel of the body and the papillae are major sites of ammonia excretion in larval *A. aegypti* (Sohal and Copeland, 1966; Donini and O'Donnell, 2005). The AeAmt1 was localized to the basal membrane of the syncytial epithelium where it was proposed to mediate NH_4^+ entry into the cytosol driven by an

electrical potential generated by the basal Na^+/K^+-ATPase (NKA) (Chasiotis et al., 2016). Although not yet localized in the anal papillae, the transcript expression of AeRh50s in the anal papillae suggests that these transporters may also be important in both ammonia entry from the haemolymph into the cytosol, and excretion into the surrounding environment (Chasiotis et al., 2016).

An understanding of how the larvae of *A. aegypti* excrete ammonia is of particular importance in light of the discovery that ammonia rich septic tanks in the Caribbean serve as a refuge for resting and breeding adult *A. aegypti*, as well as an aquatic habitat for larval development and adult emergence (Burke et al., 2010). Consequently, the significant number of larval and adult *A. aegypti* present in septic tanks was thought to explain the persistence of dengue transmission during the dry season (Burke et al., 2010). In tropical Asia another *Aedine* species, *Aedes albopictus*, was found to breed in septic tanks containing raw sewage with free ammonia levels as high as 116 mg/L (~6 mmol l^{-1}) (Lam and Dharmaraj, 1982).Given that the average ammonia levels in partially treated septic tank effluent in the United States were measured between 31-65 mg/L (Canter and Knox, 1985; Cagle and Johnson, 1994), another important consideration is the increase in anthropogenic nitrogen from septic tank effluent in ground water and other freshwater habitats where *A. aegypti* normally breed. Accumulation of nitrogen in natural waters has previously been documented (Drake and Bauder, 2005; Heatwole and McCray, 2007), and could have a significant ecological impact on the distribution and habitat availability of *A. aegypti* particularly in regions with high septic tank usage.

This study aimed to elucidate the involvement of *AeRh50-1* and *AeRh50-2* in ammonia excretion by the anal papillae. We hypothesized that at least one, if not both transporters play an important role in the excretion of ammonia at the anal papillae, and potentially the regulation of ammonia haemo-lymph levels as was shown for the basally expressed AeAmt1. dsRNA-mediated *AeRh50* knockdown was employed and changes in ammonia efflux at the anal papillae as well as haemolymph ammonia and H^+ levels were examined.

2.3 Materials and Methods

Animals

Larvae of *A. aegypti* (Liverpool) were obtained from a colony reared in the Department of Biology, York University (Toronto, ON, Canada). Larvae were reared in reverse-osmosis (RO) water at room temperature on a 12 h:12 h light:dark cycle. Larvae were fed daily with a solution of liver powder and yeast in water. Rearing water was refreshed every other day. Fourth instar larvae were used 24 h post-feeding for physiological and molecular studies.

Western Blotting

Biological samples consisting of pooled anal papillae that were isolated from 30-50 larvae under saline were collected and stored at -80°C until later processing. For examination of AeRh50 expression, samples were thawed on ice and sonicated for 2 x 10s at 5W using an XL 2000 Ultrasonic Processor (Qsonica) in a homogenization buffer containing 50 mmol l^{-1} Tris-HCl, pH 7.5, 150 mmol l^{-1} NaCl, 1% sodium deoxycholate, 1% Triton-X-100, 0.1% SDS, 1 mmol l^{-1} phenylmethylsulfonyl fluoride (PMSF) and 1:200 protease inhibitor cocktail (Sigma-Aldrich). Homogenates were then centrifuged at 10,000***g*** for 10 min at 4°C, and protein content of the collected supernatants was determined using the Bradford assay (Sigma-Aldrich) according to the manufacturer's guidelines. Samples were prepared for SDS-PAGE by heating for 5 min at 100°C in a 6x loading buffer containing 360 mmol l^{-1} Tris-HCl (pH 6.8), 12% (w/v) SDS, 30% glycerol, 600 mmol l^{-1} DTT and 0.03% (w/v) bromophenol blue. Samples were then electrophoretically separated by SDS-PAGE and Western blot analysis of AeRh50 was conducted according to procedures outlined by Chasiotis and Kelly (Chasiotis and Kelly, 2008). A custom-synthesized polyclonal antibody (1:2000 dilution) was raised in rabbit against the epitope HHKDDAYWETPAES corresponding to a 14-amino acid region of AeRh50-1 (GenScript USA Inc., Piscataway, New Jersey, USA). A cysteine was added to the C terminal histidine to facilitate conjugation with keyhole limpet hemocyanin (KLH) which is used as a carrier protein. AeRh50-2

contains a similar sequence, HHKDDVCWETPVEL thus the antibody is expected to detect both AeRh50-1 and AeRh50-2. To confirm the specificity of the antibody for AeRh50s a comparison blot was also run with the AeRh50 antibody pre-absorbed with 5x molar excess of the immunogenic peptide for 1 h at room temperature prior to applying to blots. After examination of AeRh50 expression, blots were stripped and re-probed with a 1:1000 dilution of rabbit monoclonal anti-GAPDH (Product code: 14C10) antibody (New England BioLabs, Whitby, Ontario, Canada) as loading controls. Densitometric analysis of AeRh50 and GAPDH was conducted using ImageJ 1.50i software (National Institutes of Health, USA). AeRh50 abundance was expressed as a normalized value relative to the abundance of GAPDH.

Immunohistochemistry

Immunolocalization of AeRh50, NKA and V-type H^+ ATPase (VA) in paraffin-embedded sections of anal papillae that were mounted on slides was conducted according to procedures outlined by Chasiotis and Kelly (Chasiotis et al, 2008) using a 1:40 dilution of the anti-AeRh50 antibody described above, a 1:10 dilution of a mouse monoclonal anti-α5 antibody for NKA (Douglas Fambrough, Developmental Studies Hybridoma Bank, IA, USA) or a 1:100 dilution of a mouse polyclonal anti-ATP6V0A1 antibody for VA (Abnova, Taipei, Taiwan). A sheep anti-mouse antibody conjugated to Cy2 (Jackson Immunoresearch Laboratories, West Grove, PA, USA) at a dilution of 1:500 was used to visualize both NKA and VA. A goat anti-rabbit antibody conjugated to Alexa Fluor 594 (Jackson Immunoresearch) at a dilution of 1:500 was applied to visualize AeRh50. Comparison control slides were also processed as described above with the AeRh50 antibody pre-absorbed with 10x molar excess of the immunogenic peptide for 30 min at room temperature prior to application to the slides with anal papillae sections. Stained sections on slides were preserved using ProLong Gold antifade reagent with DAPI (Life Technologies, Burlington, ON, Canada), and images of sections were captured using an Olympus IX71 inverted fluorescent microscope (Olympus Canada, Richmond Hill, ON, Canada) with

CellSense® 1.12 Digital Imaging software (Olympus Canada), and merged using Adobe Photoshop CS6 software (Adobe Systems Inc, Ottawa, ON, Canada).

dsRNA synthesis, delivery to larvae, and reverse-transcription PCR (RT-PCR)

dsRNA was prepared according to a previously established protocol (Chasiotis et al., 2016). Briefly, RNA was extracted from whole bodies of fourth instar *A. aegypti larvae*. cDNA was synthesized using the iScript™ cDNA Synthesis Kit (Bio-Rad, Mississauga, ON, Canada) and a fragment of the *AeRh50-1* (989 bp) and *AeRh50-2* (947 bp) genes were amplified by RT-PCR using primers (forward 5′ TTCACGGATTACTCAAAGGATC 3′; reverse 5′ CATAGATGGCGGAGAATAGAG 3′ for *AeRh50-1*; forward 5' GTCGCTGGATAACCTAATCG 3'; reverse 5' GCATAGTCGGTGATTTCAGG 3' for *AeRh50-2*) designed based on GenBank Accession nos. AY926463.1 and AY926464.1, respectively. A fragment of *β-lactamase* (*β-lac*) was also amplified by RT-PCR from a pGEM-T-Easy vector (kind gift from J. P. Paluzzi, York University, Toronto, ON, Canada) using the following primers: forward 5′ ATTTCCGTGTCGCCCTTATTC 3′; reverse 5′ CGTTCATCCATAGTTGCCTGAC 3′. PCR products were resolved by gel electrophoresis, extracted from the gel, and concentrated using the QIAquick Gel Extraction Kit (Qiagen Sciences, Maryland, USA). PCR products were then purified using a QIAquick PCR Purification kit (Qiagen Inc., Toronto, ON, Canada) and used to generate double stranded RNA (dsRNA) by *in vitro* transcription using the Promega T7 RiboMAX Express RNAi Kit (Promega, WI, USA). Delivery of *AeRh50-1*, *AeRh50-2*, or *β-lac* dsRNA to larvae was carried out with a modified version of a previously described protocol (Chasiotis et al., 2016; Singh et al., 2013). For *AeRh50-1* dsRNA treatment, after six days post hatching, unfed (24 hours) groups of ~25-30 larvae (3rd and 4th instar) were placed in 1.5mL centrifuge tubes containing 150 µl PCR-grade water with 0.5 µg µl^{-1} dsRNA for 2 h, and then transferred into 30 ml RO water. For *AeRh50-2* dsRNA treatment, after two days post hatching, unfed (24 hours) groups of ~50 larvae (1st and 2nd instar) were placed in 1.5mL centrifuge tubes containing 150 µl PCR-grade water with 0.5 µg

μl^{-1} dsRNA for 2 h and then transferred into 30 ml RO water. Normally 1st and 2nd instar larvae are exposed to dsRNA as outlined for *AeRh50-2*; however, knockdown of *AeRh50-1* was relatively short-lived necessitating exposure of larger 3rd and 4th instar larvae. Ingestion of the dsRNA solution in the 2 h soaking period was previously confirmed (Chasiotis et al., 2016; Singh et al., 2013). Rearing water was refreshed every 2 days following dsRNA treatment. Reductions in AeRh50 in anal papillae as a result of dsRNA treatment were examined by western blotting three days post *AeRh50-1* dsRNA treatment and six days post *AeRh50-2* dsRNA treatment (see above).

Scanning Ion-selective Electrode Technique

The scanning ion-selective electrode technique (SIET) system used in this study has been previously described (Donini and O'Donnell, 2005; Nguyen and Donini, 2010; Chasiotis et al., 2016). NH_4^+ microelectrodes were made (see below) and calibrated in solutions of 0.1, 1 and 10 mmol l^{-1} NH_4Cl. Larvae were mounted in a petri dish using beeswax, leaving the anal papillae exposed for measurements. Voltage gradients adjacent to the papillae were recorded in 0.5 mmol l^{-1} NH_4Cl. The recording protocol utilized was previously described (Chasiotis et al., 2016). Readings were taken along the middle portion to the most distal portion of the anal papillae at 5 target sites equally spaced apart. The voltage gradients obtained from the ASET software program were first converted into concentration gradients and then the concentration gradients were used to calculate the flux as outlined previously (see Chasiotis et al., 2016).

Haemolymph NH_4^+ and pH levels, and larval mortality

Haemolymph droplets were collected from larvae by making a small tear in the cuticle under paraffin oil (Sigma-Aldrich, Oakville, Canada). Levels of NH_4^+ and H^+ in collected droplets were measured using ion-selective microelectrodes as previously described (Jonusaite et al., 2011; Chasiotis et al., 2016). NH_4^+ microelectrodes were backfilled with 100 mmol l^{-1} NH_4Cl and front filled with NH_4^+ Ionophore I, Cocktail A. NH_4^+ microelectrodes were calibrated in solutions of 0.1, 1 and 10 mmol l^{-1}

NH_4Cl. H^+ microelectrodes were backfilled with 100 mmol l^{-1} NaCl/100 mmol l^{-1} sodium citrate (pH 6.0) and front filled with H^+ Ionophore I, Cocktail B. H^+ microelectrodes were calibrated in solutions of 200 mmol l^{-1} NaCl with 10 mmol l^{-1} HEPES at pH 6.0, pH 7.0 and pH 8.0. Larval mortality was assessed using the Kaplan-Meier method in Prism® 5.03 (GraphPad Software Inc., La Jolla, CA, USA). This method calculates the proportion of surviving larvae in both groups at any given time point.

Statistics

Data were analyzed using Prism® 5.03 (GraphPad Software Inc., La Jolla, CA, USA) and expressed as mean ± SEM. One-tailed t-tests were used to determine significance between control and experimental groups for AeRh50 monomer abundance following dsRNA treatment. Two-tailed t-tests were used to determine significance between control and experimental groups for all other parameters. For SIET data, a single biological replicate is defined as the average flux of 5 sites along a single papilla from a single larva. Statistical analysis of survival was calculated using the log-rank Mantel Cox test.

2.4 Results

AeRh50 expression and immunolocalisation in anal papillae

Western blot analysis of larval anal papillae AeRh50 protein expression revealed a putative monomer at ~50 kDa (predicted mass of AeRh50s is ~50 kDa) which was not detected when the antibody was pre-absorbed with the immunogenic peptide (Fig. 2-1). In addition, two non-specific bands between 63-75 kDa appeared which remained on blots probed with pre-absorbed antibody. The ~50 kDa band was used to quantify changes in AeRh50 protein abundance for dsRNA-treatment experiments.

In paraffin-embedded sections of anal papillae, AeRh50s were found to co-immunolocalise with NKA on the basal side, as well as with VA on the apical side of the epithelium (Fig. 2-2). In some

regions of the epithelium, AeRh50 immunoreactivity is observed on the outermost region of the apical membrane where the V_0 subunit is apparently absent (Fig. 2-2K,L). In control sections, immunostaining was not detected when probed with AeRh50 antibody that was pre-absorbed with the immunogenic peptide (not shown).

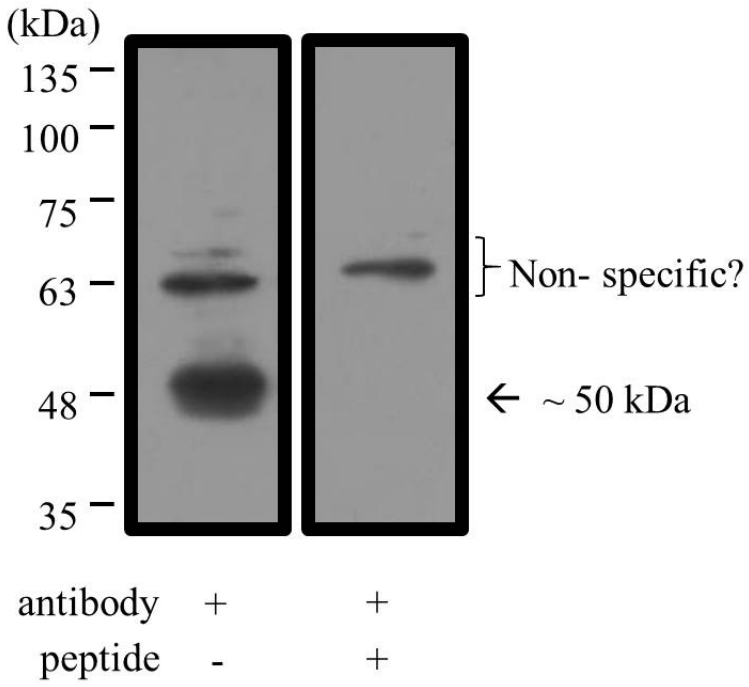

Figure 2- 1. AeRh50 expression in anal papillae of larval *Aedes aegypti*. Representative Western blot of larval anal papillae protein homogenates probed with AeRh50 antisera reveals an AeRh50 monomer at ~50 kDa (predicted mass 49.7 kDa for AeRh50-1 and 49.9 for AeRh50-2) and two non-specific bands at ~66 and 70 kDa which were not blocked by antibody pre-absorption with the immunogenic peptide.

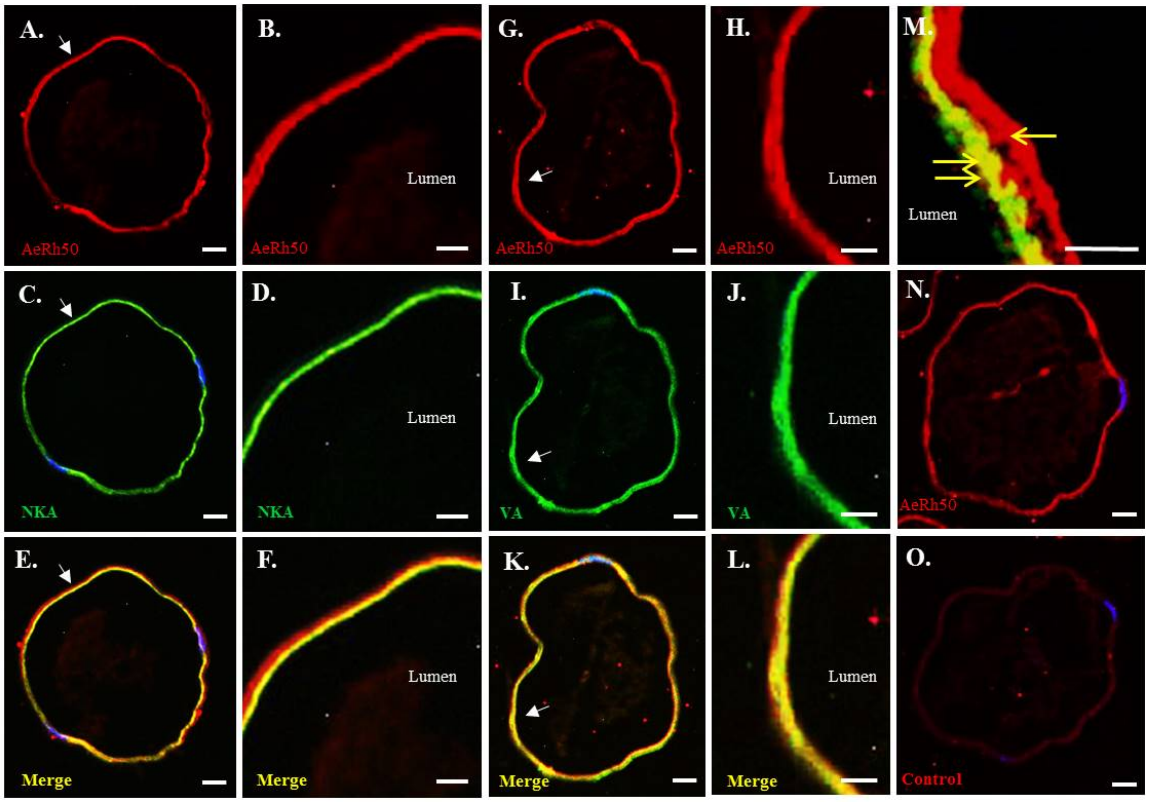

Figure 2- 2. Immunolocalisation of AeRh50 in anal papillae of larval *Aedes aegypti*. Representative paraffin-embedded sections of larval anal papillae that show immunoreactivity for: A, B, G, and H AeRh50 (red); C and D Na^+/K^+-ATPase (NKA; green); I and J V_o subunit of V-type H^+ ATPase (VA; green). E and F are merged images of A,C and B,D, respectively. K and L are merged images of G,I and H,J, respectively. nuclei were also stained with DAPI (blue). White arrows indicate areas shown at higher magnification in the panel to the immediate right. Nuclei are stained blue with DAPI. Scale bar in A., C., E., G., I., and K. = 20 µm. Scale bar in B., D., F., H., I=J., and L. = 10 µm.

dsRNA knockdown of AeRh50-1 and AeRh50-2 in the anal papillae

Protein homogenates of anal papillae from larvae treated with *AeRh50-1* dsRNA showed a significantly decreased abundance (by an apparent ~34%) of the 50 kDa band compared to the *β-Lactamase (β-Lac)* control larvae ($p = 0.04$; Fig. 2-3A,B) when sampled 3 days post dsRNA treatment. NH_4^+ fluxes from the anal papillae of *AeRh50-1* dsRNA treated larvae at 3 days post treatment were significantly lower than those recorded from anal papillae of *β-Lac* dsRNA treated larvae ($p = 0.04$; Fig. 2-3C). *AeRh50-2* dsRNA treatment resulted in a significant decrease (by an apparent ~32%) of the 50 kDa band 6 days post treatment compared with the *β-Lac* dsRNA treated larvae ($p = 0.038$) (Fig. 2-4A,B). The reduction in protein abundance of the 50 kDa band corresponds with significantly decreased NH_4^+ fluxes from the anal papillae of *AeRh50-2* dsRNA treated larvae ($p = 0.0005$) (Fig. 2-4C).

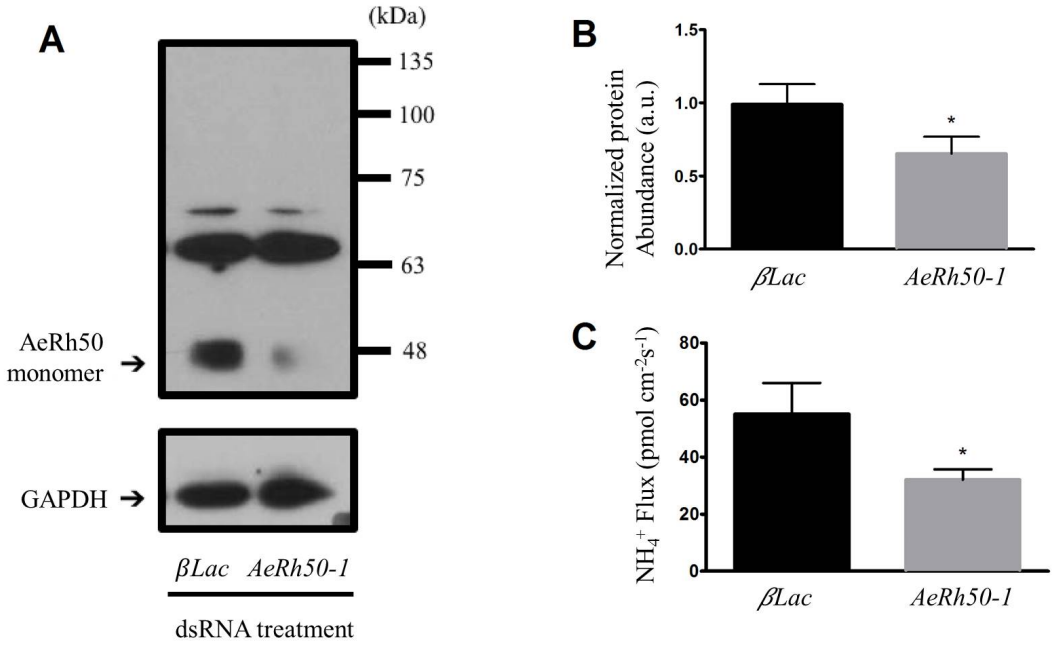

Figure 2- 3. Effects of *AeRh50-1* dsRNA treatment on AeRh50-1 abundance and NH_4^+ excretion from the anal papillae of larval *A. aegypti*. (A) Representative western blot and (B) densitometric analysis of AeRh50-1 monomer in larval anal papillae (*N=7*), and (C) scanning ion-selective electrode technique (SIET) measurements of NH_4^+ flux across the anal papillae of larvae (N=15 for control *β-Lactamase* (*β-Lac*) and N=18 for *AeRh50-1*) at 3 days following control *β-Lac* or *AeRh50-1* dsRNA treatment. AeRh50-1 monomer abundance was normalized to GAPDH and expressed relative to the *β-Lac* group. Data are expressed as means ± SEM. *; Significant difference ($P < 0.05$; two-tailed Student's t-test) from *β-Lac* group.

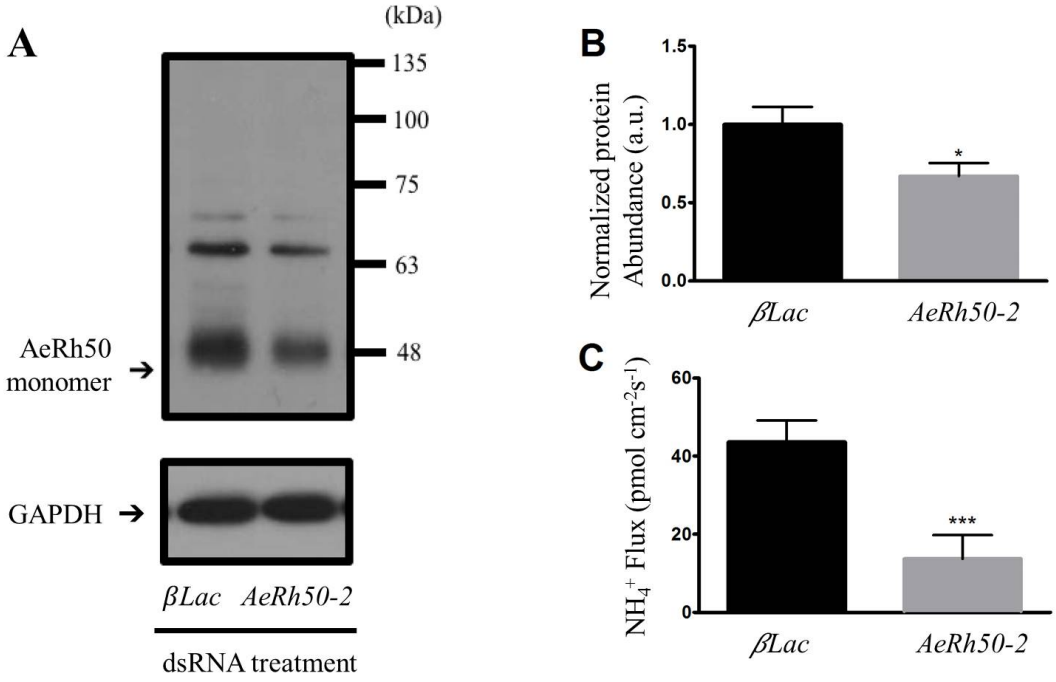

Figure 2- 4. **Effects of *AeRh50-2* dsRNA treatment on AeRh50-2 abundance and NH_4^+ excretion from the anal papillae of larval *A. aegypti*.** (A) Representative western blot and (B) densitometric analysis of AeRh50-2 monomer in larval anal papillae (*N=4*), and (C) scanning ion-selective electrode technique (SIET) measurements of NH_4^+ flux across the anal papillae of larvae (N=45 for *β-Lac* and N=44 for *AeRh50-2*) at 6 days following control *β-Lac* or *AeRh50-2* dsRNA treatment. AeRh50-2 monomer abundance was normalized to GAPDH and expressed relative to the *β-Lac* group. Data are expressed as means ± SEM. *,***; Significant difference (*P < 0.05, P < 0.001*, respectively; two-tailed Student's t-test) from *β-Lac* group.

Given the effects of AeRh50 knockdown on ammonia excretion by anal papillae, the haemolymph NH_4^+ and H^+ (pH) concentrations of the haemolymph of knockdown larvae were measured. At 3 days following *AeRh50-1* dsRNA-mediated knockdown, NH_4^+ levels in the haemolymph were significantly reduced compared to the *β-Lac* control larvae ($p = 0.019$), however, no significant change in NH_4^+ haemolymph levels were seen at 6 days post treatment with *AeRh50-2* dsRNA (Fig. 2-5A). The pH of the haemolymph was also significantly reduced at 3 days post *AeRh50-1* dsRNA treatment compared to the control group (pH= 7.93 ± 0.020 for *β-Lac* group and pH= 7.82 ± 0.015 for *AeRh50-1* group) but did not significantly differ in larvae at 6 days post treatment with *AeRh50-2* dsRNA (pH = 7.84 ± 0.105 and pH = 7.84 ± 0.078 for *β-Lac* and *AeRh50-2* groups, respectively) (Fig. 2-5B). While there was an apparent decrease in survival of larvae treated with either *AeRh50-1*- or *AeRh50-2* dsRNA, this effect was not significant ($p = 0.14$ and $p = 0.36$, respectively) (Fig. 2-6).

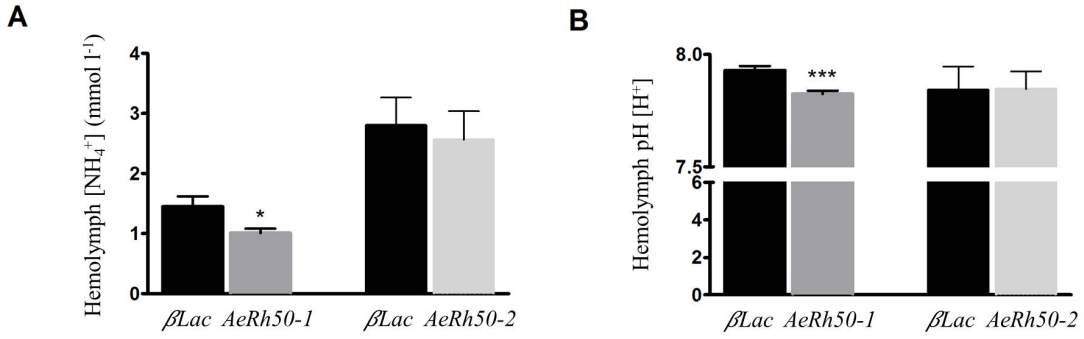

Figure 2- 5. Effects of *AeRh50-1* and *AeRh50-2* dsRNA treatment on haemolymph NH_4^+ levels and haemolymph pH of larval *A. aegypti*. (A) Ion-selective microelectrode measurements of NH_4^+ in larval haemolymph at 3 days post-*β-Lac* or *–AeRh50-1* dsRNA treatment and at 6 days post-*β-Lac* or *AeRh50-2* dsRNA treatment (N=40 for *β-Lac* and N=47 for *AeRh50-1*; N=15 for *β-Lac* and N=15 for *AeRh50-2*). (B) Ion-selective microelectrode measurements of pH of larval haemolymph at 3 days post-*β-Lac* or *–AeRh50-1* dsRNA treatment and at 6 days post-*β-Lac* or *AeRh50-2* dsRNA treatment (N=20 for *β-Lac* and N=20 for *AeRh50-1*; N=13 for *β-Lac* and N=18 for *AeRh50-2*). *,***; Significant difference ($P < 0.05$, $P < 0.001$, respectively; two-tailed Student's t-test) from *β-Lac* group.

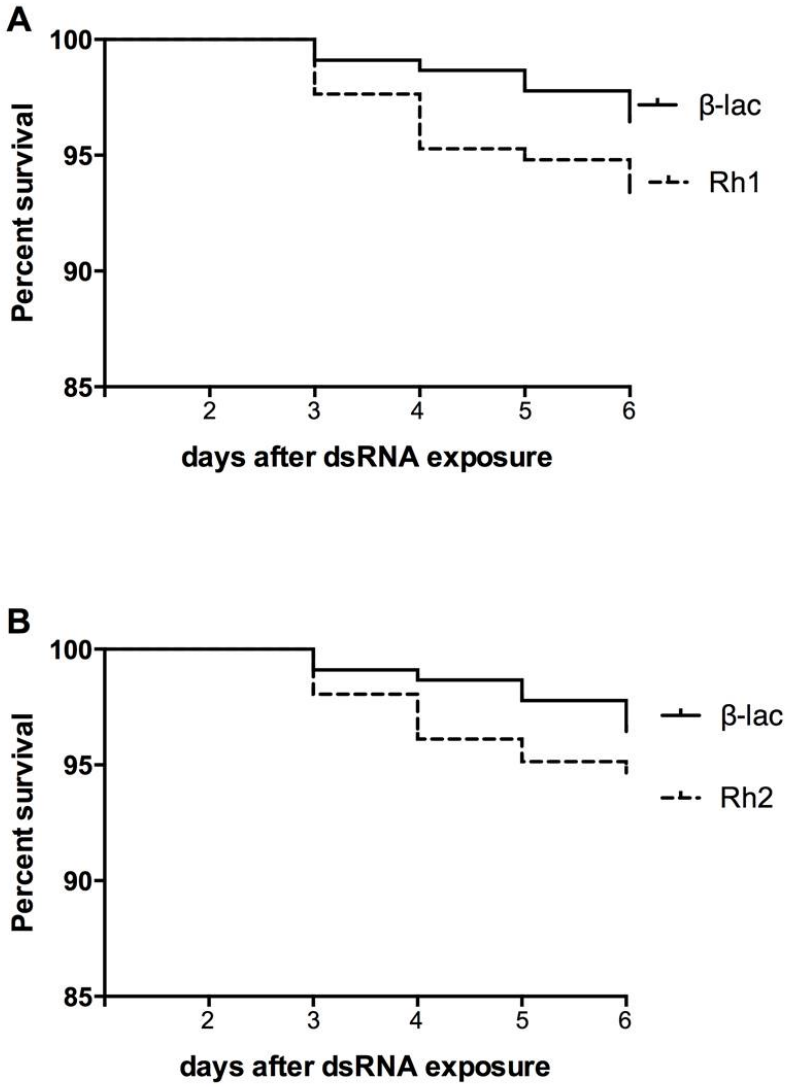

Figure 2- 6. Effects of *AeRh50-1* and *AeRh50-2* dsRNA treatment on mortality of larval *A. aegypti*. (A) Larval mortality between day 2 and day 6 following treatment with *β-Lac* or *AeRh50-1* dsRNA (N=3 groups consisting of ~60-90 larvae each, per treatment) ($p = 0.14$). (B) Larval mortality between day 2 and day 6 following treatment with *β-Lac* or *AeRh50-2* dsRNA (N=3 groups consisting of ~60-90 larvae each, per treatment) ($p = 0.35$).

2.5 Discussion

Overview

The present study demonstrates the localization of the *Aedes aegypti* AeRh50s to both the apical and basal membranes of the anal papillae epithelium. Furthermore, through dsRNA mediated knockdown of *AeRh50-1* and *AeRh50-2*, we provide evidence that the AeRh50s function to facilitate ammonia excretion by the anal papillae of larval mosquitoes. The knockdown of *AeRh50-1*, verified at the anal papillae (but not at other tissues) results in alterations of haemolymph NH_4^+ and pH.

Localization of AeRh50s in epithelium of anal papillae

Despite studies that have measured transcript expression, the localization of invertebrate Rh-50 proteins in epithelia is in its infancy. For example, one of the more completely studied Rh-50 proteins, CeRhr-1 of the nematode, can mediate ammonia transport and is expressed at the transcript level predominantly in the hypodermis where transcript abundance increases in response to high environmental ammonia (HEA), but has yet to be localized in the hypodermis (Adlimoghaddam et al., 2015; Ji et al., 2006). Similarly, a freshwater leech Rh protein, NoRhp, was shown to transport ammonia and alter transcript abundance in response to HEA; however, the protein has not been localized in tissues (Quijada-Rodriquez et al., 2015). Although we can conclude that the mosquito AeRh50s are localized on the apical and basal sides of the anal papillae epithelium it remains unclear if AeRh50-1 and AeRh50-2 are expressed on opposing membranes (apical vs basal) or within the same membranes (both apical and basal), because the antisera is expected to bind both AeRh50s. There are multiple studies of vertebrate Rh proteins that have localized these proteins to distinct sides of epithelia such as the Rhbg and Rhcg in the rat and mouse kidney (Quentin et al., 2003) and the Rhbg and Rhcg2 in the pillar cells of the pufferfish *Takifugu rubripes* (Nakada et al., 2007). It is therefore tempting to speculate that AeRh50-1 and AeRh50-2 are expressed in a mutually exclusive manner to distinct sides of the anal papillae epithelium; however, it is possible that both transporters are present and function on both

apical and basal membranes. Regardless, the protein localization of AeRh50s to the apical and basal sides of the mosquito anal papillae epithelium represents a significant step forward in the study of invertebrate Rh proteins.

Evidence that AeRh50s are involved in ammonia excretion by the anal papillae

Based on the relative transcript abundances of *AeRh50-1* and *AeRh50-2,* whereby *AeRh50-1* transcript was 10-fold greater than *AeRh50-2* (Chasiotis et al., 2016), it was postulated that AeRh50-1 would have a greater function in facilitating ammonia excretion at the anal papillae. Interestingly, dsRNA-mediated knockdown of *AeRh50-2* resulted in significantly reduced NH_4^+ efflux by 3.2-fold in comparison to a 1.7-fold reduction as a result of *AeRh50-1* dsRNA treatment (Fig. 2-4C & 2-3C, respectively). The extent of decreased protein abundance by dsRNA treatments appeared similar when considering quantification measurements of the 50 kDa band in western blots (see Figs 2-3B and 2-4B). This result suggests that, at the very least, both AeRh50s play an equally important role in ammonia excretion by the anal papillae. In fish, there are also multiple Rh protein homologs in the gills that function to facilitate ammonia excretion (Nawata et al., 2007; Nawata and Wood, 2008). The Rhcg isoforms (Rhcg1 and Rhcg2) are more abundant in the gills, kidney and skin, in contrast to *Rhbg* mRNA which is widespread throughout the body (Hung et al., 2007; Nawata et al., 2007). Although an assessment of relative transcript abundance of *AeRh50-1* and *AeRh50-2* in other tissues, as well as the specific protein localization of AeRh50-1 and AeRh50-2 of the mosquito is necessary, the expression of the two AeRh50s in the anal papillae is reminiscent of *Rhbg* and *Rhcg* in fish.

In the euryhaline crab *Carcinus maenas,* the transcript of only one Rh-protein, RhCM, has been detected and is highly expressed in the ammonia excreting gills when animals are acclimated to seawater in comparison to low expression in brackish water acclimated crabs (reviewed in Weihrauch et al., 2009). Changes in RhCM expression with increasing salinity also corresponded with increased transepithelial conductance of NH_4^+ (Spaargaren, 1990; Weihrauch et al., 2009). In mosquito anal

papillae, the AeRh50s respond with an apparent decrease in transcript abundance when larvae are exposed to HEA; however, these results were preliminary and confirmation of this result is required (see Weihrauch et al., 2012b). There are many observations from ammonia excreting tissues of freshwater animals that demonstrate varying responses between ammonia transporter transcript levels, ammonia excretion rates, and external ammonia levels. For example, HEA exposure of the fully aquatic, freshwater inhabiting African clawed frog caused a decrease in the transcript levels of *Rhbg*, VA and NKA in the dorsal and ventral skin and reduced the capacity of the skin to excrete ammonia (Cruz et al., 2013). In contrast, in the freshwater planarian *Schmidtea mediterranea*, transcript abundance of an Rh-50-like gene putatively involved in ammonia excretion increased in response to feeding where ammonia excretion rates are also increased (Weihrauch et al., 2012a). In the mangrove killifish, *Kryptolebias marmoratus*, exposure to high environmental ammonia (HEA) resulted in elevated *Rhcg2* transcript levels in the gills and elevated *Rhcg1* transcript levels in the skin (Hung et al., 2007). In the marine crab *Metacarcinus magister*, a single Rh protein, RhMM, is expressed predominantly in the gills and HEA exposure caused a doubling of RhMM expression (Martin et al., 2011). A decrease in transporter expression with increased environmental ammonia is not intuitive; regardless, as reviewed above, there are multiple examples of this scenario. In the case of larval *Aedes aegypti*, a putative decrease in AeRh50s with HEA treatment (see Weihrauch et al., 2012b) in the anal papillae may be explained as a protective mechanism against influx of ammonia through the AeRh50s under HEA conditions since it is believed that Rh-50s transport ammonia bi-directionally based on the gradient of ammonia.

Physiological studies in the unicellular green algae (Kustu and Inwood, 2006), human erythrocytes (Endeward et al., 2006), and RhAG expressed in *Xenopus* oocytes (Musa-Aziz et al., 2009) suggest that Rh-50 proteins are gas channels that also conduct CO_2. In this study, *AeRh50-1* knockdown larvae exhibited lower NH_4^+ levels and pH in the haemolymph at 3 days following dsRNA treatment (Fig. 2-5B,C). In contrast, knockdown of *AeRh50-2* had no effect on haemolymph NH_4^+ or pH (this

study) and knockdown of *AeAmt1* resulted in an increase in NH_4^+ levels of the haemolymph (Chasiotis et al., 2016). Therefore, if any of these transporters are a conduit for CO_2 it may be the AeRh50-1 since knockdown affects both haemolymph ammonia and pH. Since haemolymph parameters are a product of whole-body knockdown of these transporters these results suggest that the three transporters (AeRh50-1, AeRh50-2, AeAmt1) may be differentially expressed across tissues and/or have primarily different functions in different tissues.

Redundancies in ammonia excretion by larval mosquitoes

It is plausible to assume that other tissues besides anal papillae, and also other molecular mechanisms facilitating ammonia excretion are present in *A. aegypti*, since survival was not significantly affected by individual *AeRh50-1* and *AeRh50-2* knockdown in the anal papillae. Furthermore, larval survival was not significantly affected by individual knockdown of the basally expressed AeAmt1 in larval *Aedes aegypti* (Chasiotis et al., 2016). However, it may also be possible that a more potent dsRNA treatment causing a greater reduction in either of the AeRh50 proteins, or AeAmt1, may reveal enhanced mortality. In the case of the anal papillae the relative contributions of AeAmt1 (see Chasiotis et al., 2016) and the AeRh50s to ammonia excretion remains to be tested. Furthermore, the levels of ammonia in the haemolymph of insects in comparison to other animals demonstrate their increased tolerance to this toxic molecule (see Weihrauch et al., 2012b). For example, *Drosophila melanogaster* larvae feed and develop in media containing up to 30mM ammonia (Borash et al., 1998), and the ammonia haemolymph levels of black flies (5mM; Gordon and Bailey, 1974), *Manduca sexta* larvae (0.8mM; Weihrauch, 2006), and larval *A. aegypti* (up to ~1.5mM; Chasiotis et al., 2016) are much higher than that of fish (Wood et al., 2002), aquatic crabs (Weihrauch et al., 1999), and mammals (Cooper and Plum, 1987), where levels are no greater than 400 μM (see Weihrauch et al., 2004). Environmental ammonia levels as low as 19 μM NH_3 is lethal to crustaceans (Ostrensky et al., 1992), but remarkably, *A. aegypti* larvae exposed to 1mM NH_4Cl for 3 days not only survive, but also quickly

adjust to the high environmental ammonia conditions by increasing NH_4^+ and H^+ excretion from the anal papillae (Weihrauch et al., 2012b). Therefore it is not surprising that individual AeRh50-1, AeRh50-2 and AeAmt1 knockdown in anal papillae did not significantly affect larval survival (this study and Chasiotis et al., 2016).

Model of ammonia excretion by anal papillae

Recently, studies in mammals and fish have implicated Rh proteins in the recruitment of NH_4^+ as a substrate for net NH_3 transport (Nawata et al., 2010; Baday et al., 2015). Together with the results of this study we refine a working model of ammonia excretion by anal papillae (see Fig. 2-7) of larval *Aedes aegypti* which was first proposed in a previous study focused on AeAmt1 (Chasiotis et al., 2016). Basal expressed AeRh50s allow for NH_3 and/or potentially CO_2 (see Kutsu and Inwood, 2006; Huang, 2008) to be transported from the haemolymph into the cytosol in addition to the AeAmt1 transport of NH_4^+. A negative voltage potential within the cytosol is driven by the action of basal NKA and apical VA, which further facilitates NH_4^+ entry from the haemolymph. NHE3 is implicated in NH_4^+ transport across the apical side to the water. Apical AeRh50s are likely to facilitate ammonia excretion in conjunction with the activity of apical VA by ammonia trapping, whereby VA creates an acidified boundary layer at the apical membrane aided by cytosolic CA (Weihrauch et al., 2009; Wright and Wood, 2009). NH_3 is effectively "trapped" in the form of NH_4^+ by binding to H^+ thereby sustaining a NH_3 gradient that favors NH_3 excretion into the water.

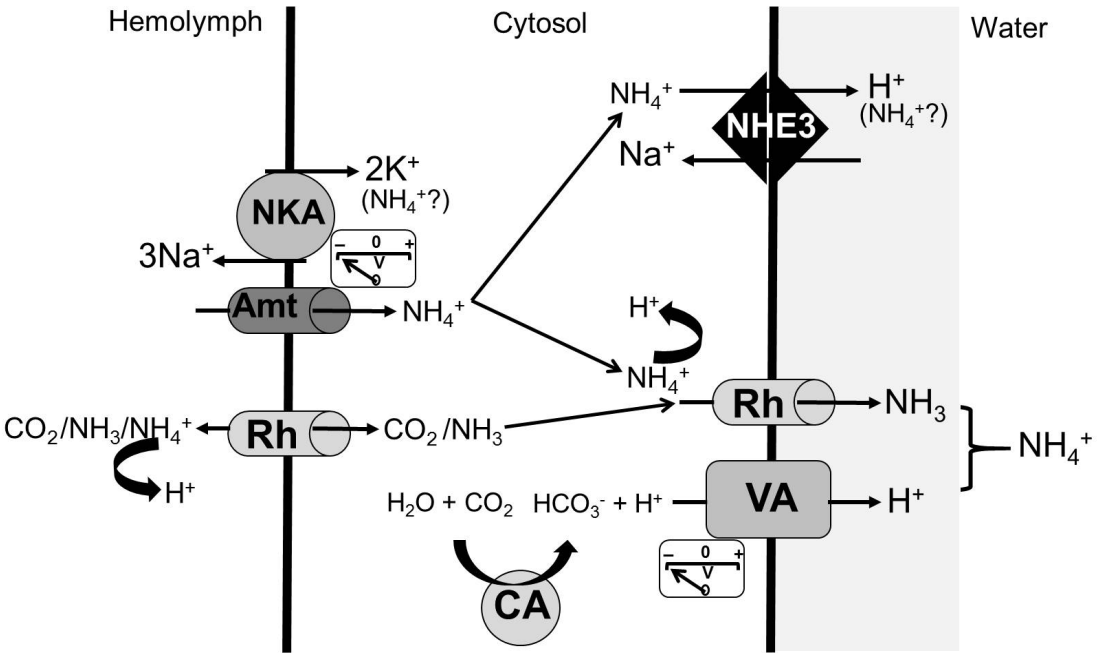

Figure 2- 7. Model of ammonia excretion mechanism in the anal papilla syncytial epithelium of the larval *A. aegypti* mosquito (adapted from Chasiotis et al., 2016). Basally expressed NKA and apically expressed VA provides a cytosol negative voltage potential that could serve to drive NH_4^+ from the haemolymph to the cytosol through AeAmt1 (Amt). NH_4^+ may also substitute for K^+ and enter directly through NKA. NH_4^+/NH_3 are also recruited by a basal AeRh50 (Rh) with NH_3 entering the cytosol. On the basal side, AeRh50 (Rh) may also transport CO_2 to the cytosol. On the apical side, NH_4^+ in the cytosol may exit to the surrounding environment through apical AeRh50s (Rh), or through NHE3 in exchange for a cation (e.g. Na^+). An apical AeRh50 transporter may also facilitate NH_3 exit from the cytosol with the aid of an ammonia-trapping mechanism whereby apical VA acidifies the papilla boundary layer. NHE3 may also contribute to the acidification of the boundary layer by transporting H^+ into the water. A basal AeRh50 can supply a cytoplasmic carbonic anhydrase (CA) with CO_2, and in turn the CA can supply H^+ to the VA, as well as contribute to the cytosol negative potential.

2.6 References

Adlimoghaddam, A., Boeckstaens, M., Marini, A.-M., Treberg, J. R., Brassinga, A.-K. C. and Weihrauch, D. (2015). Ammonia excretion in Caenorhabditis elegans: mechanism and evidence of ammonia transport of the Rhesus protein CeRhr-1. *J. Exp. Biol.* **218**, 675–683.

Baday, S., Orabi, E. A., Wang, S., Lamoureux, G. and Bernèche, S. (2015). Mechanism of NH_4^+ Recruitment and NH_3 Transport in Rh Proteins. *Structure* **23**, 1550–1557.

Borash, D. J., Gibbs, A. G., Joshi, A. and Mueller, L. D. (1998). A Genetic Polymorphism Maintained by Natural Selection in a Temporally Varying Environment. *Am. Nat.* **151**, 148–156.

Burke, R. L., Barrera, R., Lewis, M., Kluchinsky, T. and Claborn, D. (2010). Septic tanks as larval habitats for the mosquitoes *Aedes aegypti* and *Culex quinquefasciatus* in Playa-Playita, Puerto Rico. *Med. Vet. Entomol.* **24**, 117–123.

Cagle, W. A. and Johnson, L. A. (1994). Onsite intermittent sand filter systems, A regulatory approach to their study in Placer County, California. In *Proc of the 7th Natl Symposium on Individual and Small Community Sewage Systems.*, pp. 283–291. St. Joseph, MI.: ASAE.

Canter, L. W. (1985). *Septic tank system effects on ground water quality / by Larry W. Canter and Robert C. Knox*. (ed. Knox, R. C.) Chelsea, Mich: Lewis Publishers.

Chasiotis, H. and Kelly, S. P. (2008). Occludin immunolocalization and protein expression in goldfish. *J. Exp. Biol.* **211**, 1524–1534.

Chasiotis, H., Ionescu, A., Misyura, L., Bui, P., Fazio, K., Wang, J., Patrick, M., Weihrauch, D. and Donini, A. (2016). An animal homolog of plant Mep/Amt transporters promotes ammonia excretion by the anal papillae of the disease vector mosquito *Aedes aegypti*. *J. Exp. Biol.* **219**, 1346–55.

Conroy, M. J., Bullough, P. A., Merrick, M. and Avent, N. D. (2005). Modelling the human

rhesus proteins: implications for structure and function. *Br. J. Haematol.* **131**, 543–551.

Cooper, A. J. L. and Plum, F. (1987). Biochemistry and Physiology of Brain Ammonia. *Physiol. Rev.* **67**, 440–519.

Credland, P. (1976). A structural study of the anal papillae of the midge *Chironomus riparius* Meigen (Diptera: Chironomidae). *Cell Tissue Res.* **166**,.

Cruz, M. J., Sourial, M. M., Treberg, J. R., Fehsenfeld, S., Adlimoghaddam, A. and Weihrauch, D. (2013). Cutaneous nitrogen excretion in the African clawed frog *Xenopus laevis*: Effects of high environmental ammonia (HEA). *Aquat. Toxicol.* **136**–**137**, 1–12.

Donini, A. and O'Donnell, M. J. (2005). Analysis of Na^+, Cl^-, K^+, H^+ and NH_4^+ concentration gradients adjacent to the surface of anal papillae of the mosquito *Aedes aegypti*: application of self-referencing ion-selective mi. *J. Exp. Biol.* **208**, 603–10.

Drake, V. M. and Bauder, J. W. (2005). Ground water nitrate-nitrogen trends in relation to urban development, Helena, Montana, 1971-2003. *Groundw. Monit. Remediat.* **25**, 118–130.

Endeward, V., Cartron, J.-P., Ripoche, P. and Gros, G. (2006). Red cell membrane CO_2 permeability in normal human blood and in blood deficient in various blood groups, and effect of DIDS. *Transfus. Clin. Biol.* **13**, 123–127.

Gordon, R. and Bailey, C. H. (1974). Free amino acid composition of the haemolymph of the larval blackfly *Simulium venustum* (Diptera: Simuliidae). *Experientia* **30**, 902–903.

Gruswitz, F., Chaudhary, S., Ho, J. D., Schlessinger, A., Pezeshki, B., Ho, C.-M., Sali, A., Westhoff, C. M. and Stroud, R. M. (2010). Function of human Rh based on structure of RhCG at 2.1 A. *Proc. Natl. Acad. Sci.* **107**, 9638–9643.

Heatwole, K. K. and McCray, J. E. (2007). Modeling potential vadose-zone transport of nitrogen from onsite wastewater systems at the development scale. *J. Contam. Hydrol.* **91**, 184–201.

Huang, C. H. (2008). Molecular origin and variability of the Rh gene family: an overview of evolution, genetics and function. *Haematologica* **2**, 149–157.

Hung, C. Y. C., Tsui, K. N. T., Wilson, J. M., Nawata, C. M., Wood, C. M. and Wright, P. a (2007). Rhesus glycoprotein gene expression in the mangrove killifish *Kryptolebias marmoratus* exposed to elevated environmental ammonia levels and air. *J. Exp. Biol.* **210**, 2419–2429.

Ji, Q., Hashmi, S., Liu, Z., Zhang, J., Chen, Y. and Huang, C.-H. (2006). CeRh1 (rhr-1) is a dominant Rhesus gene essential for embryonic development and hypodermal function in *Caenorhabditis elegans*. *Proc. Natl. Acad. Sci. U. S. A.* **103**, 5881—5886.

Jonusaite, S., Kelly, S. P. and Donini, A. (2011). The physiological response of larval *Chironomus riparius* (Meigen) to abrupt brackish water exposure. *J. Comp. Physiol. B.* **181**, 343–52.

Khademi, S., O'Connell III, J., Remis, J., Robles-Colmenares, Y., Miercke, L. J. W. and Stroud, R. M. (2004). Mechanism of ammonia transport by Amt/MEP/Rh: Structure of AmtB at 1.35 angstroms. *Science (80-.).* **305**, 1587–1594.

Kustu, S. and Inwood, W. (2006). Biological gas channels for NH_3 and CO_2: evidence that Rh (Rhesus) proteins are CO_2 channels. *Transfus. Clin. Biol.* **13**, 103–110.

Lam, W. K. and Dharmaraj, D. (1982). A survey on mosquitoes breeding in septic tanks in several residential areas around Ipoh municipality. *Med. J. Malaysia* **37**, 114–123.

Li, X., Jayachandran, S., Nguyen, H.-H. T. and Chan, M. K. (2007). Structure of the *Nitrosomonas europaea* Rh protein. *Proc. Natl. Acad. Sci. U. S. A.* **104**, 19279–84.

Lupo, D., Li, X.-D., Durand, A., Tomizaki, T., Cherif-Zahar, B., Matassi, G., Merrick, M. and Winkler, F. K. (2007). The 1.3-A resolution structure of *Nitrosomonas europaea* Rh50 and mechanistic implications for NH_3 transport by Rhesus family proteins. *Proc. Natl. Acad. Sci. U. S. A.* **104**, 19303–19308.

Martin, M., Fehsenfeld, S., Sourial, M. M. and Weihrauch, D. (2011). Effects of high environmental ammonia on branchial ammonia excretion rates and tissue Rh-protein mRNA expression levels in seawater acclimated Dungeness crab *Metacarcinus magister*. *Comp.*

Biochem. Physiol. - A Mol. Integr. Physiol. **160**, 267–277.

Musa-Aziz, R., Chen, L.-M., Pelletier, M. F. and Boron, W. F. (2009). Relative CO_2/NH_3 selectivities of AQP1, AQP4, AQP5, AmtB, and RhAG. *Proc. Natl. Acad. Sci. U. S. A.* **106**, 5406–5411.

Nakada, T., Hoshijima, K., Esaki, M., Nagayoshi, S., Kawakami, K. and Hirose, S. (2007). Localization of ammonia transporter Rhcg1 in mitochondrion-rich cells of yolk sac, gill, and kidney of zebrafish and its ionic strength-dependent expression. *Am J Physiol Regul Integr Comp Physiol* **293**, R1743-53.

Nawata, C. M. and Wood, C. M. (2008). The effects of CO_2 and external buffering on ammonia excretion and Rhesus glycoprotein mRNA expression in rainbow trout. *J. Exp. Biol.* **211**, 3226–3236.

Nawata, C. M., Hung, C. C. Y., Tsui, T. K. N., Wilson, J. M., Wright, P. A. and Wood, C. M. (2007). Ammonia excretion in rainbow trout (*Oncorhynchus mykiss*): evidence for Rh glycoprotein and H+-ATPase involvement. *Physiol. Genomics* **31**, 463–474.

Nawata, C. M., Wood, C. M. and O'Donnell, M. J. (2010). Functional characterization of Rhesus glycoproteins from an ammoniotelic teleost, the rainbow trout, using oocyte expression and SIET analysis. *J. Exp. Biol.* **213**, 1049–1059.

Nguyen, H. and Donini, A. (2010). Larvae of the midge *Chironomus riparius* possess two distinct mechanisms for ionoregulation in response to ion-poor conditions. *Am. J. Physiol. Integr. Comp. Physiol.* **299**, R762–R773.

Ostrensky, A. and Wasielesky, J. . (1995). Acute toxicity of ammonia to various life stages of the Sao Paulo shrimp *Penaeus paulensis* Perez-Farfante, 1967. *Aquaculture* **132**, 339–347.

Perry, S. F., Braun, M. H., Noland, M., Dawdy, J. and Walsh, P. J. (2010). Do Zebrafish Rh Proteins Act as Dual Ammonia – CO_2 Channels ? *J. Exp. Zool.* **313A**, 618–621.

Quentin, F. (2003). RhBG and RhCG, the putative ammonia transporters, are expressed in the same

cells in the distal nephron. *J. Am. Soc. Nephrol.* **14**, 545–554.

Quijada-Rodriguez, A. R., Treberg, J. R. and Weihrauch, D. (2015). Mechanism of ammonia excretion in the freshwater leech *Nephelopsis obscura*: characterization of a primitive Rh protein and effects of high environmental ammonia. *Am. J. Physiol. Regul. Integr. Comp. Physiol.* ajpregu.00482.2014.

Singh, A. D., Wong, S., Ryan, C. P. and Whyard, S. (2013). Oral delivery of double-stranded RNA in larvae of the yellow fever mosquito, *Aedes aegypti*: implications for pest mosquito control. *J. Insect Sci.* **13**, 69.

Sohal, R. S. and Copeland, E. (1966). Ultrastructural variations in the anal papillae of *Aedes aegypti* (L.) at different environment salinities. *J Insect Physiol* **12**, 429–434.

Soupene, E., Chu, T., Corbin, R. W., Hunt, D. F. and Kustu, S. (2002). Gas channels for NH_3: Proteins from hyperthermophiles complement an Escherichia coli mutant. *J. Bacteriol.* **184**, 3396–3400.

Soupene, E., Inwood, W. and Kustu, S. (2004). Lack of the Rhesus protein Rh1 impairs growth of the green alga *Chlamydomonas reinhardtii* at high CO_2. *Proc. Natl. Acad. Sci. U. S. A.* **101**, 7787–7792.

Spaargaren, D. H. (1990). The effect of environmental ammonia concentrations on the ion-exchange of shore crabs, *Carcinus maenas* (L.). *Comp. Biochem. Physiol. Part C Comp. Pharmacol.* **97**, 87–91.

Weihrauch, D. (2006). Active ammonia absorption in the midgut of the Tobacco hornworm *Manduca sexta* L.: Transport studies and mRNA expression analysis of a Rhesus-like ammonia transporter. *Insect Biochem. Mol. Biol.* **36**, 808–821.

Weihrauch, D., Becker, W., Postel, U., Luck-Kopp, S. and Siebers, D. (1999). Potential of active excretion of ammonia in three different haline species of crabs. *J. Comp. Physiol. B* **169**, 25–37.

Weihrauch, D., Morris, S. and Towle, D. W. (2004). Ammonia excretion in aquatic and terrestrial

crabs. *J. Exp. Biol.* **207**, 4491–4504.

Weihrauch, D., Wilkie, M. P. and Walsh, P. J. (2009). Ammonia and urea transporters in gills of fish and aquatic crustaceans. *J. Exp. Biol.* **212**, 1716–1730.

Weihrauch, D., Donini, A. and O'Donnell, M. J. (2012a). Ammonia transport by terrestrial and aquatic insects. *J. Insect Physiol.* **58**, 473–487.

Weihrauch, D., Chan, a. C., Meyer, H., Doring, C., Sourial, M. and O'Donnell, M. J. (2012b). Ammonia excretion in the freshwater planarian *Schmidtea mediterranea*. *J. Exp. Biol.* **215**, 3242–3253.

Wood, C. M., Matsuo, A. Y. O., Gonzalez, R. J., Wilson, R. W., Patrick, M. L. and Val, A. L. (2002). Mechanisms of ion transport in Potamotrygon , a stenohaline freshwater elasmobranch native to the ion-poor blackwaters of the Rio Negro. *J. Exp* **205**, 3039–3054.

Wright, P. A. and Wood, C. M. (2009). A new paradigm for ammonia excretion in aquatic animals: role of Rhesus (Rh) glycoproteins. *J. Exp. Biol.* **212**, 2303–12.

Zheng, L., Kostrewa, D., Bernèche, S., Winkler, F. K. and Li, X.-D. (2004). The mechanism of ammonia transport based on the crystal structure of AmtB of *Escherichia coli*. *Proc. Natl. Acad. Sci. U. S. A.* **101**, 17090–5.

Chapter Three

Ammonia excretion in an osmoregulatory syncytium is facilitated by *AeAmt2*, a novel ammonia transporter in *Aedes aegypti* larvae

This chapter has been published and reproduced with permission:

Durant A.C., Donini A. (2018) Ammonia excretion in an osmoregulatory syncytium is facilitated by AeAmt2, a novel ammonia transporter in *Aedes aegypti* larvae. *Frontiers in Physiology, Invertebrate Physiology* 11 April 2018; https://doi.org/10.3389/fphys.2018.00339

3.1 Summary

The larvae of the mosquito *Aedes aegypti* inhabit ammonia rich septic tanks in tropical regions of the world that make extensive use of these systems, explaining the prevalence of disease during dry seasons. Since ammonia (NH_3/NH_4^+) is toxic to animals, an understanding of the physiological mechanisms of ammonia excretion permitting the survival of *A. aegypti* larvae in high ammonia environments is important. We have characterized a novel ammonia transporter, *AeAmt2,* belonging to the Amt/MEP/Rh family of ammonia transporters. Based on the amino acid sequence, the predicted topology of AeAmt2 consists of 11 transmembrane helices with an extracellular N-terminus and a cytoplasmic C-terminus region. Alignment of the predicted AeAmt2 amino acid sequence with other Amt/MEP proteins from plants, bacteria, and yeast highlights the presence of conserved residues characteristic of ammonia conducting channels in this protein. AeAmt2 is expressed in the ionoregulatory anal papillae of *A. aegypti* larvae where it is localized to the apical membrane of the epithelium. dsRNA-mediated knockdown of AeAmt2 results in a significant decrease in NH_4^+ efflux from the anal papillae, suggesting a key role in facilitating ammonia excretion. The effect of high environmental ammonia (HEA) on expression of AeAmt2, along with previously characterized AeAmt1, AeRh50-1, and AeRh50-2 in the anal papillae was investigated. We show that changes in expression of ammonia transporters occur in response to acute and chronic exposure to HEA, which reflects the importance of these transporters in the physiology of life in high ammonia habitats.

3.2 Introduction

Mosquito larvae (order Diptera) are found in a wide range of habitats which vary in alkalinity and ionic composition. The disease vector mosquito, *Aedes aegypti*, is historically considered a fresh water breeder where the larvae are commonly found in clean freshwater habitats including artificial containers, streams, and pools (Ramasamy et al., 2011). Few mosquito species are capable of surviving in heavily polluted waters, *A. aegypti* being one such species. In fact, there is a growing body of evidence from field studies in tropical regions of the world demonstrating that *A. aegypti* are abundant in septic tanks containing raw sewage (Banerjee et al., 2015; Barrera et al., 2008; Burke et al., 2010; Chitolina et al., 2016). In some regions, it was estimated that these cryptic aquatic environments were providing a new habitat for more than 18,000 emerging *A. aegypti* adults daily (Barrera et al., 2008). A number of observations suggest that *A. aegypti* may be well adapted to inhabiting sewage. When female *A. aegypti* were given a choice to lay their eggs in freshwater or raw sewage, there was no breeding preference displayed (Chitolina et al., 2016). Furthermore, *A. aegypti* emerging from septic tanks have longer wings and higher nutrient reserves than those emerging from freshwater (Banerjee et al., 2015). This is significant as these are positive measures of overall fitness because larval nutrient acquisition is an important determinant of successful breeding of adults. While no genetic differentiation was observed between *A. aegypti* populations from septic tanks and freshwater surface containers, it was suggested that septic tank populations may even represent a more dangerous phenotype for disease transmission (Somers et al., 2011).

Sewage contains high levels of ammonia (NH_3/NH_4^+) which is toxic to animal cells at micromolar concentrations (Weihrauch et al., 2004). Furthermore, free ammonia and ammonium salts are common in organically polluted water inhabited by these mosquitoes (Kell Reid, 1961; Mitchell and Wood, 1984). *A. aegypti* larvae are tolerant to remarkably high levels of ammonium chloride (~7mM NH_4Cl), the major toxic component of sewage, and selection towards an increased tolerance to high ammonia was observed within a single generation (Mitchell and Wood, 1984). This is unlike other

aquatic invertebrate species where levels as low as 58 μmol l^{-1} of NH_3 and 1.39 mmol l^{-1} total ammonia is lethal (Chen and Lin, 1992; O'Donnell and Donini, 2017; Weihrauch et al., 2004; Wright, 1995b). These findings raise the question of what physiological mechanisms *A. aegypti* larvae possess allowing for high ammonia tolerance. Ammonia transport and excretion is a fundamental physiological process, one that all animals possess in some capacity (Marini et al., 1994; Marini et al., 1997a; Marini et al., 2000). In *A. aegypti*, the anal papillae have been shown to excrete ammonia and research on the molecular mechanisms of ammonia excretion by these organs has recently begun (Chasiotis et al., 2016; Chapter 2).

The four anal papillae in *A. aegypti* larvae are relatively elongate sac-like structures that surround the anal opening and are the product of eversion of the hindgut tissues (Edwards and Harrison, 1983). Anal papillae are composed of a single layer of homogenous cells that form a syncytium covered by a thin cuticle. The apical surface of the epithelial cells is directed outwards and the basal membrane faces the papilla lumen. The lumen of the papillae contains haemolymph and is continuous with the hemocoel of the body (Sohal and Copeland, 1966). In *A. aegypti,* the anal papillae are important for ionoregulation whereby active uptake of ions (Na^+, Cl^-) from the surrounding dilute medium occurs in addition to ammonia excretion (Donini and O'Donnell, 2005).

Ammonia transport across biological membranes is facilitated by Methylammonium/ammonium permeases (MEP) in yeast, also known as ammonium transporters (Amt) in bacteria, as well as analogs of both in vertebrates, the conserved family of Rhesus glycoproteins (Rh proteins) (Kustu and Inwood, 2006). Invertebrates possess both Amt/MEP and Rh proteins (Gruswitz et al., 2010). The Rh proteins are glycosylated, comprising a group of Rh-50 proteins (~50 kDa) which function as trimers (Gruswitz et al., 2010). Each monomer possesses 12 transmembrane helices, one more than invertebrate, plant, and bacterial homologs, which form a triple pore for substrate transfer through each monomer comprising the trimer. The crystallographic structure of mammalian RhCG predicts the transport of NH_3 over NH_4^+, whereby RhCG recruits NH_4^+ which is then deprotonated and NH_3 is conducted

through the channel (Baday et al., 2015; Gruswitz et al., 2010; Kustu and Inwood, 2006). The proton is recycled back to the extracellular space, resulting in electroneutral transport through these passive gas channels (Li et al., 2007; Lupo et al., 2007; Weihrauch and O'Donnell, 2015). Rh proteins are also proposed to be CO_2 gas channels in addition to ammonia transporters and require a partial pressure gradient (ΔP_{NH3} and ΔP_{CO2}) for transport (Khademi et al., 2004). Amt/MEP proteins have 11 pore-forming transmembrane helices which trimerize in the membrane, forming a triple pore for ammonia transport similarly to Rh proteins (Khademi et al., 2004; Zheng et al., 2004). The crystal structure of AmtB in *Escherichia coli* indicates that the trimer has a hydrophobic pore located at the center of each monomer with an NH_3/NH_4^+ binding site at the entry of each pore, and uncharged NH_3 is transported through the channel (Mayer et al., 2006). Some plant AMTs such as the *Lycopersicon esculentum* LeAMT1;2, are electrogenic ammonia transporters which conduct NH_4^+ specifically, or act as a co-transporter for NH_3/H^+ (Ludewig et al., 2002; Mayer et al., 2006). The anal papillae epithelium is a suitable tissue for electrogenic transport of NH_4^+, because the transport activities of basolateral Na^+/K^+-ATPase (NKA) and apical V-type H^+-ATPase (VA) is expected to produce a large cytosol negative voltage potential which would favour NH_4^+ entry into the cytosol from the haemolymph (Chasiotis et al., 2016; Patrick et al., 2006a; Weihrauch et al., 2012a).

Amt/MEP and Rh proteins have been identified and characterized as ammonia transporters in anopheline and aedine mosquito species (Pitts et al., 2014; Wu et al., 2010a). We have previously identified and characterized one Amt/MEP, *AeAmt1*, and two Rh proteins, *AeRh50-1* and *AeRh50-2*, in *A. aegypti* larvae which are expressed in the ionoregulatory syncytial epithelium of the anal papillae and have been implicated in facilitating ammonia excretion within this organ (Chasiotis et al., 2016; Chapter 2). Double-stranded RNA (dsRNA)-mediated knockdown of either *AeAmt1*, *AeRh50-1*, or *AeRh50-2* within the anal papillae of *A. aegypti* larvae causes a significant decrease in NH_4^+ efflux from the papillae and altered NH_4^+ and pH levels in the haemolymph.

This suggests that each of these transporters plays a role in ammonia excretion at the anal papillae at the very least (Chasiotis et al., 2016; Chapter 2). Changes in Rh protein expression in leeches, crabs, frogs, and fish in response to high environmental ammonia (HEA) has been well documented (Cruz et al., 2013; Hung et al., 2007; Martin et al., 2011; Quijada-Rodriguez et al., 2015), however, the involvement of Amts in invertebrates and Rh proteins in mosquitoes, specifically, in response to HEA is unknown.

The aim of this study was to characterize a novel Amt protein in the anal papillae of *A. aegypti* larvae and examine changes in ammonia transporter expression in response to HEA. We hypothesized that the novel Amt protein, AeAmt2 is expressed in the anal papillae where it functions to facilitate ammonia excretion, and that HEA exposure will result in alterations of ammonia transporter expression. To test this hypothesis, we examined transcript and protein expression of *AeAmt2* and conducted functional studies using a combination of dsRNA with electrophysiology techniques. Furthermore ammonia transporter expression in response to HEA was examined.

3.3 Materials and Methods

Animals and rearing conditions

A colony of *Aedes aegypti* (Linnaeus) was established in 2007 at York University with eggs obtained from Dr. Marjorie Patrick at the University of San Diego, CA, USA. The colony has been supplemented with eggs from a colony of *Aedes aegypti* (Liverpool strain) at Simon Fraser University, B.C., Canada in the laboratory facilities of Dr. Carl Lowenberger. The procedures for rearing mosquitoes were adapted from a previously established protocol (Donini and O'Donnell, 2005). Cages containing adult mosquitoes were kept in the laboratory at room temperature and had continuous access to a 5% aqueous sucrose solution. Females were fed on warm sheep's blood in Alsever's solution (Cedarlane Laboratories, Burlington, ON. Canada). Eggs were collected on filter paper and stored dry

in plastic containers until needed. Eggs were hatched and larvae reared in dechlorinated tap water (deH_2O) in plastic containers in the laboratory. Lights on a timer located at the bench where the mosquito cages and larval containers were held simulated a 12:12 light:dark cycle. Larvae were fed daily with a solution of liver powder and yeast in water. Rearing water was refreshed every other day. Fourth instar larvae were used 24h post-feeding for physiological and molecular studies.

Animals and rearing conditions for high environmental ammonia (HEA) studies

HEA treatments conducted in this study were two-fold; (1) acute (6 hr) and semi-chronic (48 hr) exposure to HEA, and (2) rearing (7 days) in HEA. For acute (6 h) and semi-chronic (48 h) exposure to HEA studies, larvae were hatched and reared in deH_2O until reaching fourth instar when they were then transferred to either deH_2O or 5 mM NH_4Cl in deH_2O for 6 and 48 hours. For rearing in HEA experiments, larvae were hatched in deH_2O and transferred to either deH_2O or 5 mM NH_4Cl in deH_2O two days post hatching until they reached fourth instar.

Reverse-transcriptase PCR (RT-PCR) and quantitative real-time PCR (qRT-PCR)

AeAmt2 was identified by sequence alignment to the AeAmt1 nucleotide sequence using a BLAST query from the Bioinformatics Resource for Invertebrate Vectors of Human Pathogens (VectorBase) and the nucleotide database provided by the National Center for Biotechnology Information (NCBI). Partial mRNA sequences for *A. aegypti AeAmt2* (AAEL007373-RA) were used for primer design (forward primer: 5'-GCATTTTAGCGTCACTGGTC-3'; reverse primer: 5'-GGGAA-TAGGGTTATCAGCAAAC-3'; 221 bp amplicon size, 62°C annealing temperature). Primers for *AeAmt1*, *AeRh50-1*, and *AeRh50-2* were previously designed and described (Chasiotis et al., 2016). Three biological samples, each consisting of a pool of 200 anal papillae from 50 larvae were isolated and collected in cold lysis buffer with 1% 2-mercaptoethanol (Ambion, Austin, TX, USA). Total anal papillae RNA was extracted using the Purelink RNA mini kit (Ambion, Austin, TX) and was treated with the TURBO DNA-free™ Kit (Applied Biosystems, Streetsville, Ont, Canada) to remove genomic

DNA. Template cDNAs were synthesized using the iScript™ synthesis kit (Bio-Rad, Mississauga, ON, Canada) with 1 µg of total RNA for each reaction. PCR amplicons of *AeAmt2*, *AeRh50-1*, *AeRh50-2*, *AeAmt1* were resolved by agarose gel electrophoresis with ethidium bromide. AeAmt2 transcript was concentrated and purified using the QIAquick PCR Purification Kit (Qiagen, Toronto, Ont, Canada), and was sequenced (Bio Basic Inc., Markham, ON, Canada) to ensure the specificity of the product.

Quantitative real time PCR (qRT-PCR) using the primers described above was used to examine the mRNA abundance of *AeRh50-1*, *AeRh50-2*, *AeAmt1*, and *AeAmt2* in the anal papillae. qRT-PCR reactions were carried out using the CFX96™ real-time PCR detection system (Bio-Rad) and Sso-Fast™ Evagreen® Supermix (Bio-Rad) according to the manufacturer's protocol. Ribosomal *18s* RNA served as the reference gene utilizing primers that have been previously reported (Chasiotis et al., 2016; Jonusaite et al., 2016; Sanders et al., 2003). A melting curve analysis was performed after each cycle to confirm the presence of a single product. For *AeAmt2* primer optimization, a standard curve was generated to assess primer and reaction efficiency. Quantification of relative transcript abundance was determined according to the Pfaffl method (Pfaffl, 2004). For the expression profile of Amt and Rh proteins in the anal papillae, the mRNA abundance of ammonia transporter genes in the anal papillae were expressed relative to *AeRh50-1*, which was assigned a value of 1.0 after normalizing with *18s* RNA abundance. To assess effects of HEA treatment on mRNA abundance of ammonia transporter genes the mRNA abundance of each respective gene was expressed relative to the control deH_2O, which was assigned a value of 1.0 after normalizing to *18s* transcript abundance.

Western blotting and immunohistochemistry

The protein abundance of AeAmt2, AeAmt1, and AeRh50s in the anal papillae of 4th instar larvae was examined using Western blotting. Briefly, biological samples consisting of pooled anal papillae were isolated from 20–50 larvae in *A. aegypti* saline (Donini et al., 2006) and were sonicated (3× 10 seconds) in a homogenization buffer (50 mmol l^{-1} Tris-HCl pH 7.4, 1 mmol l^{-1} PMSF, 150

mmol l^{-1} NaCl, 1% sodium deoxycholate, 1% Triton X-100, 0.1% SDS, and 1:200 protease inhibitor cocktail [Sigma-Aldrich]), centrifuged at 13,000 *g* for 10 min at 4°C, and the supernatant was stored at -80°C. Samples consisting of 5 µg of protein, determined using the Bradford assay (Bio-Rad), were prepared for SDS-PAGE by heating for 5 min at 100°C in 6× loading buffer (360 mmol l^{-1} Tris-HCl pH 6.8, 12% (w/v) SDS, 30% glycerol, 600 mmol l^{-1} DTT, and 0.03% (w/v) Bromophenol blue) and then were electrophoretically separated by SDS-PAGE (12% polyacrylamide). Western blot analysis of each ammonia transporter was conducted according to an established protocol (Chasiotis and Kelly, 2008; Chasiotis et al., 2016; Chapter 2). A custom-synthesized polyclonal antibody that was raised in rabbit against a synthetic peptide corresponding to a 14-amino acid region (DKMSPQKKANDQPK) of *AeAmt2* (GenScript USA Inc., Piscataway, New Jersey, USA) was used at a 1:5000 dilution. Custom-synthesized polyclonal antibodies raised in rabbit against AeAmt1 and AeRh50s were used at dilutions of 1:500 and 1:2000 , respectively, and have been previously validated (Chasiotis et al., 2016; Chapter 2). The AeRh50 antisera is presumed to detect both AeRh50-1 and AeRh50-2 (Chapter 2). AeAmt2 antibody specificity was confirmed by running a comparison blot with AeAmt2 antibody pre-absorbed with 10× molar excess of immunogenic peptide for 1 hr at room temperature prior to application to blots. After examination of ammonia transporter expression, blots were stripped and either re-probed with a 1:1000 dilution of rabbit monoclonal anti-GAPDH antibody (14C10, New England BioLabs, Whitby, ON, Canada) following the above procedure, as specified, or total protein analysis was carried out using Coomassie total protein staining as a loading control (0.1% Coomassie R250, 50% methanol, 50% ddH_2O) (Eaton et al., 2013). Preliminary studies were used to determine which loading control was appropriate for the study treatments. For the 6 hour and 48 hour HEA exposures, GAPDH expression did not change with treatment and was therefore used as the loading control. For dsRNA and 7 day HEA treatments, GAPDH expression increased and therefore total protein was used as the loading control. Blots were incubated in Coomassie for 1 minute followed by de-staining for 3-5 minutes in de-stain solution (50% ethanol, 10% acetic acid, 40% ddH_2O). Blots were then washed in

ddH_2O for 1 minute and dried completely prior to visualization using a Gel Doc XR + system (Bio-Rad). Densitometric analysis of AeAmt2, AeAmt1, AeRh50s, GAPDH, and Coomassie total protein was conducted using ImageJ 1.50i software (National Institutes of Health, Bethesda, MD, USA).

Immunolocalization of AeAmt2 in paraffin-embedded cross sections of anal papillae was conducted using immunohistochemistry. Na^+-K^+-ATPase (NKA) and the V_0 subunit of V-type H^+ ATPase (VA) immunostaining were used as markers for the basolateral membrane and apical membrane, respectively (Patrick et al., 2006a). The procedure was carried out according to an established protocol (Chasiotis et al., 2016; Chapter 2). AeAmt2 antibody was used at a 1:500 dilution, a mouse monoclonal anti-α5 antibody for NKA (Douglas Fambrough, Developmental Studies Hybridoma Bank, IA, USA) was used at a concentration of 4.2 ug/mL (Chasiotis et al., 2016; Chapter 2; Patrick et al., 2006), and a guinea pig anti-V-type H^+-ATPase (kind gift from Dr. Weiczorek, University of Osnabruk, Germany) was used at a 1:3000 dilution. A sheep anti-mouse antibody conjugated to Cy2 and a goat anti-guinea pig antibody conjugated to AlexaFluor 647 (Jackson ImmunoResearch Laboratories, West Grove, PA, USA) at dilutions of 1:500 was used to visualize NKA and VA, respectively. A goat anti-rabbit antibody conjugated to Alexa Fluor 594 (Jackson ImmunoResearch) at a dilution of 1:500 was applied to visualize AeAmt2. Comparison control slides were also processed as described above, with control slides incubated in primary immune serum with no primary antibody. Slides were mounted using ProLong Gold antifade reagent with DAPI (Life Technologies, Burlington, ON). Fluorescence images were captured on a Zeiss LSM 700 laser scanning microscope (Zeiss, U.S.A). Images were merged using ImageJ 1.50i software (National Institutes of Health, Bethesda, MD, USA).

dsRNA synthesis and delivery

Using the NCBI nucleotide database, primers were designed for *AeAmt2* dsRNA synthesis that spans 951 bp of the partial mRNA sequence (forward: 5'-ACTCAGGCAGCACATACGG-3'; reverse: 5'-ATTGATTTCCCCCCAACTCG-3'). The purified PCR product was sequenced (The Centre for

Applied Genomics, Sick Kids Hospital, Toronto, ON) to ensure specificity of the target. A fragment of the *β-lactamase* (*β-lac*) gene was also amplified by RT-PCR from a pGEM-T-Easy vector (kind gift from Jean-Paul Paluzzi) (forward: 5'-ATTTCCGTGTCGCCCTTATTC-3'; reverse: 5'-CGTTCATCCATAGTTGCCTGAC-3', 799 bp amplicon size) and served as a control. Using the PCR product as template, RT-PCR was carried out using the *AeAmt2* and *β-lac* primers with an additional T7 promoter sequence (5'-TAATACGACTCACTATAGGG-3'). *AeAmt2* and *β-lac* PCR products with the T7 promoter were concentrated and purified using the QIAquick PCR Purification Kit (Qiagen). dsRNA was synthesized according to a previously described protocol (Chasiotis et al., 2016), using the Promega T7 RiboMAX Express RNAi kit (Promega, Madison, WI, USA) and the *AeAmt2* and *β-lac* T7 PCR products as template.

For *AeAmt2* dsRNA-mediated knockdown studies, 30 fourth instar larvae were incubated in 0.5 μg μl^{-1} dsRNA in 150 μl PCR-grade water for 2 hours (Singh et al., 2013), after which they were transferred into 50 ml of deH_2O. Larvae ingest the media that they inhabit as shown in previous studies (Chasiotis et al., 2016; Singh et al., 2013). Water was refreshed every other day and larvae were fed every other day beginning 24 h after dsRNA treatment.

Ion-selective microelectrodes (ISME) for haemolymph ion measurements

For haemolymph collection, larvae were gently blotted on filter paper to remove excess water. Larvae were then submerged in paraffin oil (Sigma-Aldrich, Oakville, ON, CA) and fine forceps were used to gently tear the cuticle without rupturing the gut tissue, releasing haemolymph into the oil. The NH_4^+ levels of the collected haemolymph droplets were measured as free ion activities using ion-selective microelectrodes (ISMEs). The construction of microelectrodes has been previously described in detail (Donini and O'Donnell, 2005). The following ionophore cocktails (Fluka, Buchs, Switzerland) and back-fill solutions (in parentheses) were used: NH_4^+ Ionophore I Cocktail A (100 mmol l^{-1} NH_4Cl).

The ISMEs were calibrated in the following solutions (mmol l^{-1}): NH_4^+; (0.1, 1, 10) NH_4Cl. Voltages were recorded and analyzed in LabChart 6 Pro software (AD Instruments Inc.).

Scanning ion-selective microelectrode technique (SIET)

The scanning ion-selective electrode technique (SIET) system used in this study to measure NH_4^+ flux from the anal papillae of larvae has been previously described (Chasiotis et al., 2016). Larvae were mounted in a Petri dish using beeswax, leaving the anal papillae exposed and immobilized for measurements. Voltage gradients over an excursion distance of 100 µm were recorded adjacent to the papillae with a NH_4^+ microelectrode (see ISME) in a 4mL bath of 0.5 mmol l^{-1} NH_4Cl in double distilled water (ddH_2O). The sampling protocol utilized here was outlined elsewhere (Chasiotis et al., 2016). Readings were taken along the middle to distal portion of the anal papillae at five equally spaced sites. Background voltage gradients were taken 3000 µm away from the anal papillae using the same sampling protocol and were subtracted from the voltage gradients recorded at the papillae. To calculate NH_4^+ flux, voltage gradients were used to calculate NH_4^+ concentration gradients using the following formula:

$$\Delta C = C_B \, x \, 10^{(\Delta V/S)} - C_B,$$

where ΔC is the concentration gradient (µmol l^{-1} cm^{-3}), C_B is the background concentration of NH_4^+ in the bath solution, ΔV is the voltage difference between the two points, and S is the slope of the electrode (the voltage difference for a 10-fold difference in NH_4^+ concentration). The NH_4^+ flux was then calculated using the concentration gradient (ΔC) and Fick's law of diffusion:

$$J = D(\Delta C)/\Delta X,$$

where J is the net flux of the NH_4^+ (pmol cm^{-2} s^{-1}), D is the diffusion coefficient of NH_4^+ (2.09×10^{-5} cm^2 s^{-1}), ΔC is the concentration gradient calculated above, and ΔX is the excursion distance used to measure the voltage gradients (here 0.01cm). The NH_4^+ fluxes were recorded from larvae treated with

β-lac dsRNA (control), AeAmt2 dsRNA, or a combination of AeAmt1, AeAmt2, AeRh50-1, and AeRh50-2 dsRNA, where specified.

Statistical analysis and phylogeny

Statistical analyses in this study were computed using Prism® 7.00 (GraphPad Software, La Jolla, CA, USA). An unpaired two-tailed t-test was performed for comparisons between two groups, unless specified. For comparisons of multiple groups for a single treatment (qRT-PCR studies), a one-way ANOVA was performed using the Holm-Sidak method for multiple comparisons. The adjusted P value accounting for multiple testing is indicated. For SIET data, a single biological replicate is defined as the average flux from 5 sites along a single papilla from a single larva.

An unrooted maximum likelihood tree based on the JTT matrix-based model was constructed in MEGA7 from multiple sequence alignment of 16 amino acid sequences using Clustal X (Kumar et al., 2016). The Protter protein visualization software was used to generate the transmembrane plot of AeAmt2 (Omasits et al., 2014).

3.4 Results

Characterization, expression, and localization of AeAmt2 in the anal papillae

AeAmt2 is a member of the Amt family of ammonia transporters, sharing significant homology with putative or confirmed ammonia transporter proteins from other insects and to a lesser extent, Amts from plants (Fig. 3-1). Multiple amino acid sequence alignment of 8 members of the Amt/MEP/Rh family illustrates that the highly conserved residues in this family are also conserved in AeAmt2 (Fig. 3-2). The transcript of *AeAmt2* is predicted to encode a peptide of 585 amino acid residues with a predicted molecular mass of 63.31 kDa (VectorBase) comprising 11 transmembrane helices and an extracellular N-terminus and intracellular C-terminus (Fig. 3-3). To determine whether *AeAmt2* was

expressed in the anal papillae, RT-PCR and agarose gel electrophoresis was performed (Fig. 3-4A). A single distinct product for *AeAmt2* was observed at 220 base pairs. qRT-PCR was then used to examine relative *AeAmt2* transcript abundance in the anal papillae along with *AeAmt1*, *AeRh50-1*, and *AeRh50-2* (Fig. 3-4B). *AeAmt2* mRNA abundance in the anal papillae was significantly lower in comparison to all other ammonia transporter mRNA examined, being ~50 and ~2500 times less abundant than *AeRh50-1* and AeAmt1 within this organ, respectively. Western blot analysis in combination with a peptide block revealed one specific, putative AeAmt2 protein band in the anal papillae that does not appear when the antibody is preabsorbed with immunogenic peptide (Fig. 3-4C). This putative AeAmt2 is 55 kDa in molecular mass. For densitometric analysis of AeAmt2 for all experiments, the 55 kDa band was used for protein quantification.

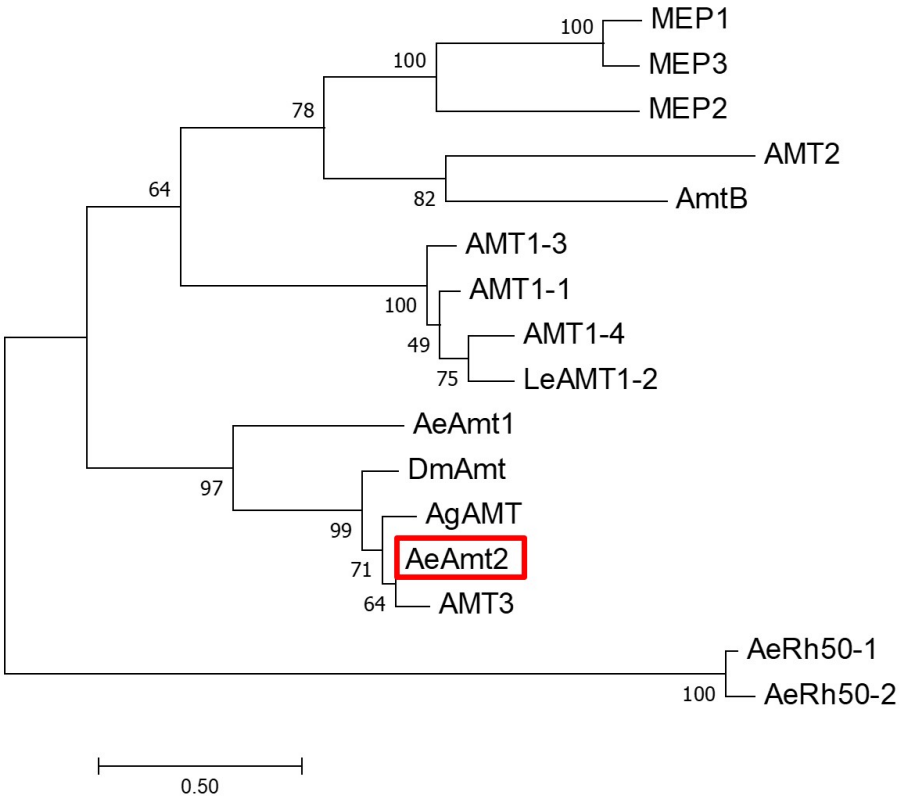

Figure 3- 1. Unrooted maximum likelihood tree for 16 ammonium transporters (Amt), Rhesus glycoproteins (Rh) and methylammonium permeases (Mep). The percentage of trees in which the associated taxa clustered together from 500 replicates is shown next to the branches. The scale bar represents the number of amino acid substitutes per site, with tree branches drawn to scale. The boxed sequence is the subject of the current study. The analysis involved the multiple alignment of 16 full length amino acid sequences of 16 different genes using Clustal X prior to tree construction. Species name, gene, and GenBank accession number (in parentheses): *Saccharomyces cerevisiae* MEP1 (NP_011636), *Saccharomyces cerevisiae* MEP3 (EGA76487), *Saccharomyces cerevisiae* MEP2 (NP_011636), *Arabidopsis thaliana* AMT2 NC_025010.1), *Escherichia coli* AmtB (Z71418.1), *Arabidopsis thaliana AMT 1-3* (NC_025010.1), *Arabidopsis thaliana* AMT 1-1 (NC_025010.1), *Arabidopsis thaliana* AMT 1-4 (NC_025010.1), *Lycopersicon esculentum* LeAMT1-2 (NC_025010.1), *Aedes aegypti AeAmt1* (XP_001652713.1), *Drosophila melanogaster* DmAmt (NP_001097800), *Anopheles gambiae* AgAMT (XM_318439), *Aedes aegypti* AeAmt2 (A0A1S4FGF9), *Aedes albopictus* AMT3 (XM_020076522), *Aedes aegypti* AeRh50-1 (AY926463.1), *Aedes aegypti* AeRh50-2 (AY926464.1).

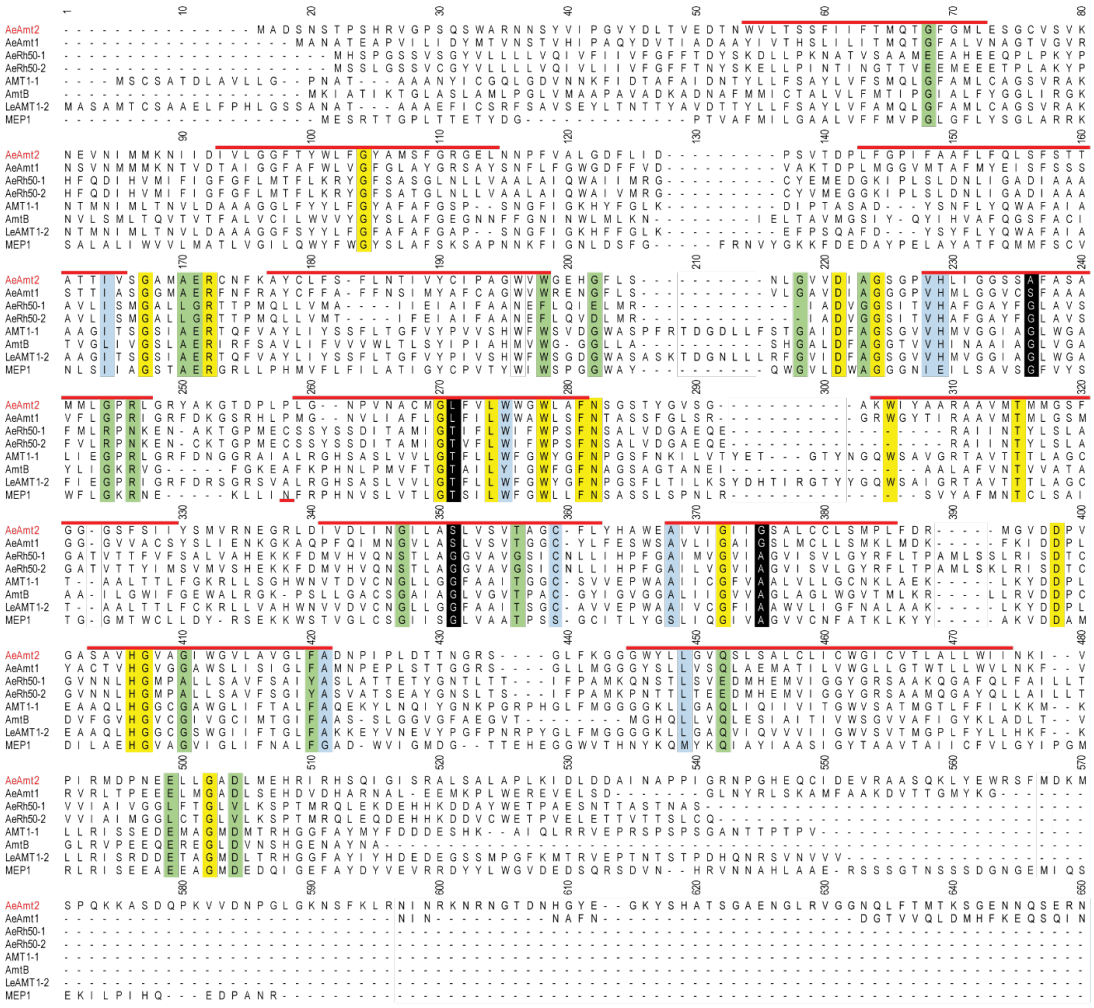

Figure 3- 2. Amino acid sequence alignment of AeAmt2 and selected members of the Amt/MEP/Rh family. *A. aegypti* AeAmt2 is labelled in red and predicted transmembrane helices from 1-11 beginning at residue 54 are indicated by the red lines (VectorBase). Sequence number according to LeAMT1-2 of *L. esculentum* is indicated, and 577 (out of 585 total) amino acid residues for AeAmt2 are shown. Highly conserved residues are highlighted in yellow, mostly conserved residues (7 out of 8 members have conserved amino acid residues) are highlighted in blue, highly conserved sequences in Amt/MEP proteins but not metazoan Rh proteins are highlighted in green, and conserved residues between AeAmt1 and AeAmt2 in *A. aegypti* that are different to the conserved residues in the other members are highlighted in black. Species names corresponding to amino acid sequences of ammonia transporters are as follows (in parentheses): AeAmt2 (*A. aegypti*), AeAmt1 (*A. aegypti*), AmtB (*E. coli*), AMT1-1 (*A. thaliana*), MEP1 (*S. cerevisiae*), Le-AMT1-2 (*L. esculentum*), AeRh50-1 (*A. aegypti*), and AeRh50-2 (*A. aegypti*). The alignment was constructed using the ClustalW algorithm.

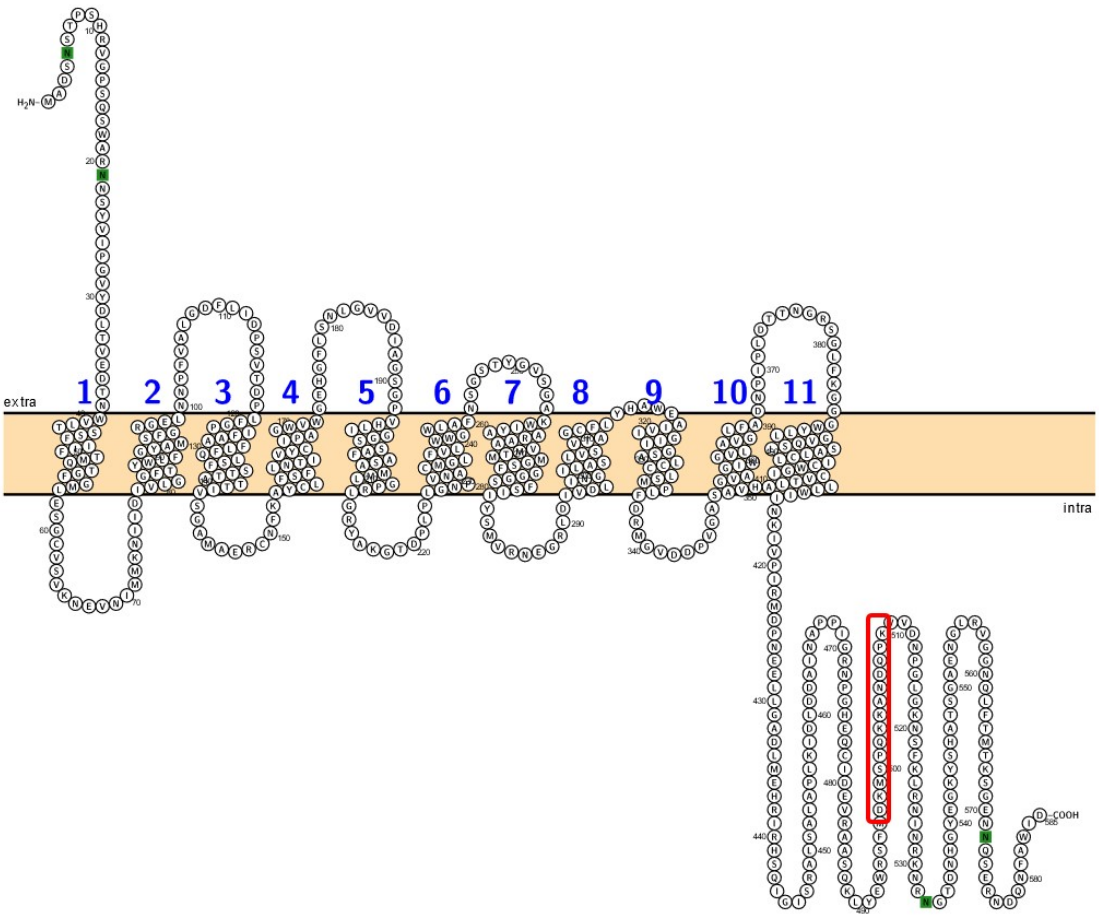

Figure 3- 3. Amino acid plot of *Aedes aegypti* AeAmt2. The plot of predicted sequence features of AeAmt2 depicts 11 transmembrane domains, an extracellular (extra) N-terminus and an intracellular (intra) C-terminal region. Amino acids highlighted in green represent N-glycosylation sites. The amino acid sequence boxed in red represents the epitope used to generate the custom AeAmt2 antibody used in this study (see Methods).

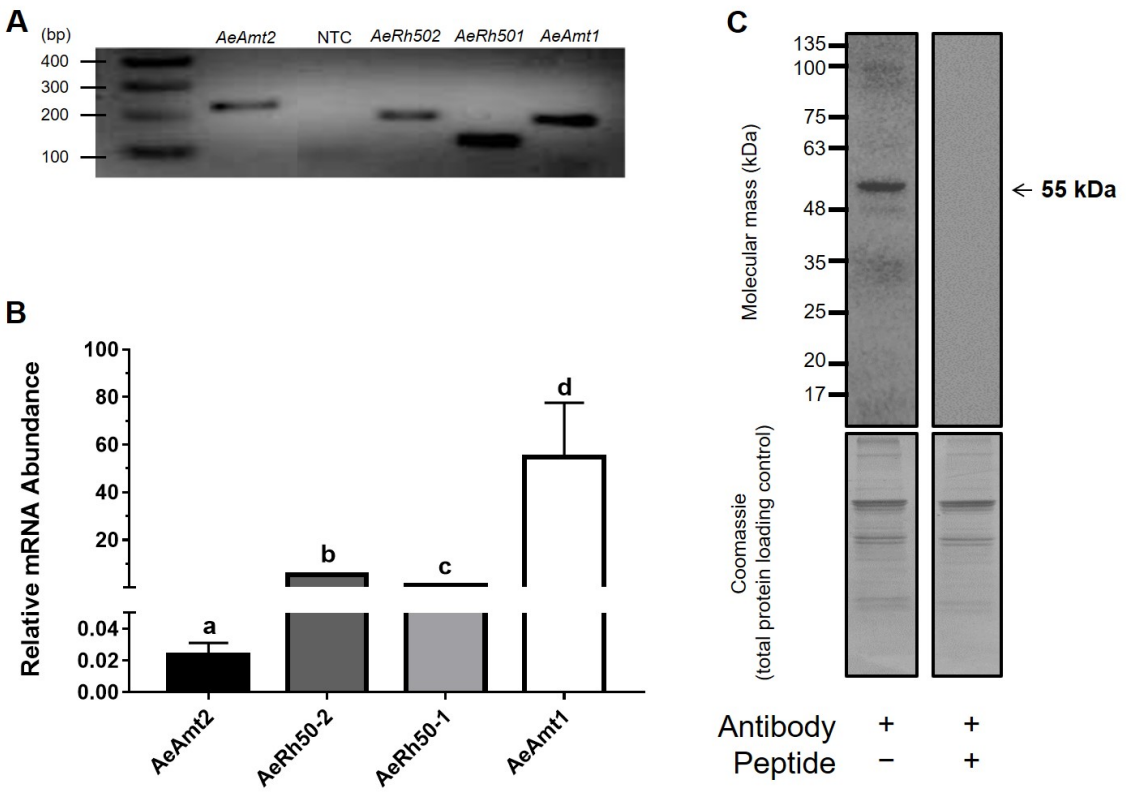

Figure 3- 4. **Ammonia transporter expression in the anal papillae of larval *A. aegypti*. (A)** RT-PCR amplicon of *AeAmt2,* the corresponding no template control (NTC) for *AeAmt2* primers, *AeRh50-2*, *AeRh50-1*, and *AeAmt1* expression in the anal papillae resolved by gel electrophoresis. **(B)** Comparison of *AeAmt2, AeRh50-1*, *AeRh50-2*, and *AeAmt1* mRNA abundance in the anal papillae. Each gene was normalized to 18s ribosomal RNA abundance in the anal papillae and was expressed relative to *AeRh50-1* (assigned a value of 1). The dashed line illustrates y = 1. Data are expressed as mean values ± SEM (n=3). Letters denote significant differences in relative mRNA abundance based on a One-way ANOVA (Holm-Sidak for multiple comparisons) of log transformed values ($p = 0.00002$). **(C)** Representative Western blot of larval anal papillae homogenates probed with AeAmt2 antisera revealing a single putative monomer at ~55 kDa (top panel). The single 55 kDa band was blocked by antibody pre-absorption with the immunogenic peptide. Coomassie total protein staining, used as a loading control, is shown in the lower panel.

The ion-motive pumps V-type H^+-ATPase (VA) and Na^+/K^+-ATPase (NKA) have been localized to the apical and basolateral membranes, respectively, within the anal papillae epithelium (Patrick et al., 2006a). In paraffin-embedded cross sections of anal papillae from fourth instar larvae reared in deH_2O, AeAmt2 immunostaining (Fig. 3-5A), apical VA immunostaining (Fig. 3-5B) co-immunolocalize when the images are merged, indicated by the yellow fluorescence (Fig. 3-5D). Nuclei staining with DAPI (blue) is visible in anal papillae cross sections (Fig. 3-5C-D). Conversely, AeAmt2 (Fig. 5E) and NKA immunostaining (Fig. 3-5F) do not appear to co-immunolocalize when merged (Fig. 5H). This is most clearly visible at regions surrounding the nuclei (Fig. 3-5G-H) indicated by the white arrows, showing separation of basolateral NKA staining and AeAmt2 staining. Yellow fluorescence was observed irregularly in merged images of NKA and AeAmt2 staining, which we believe is the result of membrane folding due to tissue sectioning. No immunofluorescence was observed in negative control slides examined at the same exposure as experimental slides (Fig. 3-5I).

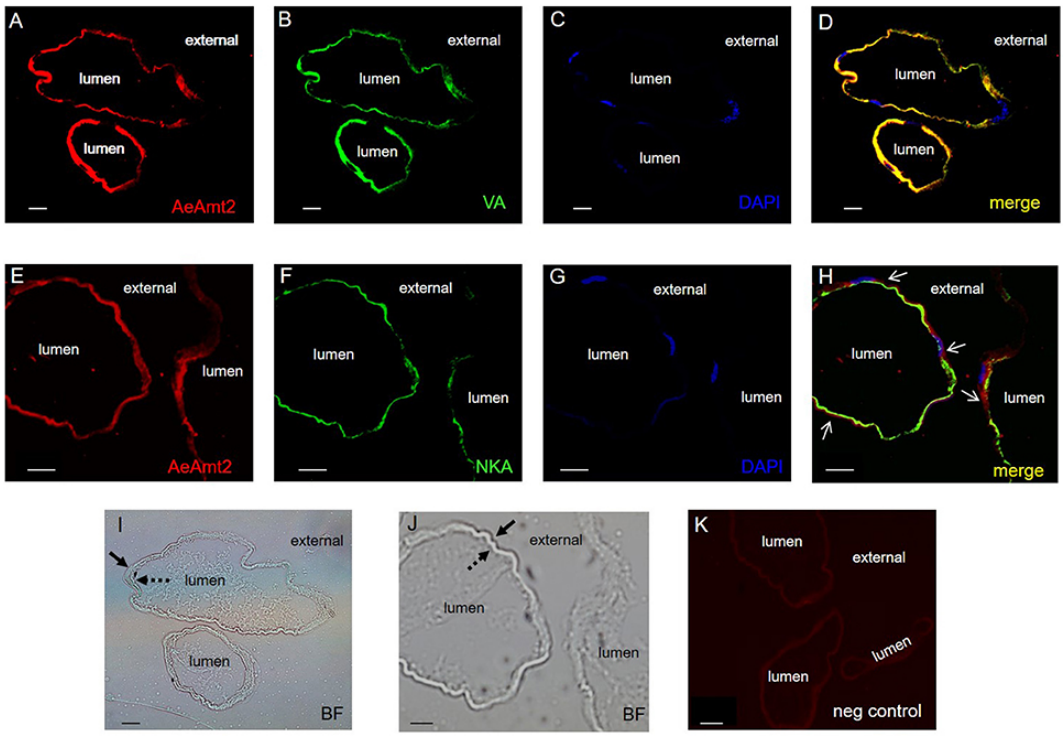

Figure 3- 5. Immunolocalization of AeAmt2 in the anal papillae of *A. aegypti* larvae. Representative paraffin-embedded cross sections of anal papillae showing immunoreactivity for: (**A,E**) AeAmt2 (red), (**B**) the V_0 subunit of V-type H^+ ATPase (VA, green), (**F**) Na^+-K^+-ATPase (NKA, green), and (**C,G**) nuclei staining with DAPI (blue). (**D**) Merged image of AeAmt2, VA, and DAPI, and (H) merged image of AeAmt2, NKA, and DAPI. White arrows indicate areas with nuclei, where separation of the apical and basolateral membranes is observed. Cross sections of anal papillae in brightfield (BF) corresponding to (**I**) panels A-D and (**J**) panels E-H, demonstrating the apical (solid arrows) and basolateral (dashed arrows). (K) Control cross section of anal papillae (primary antibodies omitted). Scale bars (**A-K**): 20 µM.

AeAmt2 dsRNA knockdown in the anal papillae and NH_4^+ flux

AeAmt2 protein abundance in the anal papillae was significantly reduced by dsRNA knockdown two days post treatment and returned to control levels thereafter (Fig. 3-6A). As a result, functional analyses in response to AeAmt2 protein knockdown was performed two days post dsRNA treatment. NH_4^+ efflux from the anal papillae was significantly reduced by 3-fold at two days post *AeAmt2* dsRNA treatment (Fig. 3-6B), but NH_4^+ haemolymph levels were unchanged in response to dsRNA-mediated AeAmt2 knockdown in the anal papillae (Fig. 3-6C). A summarized model of the current mechanisms of ammonia excretion in the anal papillae, reflecting the contribution of AeAmt2 in facilitating this process is provided (Fig. 3-7).

Effects of HEA on ammonia transporter expression within the anal papillae

The acute (6 hr), semi-chronic (48 hr), and chronic (7 days) changes that occur in ammonia transporter transcript and protein abundance in the anal papillae in response to HEA (5 mM NH_4Cl) were examined (Fig. 3-8, Fig. 3-9). Significant alterations to both mRNA and protein abundance were evident but did not always follow the same trends. The mRNA abundance of *AeAmt1, AeAmt2* and *AeRh50-2* followed the same trend in response to HEA; however, the abundance of their respective protein did not. After larvae were exposed to HEA for 6 hr, the mRNA abundance of *AeAmt1, AeAmt2* and *AeRh50-2* in anal papillae was 10, 3 and 20-fold higher than that of controls (Fig. 3-8). The protein abundance of AeAmt1 in anal papillae was significantly lower after 6 hr larval exposure to HEA compared to controls (Fig. 3-9A), whereas there was no difference in the protein abundance of AeAmt2 or the AeRh50s after 6 hr (Fig. 3-9B-C). When larvae were exposed for 48 hr to HEA there was no difference in mRNA abundance of any of the ammonia transporter genes in the anal papillae compared to controls (Fig. 3-8A-C); however, the protein abundance of AeAmt1 was significantly higher (Fig. 3-9A). When larvae were reared for 7 days in HEA (5 mM NH_4Cl), AeAmt1 protein abundance did

not change (Fig. 3-9A), however, significant decreases in AeAmt2 and AeRh50s protein abundance by 60% and 77%, respectively, was observed (Fig. 3-9B-C).

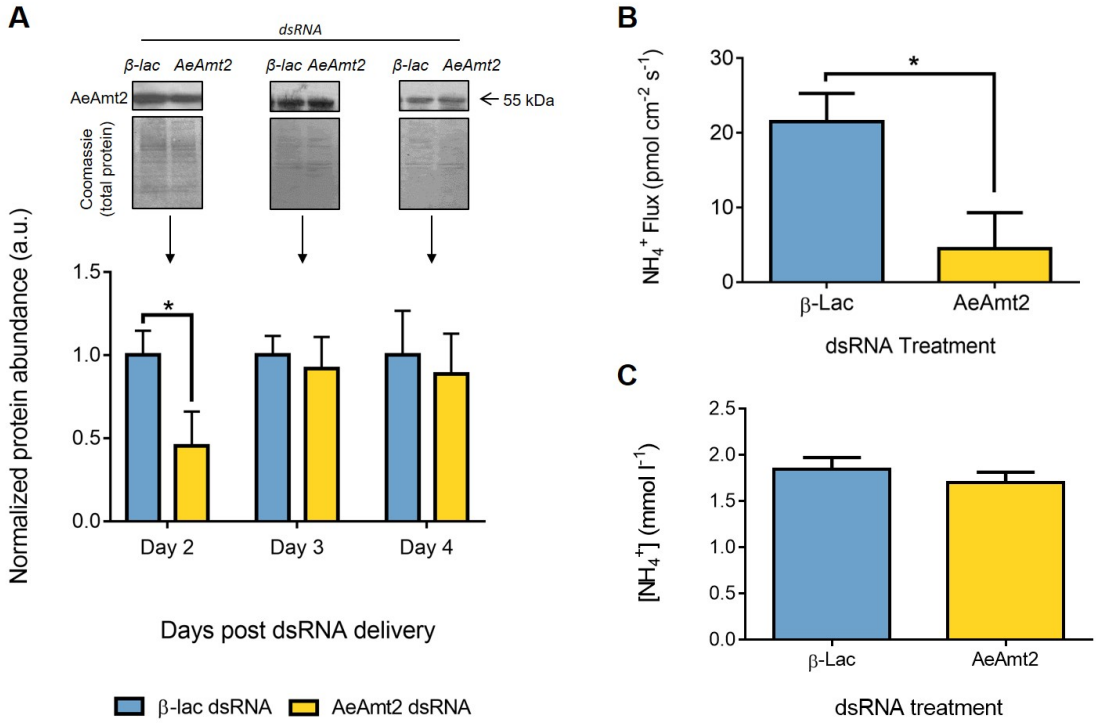

Figure 3- 6. Effects of *AeAmt2* dsRNA treatment on AeAmt2 abundance in the anal papillae, NH_4^+ excretion from the anal papillae, and NH_4^+ concentration in the haemolymph. (A) Representative Western blots (1 representative of 3 replicates) and densitometric analysis of AeAmt2 (55 kDa) in the anal papillae on days 2-4 following dsRNA treatment. Each group was normalized to Coomassie total protein staining, used as a loading control, and is expressed relative to the *β-lac* control group (assigned a value of 1, n=3). Asterisk denotes a significant difference in normalized protein expression compared to the *β-lac* control group based on an unpaired one-tailed t-test of relative density ($p = 0.0491$). (B) Scanning ion-selective electrode technique (SIET) measurements of NH_4^+ flux across the anal papillae epithelium 2 days post *β-lac* and *AeAmt2* dsRNA treatment (n=10). Asterisk denotes a significant difference in NH_4^+ efflux compared to the *β-lac* control group based on an unpaired t-test ($p = 0.0125$). (C) Ion-selective microelectrode measurements of NH_4^+ concentration in the haemolymph of larvae at 2 days post *β-lac* and *AeAmt2* dsRNA treatment (n = 10). Data is shown as mean values ± SEM.

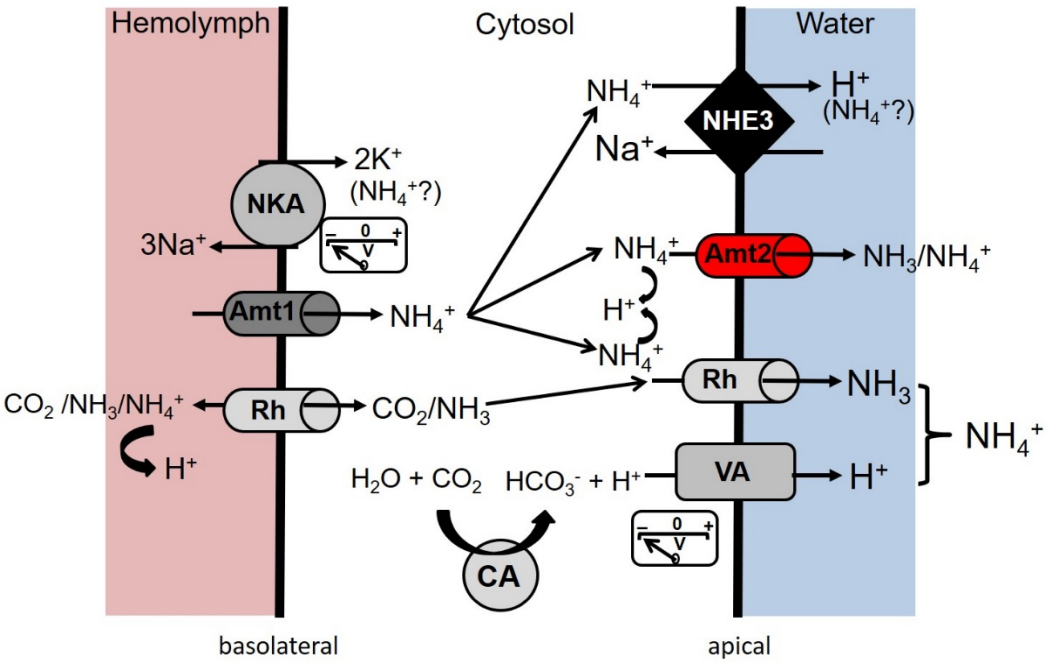

Figure 3- 7. Current model of putative transcellular ammonia (NH_3/NH_4^+) transport mechanisms in the anal papillae epithelium of *A. aegypti* larvae in freshwater conditions (adapted from Chasiotis et al., 2016). Basolateral NKA provides a cytosol negative voltage potential that could serve to drive NH_4^+ from the haemolymph to the cytosol through AeAmt1 (Amt1). Partial pressure gradient ($\Delta P_{NH3/CO2}$) driven entry of CO_2 and NH_3 into the cytosol occurs through one of the two Rh proteins (AeRh50-1 or AeRh50-2). On the apical side, AeAmt2 facilitates NH_3/NH_4^+ exit from the cytosol to the aqueous habitat either through NH_4^+ transport, NH_3 transport following NH_4^+ recruitment and deprotonation, or NH_3/H^+ co-transport. NH_4^+ in the cytosol may exit from the apical side to the aqueous habitat through the sodium-hydrogen exchanger 3 (NHE3) in exchange for Na^+. An Rh protein (Rh) on the apical side may function to excrete NH_3 through an ammonia-trapping mechanism exploiting an acidified boundary layer generated by apical VA and partly by NHE3. Cytoplasmic carbonic anhydrase (CA) contributes to the cytosol negative voltage potential and the maintenance of the acidified boundary layer by supplying H^+ for VA.

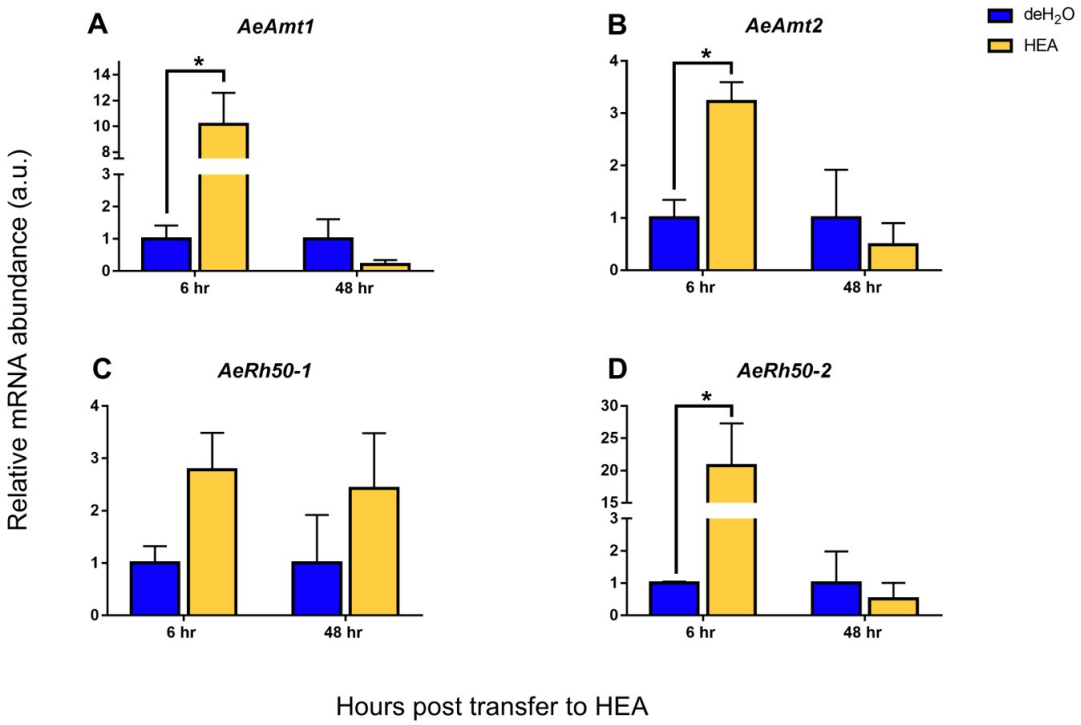

Figure 3- 8. Effects of high environmental ammonia (HEA) on transcript abundance of ammonia transporter genes in the anal papillae of *A. aegypti* larvae. Relative mRNA abundance of (A) *AeAmt1*, (B) *AeAmt2*, (C) *AeRh50-1*, and (D) *AeRh50-2* at 6 hr and 48 hr post transfer to dechlorinated tap water (deH_2O) or HEA (5mM NH_4Cl) (n = 3). Each gene was normalized to 18s ribosomal RNA abundance and expressed relative to levels in the control deH_2O group (assigned a value of 1). Data is shown as mean values ± SEM. Asterisks denote statistically significant differences between deH_2O and HEA groups (Unpaired t-test, $p \leq 0.05$).

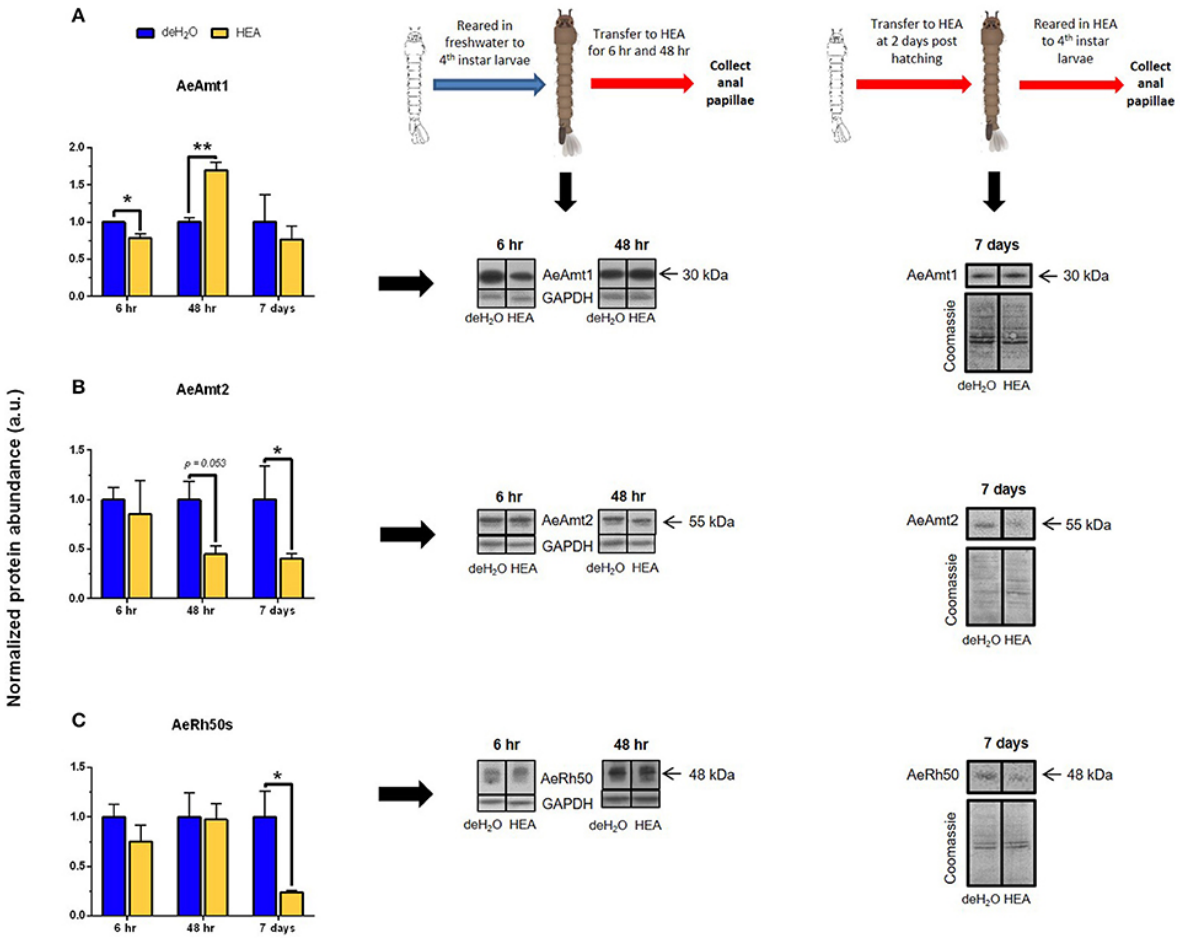

Figure 3- 9. Effects of high environmental ammonia (HEA) exposure on protein abundance of ammonia transporter genes in the anal papillae of fourth instar *A. aegypti* larvae. (A) AeAmt1 normalized monomer (30 kDa) abundance, (B) AeAmt2 normalized monomer (55 kDa) abundance, and (C) AeRh50s normalized monomer (48 kDa) abundance, and corresponding representative Western blots (right panels, 1 representative of 3 replicates) at 6 hr, 48 hr, and 7 days in dechlorinated tap water (deH_2O) or HEA (5mM NH_4Cl) (n = 3). For 6 hr and 48 hr HEA exposure, protein abundance was normalized to GAPDH abundance in the anal papillae. For 7-day HEA exposure, protein abundance was normalized to total protein (Coomassie). Normalized protein abundance for each protein is expressed relative to the control deH_2O group (assigned a value of 1). Data is shown as mean values ± SEM. Asterisks denote statistically significant differences between deH_2O and HEA groups (unpaired t-test, $p \leq 0.05$ [*], $p \leq 0.005$ [**]).

3.5 Discussion

A novel putative ammonia transporter of *Aedes aegypti*, AeAmt2

In the present study we have identified and characterized a novel putative ammonia transporter, *AeAmt2*, in the mosquito *A. aegypti*. This protein aligns with members of the family of ammonium transporters (Amt/MEP/Rh) from plants, bacteria, fungi, and vertebrates and shares high sequence homology with antennal-expressed AgAMT (Pitts et al., 2014) of the mosquito *A. gambiae*, the antennal-expressed DmAmt from the fruitfly *D. melanogaster* (Menuz et al., 2014), and an uncharacterized AMT3 in the mosquito *A. albopictus*. *A. aegypti* AeAmt2 and other insect Amts cluster with some electrogenic plant Amts (e.g. LeAMT1;2) in comparison to electroneutral bacterial Amts (e.g. AmtB) (See Fig. 3-1).

Similar to other Amt proteins, AeAmt2 is comprised of eleven transmembrane helices which vary in length (19-30 amino acids), and possesses the common extracellular N-terminus and intracellular C-terminus topology conserved in this family (Severi et al., 2007). The cytoplasmic C-terminus of AeAmt2 is notably longer in comparison to other members of the Amt/MEP/Rh family (Figs. 3-2, 3-3). Multiple sequence alignment of amino acid residues from *A. aegypti* Amt and Rh proteins, specifically AeAmt2, with other Amt/MEP proteins from plants, fungi, and bacteria demonstrate the presence of highly conserved residues which cluster around the narrow hydrophobic pore formed by the monomer (Khademi et al., 2004; Zheng et al., 2004). Similar to the bacterial AmtB, two highly conserved histidine residues (H229 and H406) are located at the N-termini of pseudo-symmetric transmembrane helices 5 and 10 of the AeAmt2 monomer (Zheng et al., 2004). The imidazole side chains of H229 and H406 and the acidic side chains of the preceding highly conserved aspartates (D221 and D398) play a role in hydrogen bonding and structural support, respectively (Zheng et al., 2004). Two highly conserved threonine residues (T315 and T356) among the Amt/MEP/Rh family which are present in AeAmt2 were suggested to be functionally relevant, contributing to a tightly-packed pore surface on the periplasmic side of the monomer (Khademi et al., 2004; Zheng et al., 2004). Furthermore,

mutation of a highly conserved tryptophan 148 residue (W198 in the present study) at the periplasmic entry of the hydrophobic pore of each monomer in Amt/MEP proteins, also conserved in transmembrane helix four of AeAmt2, demonstrated that the substrate of the channel is an ion and W148 is important for restricting the conductance and increasing selectivity of AmtB to NH_4^+ (Fong et al., 2007). Together, this structural information suggests that AeAmt2 possesses all the ammonia transporting capabilities of other known ammonia transporters.

Expression of AeAmt2 in the larval anal papillae

The anal papillae of *A. aegypti* larvae are important organs for the excretion of ammonia directly into the aquatic environment (Donini and O'Donnell, 2005). The syncytial epithelium of the anal papillae expresses the ammonia transporters, *AeAmt1*, *AeRh50-1* and *AeRh50-2* and knockdown experiments revealed their importance in ammonia transport by the anal papillae (Chasiotis et al., 2016; Chapter 2). We detected *AeAmt2* mRNA in the anal papillae but the transcript abundance of *AeAmt2* was significantly lower than that of the other ammonia transporters (Fig. 3-4). An antibody generated against a unique sequence in the predicted cytosolic region of the AeAmt2 protein detected a 55 kDa signal in western blots which was abolished by pre-incubation of the antisera with immunogenic peptide. Occasionally, 48 kDa and 63 kDa signals also appeared on blots (not shown). The 63 kDa signal corresponds to the predicted mass of the full-length sequence of the AeAmt2; however, since this only occasionally appeared while the 55 kDa band consistently appeared, we suggest that AeAmt2 may undergo post-translational processing. For example, the mature, functional bacterial AmtB protein is derived from cleavage of a signal sequence from the preprotein (Thornton et al., 2006). The dichotomy of relatively low *AeAmt2* mRNA levels but high protein abundance that we observed could simply be a result of low protein turnover, discussed below.

AMT/Mep/Rh protein monomers are known to trimerize in the membrane when functional (Gruswitz et al., 2010; Khademi et al., 2004; Zheng et al., 2004). We did not see the trimeric form in

western blots likely because of the denaturing conditions used, separating the trimeric forms into respective monomers (Severi et al., 2007). The significance of the trimeric arrangement of Amt/MEP/Rh proteins is attributed to interactions with the trimeric regulatory P_{II} protein, GlnB or its homolog GlnK in prokaryotes, with each monomer of the Amt/MEP/Rh trimer conducting substrate independently (Conroy et al., 2007; Coutts et al., 2002; Gruswitz et al., 2007). The regulatory P_{II} proteins are stable trimers with extended T-loops protruding from each monomer (Andrade and Einsle, 2007). In *Azotobacter vinelandii*, evidence of a direct association of GlnK with the cytoplasmic face of Amt-1 in response to high levels of ammonium in the cell was provided (Coutts et al., 2002), and physical obstruction of the pores of each monomer of AmtB from *E. coli* through the insertion of the T-loops of the trimeric GlnK deep into each pore was shown (Conroy et al., 2007; Gruswitz et al., 2007). Furthermore, the regulation of Amt proteins in plants through post-translational modifications may provide insight into the mechanisms of regulation for invertebrate Amts which is presently unknown. *A. thaliana* AtAmt1;2 activity is regulated by phosphorylation, whereby dephosphorylation of all monomers comprising the trimer is essential for activation of ammonia transport with each monomer functioning independently (Neuhäuser et al., 2007).

Studies on mutant variants at the conserved cytoplasmic C-terminus region of AmtB proceeding transmembrane helix 11 in *E. coli* may imply an important functional or structural role at this region (Severi et al., 2007). Mutants were either inhibited in their ammonia transporting capabilities or were completely void of activity altogether, suggesting a gating mechanism of the trimer through the carboxyl tail of a single monomer. Mutation of a single glycine residue (G502 in this study, Fig. 3-2) in the cytoplasmic C-terminus region, conserved in AeAmt2, within a single monomer led to cross-inhibition of NH_4^+ transport within the entire trimer in some plant Amts (Ludewig et al., 2003; Neuhäuser et al., 2007). The extensive cytoplasmic C-terminus of AeAmt2 in comparison to that of other members, possessing two putative N-glycosylation sites (Fig. 3-3) and approximately 14 putative phosphorylation sites [not shown; (Blom et al., 2004)], may suggest a more complex role of this region.

Regulation of AeAmt2 protein by any of the mechanisms described in other members of the Amt/MEP/Rh family outlined above are quite possible and require further investigation.

Immunohistochemistry on cross sections of anal papillae revealed that AeAmt2 is localized to the apical, water facing membrane of the epithelium. This is only the second cellular localization of an Amt protein in a functioning organ of an animal, and the first apical localization of an Amt protein in animals. An apical localization of AeAmt2 was unsurprising based on the distribution of Rh proteins in the anal papillae of *A. aegypti* larvae and the cortex cells of the rat kidney to opposite membranes (Chapter 2; Quentin, 2003).

Functional Consequences of AeAmt2 protein knockdown in the anal papillae of larvae

RNA interference techniques in combination with SIET were used to elucidate an ammonia-transporting function of AeAmt2 directly at the anal papillae. dsRNA-mediated knockdown of AeAmt2 protein, verified in anal papillae to be ~50% at two days post dsRNA treatment resulted in a significant decrease in NH_4^+ efflux from the anal papillae, indicating that AeAmt2 is functioning to facilitate ammonia excretion within this organ. The current working model of transcellular ammonia excretion in the syncytial anal papillae epithelium has been updated to reflect the contribution of AeAmt2 (Fig. 3-7) (Chasiotis et al., 2016). On the apical side of the epithelium, AeAmt2 likely facilitates NH_4^+ transport from the cytosol to the external surroundings for excretion by means of three possible mechanisms. Through electroneutral transport, an AeAmt2 trimer can recruit NH_4^+ from the cytosol where the proton is stripped and NH_3 traverses the triple pore for excretion (McDonald and Ward, 2016b; Soupene et al., 1998). By contrast, electrogenic transport of NH_4^+ at the apical membrane of papillae can occur through AeAmt2 function as a NH_4^+ uniporter, as a co-transporter for NH_3/H^+, or as an NH_4^+/H^+ antiporter (Ludewig et al., 2002; Neuhäuser and Ludewig, 2014). The former two possibilities are unlikely due to the cytosolic negative potential of the anal papillae epithelium, driven largely by apical VA. A mechanism of NH_4^+/H^+ antiport by AeAmt2 is more plausible, with VA

providing the H^+ gradient facilitating NH_4^+ exchange. In this manner, H^+ is moved along its own electrochemical gradient allowing NH_4^+ to be moved against its electrochemical gradient.

The knockdown of AeAmt2 is assumed to be systemic but this did not have an effect on haemolymph NH_4^+ levels. Similarly, the knockdown of AeRh50-2 did not affect haemolymph NH_4^+ levels in larvae (Chapter 2). In contrast, the knockdown of either AeAmt1 or AeRh50-1 results in alterations to haemolymph NH_4^+ levels whereby AeAmt1 knockdown causes an increase in NH_4^+, and AeRh50-1 knockdown results in decreased NH_4^+ levels and an acidification of the haemolymph (Chasiotis et al., 2016; Chapter 2). Our interpretation of these results assumes a key role of the anal papillae in ammonia excretion; however, we do not propose that these are the only organs responsible for ammonia excretion. Decreasing AeAmt1 expression in papillae would decrease ammonia clearance from the haemolymph across the basal side of the papillae epithelia resulting in the observed increase of NH_4^+ haemolymph levels. In contrast, decreasing AeRh50-1 expression could lead to decreased haemolymph NH_4^+ levels if AeRh50-1 is on the basal side of the papillae epithelia because it could mediate backflux of ammonia to the haemolymph when cytosolic levels become too high which may be expected since ammonia transport by AeAmt1 is energized by the activity of Na^+/K^+-ATPase (Chasiotis et al., 2016). The finding that haemolymph NH_4^+ levels are unaltered by AeAmt2 knockdown may suggest that disruption of apical pathways of ammonia excretion at the papillae are not as impactful to systemic haemolymph ammonia levels. This lends credence to the suggestion that AeRh50-2 may be expressed apically, as AeRh50-2 knockdown does not affect NH_4^+ haemolymph levels. Collectively, these results may also suggest that AeAmt1 function in the anal papillae is the most important for systemic regulation of ammonia levels with respect to the other three ammonia transporters expressed in the anal papillae.

Ammonia transporter expression in response to HEA

In HEA conditions, larvae are faced with the challenge of combatting significant inwardly directed partial pressure (ΔP_{NH3}) and NH_4^+ electrochemical gradients at the anal papillae and other osmoregulatory organs (Weihrauch et al., 2012a). Traditionally thought to be a passive process in aquatic animals, active ammonia excretion against a 4-8 fold inwardly directed ammonia gradient has been well documented in the gills of crabs (Weihrauch et al., 2004). We quantified the expression of AeAmts and AeRh50s at both the transcript and protein level in the anal papillae of larvae exposed to acute (6 hr), semi-chronic (48 hr) and long term (7 days) HEA exposure (5mM NH_4Cl). Significant increases in the mRNA abundance of both *AeAmts* as well as *AeRh50-2* in the anal papillae were observed after 6 h exposure to HEA (see Fig. 3-8), as well as a decrease in AeAmt1 protein levels (see Fig. 3-9). After 48 hr in HEA, mRNA abundance of both AeAmts and both AeRh50s were no different than those in control larvae (Fig. 3-8); however, an increase in basolateral AeAmt1 and a decrease in apical AeAmt2 protein abundance in the anal papillae was observed when compared with levels in control larvae (Fig. 3-9). This result was similar to that found for a 7-day HEA exposure in that AeAmt2 protein abundance decreased relative to controls and AeAmt1 protein abundance remained unchanged (Fig. 3-9). The finding that expression of a basolateral Amt (AeAmt1) is either unaffected or increases, and an apical Amt (AeAmt2) decreases simultaneously in response to HEA suggests a mechanism of ammonia clearance from the haemolymph whilst limiting NH_4^+ influx at the apical membrane. This may imply that AeAmt1 is the key driver of ammonia excretion in the anal papillae irrespective of external NH_4^+ levels. AeAmt1 function is likely driven by NKA activity (secondary active transport), as supported by pharmacological evidence (see Chasiotis et al., 2016) and would not be affected by changing NH_3/NH_4^+ gradients, whereas a decrease in apical transporter expression may limit NH_3/NH_4^+ influx into the anal papillae cytosol in HEA conditions. We were unable to discern specific changes in AeRh50-1 and AeRh50-2 protein abundance because the antibody detects both (Chapter 2).

Nevertheless, it may be reasoned that the increase in *AeRh50-2* mRNA abundance after 6hr in HEA led to changes in protein abundance of AeRh50-2.

Overall, the immediate and long term responses to HEA is reflective of the importance of these transporters in regulating ammonia excretion within the anal papillae against an inwardly directed gradient, where larvae have been shown to tolerate NH_4^+ haemolymph levels of between 1-3 mmol l^{-1} under normal freshwater conditions (Chasiotis et al., 2016; Chapter 2). It is also very likely that due to post-translational modifications or conformational changes regulating Amt and Rh protein activity, turnover numbers of these proteins are limited even in HEA conditions. In this manner, changes in the activity of Amt and Rh proteins may be more indicative of their role in facilitating ammonia excretion in response to HEA.

In general, *A. aegypti* larvae appear to be more tolerant of high ammonia haemolymph levels and HEA in comparison to other aquatic invertebrates (O'Donnell and Donini, 2017; Weihrauch et al., 2004). HEA levels of 5 mmol l^{-1} NH_4Cl and above are lethal to the freshwater planarian, *Schmidtea mediterranea*, within 48 hours (Weihrauch et al., 2012b). However, a significant increase in the mRNA of a Rh-like transporter upon exposure to 1 mmol l^{-1} for 48 hr was reported. In the freshwater leech *Nephelopsis obscura*, increases in ammonia excretion within 1 h of exposure to HEA (1 mmol l^{-1} NH_4Cl) was attributed to increases in metabolic rates due to stress, and mRNA levels of NoRhp, an Rh transporter, in the gills decreased after 7 days in HEA (Quijada-Rodriguez et al., 2015). Evidence that apical AeAmt2 and AeRh50 protein decreases in response to long term exposure to HEA may suggest a regulatory mechanism which prevents both chemical and/or electrochemical driven influx of ammonia at the anal papillae.

Summary

The quality of larval habitats for egg hatching and development is a strong determinant of the selection of breeding sites for female *A. aegypti* (Chitolina et al., 2016). Vector control and

surveillance programs are directly influenced by where mosquitoes breed (Banerjee et al., 2015; Barrera et al., 2008), highlighting the importance of understanding how *A. aegypti* can adapt to ammonia-rich raw sewage in septic tanks. Septic tank usage is common and widespread in tropical regions where *A. aegypti* are most prevalent which may explain the persistence of disease during dry periods or following control measures, such as removing artificial water containers (Burke et al., 2010). The aim of this study was to further our understanding of the molecular and physiological mechanisms of ammonia excretion in *A. aegypti* larvae attributing to their tolerance of HEA.

We have identified and characterized a novel ammonia transporter, *AeAmt2*, belonging to the Amt/MEP/Rh family of conserved ammonia transporters in bacteria, plants and animals. This is only the second characterization and localization of an Amt protein in an animal. *AeAmt2* is expressed in the osmoregulatory anal papillae which are important organs for the excretion of ammonia directly from the haemolymph of *A. aegypti* larvae (Donini and O'Donnell, 2005). The apical localization of AeAmt2 in the anal papillae epithelium of *A. aegypti* larvae is the first apical localization of an Amt protein in animals. AeAmt2 plays a significant role in facilitating ammonia excretion from the anal papillae demonstrated by dsRNA-mediated knockdown studies using SIET. Furthermore, the involvement of AeAmt1, AeAmt2, AeRh50-1, and AeRh50-2 in facilitating ammonia excretion and the maintenance of ammonia haemolymph levels in response to HEA was investigated, providing insight into the tolerance of *A. aegypti* larvae to high ammonia. This is one of few comprehensive studies of the physiological mechanisms underlying ammonia excretion in *A. aegypti* larvae permitting them to survive and thrive in HEA habitats such as septic tanks.

3.6 References

Andrade, S. L. A. and Einsle, O. (2007). The Amt/Mep/Rh family of ammonium transport proteins (Review). *Mol. Membr. Biol.* **24**, 357–365.

Baday, S., Orabi, E. A., Wang, S., Lamoureux, G. and Bernèche, S. (2015). Mechanism of NH_4^+ Recruitment and NH_3 Transport in Rh Proteins. *Structure* **23**, 1550–1557.

Banerjee, S., Mohan, S., Saha, N., Mohanty, S. P., Saha, G. K. and Aditya, G. (2015). Pupal productivity & nutrient reserves of *Aedes* mosquitoes breeding in sewage drains & other habitats of Kolkata, India: Implications for habitat expansion & vector management. *Indian J. Med. Res.* **142**, 87–94.

Barrera, R., Amador, M., Diaz, A., Smith, J., Munoz-Jordan, J. L. and Rosario, Y. (2008). Unusual productivity of *Aedes aegypti* in septic tanks and its implications for dengue control. *Med. Vet. Entomol.* **22**, 62–69.

Blom, N., Sicheritz-pontén, T., Gupta, R., Gammeltoft, S. and Brunak, S. (2004). Prediction of post-translational glycosylation and phosphorylation of proteins from the amino acid sequence. 1633–1649.

Burke, R. L., Barrera, R., Lewis, M., Kluchinsky, T. and Claborn, D. (2010). Septic tanks as larval habitats for the mosquitoes *Aedes aegypti* and *Culex quinquefasciatus* in Playa-Playita, Puerto Rico. *Med. Vet. Entomol.* **24**, 117–123.

Chasiotis, H. and Kelly, S. P. (2008). Occludin immunolocalization and protein expression in goldfish. *J. Exp. Biol.* **211**, 1524–1534.

Chasiotis, H., Ionescu, A., Misyura, L., Bui, P., Fazio, K., Wang, J., Patrick, M., Weihrauch, D. and Donini, A. (2016). An animal homolog of plant Mep/Amt transporters promotes ammonia excretion by the anal papillae of the disease vector mosquito *Aedes aegypti*. *J. Exp. Biol.* **219**, 1346–55.

Chen, J. C. and Lin, C. Y. (1992). Lethal effects of ammonia on *Penaeus chinensis* Osbeck juveniles at different salinity levels. *J. Exp. Mar. Bio. Ecol.* **156**, 139–148.

Chitolina, R. F., Anjos, F. A., Lima, T. S., Castro, E. A. and Costa-Ribeiro, M. C. V. (2016). Raw sewage as breeding site to *Aedes (Stegomyia) aegypti* (Diptera, culicidae). *Acta Trop.* **164**, 290–296.

Conroy, M. J., Durand, A., Lupo, D., Li, X.-D., Bullough, P. A., Winkler, F. K. and Merrick, M. (2007). The crystal structure of the *Escherichia coli* AmtB-GlnK complex reveals how GlnK regulates the ammonia channel. *Proc. Natl. Acad. Sci. U. S. A.* **104**, 1213–1218.

Coutts, G., Thomas, G., Blakey, D. and Merrick, M. (2002). Membrane sequestration of the signal transduction protein GlnK by the ammonium transporter AmtB. *EMBO J.* **21**, 536–545.

Cruz, M. J., Sourial, M. M., Treberg, J. R., Fehsenfeld, S., Adlimoghaddam, A. and Weihrauch, D. (2013). Cutaneous nitrogen excretion in the African clawed frog *Xenopus laevis*: Effects of high environmental ammonia (HEA). *Aquat. Toxicol.* **136**–**137**, 1–12.

Donini, A. and O'Donnell, M. J. (2005). Analysis of Na^+, Cl^-, K^+, H^+ and NH_4^+ concentration gradients adjacent to the surface of anal papillae of the mosquito *Aedes aegypti*: application of self-referencing ion-selective mi. *J. Exp. Biol.* **208**, 603–10.

Durant, A. C., Chasiotis, H., Misyura, L. and Donini, A. (2017). *Aedes aegypti* Rhesus glycoproteins contribute to ammonia excretion by larval anal papillae. *J. Exp. Biol.* **220**, 588–596.

Eaton, S. L., Roche, S. L., Llavero Hurtado, M., Oldknow, K. J., Farquharson, C., Gillingwater, T. H. and Wishart, T. M. (2013). Total protein analysis as a reliable loading control for quantitative fluorescent western blotting. *PLoS One* **8**, 1–9.

Edwards, H. A. and Harrison, J. B. (1983). An osmoregulatory syncytium and associated cells in a freshwater mosquito. *Tissue Cell* **15**, 271–280.

Fong, R. N., Kim, K.-S., Yoshihara, C., Inwood, W. B. and Kustu, S. (2007). The W148L

substitution in the *Escherichia coli* ammonium channel AmtB increases flux and indicates that the substrate is an ion. *Proc. Natl. Acad. Sci. U. S. A.* **104**, 18706–11.

Gruswitz, F., O'Connell, J. and Stroud, R. M. (2007). Inhibitory complex of the transmembrane ammonia channel, AmtB, and the cytosolic regulatory protein, GlnK, at 1.96 A. *Proc. Natl. Acad. Sci.* **104**, 42–47.

Gruswitz, F., Chaudhary, S., Ho, J. D., Schlessinger, A., Pezeshki, B., Ho, C.-M., Sali, A., Westhoff, C. M. and Stroud, R. M. (2010). Function of human Rh based on structure of RhCG at 2.1 A. *Proc. Natl. Acad. Sci.* **107**, 9638–9643.

Hung, C. Y. C., Tsui, K. N. T., Wilson, J. M., Nawata, C. M., Wood, C. M. and Wright, P. a (2007). Rhesus glycoprotein gene expression in the mangrove killifish *Kryptolebias marmoratus* exposed to elevated environmental ammonia levels and air. *J. Exp. Biol.* **210**, 2419–2429.

Jonusaite, S., Kelly, S. P. and Donini, A. (2016). The response of claudin-like transmembrane septate junction proteins to altered environmental ion levels in the larval mosquito *Aedes aegypti*. *J. Comp. Physiol. B Biochem. Syst. Environ. Physiol.* **186**, 589–602.

Kell Reid, G. (1961). *Ecology of inland waters and estuaries*. New York: Reinhold.

Khademi, S., O'Connell III, J., Remis, J., Robles-Colmenares, Y., Miercke, L. J. W. and Stroud, R. M. (2004). Mechanism of ammonia transport by Amt/MEP/Rh: Structure of AmtB at 1.35 angstroms. *Science (80-.).* **305**, 1587–1594.

Kumar, S., Stecher, G. and Tamura, K. (2016). MEGA7: Molecular Evolutionary Genetics Analysis Version 7.0 for Bigger Datasets. *Mol. Biol. Evol.* **33**, 1870–1874.

Kustu, S. and Inwood, W. (2006). Biological gas channels for NH_3 and CO_2: evidence that Rh (Rhesus) proteins are CO_2 channels. *Transfus. Clin. Biol.* **13**, 103–110.

Li, X., Jayachandran, S., Nguyen, H.-H. T. and Chan, M. K. (2007). Structure of the *Nitrosomonas europaea* Rh protein. *Proc. Natl. Acad. Sci. U. S. A.* **104**, 19279–84.

Ludewig, U., Von Wiren, N. and Frommer, W. B. (2002). Uniport of NH_4^+ by the root hair plasma membrane ammonium transporter LeAMT1;1. *J. Biol. Chem.* **277**, 13548–13555.

Ludewig, U., Wilken, S., Wu, B., Jost, W., Obrdlik, P., Bakkoury, M. El, Marini, A., Andre, B., Hamacher, T., Boles, E., et al. (2003). Homo- and hetero-oligomerization of Ammonium Transporter-1 NH_4^+ Uniporters. **278**, 45603–45610.

Lupo, D., Li, X.-D., Durand, A., Tomizaki, T., Cherif-Zahar, B., Matassi, G., Merrick, M. and Winkler, F. K. (2007). The 1.3-A resolution structure of *Nitrosomonas europaea* Rh50 and mechanistic implications for NH_3 transport by Rhesus family proteins. *Proc. Natl. Acad. Sci. U. S. A.* **104**, 19303–19308.

Marini, A. M., Vissers, S., Urrestarazu, A. and Andre, B. (1994). Cloning and expression of the MEP1 gene encoding an ammonium transporter in *Saccharomyces cerevisiae*. *Embo J* **13**, 3456–3463.

Marini, A. M., Soussi-Boudekou, S., Vissers, S. and Andre, B. (1997). A family of ammonium transporters in *Saccharomyces cerevisiae*. *Mol. Cell. Biol.* **17**, 4282–93.

Marini, a M., Matassi, G., Raynal, V., André, B., Cartron, J. P. and Chérif-Zahar, B. (2000). The human Rhesus-associated RhAG protein and a kidney homologue promote ammonium transport in yeast. *Nat. Genet.* **26**, 341–344.

Martin, M., Fehsenfeld, S., Sourial, M. M. and Weihrauch, D. (2011). Effects of high environmental ammonia on branchial ammonia excretion rates and tissue Rh-protein mRNA expression levels in seawater acclimated Dungeness crab *Metacarcinus magister*. *Comp. Biochem. Physiol. - A Mol. Integr. Physiol.* **160**, 267–277.

Mayer, M., Schaaf, G., Mouro, I., Lopez, C., Colin, Y., Neumann, P., Cartron, J.-P. and Ludewig, U. (2006). Different transport mechanisms in plant and human AMT/Rh-type ammonium transporters. *J. Gen. Physiol.* **127**, 133–144.

McDonald, T. R. and Ward, J. M. (2016). Evolution of Electrogenic Ammonium Transporters

(AMTs). *Front. Plant Sci.* **7**, 352.

Menuz, K., Larter, N. K., Park, J. and Carlson, J. R. (2014). An RNA-Seq screen of the *Drosophila* antenna identifies a transporter necessary for ammonia detection. *PLoS Genet.* **10**,.

Mitchell, M. J. and Wood, R. J. (1984). Genetic variation in tolerance of ammonium chloride in *Aedes aegypti*. *Mosq. News* **44**, 498–501.

Neuhäuser, B. and Ludewig, U. (2014). Uncoupling of ionic currents from substrate transport in the plant ammonium transporter AtAMT1;2. *J. Biol. Chem.* **289**, 11650–11655.

Neuhäuser, B., Dynowski, M., Mayer, M. and Ludewig, U. (2007). Regulation of NH_4^+ transport by essential cross talk between AMT monomers through the carboxyl tails. *Plant Physiol.* **143**, 1651–1659.

Omasits, U., Ahrens, C. H., M??ller, S. and Wollscheid, B. (2014). Protter: Interactive protein feature visualization and integration with experimental proteomic data. *Bioinformatics* **30**, 884–886.

Patrick, M. L., Aimanova, K., Sanders, H. R. and Gill, S. S. (2006). P-type Na^+/K^+-ATPase and V-type H^+-ATPase expression patterns in the osmoregulatory organs of larval and adult mosquito *Aedes aegypti*. *J. Exp. Biol.* **209**, 4638–51.

Pfaffl, M. (2004). Quantification strategies in real-time PCR. *A-Z Quant. PCR* 87–112.

Pitts, R. J., Derryberry, S. L., Pulous, F. E. and Zwiebel, L. J. (2014). Antennal-expressed ammonium transporters in the malaria vector mosquito *Anopheles gambiae*. *PLoS One* **9**,.

Quentin, F. (2003). RhBG and RhCG, the putative ammonia transporters, are expressed in the same cells in the distal nephron. *J. Am. Soc. Nephrol.* **14**, 545–554.

Quijada-Rodriguez, A. R., Treberg, J. R. and Weihrauch, D. (2015). Mechanism of ammonia excretion in the freshwater leech *Nephelopsis obscura*: characterization of a primitive Rh protein and effects of high environmental ammonia. *Am. J. Physiol. Regul. Integr. Comp. Physiol.* ajpregu.00482.2014.

Ramasamy, R., Surendran, S. N., Jude, P. J., Dharshini, S. and Vinobaba, M. (2011). Larval development of *Aedes aegypti* and *Aedes albopictus* in peri-urban brackish water and its implications for transmission of arboviral diseases. *PLoS Negl Trop Dis* **5**, e1369.

Sanders, H. R., Evans, A. M., Ross, L. S. and Gill, S. S. (2003). Blood meal induces global changes in midgut gene expression in the disease vector, *Aedes aegypti*. *Insect Biochem. Mol. Biol.* **33**, 1105–1122.

Severi, E., Javelle, A. and Merrick, M. (2007). The conserved carboxy-terminal region of the ammonia channel AmtB plays a critical role in channel function. *Mol. Membr. Biol.* **24**, 161–171.

Singh, A. D., Wong, S., Ryan, C. P. and Whyard, S. (2013). Oral delivery of double-stranded RNA in larvae of the yellow fever mosquito, *Aedes aegypti*: implications for pest mosquito control. *J. Insect Sci.* **13**, 69.

Sohal, R. S. and Copeland, E. (1966). Ultrastructural variations in the anal papillae of *Aedes aegypti* (L.) at different environment salinities. *J Insect Physiol* **12**, 429–434.

Somers, G., Brown, J. E., Barrera, R. and Powell, J. R. (2011). Genetics and morphology of *Aedes aegypti* (Diptera: Culicidae) in septic tanks in Puerto Rico. *J. Med. Entomol.* **48**, 1095–1102.

Soupene, E., He, L., Yan, D. and Kustu, S. (1998). Ammonia acquisition in enteric bacteria: physiological role of the ammonium/methylammonium transport B (AmtB) protein. *Proc. Natl. Acad. Sci. U. S. A.* **95**, 7030–4.

Thornton, J., Blakey, D., Scanlon, E. and Merrick, M. (2006). The ammonia channel protein AmtB from *Escherichia coli* is a polytopic membrane protein with a cleavable signal peptide. *FEMS Microbiol. Lett.* **258**, 114–120.

Weihrauch, D. and Donnell, M. O. (2017). *Acid-Base Balance and Nitrogen Excretion in Invertebrates*.

Weihrauch, D. and O'Donnell, M. J. (2015). Links between osmoregulation and nitrogen-excretion in insects and crustaceans. *Integr. Comp. Biol.* **55**, 816–829.

Weihrauch, D., Morris, S. and Towle, D. W. (2004). Ammonia excretion in aquatic and terrestrial crabs. *J. Exp. Biol.* **207**, 4491–4504.

Weihrauch, D., Donini, A. and O'Donnell, M. J. (2012a). Ammonia transport by terrestrial and aquatic insects. *J. Insect Physiol.* **58**, 473–487.

Weihrauch, D., Chan, a. C., Meyer, H., Doring, C., Sourial, M. and O'Donnell, M. J. (2012b). Ammonia excretion in the freshwater planarian *Schmidtea mediterranea*. *J. Exp. Biol.* **215**, 3242–3253.

Wood, C., Part, P. and Wright, P. (1995). Ammonia and urea metabolism in relation to gill function and acid-base balance in a marine elasmobranch, the spiny dogfish (*Squalus acanthias*). *J. Exp. Biol.* **198**, 1545–58.

Wright, P. (1995). Nitrogen excretion : three end products , many physiological roles. *J. Exp. Biol.* **281**, 273–281.

Wu, Y., Zheng, X., Zhang, M., He, A., Li, Z. and Zhan, X. (2010). Cloning and functional expression of Rh50-like glycoprotein, a putative ammonia channel, in *Aedes albopictus* mosquitoes. *J. Insect Physiol.* **56**, 1599–1610.

Zheng, L., Kostrewa, D., Bernèche, S., Winkler, F. K. and Li, X.-D. (2004). The mechanism of ammonia transport based on the crystal structure of AmtB of *Escherichia coli*. *Proc. Natl. Acad. Sci. U. S. A.* **101**, 17090–5.

Chapter Four

Evidence that Rh proteins in the anal papillae of the freshwater mosquito *Aedes aegypti* are involved in the regulation of acid base balance in elevated salt and ammonia environments

This chapter has been published and reproduced with permission:

Durant A.C., Donini A (2018) Evidence that Rh proteins in the anal papillae of the freshwater mosquito *Aedes aegypti* are involved in the regulation of acid base balance in elevated salt and ammonia environments. *Journal of Experimental Biology* 221, doi: 10.1242/jeb.186866

4.1 Summary

Aedes aegypti commonly inhabit ammonia rich sewage effluents in tropical regions of the world where the adults are responsible for the spread of disease. Studies have shown the importance of the anal papillae of *Aedes aegypti* in ion uptake and ammonia excretion. The anal papillae express ammonia transporters and Rh proteins which are involved in ammonia excretion and studies have primarily focused on understanding these mechanisms in freshwater. In this study, effects of rearing larvae in salt (5 mmol l^{-1} NaCl) or ammonia (5 mmol l^{-1} NH_4Cl) on physiological endpoints of ammonia and ion regulation are assessed. In anal papillae of NaCl reared larvae, Rh protein expression increased, NHE3 transcript abundance decreased and NH_4^+ excretion increased, and this coincided with decreased haemolymph [NH_4^+] and pH. We propose that under these conditions larvae excrete more NH_4^+ through Rh proteins as a means of eliminating acid from the haemolymph. In anal papillae of NH_4Cl reared larvae, expression of an apical ammonia transporter and the Rh proteins decreased, the activities of NKA and VA decreased and increased, respectively and this coincided with haemolymph acidification. The results present evidence for a role of Rh proteins in acid base balance in response to elevated levels of salt, whereby ammonia is excreted as an acid equivalent.

4.2 Introduction

Like many aquatic invertebrate and vertebrate animals, the larvae of most mosquito species inhabit freshwater systems which can vary remarkably in water chemistry, including in ionic composition and pH (Patrick et al., 2002b; Patrick et al., 2002a). While freshwater NaCl concentrations can range between 0 to 8 mmol l^{-1}, mosquito larvae maintain much higher haemolymph ion levels in comparison to the surrounding environment ($[Na^+]$ = 85.1±2.2 mmol l^{-1} and $[Cl^-]$ = 65.8±5.2 mmol l^{-1}) (Donini and O'Donnell, 2005; Patrick et al., 2002a). This presents a challenge to haemolymph ion homeostasis in a relatively hypo-osmotic environment. Strategies of counteracting ion loss and water gain have been investigated in aquatic dipteran larvae, which have proven to be effective osmoregulators in varying environmental salinity (Akhter et al., 2017; Jonusaite et al., 2011; Nguyen and Donini, 2010; Patrick et al., 2001). Furthermore, aquatic invertebrates, and insects in particular, are among the most pH tolerant animals on the planet (Matthews, 2017). Mosquito larvae have been shown to tolerate chronic exposure to highly alkaline or acidic water (pH 4 to pH 11) in nature and under laboratory conditions with minor effects on haemolymph pH, growth, and development (Clark, 2004). Acidified water coupled to ion poor conditions can be particularly challenging, as the excretion of acid-base equivalents is coupled to the uptake of certain ions which are limited (Vangenechten et al., 1989).

The regulation of haemolymph ion composition and pH, which are often linked, is essential for homeostasis and survival in freshwater systems with varying water chemistry. In addition to ventilation and buffering strategies, aquatic insects regulate their haemolymph pH and osmolarity through the active uptake and excretion of ions and acid-base equivalents internally between the haemolymph and gut lumen, or with the external environment (Matthews, 2017). For most air-breathing aquatic insects, such as mosquito larvae, ions and acid-base equivalents are absorbed or excreted directly between the haemolymph and the surroundings through ion-permeable epithelia. This is unlike water breathing

aquatic insects, such as the aquatic nymphs of mayflies, which possess ionocyte-dense tracheal gills for active ion-transport (Nowghani et al., 2017).

Many air-breathing aquatic dipteran larvae possess dedicated iono- and osmoregulatory organs known as anal papillae (Koch, 1938; Wigglesworth, 1932). The four anal papillae in larval *A. aegypti* are elongate sac-like projections of the cuticle that surround the anal opening, with a lumen that is continuous with the hemocoel of the body (Copeland, 1964; Sohal and Copeland, 1966). The thin cuticle, syncytial epithelium, and relatively small surface area of the anal papillae restricts ion and water movement to this organ, while a relatively impermeable integument covers the rest of the body (Wigglesworth, 1932). These morphological features enable the anal papillae to function as major ion exchange organs. The anal papillae are the site of Na^+, Cl^-, and K^+ uptake and the excretion of acid-base equivalents (H^+, NH_4^+, HCO_3^-) in mosquito larvae (Donini and O'Donnell, 2005; Patrick et al., 2001; Stobbart, 1965; Stobbart, 1971). However, until more recently there remained limited evidence of a role for the anal papillae in pH homeostasis (Clark et al., 2007).

Ammonia (NH_3/NH_4^+) is generated through metabolic processes, primarily the deamination of amino acids, and can be used as an acid-base equivalent (Onken and Moffett, 2017). At physiological pH (~7.4; pKa = 9.4)), only 1.7% of total ammonia is present as NH_3 (Weiner and Verlander, 2017). The predominant ionic form, NH_4^+, acts as an H^+ equivalent that can alter intracellular and extracellular pH when transported (Weihrauch and Allen, 2018a). However, the extent to which ammonia transport is used to mitigate changes in pH of internal fluids of aquatic invertebrates remains poorly understood. Evidence of a link between ion transport, pH homeostasis, and ammonia excretion in the anal papillae epithelium of *A. aegypti* larvae has been shown through electrophysiology and pharmacological studies. Upon exposure of *A. aegypti* larvae to 30% seawater, haemolymph Na^+, Cl^-, and H^+ concentrations increased within hours, coupled with a decrease in Na^+ and Cl^- uptake at the anal papillae (Donini et al., 2007). Independent uptake of Na^+ and Cl^- was also suggested based on differences in measured

uptake kinetics of each ion. The inhibition of basolateral Na^+/K^+-ATPase (NKA), which functions to maintain a negative cell potential and low [Na^+] in the cytosol, causes significant reductions in NH_4^+ efflux at the anal papillae (Chasiotis et al., 2016; Patrick et al., 2006a). The efflux of H^+ driven by apical V-type-H^+-ATPase (VA) contributes to the negative intracellular voltage generated by NKA, facilitating NH_3 efflux likely through an ammonia trapping mechanism at the apical membrane whereby NH_3 combines with H^+ on the external side which maintains an NH_3 gradient favoring excretion (Chasiotis et al., 2016; Chapter 2; Weihrauch et al., 2009). Inhibition of VA also results in a significant reduction in ammonia excretion at the anal papillae epithelium, implicating VA and NKA in the process of ammonia excretion which is likely to stem from establishing the cytosol negative electrical potential and ammonia trapping. Additionally, the negative cytosolic voltage generated by NKA and VA is important in energizing Na^+ uptake in other aquatic invertebrates (Onken, 2003; Onken and Riestenpatt, 2002). Interestingly, inhibition of an apical Na^+/H^+ exchanger 3 (NHE3, SLC 9 family) decreases NH_4^+ excretion at the anal papillae in *A. aegypti* larvae, suggesting that this transporter may either contribute to ammonia trapping or perhaps directly conduct NH_4^+ across the apical membrane (Chasiotis et al., 2016).

A. aegypti possess two homologs of the vertebrate Rhesus glycoproteins (Rh proteins), *AeRh50-1* and *AeRh50-2*, which have been localized to the apical and basolateral membranes of the anal papillae epithelium (Chapter 2). It has been suggested that Rh proteins may transport NH_3 as well as CO_2; however, the specific transport substrate(s) of Rh proteins remains to be determined (Kustu and Inwood, 2006; Weihrauch et al., 2004; Weiner and Verlander, 2017). In *A. aegypti* larvae, knockdown studies of both AeRh50-1 and AeRh50-2 proteins results in significant reductions in ammonia efflux (Chapter 2). A decrease in [NH_4^+] in the haemolymph coupled with an acidification of haemolymph was also observed in response to *AeRh50-1* knockdown and it was suggested that this may occur if AeRh50-1 was capable of CO_2 transport. The partial pressure gradient of CO_2 plays a significant role in the acid-base balance of body fluids of aquatic animals (Nawata and Wood, 2008), and in this

respect it was speculated that AeRh50-1 may mediate CO_2 excretion through the anal papillae with dsRNA-mediated knockdown resulting in accumulation of CO_2 in the haemolymph; however, no measurements of CO_2 have been performed in relation to these studies (Chapter 4).

There is currently little known about the transport mechanisms used by mosquito larvae to achieve their acid-base balance, with some evidence demonstrating a role of the anal papillae in pH homeostasis (Clark et al., 2007). Given the lack of information on the contribution of ammonia transport and the function of the anal papillae in acid-base balance in mosquito larvae, as well as the link between ion uptake and excretion of acid and base equivalents, we examined the transport rates and haemolymph levels of Na^+, NH_4^+, and pH in response to HEA and moderate levels of NaCl (approximately 10 times higher than freshwater levels). We hypothesized that haemolymph pH regulation is partly achieved through modulation of NH_4^+ excretion, an H^+ equivalent, by the anal papillae. If this occurs, then increased NH_4^+ excretion at the anal papillae in conjunction with acidification of the haemolymph might be observed. Furthermore, changes in the magnitude of NH_4^+ excretion by anal papillae may be representative of changes in ammonia transporter expression.

4.3 Materials and Methods

Animals

Aedes aegypti larvae (Liverpool) were obtained from a colony reared in the Department of Biology, York University (Toronto, ON, Canada). Larvae were reared in dechlorinated tap water (deH_2O) at room temperature (21°C) on a 12h:12h light:dark cycle. Larvae were fed daily with a 1:1 solution of liver powder and yeast in water. Rearing water was refreshed every other day. For rearing treatments employed in this study, larvae were hatched in deH_2O ([Ion] μmol l^{-1}: [Na^+] 590, [Cl^-] 920, [Ca^{2+}] 760, [K^+] 43, pH 7.35) and transferred to either 5 mmol l^{-1} NaCl (in deH_2O, pH = 7.35) or 5 mmol l^{-1} NH_4Cl (in deH_2O, pH = 7.35) at two days post-hatching (Nguyen and Donini, 2010). Control larvae were maintained in deH_2O. *A. aegypti* larvae were reared in the respective treatments following

the protocol above, until reaching 4th instar (approximately 7 days). Fourth instar larvae from each treatment were used 24h post-feeding for all physiological and molecular studies.

RNA extraction and quantitative real-time PCR (qRT-PCR)

Partial mRNA sequences for *A. aegypti* NHE3 (AAEL001503) were used for primer design (forward primer: 5'- CTACCTGGCGTATCTGAATGC-3'; reverse primer: 5'-CGTATTT-GATGGTCGTGTGC-3'; 131 bp amplicon size, 58°C annealing temperature). The purified RT-PCR product, resolved by gel electrophoresis, was sequenced at The Centre for Applied Genomics (TCAG), The Hospital for Sick Children, to confirm NHE3 sequence specificity. Three biological samples, each consisting of a pool of 200 anal papillae from 50 larvae were isolated and collected in cold lysis buffer with 1% 2-mercaptoethanol (Ambion, Austin, TX, USA). Total anal papillae RNA was extracted using the Purelink RNA mini kit (Ambion, Austin, TX) and genomic DNA was removed with an RNAse-free DNAse using the TURBO DNA-free™ Kit (Applied Biosystems, Streetsville, Ont, Canada). cDNA was synthesized using the iScript™ synthesis kit (Bio-Rad, Mississauga, ON, Canada) with 0.75 µg of total RNA for each reaction.

Quantitative real time PCR (qRT-PCR) using the primers described above was used to examine the relative mRNA abundance of NHE3 in the anal papillae of *A. aegypti* larvae. qRT-PCR reactions were carried out using the CFX96™ real-time PCR detection system (Bio-Rad) and SsoFast™ Evagreen® Supermix (Bio-Rad) according to the manufacturer's protocol. Ribosomal protein 49 (rp49) RNA served as the reference gene utilizing primers that have been previously designed and utilized (Paluzzi et al., 2014). A melting curve analysis was performed after each cycle to confirm the presence of a single product. Quantification of relative transcript abundance was determined according to the Pfaffl method (Pfaffl, 2004). The mRNA abundance of NHE3 in the anal papillae of larvae from each rearing condition (NaCl and HEA) was expressed relative to the control deH_2O, which was assigned a value of 1.0 after normalizing to *rp49* transcript abundance.

Western blotting

Changes in the protein abundances of AeAmt1, AeAmt2, and AeRh50s in response to rearing in HEA (5 mmol l^{-1} NH_4Cl) has been previously documented (Chapter 4). Here, the protein abundances of AeAmt1, AeAmt2, and AeRh50s in the anal papillae of 4th instar larvae in response to 5 mmol l^{-1} NaCl was examined using Western blotting following an established protocol (Chasiotis and Kelly, 2008). Three biological samples consisting of pooled anal papillae were isolated from 30 larvae in *A. aegypti* saline (Donini et al., 2007) and were sonicated (3× 10 seconds) on ice in a homogenization buffer (50 mmol l^{-1} Tris-HCl pH 7.4, 1 mmol l^{-1} PMSF, 150 mmol l^{-1} NaCl, 1% sodium deoxycholate, 1% Triton X-100, 0.1% SDS, and 1:200 protease inhibitor cocktail [Sigma-Aldrich]), centrifuged at 13,000 *g* for 10 min at 4°C, and the supernatant was collected and stored at -80°C. The preparation of samples consisted of 5 µg of protein from anal papillae (Bradford Assay, Bio-Rad) in radioimmuno-precipitation assay (RIPA) homogenization buffer and 6× loading buffer (360 mmol l^{-1} Tris-HCl pH 6.8, 12% (w/v) SDS, 30% glycerol, 600 mmol l^{-1} DTT, and 0.03% (w/v) Bromophenol blue) for a total sample volume of 25 µL. Samples were prepared for SDS-PAGE by heating for 5 min at 100°C, and then were electrophoretically separated by SDS-PAGE (12% polyacrylamide). Western blot analysis of AeAmt1, AeAmt2, and AeRh50s was conducted according to an established protocol (Chasiotis and Kelly, 2008; Chasiotis et al., 2016; Chapter 2). Custom-synthesized polyclonal antibodies raised in rabbit against AeAmt1, AeAmt2, and AeRh50s were used at dilutions of 1:500, 1:5000 and 1:2000, respectively, and have been previously validated (Chasiotis et al., 2016; Chapter 3, 2018; Chapter 2). The AeRh50 antisera is presumed to detect both AeRh50-1 and AeRh50-2 due to high epitope sequence similarity (Chapter 2). Following chemiluminescent detection of ammonia transporter expression using a Gel Doc XR^+ system (Bio-Rad), blots were stripped using stripping buffer (20 mmol l^{-1} magnesium acetate, 30 mmol l^{-1} KCl, 0.1M glycine, pH = 2.2) and total protein analysis was carried out using Coomassie total protein staining as a loading control (0.1% Coomassie R250, 50% methanol, 50% ddH_2O) (Eaton et al., 2013). Blots were incubated in Coomassie for 1 minute followed by de-staining

for 3-5 minutes in de-stain solution (50% ethanol, 10% acetic acid, 40% ddH_2O). Blots were rinsed in ddH_2O for 1 minute, dried completely, and visualized using a Gel Doc XR + system (Bio-Rad). Densitometric analysis of AeAmt1, AeAmt2, AeRh50s, and Coomassie total protein was conducted using ImageJ 1.50i software (National Institutes of Health, Bethesda, MD, USA).

Ion-selective microelectrodes (ISME) and scanning ion-selective microelectrode technique (SIET)

Haemolymph was collected by gently blotting *A. aegypti* larvae on filter paper to remove excess water, submerging the larvae in paraffin oil (Sigma-Aldrich, Oakville, ON, CA), and gently tearing the cuticle with fine forceps to release a droplet of haemolymph into the oil. Na^+, NH_4^+, and pH concentrations in the haemolymph were determined by measuring the activities of the free ions (Na^+, NH_4^+, H^+) using ion-selective microelectrodes (ISMEs) (Donini and O'Donnell, 2005). The following ionophore cocktails (Fluka, Buchs, Switzerland) and back-fill solutions (in parentheses) were used: NH_4^+ Ionophore I Cocktail A (100 mmol l^{-1} NH_4Cl); Na^+ Ionophore II Cocktail A (100 mmol l^{-1} NaCl); and H^+ Ionophore I Cocktail B (100 mmol l^{-1} NaCl/100 mmol l^{-1} sodium citrate, pH 6.0). The ISMEs were calibrated after every 5 haemolymph measurements in the following solutions (mmol l^{-1}): NH_4^+, 0.1, 1, 10 NH_4Cl; Na^+, 30 NaCl +270 LiCl and 300 NaCl; and H^+, 100 mmol l^{-1} NaCl and 100 mmol l^{-1} sodium citrate at pH 6.0, 7.0, and 8.0 (using NaOH or HCl). Voltages were recorded and analyzed in LabChart 6 Pro software (AD Instruments Inc.).

The scanning ion-selective electrode technique (SIET) system protocol used in this study to measure NH_4^+ and Na^+ flux at the anal papillae of larvae has been detailed previously (Chasiotis et al., 2016). Larvae were mounted alive in a Petri dish using beeswax and submerged in 4 ml of bath solution (2.5 mmol l^{-1} NH_4Cl and 5 mmol l^{-1} NaCl in double-distilled H_2O), leaving the anal papillae exposed and immobilized for measurements. ISMEs were calibrated after every 4 larvae measurements in 0.1, 1 and 10 mmol l^{-1} of NaCl in ddH_2O for Na^+ and 0.1, 1, and 10 mmol l^{-1} of NH_4Cl for NH_4^+ in ddH_2O. Voltage gradients over an excursion distance of 100 μm were recorded adjacent to the papillae with

both Na^+ and NH_4^+ microelectrodes (see ISME above) at the exact same site at the same time. The sampling protocol utilized here has been outlined previously (Chasiotis et al., 2016). Readings were taken along the lateral to distal portion of the anal papillae at five equidistant sites. Background voltage gradients were taken 3000 µm away from the anal papillae using the same sampling protocol and were subtracted from the voltage gradients recorded at the papillae. To calculate Na^+ and NH_4^+ flux, voltage gradients were used to calculate Na^+ and NH_4^+ concentration gradients, and the Na^+ and NH_4^+ flux was then calculated using the concentration gradients with Fick's law of diffusion. For SIET measurements, a single biological replicate is defined as the average flux from 4 repeated measurements at each of 5 sites along a single anal papilla from a single larva.

NKA and VA activity assay

The NKA and VA activity assay used in this study was adapted from McCormick and has been outlined previously in detail (Jonusaite et al., 2011; Mccormick, 1993). This assay is dependent on the enzymatic coupling of NKA inhibitor ouabain (Sigma-Aldrich Canada Ltd.) or VA inhibitor bafilomycin (LC Laboratories, Woburn, MA, USA) sensitive hydrolysis of adenosine triphosphate (ATP) with the oxidation of reduced nicotinamide adenine dinucleotide (NADH), with NADH disappearance being directly measured in a microplate spectrophotometer. Briefly, anal papillae from 30 larvae were collected in 1.5 ml centrifuge tubes, flash-frozen in liquid nitrogen and stored at -80°C. Samples were later thawed on ice, and 100 µl of homogenizing buffer (four parts SEI, composing of 150 mmol l^{-1} sucrose/10mmol l^{-1} Na_2EDTA/50mmol l^{-1} imidazole; pH 7.3 and one-part SEID, composed of 0.5% deoxycholic acid in SEI) was added to each tube. Samples were sonicated on ice for 10 seconds at 5 W using an XL 2000 Ultrasonic Processor (Qsonica), and were then centrifuged at 10,000 *g* for 10 min at 4°C. The supernatants of each sample (100 µl) were transferred to 1.5 ml centrifuge tubes and stored at -80°C.

Three assay solutions (A, B, and C) were freshly prepared having a composition of: (A) 5 units ml^{-1} pyruvate kinase, 2.8 mmol l^{-1} phosphoenolpyruvate, 4 units ml^{-1} lactate dehydrogenase, 3.5 mmol l^{-1} ATP, 0.24 mmol l^{-1} NADH, 50 mmol l^{-1} imidazole, pH 7.5; (B) solution A/ 5 mmol l^{-1} ouabain; (C) solution A/ 10 µmol l^{-1} bafilomycin. Each solution (A, B, and C) was mixed separately with a salt solution (composition of 189 mmol l^{-1} NaCl, 10.5 mmol l^{-1} $MgCl_2$, 42 mmol l^{-1} KCl, 50 mmol l^{-1} imidazole, pH 7.5) with a 3:1 ratio and kept on ice. An adenosine diphosphate standard curve was first run using the 3:1 solution A and salt solution to ensure that all reagents were working appropriately. ADP (Sigma-Aldrich) standards were prepared using a 4 mmol l^{-1} ADP stock and 50 mmol l^{-1} imidazole buffer at concentrations of 0 nmol l^{-1} of ADP/10 µl, 5 nmol l^{-1} of ADP/10 µl, 10 nmol l^{-1} of ADP/10 µl, 20 nmol l^{-1} of ADP/10 µl, and 40 nmol l^{-1} of ADP/10 µl. Each standard (10 µl) was added in duplicates to a 96-well microplate (BD Falcon™) and 200 µl of 3:1 Solution A and salt solution was added to each well. A linear rate of NADH disappearance was measured at 340 nm using a thermos Multiscan Spectrum microplate spectrophotometer (Thermo Electron Co., San Jose, USA) at 25°C. Absorbance spectra were recorded and analyzed using the SkanIt version 2.2 software, which yielded a slope of -0.0128. Samples of anal papillae homogenates were thawed on ice. Six replicates (10 µl in each well) from each sample were added to the microplate on ice, followed by the addition of 3:1 Solution A and salt solution to two wells of each sample, 3:1 Solution B and salt solution to two wells of each sample, and 3:1 Solution C and salt solution to two wells of each sample. A decrease in NADH absorbance was measured every minute for 30 min at 340 nm, and NKA and VA activity was calculated using the following equation:

$$\text{NKA or VA activity} = ((\Delta\text{ATPase}/S)/[P]) \; x \; 60 \text{ (min)},$$

where ΔATPase is the difference in ATP hydrolysis in the absence and presence of inhibitors ouabain or bafilomycin, S is the slope of the ADP standard curve, $[P]$ is the protein concentration of the sample (Bradford assay, Sigma-Aldrich Canada, Ltd.). The final ATPase activity was expressed as µmoles of ADP per milligram of protein per hour.

Statistical analyses

Statistical analyses for all experiments were computed using Prism® 7.00 (GraphPad Software, La Jolla, CA, USA), detailed in the caption of each figure. For analyses of multiple groups using a One-Way ANOVA, pairwise multiple comparisons were performed using the Tukey multiple comparisons test, unless specified otherwise, and the adjusted *P*-value is indicated.

4.4 Results

Expression of AeAmt1, AeAmt2, and AeRh50s in the anal papillae in response to NaCl

Changes in protein expression of ammonia transporters in the anal papillae were examined in response to rearing of *A. aegypti* larvae in 5 mmol l^{-1} NaCl (Fig. 4-1). AeAmt1 and AeAmt2 protein abundance was unchanged in the anal papillae of deH_2O and 5 mmol l^{-1} NaCl reared larvae (Fig. 4-1 A-B). A five-fold increase in protein abundance of AeRh50s in the anal papillae was observed compared to deH_2O control levels in response to rearing in 5 mmol l^{-1} NaCl (Fig. 4-1C; $P = 0.0335$).

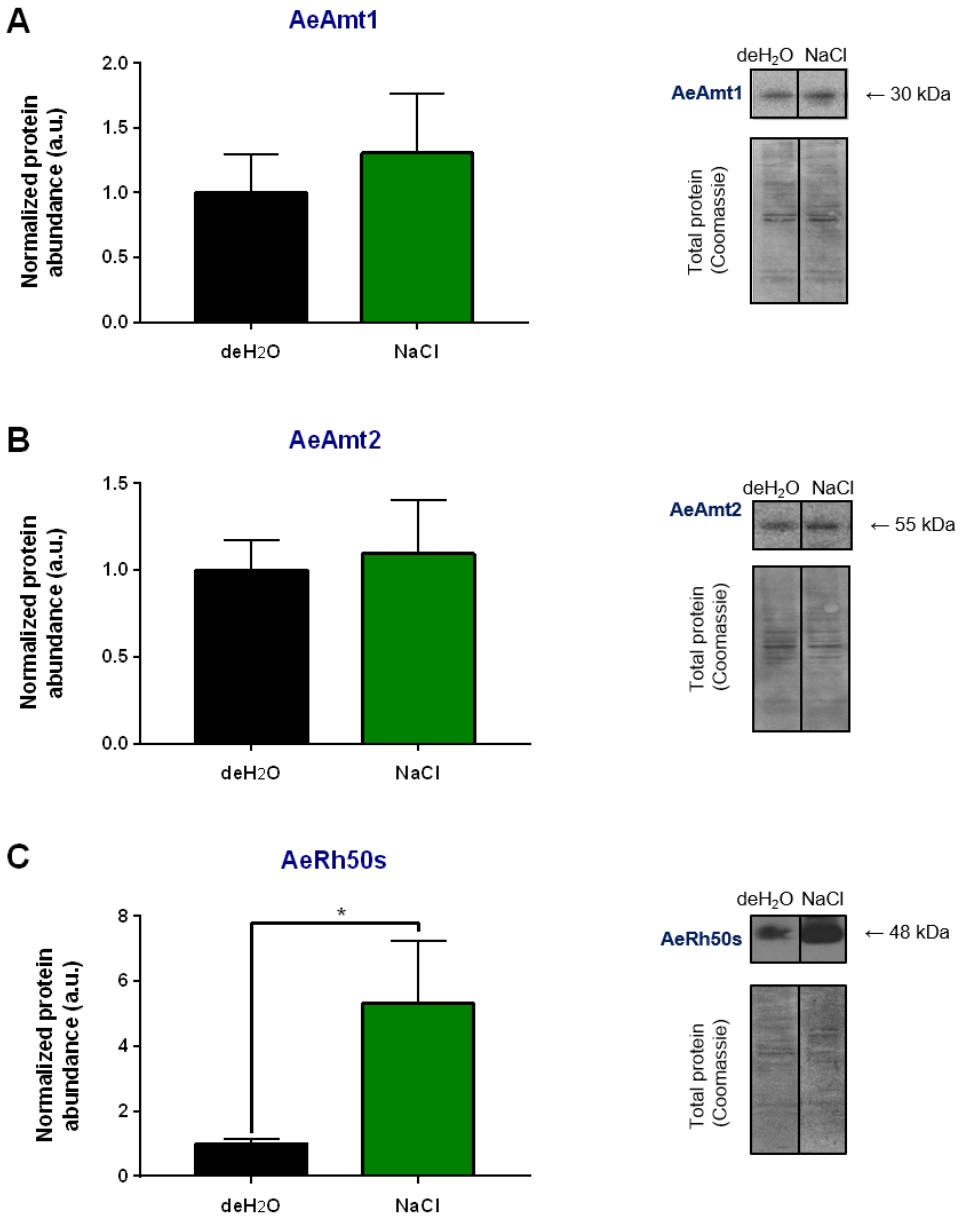

Figure 4- 1. Effect of rearing in NaCl on the protein abundance of ammonia transporters in the anal papillae of 4th instar *Aedes aegypti* larvae. Densitometric analysis and representative western blots of (A) AeAmt1 monomer (30 kDa), (B) AeAmt2 monomer (55 kDa), and (C) AeRh50s monomer (48 kDa) abundance in anal papillae of larvae reared in either dechlorinated tap water (deH_2O) or NaCl (5 mmol l^{-1}). Protein abundance of ammonia transporters was normalized to total protein (Coomassie) in the anal papillae. The control (deH_2O) group was assigned a value of 1, and normalized protein abundance in the NaCl group is expressed relative to the control group. Data is shown as mean values ± S.E.M (N = 5-6). An asterisk denotes a significant difference from the control deH_2O group (two-tailed, Unpaired t-test; P = 0.0335 for panel C).

Na^+ and NH_4^+ flux at the anal papillae in response to rearing in NaCl and HEA

Na^+ and NH_4^+ fluxes at the anal papillae of 4th instar larvae reared in deH_2O, 5 mmol l^{-1} NaCl, and 5 mmol l^{-1} NH_4Cl (HEA) were measured using SIET (Fig. 4-2). While there was an apparent trend towards decreased Na^+ absorption at the anal papillae of larvae reared in NaCl and an apparent reversal of Na^+ flux for larvae reared in NH_4Cl, compared to the deH_2O control, no statistically significant change in Na^+ flux was observed in response to the respective rearing conditions (Fig. 4-2). In contrast, *A. aegypti* larvae reared in 5 mmol l^{-1} NaCl had significantly higher NH_4^+ efflux rates, an approximate 7-fold increase, compared to the average flux measured for deH_2O reared larvae (Fig. 4-2). Larvae reared in 5 mmol l^{-1} NH_4Cl showed similar NH_4^+ fluxes at the anal papillae compared to deH_2O controls levels (Fig. 4-2).

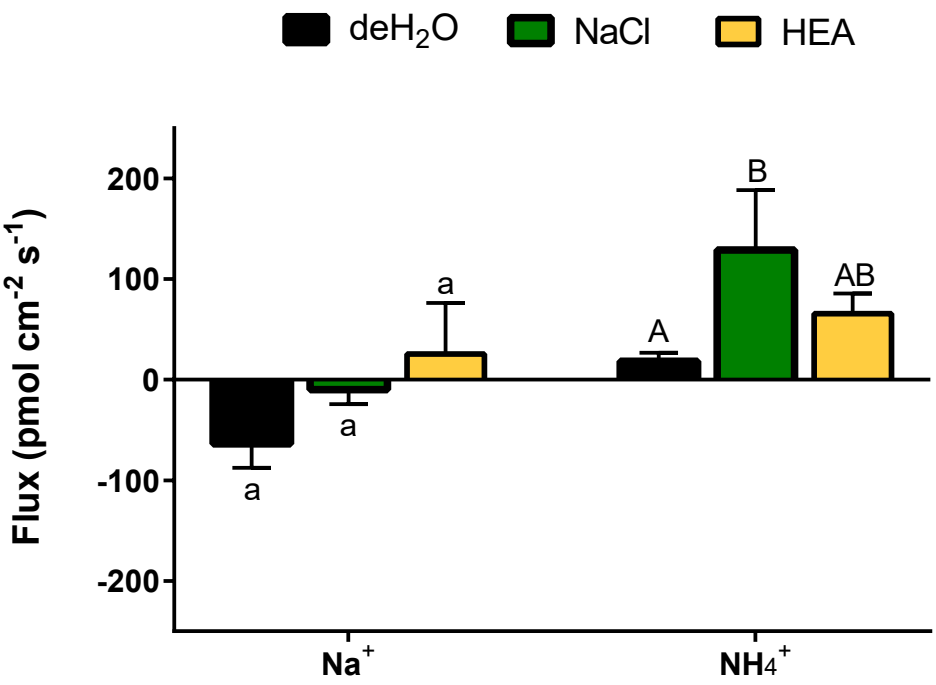

Figure 4- 2. Effect of rearing in NaCl and HEA (NH_4Cl) on Na^+ and NH_4^+ flux at the anal papillae of 4th instar *Aedes aegypti* larvae. Scanning ion-selective electrode technique (SIET) measurements of Na^+ and NH_4^+ flux across the anal papillae epithelium of larvae reared in either dechlorinated tap water (deH_2O) or NaCl (5 mmol l^{-1}). Data is shown as mean values ± S.E.M (*N* = 9-11). Different letters denote a significant difference in flux between groups based on a one-way ANOVA for each ion (Fisher's LSD test, *P = 0.0384)*.

NKA and VA activity in the anal papillae of larvae reared in NaCl and HEA

The activity of the primary ionomotive pumps, NKA and VA, in the anal papillae of 4th instar larvae reared in deH_2O, 5 mmol l^{-1} NaCl, and 5 mmol l^{-1} NH_4Cl was examined (Fig. 4-3). The activities of NKA and VA in the anal papillae d in larvae reared in NaCl did not change when compared to NKA and VA activities in the anal papillae of control deH_2O reared larvae. In contrast, NKA activity in the anal papillae was significantly reduced in larvae reared in HEA compared to activity levels in deH_2O and NaCl (Fig. 4-3; P = 0.0357). Furthermore, VA activity in the anal papillae of larvae reared in HEA was significantly higher than the VA activity in the papillae of larvae reared in deH_2O and NaCl (P *=0.005).*

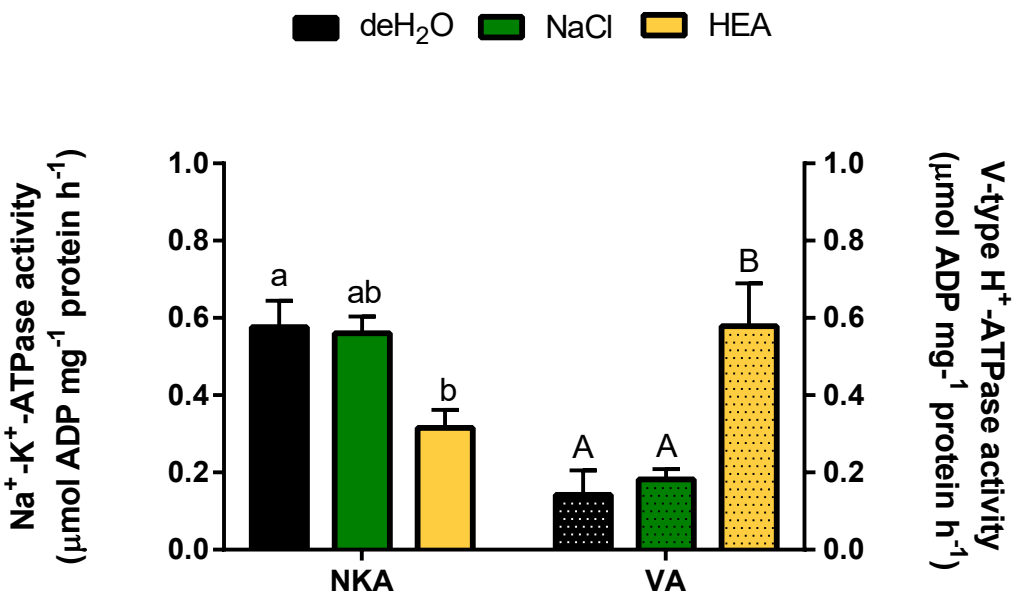

Figure 4- 3. Effect of rearing in NaCl and HEA (NH_4Cl) on $Na^{+/}K^{+}$-ATPase (NKA) activity and V-type-H^{+}-ATPase (VA) activity in the anal papillae of 4th instar *Aedes aegypti* larvae. NKA and VA activities in the anal papillae of larvae reared in dechlorinated tap water (deH_2O), NaCl (5 mmol l^{-1}) or NH_4Cl (5 mmol l^{-1}) were measured. Different letters denote a significant difference between rearing groups (one-way ANOVA, Tukey's multiple comparisons test, $P = 0.0357$ for NKA and $P \leq 0.005$ for VA). All data are expressed as mean ± S.E.M (N = 3-5 for each treatment group).

Changes in haemolymph ion levels and pH in response to rearing in NaCl and HEA

Haemolymph Na^+, NH_4^+, and pH levels in the haemolymph of 4th instar *A. aegypti* larvae reared in deH_2O, 5 mmol l^{-1} NaCl, and 5 mmol l^{-1} NH_4Cl were measured using ISMEs (Fig. 4-4). No significant difference in haemolymph Na^+ levels were observed between larvae reared in deH_2O and NaCl, or deH_2O and HEA, respectively (Fig. 4-4A). However, larvae reared in NaCl had a significantly higher Na^+ haemolymph concentration compared to larvae reared in HEA (Fig. 4-4A). The haemolymph NH_4^+ concentration decreased in NaCl reared larvae compared to the deH_2O control and HEA larvae (Fig. 4-4B). While there was a trend towards increased NH_4^+ levels in the haemolymph of HEA reared larvae compared to the deH_2O control, this change was not significant (P = 0.0922). *A. aegypti* larvae reared in NaCl and HEA had significantly lower haemolymph pH levels in comparison to larvae reared in deH_2O (Fig. 4-4C).

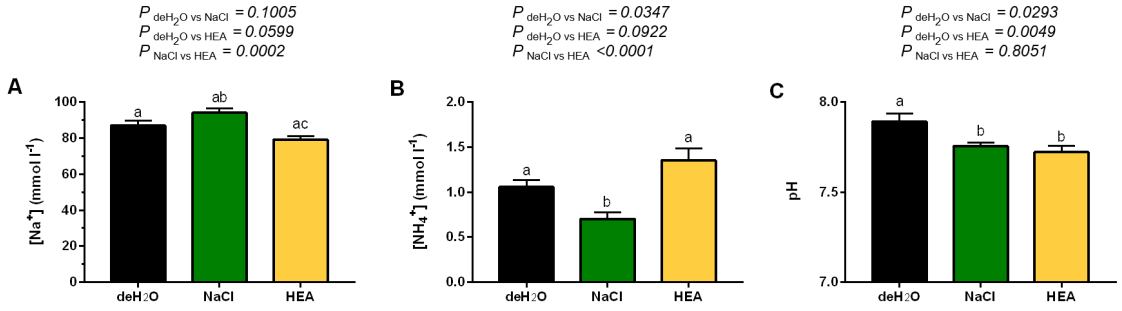

Figure 4- 4. Effect of rearing in NaCl and HEA (NH_4Cl) on Na^+, NH_4^+, and pH levels in the haemolymph of 4th instar *Aedes aegypti* larvae. Ion-selective micro-electrode measurements of (A) NH_4^+, (B) Na^+, and (C) H^+ concentrations (expressed as pH) in the haemolymph of larvae at 7 days of rearing in either dechlorinated tap water (deH_2O), NaCl (5 mmol l^{-1}), or NH_4Cl (5 mmol l^{-1}). Different letters denote a significant difference in ion levels based on a one-way ANOVA (Tukey's multiple comparisons test; adjusted *P* values indicated above each panel, A-C). Data is shown as mean values ± S.E.M *(N*= 10-11 for Na^+, *N* = 8-10 for NH_4^+, *N* = 10-12 for pH).

Changes in NHE3 mRNA expression in response to rearing in NaCl and HEA

The mRNA abundance of NHE3 in the anal papillae of larvae reared in deH_2O, 5 mmol l^{-1} NaCl, and 5 mmol l^{-1} NH_4Cl were measured (Fig. 4-5). NHE3 transcript abundance, normalized to ribosomal protein 49 (rp49) abundance in the anal papillae, did not change in larvae reared in HEA in comparison to larvae reared in deH_2O (Fig. 4-5). A significant decrease in NHE3 mRNA was observed in larvae reared in NaCl compared to deH_2O (an approximate 75% reduction) and HEA-reared larvae.

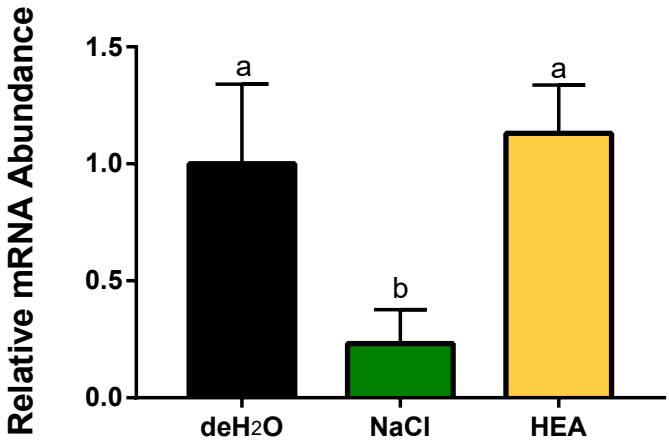

Figure 4- 5. Effect of rearing in NaCl and HEA (NH_4Cl) on the relative mRNA abundance of *NHE3* in the anal papillae of 4th instar *Aedes aegypti* larvae. Relative *NHE3* mRNA abundance in the anal papillae was measured using qRT-PCR and was normalized to ribosomal protein 49 (rp49). NHE3 mRNA abundance in NaCl and HEA treatments are expressed relative to deH_2O levels (assigned a value of 1). Different letters denote a significant difference in mRNA abundance based on a one-way ANOVA of log-transformed normalized values (Fisher's LSD test; $P < 0.05$). Data is shown as mean values ± S.E.M ($N = 3$).

4.5 Discussion

Overview

This study describes the novel physiological mechanisms used by *A. aegypti* larvae to accomplish ammonia excretion, acid-base balance, and haemolymph ion homeostasis when faced with varying aquatic environments. Based on our previous work, we hypothesized that ammonia excretion at the anal papillae through ammonia transporters could be utilized for acid base regulation. We found that haemolymph acidification was a common consequence of exposing larvae to HEA or moderate levels of NaCl. This was coupled to alterations in ammonia transporter expression in the anal papillae, and in the case of NaCl exposure, elevated ammonia excretion rates at the anal papillae. The results support the hypothesis that ammonia excretion at the anal papillae may be used to excrete acid when haemolymph acidification occurs.

HEA Rearing

In a recent study, we examined the effects of rearing *A. aegypti* larvae in HEA on the expression of ammonia transporters in the anal papillae (Chapter 3). We reported a decrease in the protein abundance of apical AeAmt2 and the AeRh50s, while the basolateral AeAmt1 protein abundance did not change compared to control larvae reared in deH_2O. While we do not know whether NHE3 protein abundance is altered, here we add that the mRNA abundance of apical NHE3 remains unchanged in response to rearing in HEA, while the activities of basolateral NKA decreases and the apical VA increases, respectively, in the anal papillae of HEA reared larvae (Figures 4-3 and 4-5). Although the transporters involved in ammonia excretion and ion transport in the anal papillae of mosquito larvae are similar to those found in other aquatic invertebrates and vertebrates (e.g. fish), the alterations in expression reported here demonstrate differences in how these transporters are utilized for ammonia excretion. For example, in the freshwater goldfish and common carp gills, exposure to HEA results in an increase in apical Rhcg mRNA expression and NKA activity (Sinha et al., 2013; Sinha et al., 2016).

Similar responses are observed in a freshwater shrimp and flatworm, where NKA activity increases and the expression of a Rh protein increases (Pinto et al., 2016; Weihrauch et al., 2012b). These responses are the opposite of what is observed in the anal papillae of mosquito larvae in the present study, which are consistent with the freshwater leech whereby Rh protein expression and NKA activity both decrease upon HEA exposure (Quijada-Rodriguez et al., 2015). A decrease in expression of apical AeAmt2 and AeRh50s may be a response to limit the entry of ammonia from the water in the face of a gradient that no longer favours excretion into the water. In fact, we measured haemolymph ammonia levels of ~ 1.4 mmol l^{-1} in HEA exposed larvae (Figure 4-4) which is considerably lower than the external HEA treatment of 5 mmol l^{-1} and would therefore favour ammonia entry; however, it must be noted that we have not measured cytosolic ammonia levels in the syncytial anal papillae epithelium. In the marine crab, *Metacarcinus magister*, a 7-day exposure to 1 mmol l^{-1} ammonia caused an increase in haemolymph ammonia to levels close to 1 mmol l^{-1} and a similar response was proposed for the freshwater leech, *Nephelopsis obscura* (Martin et al., 2011; Quijada-Rodriguez et al., 2015). It was suggested that this increase in haemolymph ammonia permits ammonia excretion in HEA by minimizing the ammonia gradient that would otherwise lead to ammonia entry. This is in contrast to our findings in the mosquito larvae, which appear to maintain haemolymph ammonia levels that are lower than the external ammonia levels. The unaltered basal expression of AeAmt1, which has been proposed to transport NH_4^+ from haemolymph to cytosol and is driven by the cytosol negative potential generated by basal NKA and apical VA, could maintain cytosol ammonia levels higher than the haemolymph, thus supporting ammonia excretion across the apical membrane (Chasiotis et al., 2016). In this case, the electrical potential is more important than the ammonia concentration gradient. Although NKA activity decreases in HEA, the elevated VA activity may compensate to maintain the cytosol negative potential in the anal papillae. Ammonia excretion is still evident in papillae of HEA exposed larvae because ammonia excretion rates which were similar to those recorded from papillae of control larvae

were measured in water with 2.5 mmol l^{-1} NH_4Cl (and 5 mmol l^{-1} NaCl) which represents an inward directed ammonia gradient relative to the haemolymph ammonia levels (Figure 4-2).

A reduction in Na^+ uptake at the anal papillae in a bath containing 5 mmol l^{-1} NaCl and 2.5 mmol l^{-1} NH_4Cl was previously demonstrated (Weihrauch et al., 2012a). Larvae exposed to HEA showed a trend towards a lower haemolymph [Na^+] (Figure 4-4A, $p = 0.059$, Tukey's) as well as lower haemolymph pH compared to control larvae (Figure 4-4C). Similar findings were reported for some crustaceans exposed to HEA (Chen and Chen, 1996; Harris et al., 2001; Young-Lai et al., 1991). The prevailing theory for a reduction in haemolymph [Na^+] caused by ammonia exposure is the impairment of an apical Na^+/NH_4^+ transport system (Chen and Chen, 1996; Harris et al., 2001; Romano and Zeng, 2007), which may involve a transport metabolon comprised of VA, NHE3 and Rh proteins (Shih et al., 2012; Shih et al., 2013; Wright and Wood, 2009; Wu et al., 2010b). The findings of a trend towards reduced haemolymph [Na^+] in HEA larvae, coupled with the observation that NH_4^+ fluxes from anal papillae in a bath containing NaCl are statistically similar to those measured from control larvae, do not support a mechanism of Na^+/NH_4^+ exchange at the anal papillae. Furthermore, papillae from HEA exposed larvae showed a mean Na^+ excretion in tandem with NH_4^+ excretion suggesting that ammonia excretion and Na^+ uptake mechanisms are not linked when larvae are reared in HEA (Figure 4-2). Additionally, the loss of Na^+ at the anal papillae is likely responsible for the apparent decrease in haemolymph [Na^+] and the decrease in NKA activity in HEA, which is important for Na^+ uptake also suggests that Na^+/NH_4^+ exchange seems unlikely at the anal papillae.

Lastly, the lower haemolymph pH of larvae reared in HEA could be the result of deprotonation of NH_4^+ whereby NH_3 diffuses across cellular membranes and H^+ remains in the haemolymph, leading to acidification. The NH_4^+ levels in the haemolymph of HEA exposed larvae were ~ 1.4 mmol l^{-1} compared to levels in control larvae of ~ 1 mmol l^{-1} ($p = 0.09$ Tukey's). This apparent elevation in haemolymph ammonia may have been sufficient to acidify the haemolymph. However, the relative amount of deprotonation of NH_4^+ would be minimal at a pH of ~7.7. An alternative explanation is that

larvae intentionally decrease their haemolymph pH from ~7.9 to ~7.7 in order to limit deprotonation of the elevated NH_4^+ in the haemolymph. This has been suggested in copepods that accumulate high levels of ammonia in the haemolymph during diapause (Schründer et al., 2013). Another explanation may be that the acidification of the haemolymph is a consequence of the downregulation of AeRh50 expression. A previous study noted that RNAi mediated knockdown of AeRh50-1 in the anal papillae resulted in haemolymph acidification (Chapter 2). This is similar to the effect of HEA rearing whereby AeRh50 expression is downregulated and haemolymph acidification occurs (Chapter 4). We previously speculated that this acidification could arise if AeRh50-1 is capable of transporting CO_2 and is located on the basal membrane of the anal papillae epithelium. If this were the case then downregulation of AeRh50-1 in response to HEA would result in a buildup of bicarbonate and protons in the haemolymph; however, at this time there is no conclusive evidence that Rh proteins transport CO_2 and studies to determine the transport substrate of these transporters continue to be very important.

NaCl Rearing

Rearing of *A. aegypti* larvae in 5 mmol l^{-1} NaCl did not affect the abundance of either AeAmt1 or AeAmt2 protein in the anal papillae but increased the abundance of the AeRh50 protein by 5 times the levels detected in deH_2O-reared larvae (Figure 4-1). These observations on the expression of ammonia transporters in the anal papillae coincide with significantly higher NH_4^+ excretion from the anal papillae of NaCl reared larvae and decreased haemolymph NH_4^+ levels, suggesting that the elevated ammonia excretion occurs through the AeRh50 proteins. As previously mentioned, Rh proteins are proposed gas channels which were shown to transport NH_3 by recruitment of NH_4^+ and subsequent deprotonation (Baday et al., 2015; Kustu and Inwood, 2006). We propose that the electrical component of the electrochemical gradient drives NH_4^+ into the cytosol of the anal papillae epithelium through AeAmt1 and that ammonia exits primarily through an apical AeRh50 protein, which can recruit NH_4^+ that is accumulating in the cytosol and transport NH_3 to the water. The resulting protons in the cytosol

can be removed through VA which functions with the apical AeRh50 in an ammonia trapping mechanism. In the present study, the observed increase in ammonia excretion and AeRh50 expression at the anal papillae of NaCl reared larvae was unexpected, however, may be explained by ammonia excretion being utilized to remove acid from the haemolymph. This has been proposed for crustaceans (Fehsenfeld and Weihrauch, 2017).

Acidification of the haemolymph in aquatic animals exposed to salt is thought to occur because of a down regulation of Na^+ uptake which is coupled with H^+ secretion (Henry and Cameron, 1982; Maxime et al., 1990; Truchot, 1981; Truchot and Nonnotte, 1990). This acidification of the haemolymph was shown to occur in *A. aegypti* larvae that were transferred to relatively high salt levels (Donini et al., 2007). Evidence that Na^+ uptake is associated with H^+ secretion in *A. aegypti* has been presented (Patrick et al., 2002a; Stobbart, 1967) and we have shown that Na^+ uptake at the papillae is likely to occur through a putative Na^+ channel driven by the electrical gradient established by the apical VA which secretes H^+ into the water (Del Duca et al., 2011). We have since shown the expression of NHE3 on the apical side of the anal papilla epithelium and cannot rule out the possibility of Na^+ uptake coupled to H^+ secretion via this transporter (Chasiotis et al., 2016). Although there is a trend towards a decrease in Na^+ uptake at the anal papillae of NaCl reared larvae, the VA activity was no different than that found in control larvae. The mRNA abundance of the NHE3 was reduced to ~1/4 the levels in controls and although it is tempting to speculate that the trend towards a decrease in Na^+ uptake and the acidification of the haemolymph may be the result of reduced NHE3 expression at the anal papillae; the protein levels of NHE3 need to be measured.

The acidification of the haemolymph in NaCl reared larvae is also likely to release more CO_2 in the haemolymph because of the buffering properties of bicarbonate. As a result, the larvae would require an outlet for the increased CO_2 levels in the haemolymph. The increased expression of the AeRh50s in the anal papillae might provide the means to eliminate the excess CO_2 if these transporters were capable of CO_2 transport. In fish, algae and bacteria there is some evidence that Rh proteins may

be capable of transporting CO_2 (Perry et al., 2010; Soupene et al., 2002; Soupene et al., 2004). If *Aedes aegypti* Rh proteins are able to transport CO_2 then they may also be utilized for acid-base balance in this manner; however, more research is required to ascertain the transport substrates of these transporters..

Perspectives and Conclusions

In summary, In HEA, the apical ammonia transporters in the anal papillae appear to be detrimental and are downregulated in order to limit ammonia entry into the cytosol, whereas the basal AeAmt1 expression remains unaltered, with NH_4^+ excretion being maintained against an inward gradient. In moderate levels of salt, we propose that the main physiological challenge of *A. aegypti* larvae is haemolymph acidosis similar to other aquatic organisms (Fehsenfeld and Weihrauch, 2017). We show that elevated AeRh50 protein abundance coupled with an increase in excretion of NH_4^+ at the anal papillae and a haemolymph acidosis occurs in response to salt, suggesting an important role for Rh proteins in acid-base regulation. We therefore accept the hypothesis that NH_4^+ excretion at the anal papillae is utilized to remove acid from the haemolymph.

4.6 References

Akhter, H., Misyura, L., Bui, P. and Donini, A. (2017). Salinity responsive aquaporins in the anal papillae of the larval mosquito, *Aedes aegypti*. *Comp. Biochem. Physiol. -Part A Mol. Integr. Physiol.* **203**, 144–151.

Baday, S., Orabi, E. A., Wang, S., Lamoureux, G. and Bernèche, S. (2015). Mechanism of NH_4^+ Recruitment and NH_3 Transport in Rh Proteins. *Structure* **23**, 1550–1557.

Chasiotis, H. and Kelly, S. P. (2008). Occludin immunolocalization and protein expression in goldfish. *J. Exp. Biol.* **211**, 1524–1534.

Chasiotis, H., Ionescu, A., Misyura, L., Bui, P., Fazio, K., Wang, J., Patrick, M., Weihrauch, D. and Donini, A. (2016). An animal homolog of plant Mep/Amt transporters promotes ammonia excretion by the anal papillae of the disease vector mosquito *Aedes aegypti*. *J. Exp. Biol.* **219**, 1346–55.

Chen, J.-C. and Chen, C.-T. (1996). Changes of osmotic and electrolyte concentrations in the haemolymph of *Penaeus japonicus* exposed to ambient ammonia. *Comp. Biochem. Physiol.* **114C**, 35–38.

Clark, T. M. (2004). pH tolerances and regulatory abilities of freshwater and euryhaline Aedine mosquito larvae. *J. Exp. Biol.* **207**, 2297–2304.

Clark, T. M., Vieira, M. A. L., Huegel, K. L., Flury, D. and Carper, M. (2007). Strategies for regulation of haemolymph pH in acidic and alkaline water by the larval mosquito *Aedes aegypti* (L.) (Diptera; Culicidae). *J. Exp. Biol.* **210**, 4359–4367.

Copeland, E. (1964). A mitochondrial pump in the cells of the anal papillae of mosquito larvae. *J. Cell Biol.* **23**, 253–263.

Del Duca, O., Nasirian, A., Galperin, V. and Donini, A. (2011). Pharmacological characterisation of apical Na^+ and Cl^- transport mechanisms of the anal papillae in the larval mosquito *Aedes aegypti*. *J. Exp. Biol.* **214**, 3992–3999.

Donini, A. and O'Donnell, M. J. (2005). Analysis of Na^+, Cl^-, K^+, H^+ and NH_4^+ concentration gradients adjacent to the surface of anal papillae of the mosquito *Aedes aegypti*: application of self-referencing ion-selective mi. *J. Exp. Biol.* **208**, 603–10.

Donini, A., Gaidhu, M. P., Strasberg, D. R. and O'donnell, M. J. (2007). Changing salinity induces alterations in haemolymph ion concentrations and Na^+ and Cl^- transport kinetics of the anal papillae in the larval mosquito, *Aedes aegypti*. *J. Exp. Biol.* **210**, 983–992.

Durant, A. C. and Donini, A. (2018). Ammonia excretion in an osmoregulatory syncytium is facilitated by AeAmt2, a novel ammonia transporter in *Aedes aegypti* larvae. *Front. Physiol.* **9**,.

Durant, A. C., Chasiotis, H., Misyura, L. and Donini, A. (2017). *Aedes aegypti* Rhesus glycoproteins contribute to ammonia excretion by larval anal papillae. *J. Exp. Biol.* **220**, 588–596.

Eaton, S. L., Roche, S. L., Llavero Hurtado, M., Oldknow, K. J., Farquharson, C., Gillingwater, T. H. and Wishart, T. M. (2013). Total protein analysis as a reliable loading control for quantitative fluorescent western blotting. *PLoS One* **8**, 1–9.

Fehsenfeld, S. and Weihrauch, D. (2017). Acid--base regulation in aquatic decapod crustaceans. In *Acid-Base Balance and Nitrogen Excretion in Invertebrates: Mechanisms and Strategies in Various Invertebrate Groups with Considerations of Challenges Caused by Ocean Acidification* (ed. Weihrauch, D.) and O'Donnell, M.), pp. 151–191. Cham: Springer International Publishing.

Harris, R., Coley, S., Collins, S. and McCabe, R. (2001). Ammonia uptake and its effects on ionoregulation in the freshwater crayfish *Pacifastacus leniusculus* (Dana). *J. Comp. Physiol. - B Biochem. Syst. Environ. Physiol.* **171**, 681–693.

Henry, R. P. and Cameron, J. N. (1982). Acid-base balance in Callinectes sapidus during acclimation from high to low salinity. *J. Exp. Biol.* **101**, 255–264.

Jonusaite, S., Kelly, S. P. and Donini, A. (2011). The physiological response of larval *Chironomus riparius* (Meigen) to abrupt brackish water exposure. *J. Comp. Physiol. B.* **181**, 343–52.

Koch, H. J. (1938). The absorption of chloride ions by the anal papillae of diptera larvae. *J. Exp. Biol.* **15**, 152–160.

Kustu, S. and Inwood, W. (2006). Biological gas channels for NH_3 and CO_2: evidence that Rh (Rhesus) proteins are CO_2 channels. *Transfus. Clin. Biol.* **13**, 103–110.

Martin, M., Fehsenfeld, S., Sourial, M. M. and Weihrauch, D. (2011). Effects of high environmental ammonia on branchial ammonia excretion rates and tissue Rh-protein mRNA expression levels in seawater acclimated Dungeness crab *Metacarcinus magister*. *Comp. Biochem. Physiol. - A Mol. Integr. Physiol.* **160**, 267–277.

Matthews, P. G. D. (2017). Acid-base regulation in insect haemolymph. In *Acid-Base Balance and Nitrogen Excretion in Invertebrates* (ed. Weihrauch, D.) and O'Donnell, M. J.), pp. 219–238. Cham, Switzerland: Springer.

Maxime, V., Peyraud-Waitzenergger, M., Claireaux, G. and Peyraud, C. (1990). Effects of rapid transfer from sea water to fresh water on respiratory variables, blood acid-base status and O_2 affinity of haemoglobin in Atlantic salmon (*Salmo salar* L.). *J. Comp. Physiol. B* **160**, 31–39.

Mccormick, S. D. (1993). Methods for non biopsy and measurement of Na^+, K^+-ATPase activity. *Can. J. Aquat. Sci.* **50**, 9–11.

Nawata, C. M. and Wood, C. M. (2008). The effects of CO_2 and external buffering on ammonia excretion and Rhesus glycoprotein mRNA expression in rainbow trout. *J. Exp. Biol.* **211**, 3226–3236.

Nguyen, H. and Donini, A. (2010). Larvae of the midge *Chironomus riparius* possess two distinct mechanisms for ionoregulation in response to ion-poor conditions. *Am. J. Physiol. Integr. Comp. Physiol.* **299**, R762–R773.

Nowghani, F., Jonusaite, S., Watson-Leung, T., Donini, A. and Kelly, S. P. (2017). Strategies of ionoregulation in the freshwater nymph of the mayfly *Hexagenia rigida*. *J. Exp. Biol.* **220**, 3997–4006.

Onken, H. (2003). Active NaCl absorption across posterior gills of hyperosmoregulating *Chasmagnathus granulatus*. *J. Exp. Biol.* **206**, 1017–1023.

Onken, H. and Moffett, D. F. (2017). Acid-base loops in insect larvae with extremely alkaline midgut regions. In *Acid-Base Balance and Nitrogen Excretion in Invertebrates* (ed. Weihrauch, D. and O'Donnell, M. J.), pp. 239–260. Cham, Switzerland: Springer.

Onken, H. and Riestenpatt, S. (2002). Ion transport across posterior gills of hyperosmoregulating shore crabs (*Carcinus maenas*): amiloride blocks the cuticular Na(+) conductance and induces current-noise. *J. Exp. Biol.* **205**, 523–31.

Paluzzi, J. P., Vanderveken, M. and O'Donnell, M. J. (2014). The heterodimeric glycoprotein hormone, GPA2/GPB5, regulates ion transport across the hindgut of the adult mosquito, *Aedes aegypti*. *PLoS One* **9**, e86386.

Patrick, M. L., Gonzalez, R. J. and Bradley, T. J. (2001). Sodium and chloride regulation in freshwater and osmoconforming larvae of Culex mosquitoes. *J. Exp. Biol.* **204**, 3345–3354.

Patrick, M. L., Ferreira, R. L., Gonzalez, R. J., Wood, C. M., Wilson, R. W., Bradley, T. J. and Val, A. L. (2002a). Ion regulatory patterns of mosquito larvae collected from breeding sites in the Amazon rain forest. *Physiol. Biochem. Zool.* **75**, 215–222.

Patrick, M. L., Gonzalez, R. J., Wood, C. M., Wilson, R. W., Bradley, T. J. and Val, A. L. (2002b). The characterization of ion regulation in Amazonian mosquito larvae: Evidence of phenotypic plasticity, population-based disparity, and novel mechanisms of ion ptake. *Physiol. Biochem. Zool.* **75**, 223–236.

Patrick, M. L., Aimanova, K., Sanders, H. R. and Gill, S. S. (2006). P-type Na^+/K^+-ATPase and V-type H^+-ATPase expression patterns in the osmoregulatory organs of larval and adult mosquito *Aedes aegypti*. *J. Exp. Biol.* **209**, 4638–51.

Perry, S. F., Braun, M. H., Noland, M., Dawdy, J. and Walsh, P. J. (2010). Do zebrafish Rh proteins act as dual ammonia – CO_2 hannels ? *J. Exp. Zool.* **313A**, 618–621.

Pfaffl, M. (2004). Quantification strategies in real-time PCR. *A-Z Quant. PCR* 87–112.

Pinto, M. R., Lucena, M. N., Oliveira, R., Alves, E., Mcnamara, J. C. and Leone, F. A. (2016). Effects of ammonia stress in the Amazon river shrimp Macrobrachium. *Aquat. Toxicol.* **170**, 13–23.

Quijada-Rodriguez, A. R., Treberg, J. R. and Weihrauch, D. (2015). Mechanism of ammonia excretion in the freshwater leech *Nephelopsis obscura*: characterization of a primitive Rh protein and effects of high environmental ammonia. *Am. J. Physiol. Regul. Integr. Comp. Physiol.* ajpregu.00482.2014.

Romano, N. and Zeng, C. (2007). Acute toxicity of ammonia and its effects on the haemolymph osmolality , ammonia-N , pH and ionic composition of early juvenile mud crabs , *Scylla serrata* (Forskål). *Comp. Biochem. Physiol. Part A* **148**, 278–285.

Schründer, S., Schnack-schiel, S. B., Auel, H. and Sartoris, F. J. (2013). Control of diapause by acidic pH and Aammonium accumulation in the haemolymph of ntarctic copepods. *PLoS One* **8**, 1–9.

Shih, T., Horng, J., Liu, S., Hwang, P. and Lin, L. (2012). Rhcg1 and NHE3b are involved in ammonium-dependent sodium uptake by zebrafish larvae acclimated to low-sodium water. *Am J Physiol Regul Integr Comp Physiol* **302**, 84–93.

Shih, T.-H., Horng, J.-L., Lai, Y.-T. and Lin, L.-Y. (2013). Rhcg1 and Rhbg mediate ammonia excretion by ionocytes and keratinocytes in the skin of zebrafish larvae: H^+-ATPase-linked active ammonia excretion by ionocytes. *Am. J. Physiol. Integr. Comp. Physiol.* **304**, R1130–R1138.

Sinha, A. K., Liew, H. J., Nawata, C. M., Blust, R., Wood, C. M. and Boeck, G. De (2013). Modulation of Rh glycoproteins , ammonia excretion and Na^+ fluxes in three freshwater teleosts when exposed chronically to high environmental ammonia. *J. Exp. Biol.* 2917–2930.

Sinha, A. K., Kapotwe, M., Boki, S., Montes, S., Shrivastava, J., Blust, R. and Boeck, G. De

(2016). Differential modulation of ammonia excretion , Rhesus glycoproteins and ion-regulation in common carp (*Cyprinus carpio*) following individual and combined exposure to waterborne copper and ammonia. *Aquat. Toxicol.* **170**, 129–141.

Sohal, R. S. and Copeland, E. (1966). Ultrastructural variations in the anal papillae of *Aedes aegypti* (L.) at different environment salinities. *J Insect Physiol* **12**, 429–434.

Soupene, E., Chu, T., Corbin, R. W., Hunt, D. F. and Kustu, S. (2002). Gas channels for NH3: Proteins from hyperthermophiles complement an *Escherichia coli* mutant. *J. Bacteriol.* **184**, 3396–3400.

Soupene, E., Inwood, W. and Kustu, S. (2004). Lack of the Rhesus protein Rh1 impairs growth of the green alga *Chlamydomonas reinhardtii* at high CO_2. *Proc. Natl. Acad. Sci. U. S. A.* **101**, 7787–7792.

Stobbart, B. Y. R. H. (1965). The effect of some anions and cations upon the fluxes and net uptake of sodium in the larva of *Aedes aegypti* (L). 29–44.

Stobbart, R. H. (1967). The effect of some anions and cations upon the fluxes and net uptake of chloride in the larva of *Aedes aegypti* (L.). *J. Exp. Biol.* **47**, 35–57.

Stobbart, R. H. (1971). Evidence for Na^+/H^+ and Cl^-/HCO_3^- exchanges during independent sodium and chloride uptake by the larva of the mosquito *Aedes aegypti* (L.). *Jeb* **54**, 19–27.

Truchot, J. (1981). Acid-base state on the blood acid-base balance in the euryhaline crab. *Comp. Biochem. Physiol.* **68A**, 555–561.

Truchot, J. and Nonnotte, G. (1990). Time course of extracellular acid-base adjustments under hypo- or hyperosmotic conditions in the euryhaline fish *Platichthys ftesus*. *J. Fish Biol.* 181–190.

Vangenechten, J. H. D., Witters, H. and Vanderborght, O. L. J. (1989). Laboratory studies on invertebrate survival and physiology in acid waters. In *Acid Toxicity and Aquatic Animals.* (ed. Morris, R.), Taylor, E. W.), and Brown, D. J. A.), pp. 153–169. Cambridge: Cambridge University Press.

Weihrauch, D., Morris, S. and Towle, D. W. (2004). Ammonia excretion in aquatic and terrestrial crabs. *J. Exp. Biol.* **207**, 4491–4504.

Weihrauch, D., Wilkie, M. P. and Walsh, P. J. (2009). Ammonia and urea transporters in gills of fish and aquatic crustaceans. *J. Exp. Biol.* **212**, 1716–1730.

Weihrauch, D., Chan, a. C., Meyer, H., Doring, C., Sourial, M. and O'Donnell, M. J. (2012a). Ammonia excretion in the freshwater planarian *Schmidtea mediterranea*. *J. Exp. Biol.* **215**, 3242–3253.

Weihrauch, D., Donini, A. and O'Donnell, M. J. (2012b). Ammonia transport by terrestrial and aquatic insects. *J. Insect Physiol.* **58**, 473–487.

Weihrauch, D., Joseph, G. and Allen, P. (2018). Ammonia excretion in aquatic invertebrates: new insights and questions. *J. Exp. Biol.* **221**, 1–11.

Weiner, I. D. and Verlander, J. W. (2017). Ammonia transporters and their role in acid-base balance. *Physiol. Rev.* **97**, 465–494.

Wigglesworth, V. B. (1932). The function of the anal gills of the mosquito larva. *J. Exp. Biol.* **10**, 16–26.

Wright, P. A. and Wood, C. M. (2009). A new paradigm for ammonia excretion in aquatic animals: role of Rhesus (Rh) glycoproteins. *J. Exp. Biol.* **212**, 2303–12.

Wu, S.-C., Horng, J.-L., Liu, S.-T., Hwang, P.-P., Wen, Z.-H., Lin, C.-S. and Lin, L.-Y. (2010). Ammonium-dependent sodium uptake in mitochondrion-rich cells of medaka (*Oryzias latipes*) larvae. *AJP Cell Physiol.* **298**, C237–C250.

Young-Lai, W. W., Charmantier-Daures, M. and Charmantier, G. (1991). Effect of ammonia on survival and osmoregulation in different life stages of the lobster *Homarus americanus*. *Mar. Biol.* **110**, 293–300.

Chapter Five

Development of *Aedes aegypti* (Diptera, Culicidae) mosquito larvae in high ammonia sewage in septic tanks causes alterations in ammonia excretion, ammonia transporter expression, and osmoregulation

This chapter has been published and reproduced with permission:

Durant A.C., Donini A. (2019) Development of *Aedes aegypti* (Diptera, Culicidae) mosquito larvae in high ammonia sewage in septic tanks causes alterations in ammonia excretion, ammonia transporter expression and osmoregulation. *Scientific Reports* 9, 19028.

5.1 Summary

Larvae of the disease vector mosquito, *Aedes aegypti* (L.) readily develop in ammonia rich sewage in the British Virgin Islands. To understand how the larvae survive in ammonia levels that are lethal to most animals, an examination of ammonia excretory physiology in larvae collected from septic-water and freshwater was carried out. *A. aegypti* larvae were found to be remarkably plastic in dealing with high external ammonia through the modulation of NH_4^+ excretion at the anal papillae, measured using the scanning ion-selective electrode technique (SIET), and NH_4^+ secretion in the primary urine by the Malpighian tubules when developing in septic water. Ammonia transporters, Amt and Rh proteins, are expressed in ionoregulatory and excretory organs, with increases in Rh protein, Na^+-K^+-ATPase, and V-type-H^+-ATPase expression observed in the Malpighian tubules, hindgut, and anal papillae in septic-water larvae. A comparative approach using laboratory *A. aegypti* larvae reared in high ammonia septic-water revealed similar responses to collected *A. aegypti* with regard to altered ammonia secretion and haemolymph ion composition. Results suggest that the observed alterations in excretory physiology of larvae developing in septic-water is a consequence of the high ammonia levels and that *A. aegypti* larvae may rely on ammonia transporting proteins coupled to active transport to survive in septic-water.

5.2 Introduction

The mosquito *Aedes aegypti* (L.) is a medically and economically important species because it is the vector of the arboviruses that cause dengue, Zika, chikungunya and yellow fever. (Bhatt et al., 2013; Gubler, 1998). The aquatic larvae of *Aedes aegypti* were considered to inhabit clean urban freshwater environments in close proximity to humans; however, over the last few decades, there have been numerous reports of this species exploiting more cryptic, and previously overlooked habitats such as raw sewage and domestic sewage in subterranean septic tanks (Burke et al., 2010; Irving-Bell et al., 1987; Lam and Dharmaraj, 1982) For example, during dry months in central Nigeria, *A. aegypti* was shown to preferentially breed in containers with septic water over clean water sources (Irving-Bell et al., 1987). Similar choice assay experiments in a laboratory setting found no differences in the reproductive physiology or selection of oviposition sites by adult *A. aegypti* females provided with freshwater and raw sewage (Chitolina et al., 2016). Habitat expansion of *A. aegypti* to septic tanks was documented in a 1,400 household town of Puerto Rico where it was estimated that septic tanks were yielding tens of thousands of mosquitoes daily (Barrera et al., 2008). Furthermore, this phenomena is not limited to *A. aegypti* and is not just an issue in areas with regular domestic septic tank usage or poor sanitation practices since the mosquito *Culex quinquefasciatus*, an important vector for West Nile virus, was found in greatest abundance in septic tanks and sewage treatment plants in the Florida Keys (Hribar, 2007). While there appears to be no genetic differentiation between populations of *A. aegypti* emerging from septic/sewage water and freshwater habitats, pupal biomass, adult wing length and nutrient reserves were significantly higher in *A. aegypti* from sewage water compared to man-made and natural freshwater habitats (Banerjee et al., 2015; Mackay et al., 2009; Somers et al., 2011). It now appears that septic systems serve as a year-round, permanent refuge for emerging *A. aegypti*, irrespective of rainfall amounts and wet/dry seasons (Mackay et al., 2009). These findings have serious implications for vector control programs, which traditionally focus efforts on limiting mosquito breeding in freshwater habitats during wet seasons. Furthermore, development of *A. aegypti* larvae in raw sewage

can have grave consequences in terms of disease transmission as was shown recently in a study that demonstrated the larvae and pupae can acquire Zika virus in contaminated aquatic systems containing low levels of the virus (Du et al., 2019).

It is clearly beneficial for mosquitoes to seek out protected, predator free breeding habitats rich in organic matter, such as septic tanks, but these habitats also contain ammonia (NH_3/NH_4^+) which is toxic at micromolar concentrations to most animals. Earlier studies examining the tolerance of *A. aegypti* larvae to synthetic sewage containing high levels of ammonium chloride (NH_4Cl) found that the mean [NH_4Cl] that is lethal to 50% of the exposed individuals (LC_{50}) was between ~ 2.20-3.57 mmol l^{-1} for different strains of larvae from different geographical regions including Puerto Rico, El Salvador, Africa (3 different strains), India, Sri Lanka, and Malaysia (Mitchell and Wood, 1984; Pope and Wood, 1981). The mean LC_{50} increased to ~12 mmol l^{-1} when larvae were selected over three generations of rearing in high ammonia synthetic sewage. Outside of controlled laboratory studies, high levels of ammonia (~2-4 mmol l^{-1}) in septic tanks with actively breeding *Aedes* species (*A. aegypti* and *A. albopictus*) has been documented (Chitolina et al., 2016; Lam and Dharmaraj, 1982). Therefore, *Aedes aegypti* display a remarkable tolerance to high ammonia and effective surveillance and intervention methods to prevent breeding in septic tanks has been recommended in order to achieve successful mosquito control and disease prevention programs (Burke et al., 2010; Mackay et al., 2009).

Ammonia toxicity in animals is caused by a number of mechanisms that have been previously outlined(Weihrauch et al., 2009; Weihrauch et al., 2012a; Wright, 1995a). Animals have developed strategies to minimize ammonia toxicity which include mechanisms to sequester and excrete ammonia (Weihrauch and Allen, 2018b; Weihrauch et al., 2009; Wright, 1995b). The larvae of *A. aegypti* excrete relatively high levels of ammonium (NH_4^+) from the anal papillae (AP) (Donini and O'Donnell, 2005; Weihrauch et al., 2012a). The four AP are sac-like structures that surround the anus and protrude from the terminal segment of the animal. Each AP is comprised of a syncytial epithelium with the apical cell

surface directed outwards to the environment, and the basolateral cell surface facing the lumen which is continuous with the haemocoel (Clements, 1992). This morphology allows for the direct excretion of ammonia into the aquatic environment from the AP, and these organs express a number of ammonia-transporting proteins which have been shown to play a role in ammonia excretion in laboratory reared *A. aegypti* (Chasiotis et al., 2016; Donini and O'Donnell, 2005; Chapter 3; Chapter 2; Weihrauch et al., 2012a). The AP of laboratory reared *Aedes aegypti* express two vertebrate-like Rhesus (Rh) proteins, AeRh50-1 and AeRh50-2, and two phylogenetically related ammonium transporters (Amts), AeAmt1 and AeAmt2, which group together with functionally similar Amts from plants (Chasiotis et al., 2016; Chapter 3; Weihrauch et al., 2012a). Within the AP epithelium, AeAmt1 and AeAmt2 are localized on the basal and apical sides of the epithelium, respectively, and Rh proteins are localized to both apical and basal membranes (Chasiotis et al., 2016; Chapter 3; Chapter 2). Knockdown using RNAi in these studies implicated all four proteins in the process of ammonia excretion and, in part, the regulation of acid-base balance at the AP. Furthermore, Amt and Rh protein mRNA and protein abundances are altered in response to rearing in high environmental ammonia (HEA) conditions, presumably in order to prevent ammonia influx and to continue to facilitate ammonia efflux at the AP against an inwardly directed gradient (Chapter 3; Chapter 4).

Apart from the anal papillae which are only found in some fly (Dipteran) larvae, the main excretory organs of insects are the Malpighian tubules (MT) and rectum (RM) and these have been shown to excrete ammonia in locusts and *Drosophila* (Browne and O'Donnell, 2013; Stagg et al., 1991; Thomson et al., 1988). In laboratory reared adult *A. aegypti* ammonia is excreted after a blood meal and also after feeding on solutions containing ammonia; however, it is not yet clear which organs are involved (Mazzalupo et al., 2016; Scaraffia et al., 2006). In *Manduca sexta*, an Rh-like ammonia transporter (*RhMS*) was shown to have high levels of expression in the MT and gut, and an Rh protein in *Aedes albopictus*, *AalRh50*, was upregulated in the midgut and MT of adult females following blood

feeding (Weihrauch, 2006; Wu et al., 2010a).To the best of our knowledge, no studies have been performed to assess ammonia transport by the MT and rectum of mosquito larvae and despite the importance of the AP in ammonia excretion, one might assume that these organs are also contributing. Furthermore, epithelia of other organs comprising the gastrointestinal tract may aid in regulating ammonia levels during digestion of protein. Specifically, the gastric caeca (GC) which transport ions and other solutes (D'Silva et al., 2017; Volkmann and Peters, 1989a; Volkmann and Peters, 1989b), and the anterior and posterior midgut (AMG, PMG) which are important in digestion with the PMG being comprised of cells that resemble the resorbing/secreting cells found in the GC (Clements, 1992).

Given that sewage contaminated water is being exploited as a suitable habitat by the disease vector mosquito *A. aegypti,* and this species' remarkable ability to survive in high ammonia environments, the objectives of this study were two-fold; 1) to examine if ammonia transporter expression and rates of ammonia transport in organs of field collected *A. aegypti* larvae from sewage contaminated water and freshwater are different, and 2) to evaluate if differences exist in how laboratory and field collected *A. aegypti* larvae modulate ammonia transporter expression and ammonia transport in organs when exposed to sewage contaminated water. We hypothesized that field collected *A. aegypti* larvae from sewage contaminated water are capable of tolerating high ammonia concentrations by adjusting their physiology in part through altering ammonia transporter (Rh and Amt) expression and function in excretory organs such as the AP, Malpighian tubules and gut.

5.3 Materials and Methods

Mosquito collection sites

A. aegypti larvae were collected from freshwater (FW) artificial containers (4 different artificial containers in three urbanized areas) and septic tanks (6 different septic tanks within 4 areas) in urbanized areas of the British Virgin Islands (B.V.I.) in August and December of 2018 (wet and dry seasons, respectively, Fig. 5-1). Prior to collection of *Aedes aegypti* larvae from each site, ammonia (NH_3/NH_4^+)

test strips (Tetra EasyStrips) were used to confirm high total ammonia levels in septic water compared to freshwater levels. *A. aegypti* was distinguished from other species collected using an Identification Key of Medically Important Mosquito Species developed by the Walter Reed Biosystematics Unit (WRBU, Smithsonian Institution(Wilkerson et al., 2015)). The septic tanks are domestic sewage systems comprised of a mixture of 'black water' which has come into contact with fecal matter from toilets and contains around 90% of a household's nitrogenous waste as well as the majority of pathogens, and "grey water" generally produced from bath, kitchen and laundry waste (Luostarinen et al., 2007; Terpstra, 1999). The freshwater artificial containers included discarded paint cans, sail cloth (canvas), buckets, and large barrels that had collected rainwater. Samples of raw septic water (5 mL) were collected and immediately frozen at -30°C for later analysis.

Mosquito rearing, experimental treatments and organ sample collection

A. aegypti larvae were collected from the sites described above using fine nylon mesh nets and were reared to 4th instar in 1 litre of water from their respective collection sites in aerated plastic containers (18 x 14 x 10 cm) outdoors in the shade. Separate containers held under the same conditions were utilized to hatch eggs from a laboratory reared colony in either freshwater or septic water obtained from the collection sites (Laboratory colony from Department of Biology, York University, Toronto, ON, Canada; Details on the establishment of this colony and rearing conditions of the colony have been described in detail in a previous study (Chapter 3)). All groups of larvae whether field collected or originating from the laboratory colony were fed ¼ teaspoon of Tetrafin goldfish food flakes every other day (Tetra, Melle, Germany). For laboratory sourced larvae two containers of field collected freshwater (from two separate sites where wild larvae were collected) and two containers of septic water (from two separate sites where wild larvae were collected from) were used for hatching ~100 larvae in each container. For wild collected larvae, the larvae were set up in separate containers in their respective collected septic water or freshwater. In the case of wild collected larvae, the number of

larvae and rearing density differed depending on how many larvae could be collected from the sites. Upon reaching 4th instar, the field collected and laboratory originating larvae were either fixed in Bouin's solution and subsequently stored in cold 70% ethanol for immunohistology (see Immunohistochemistry section below), or their organs were dissected on ice in Dulbecco's phosphate-buffered saline (DPBS, Thermo Fisher Scientific) and stored at -30°C until processing (see Western blotting section below). Fixed larvae and frozen organ samples were transported to York University, Toronto, ON, Canada on ice with expedited overnight service (FedEx, Mississauga, ON, Canada). Some larvae were also transported live back to Toronto, ON, Canada in their respective rearing water with the same service in order to conduct electrophysiology experiments (see below). These larvae were subsequently held in the laboratory at 26°C on a 12h:12h light:dark cycle, the same parameters utilized to rear the laboratory colony. Importation of *A. aegypti* from the B.V.I. into Canada followed the guidelines of the Government of Canada (Office of the Chief Plant Health Officer, Plant Health and Biosecurity Directorate Canadian Food Inspection Agency).

Measurement of physicochemical properties of freshwater and septic water from larvae collection sites

The osmolarity of septic water samples (10 µl per sample) from domestic septic tanks was measured using a Precision Systems Osmette II™ osmometer (Thermo Fisher Scientific) which uses a one-step freezing point measurement of osmolality between 0 to 2000 mOsm/L. Total ammonia [NH_3/NH_4^+] in each septic water sample was determined using a colorimetric assay in which a blue indophenol compound is formed (Verdouw et al., 1978). The absorbance spectra were read at 650 nm using a thermo Multiscan Spectrum microplate spectrophotometer (Thermo Electron Co., San Jose, USA) at room temperature. The concentration of free inorganic ions (NH_4^+, H^+, Na^+, K^+) were measured using ion-selective microelectrodes (ISMEs, see below). Septic water [Cl^-] levels were determined using a colorimetric assay which was measured in a spectrophotometer (Zall et al., 1956).

Ion Selective Micro-Electrodes (ISMEs)

ISMEs selective for NH_4^+, Na^+, K^+ and H^+ were constructed according to an established protocol (Donini and O'Donnell, 2005). The ISMEs were used to measure haemolymph ion (NH_4^+, H^+, Na^+, K^+) activities, Malpighian tubule fluid secretion ion activities, and for Scanning Ion-selective Electrode Technique (SIET) ion flux measurements at the anal papillae. The tips of ISMEs for haemolymph sampling and Malpighian tubule (MT) fluid secretion sampling were coated with polyvinylchloride (PVC, Fluka) in tetrahydrofuran (THF, Fluka) as previously described (Donini and O'Donnell, 2005). The ISMEs were calibrated after every 2 samples in the following solutions (mmol l^{-1}): NH_4^+, 0.2, 2, 20 NH_4Cl; Na^+, 30 NaCl +270 LiCl and 300 NaCl; H^+, 100 mmol l^{-1} NaCl and 100 mmol l^{-1} sodium citrate at pH 7.0, 8.0 and 9.0 (pH adjusted by tritration with NaOH or HCl); and K^+, 0.5, 5, and 50 KCl. The NH_4^+ ISMEs for SIET were calibrated in 0.1, 1 and 10 mmol l^{-1} NH_4Cl.

Haemolymph and Malpighian tubule fluid secretion sampling

Haemolymph was collected from larvae following a previously established protocol (Chapter 3). Haemolymph NH_4^+, H^+, Na^+, and K^+ levels of the collected haemolymph droplets under mineral oil were measured as free ion activities using ion-selective microelectrodes (ISMEs). Voltages were recorded with an ML165 pH Amp connected to a PowerLab 4/30 and analyzed in LabChart 6 Pro software (AD Instruments Inc, Colorado Springs, CO, USA).

A modified Ramsay assay described in Misyura *et al.* was used to collect secreted primary urine droplets from MTs of *A. aegypti* larvae (Misyura et al., 2017). The MTs were left to secrete for 60 mins at room temperature with the distal 1/3 portion bathed in a saline droplet containing 2 mmol l^{-1} of NH_4Cl. Fluid secretion rates were calculated by dividing the volume of the secreted droplet by the time it took for the droplet to form. ISMEs were used to measure [NH_4^+] within the secreted fluid.

NH_4^+ flux measurements using SIET

NH_4^+ flux at the anal papillae of *A. aegypti* larvae was measured using the scanning ion-selective electrode technique (SIET) and has been described in detail elsewhere (Chasiotis et al., 2016; Donini and O'Donnell, 2005; Chapter 3). Briefly, NH_4^+ voltage gradients over an excursion distance of 100 µm were recorded adjacent to the papillae with an ISME selective for NH_4^+. Fluxes were measured in the rearing water of each group of larvae (freshwater for FW-reared larvae and septic water for Septic-reared larvae). Flux measurements were taken along the middle to distal portion of the anal papillae at four equally spaced sites. Background voltage gradients were taken 3 cm away from the anal papillae using the same sampling protocol and were subtracted from the voltage gradients recorded at the papillae. For SIET measurements, a single biological replicate (n = 1*)* is defined as the average flux from 4 repeated measurements at each of the 4 equidistant sites along a single anal papilla from a single larva.

Body weight and total body moisture

Body weight and body water content were measured from laboratory 4th instar larvae reared in both FW and septic water. The larvae were first placed on tissue paper which allowed all external body surface moisture to be absorbed. The body weight of larvae was recorded (to the nearest microgram, µg) using a UMX2 Automated-S microbalance (Mettler Toledo, Greifensee, Switzerland). Larvae were then placed in a conventional oven at 60°C for 48 hr to dehydrate and were subsequently reweighed. Total body water content (% of larval weight prior to dehydration) was then calculated using the difference in the mass of the larvae before and after dehydration.

Western blotting and immunohistochemistry

Quantification of AeAmt1, AeAmt2, and AeRh50 protein abundances in *A. aegypti* larvae using Western blotting has been previously established (Chasiotis and Kelly, 2008; Chapter 3). The present study examined AeAmt1, AeAmt2, and AeRh50 protein abundance in the carcass (CAR), whole

gut (WG), and anal papillae (AP) of B.V.I. collected larvae, and in the gastric caecae (GC), anterior midgut (AMG), posterior midgut (PMG), hindgut (HG), Malpighian tubules (MT), and the anal papillae (AP) of laboratory larvae, which were reared in either B.V.I. collected freshwater or septic water. The CAR of larvae in this study is defined as all organs, tissues and cuticle *not* including organs of the alimentary canal and anal papillae, and the WG includes all organs of the alimentary canal (GC, AMG, PMG, HG, MT). Note that GC and AMG are not presented in our normalized protein abundance data for laboratory larvae, as we did not detect ammonia transporter expression in those organs in either FW or septic water reared laboratory larvae. For B.V.I. collected larvae, 3 biological samples were collected from a total of 90 FW and 90 septic water larvae, where 1 biological sample consisted of the CAR, WG or AP of 30 larvae. Protein samples were initially collected and stored in *A. aegypti* saline described previously (Donini et al., 2007). Samples of laboratory larvae reared in B.V.I. FW and septic water were similarly collected with 3 and 4 biological samples for FW and septic water, respectively; however, each of these samples were from 50 larvae. Proteins in samples were electrophoretically separated by sodium dodecyl sulphate polyacrylamide gel electrophoresis (SDS-PAGE) as described in detail by Durant and Donini by loading 5 µg (for AP) or 15 µg (for all other organs) of protein (Bradford Assay, Bio-Rad) in RIPA homogenization buffer and 6× loading buffer (Chapter 4). Custom-synthesized polyclonal antibodies raised in rabbit against AeAmt1, AeAmt2, and AeRh50s were used at dilutions of 7.46 X 10^{-04}, 3.57 X 10^{-04}, and 4.29 X 10^{-04} µg μL^{-1} respectively, and have been previously described and used on larvae of *A.* aegypti (Chasiotis et al., 2016; Chapter 3; Chapter 2). Due to a high epitope sequence similarity between AeRh50-1 and AeRh50-2, the AeRh50 antisera (designed against AeRh50-1) is presumed to detect both AeRh50-1 and AeRh50-2 protein (Chapter 2). Therefore, AeRh50 protein abundance is reported as the combination of both AeRh50-1 and AeRh50-2. Total protein analysis as a loading control was carried out using Coomassie total protein staining (Chapter 3; Eaton et al., 2013). Densitometric analysis of AeAmt1, AeAmt2, AeRh50s, and Coomassie

total protein was conducted using ImageJ 1.50i software (National Institutes of Health, Bethesda, MD, USA).

AeAmt1, AeAmt2, and AeRh50 immunolocalization in paraffin-embedded cross and transverse sections (5 µm thick) of the *A. aegypti* WG, CAR, and AP was carried out on 10 larvae for each treatment according to an established protocol with the antisera used at dilutions of 9.33 X 10^{-03}, 2.86 X 10^{-03}, and 6.44 X 10^{-03} µg $µL^{-1}$, respectively (Chasiotis et al., 2016; Chapter 3; Chapter 2). Na^+-K^+-ATPase (NKA) and the V_1 subunit of V-type H^+-ATPase (VA) immunostaining were used as markers for the basolateral and apical membranes, respectively, of organs comprising the alimentary canal(Patrick et al., 2006a). Note that VA is localized to the basolateral membrane in the anterior midgut (AMG) of *A. aegypti* larvae, where NKA immunostaining appears to be absent (Patrick et al., 2006a). A mouse monoclonal anti-α5 antibody for NKA (Douglas Fambrough, Developmental Studies Hybridoma Bank, IA, USA) was used at a 1:10 dilution, and a guinea pig anti-V-type H^+-ATPase (kind gift from Dr. Weiczorek, University of Osnabruk, Germany) was used at a 1:5000 dilution (Chasiotis et al., 2016; Chapter 3; Patrick et al., 2006). A sheep anti-mouse antibody conjugated to Cy2 and a goat anti-guinea pig antibody conjugated to AlexaFluor 647 (Jackson ImmunoResearch Laboratories, West Grove, PA, USA) at dilutions of 1:500 were used to visualize NKA and VA, respectively. To visualize AeAmt1, AeAmt2 and AeRh50, a goat anti-rabbit antibody conjugated to Alexa Fluor 594 (Jackson ImmunoResearch) at a dilution of 1:500 for all slides was applied (Chasiotis et al., 2016; Chapter 2). Control slides were only incubated with primary immune serum (primary antibody omitted) and processed according to the procedure above. Slides were mounted using with mount media containing DAPI for nuclei staining (ProLong Gold antifade reagent, Life Technologies, Burlington, ON). Fluorescence images were captured on an Olympus IX81 inverted microscope (Olympus Canada, Richmond Hill, ON, Canada) equipped with an X-CITE 120XL Fluorescent Illuminator (X-CITE, Mississauga, ON, Canada)(Misyura et al., 2017; Nowghani et al., 2019). Images were merged using ImageJ 1.50i software (National Institutes of Health, Bethesda, MD, USA).

Statistical analyses

Data were analyzed using GraphPad Prism 7.00 (GraphPad Software Inc., La Jolla, CA, USA) and were expressed as mean ± S.E.M. All experimental measurements were analyzed using the Student's *t*-test ($p < 0.05$) or Two-way ANOVA (Bonferonni's multiple comparisons test, adjust p value < 0.05) on log transformed values for normalized data and raw values for all other data, as specified.

5.4 Results

Physicochemical analysis of freshwater and septic water from larvae collection sites

A. aegypti larvae were collected from artificial containers containing freshwater and residential septic tanks containing sewage water in urbanized regions of the British Virgin Islands (indicated in Fig. 5-1). Field assessments of total ammonia [NH_3/NH_4^+] in FW containers (Fig. 5-2A) and septic water from septic tanks (Fig. 5-2B) using ammonia test strips (Tetra EasyStrips) were carried out. Lower levels of ammonia in FW (~0.015 mmol l^{-1}) were detected relative to those in septic water (~ 5 mmol l^{-1}). Ammonia test strips from each of the FW containers and septic tank sites in which *A. aegypti* larvae were collected from in this study are also presented to demonstrate differences in field estimates of total ammonia between FW and septic water (Fig. 5-S1). The osmolarity, concentration of inorganic ions, and total ammonia [NH_3/NH_4^+] levels in septic water collected from three septic tanks was also measured in the laboratory (Table 5-1). Mean osmolarity (29 mOsm l^{-1}) was approximately 10 times less than the haemolymph osmolarity of *A. aegypti* larvae (Edwards, 1982). High levels of total ammonia [NH_3/NH_4^+] and ammonium [NH_4^+] were measured in septic water (7.8 and 4.6 mmol l^{-1}, respectively), corresponding with crude assessments using ammonia test strips (see above). The mean septic water pH was alkaline (pH 8.5), and moderate amounts of Cl^-, Na^+, and to a lesser extent, K^+, was measured (8.2, 4.3, and 1.2 mmol l^{-1}, respectively) (Table 5-1). Measurements of [NH_4^+] in FW from artificial containers containing larvae were much lower ($\leq 0.387 \pm 0.015$ mmol l^{-1}) with osmolarity between 0-5 mOsm l^{-1} (data not shown).

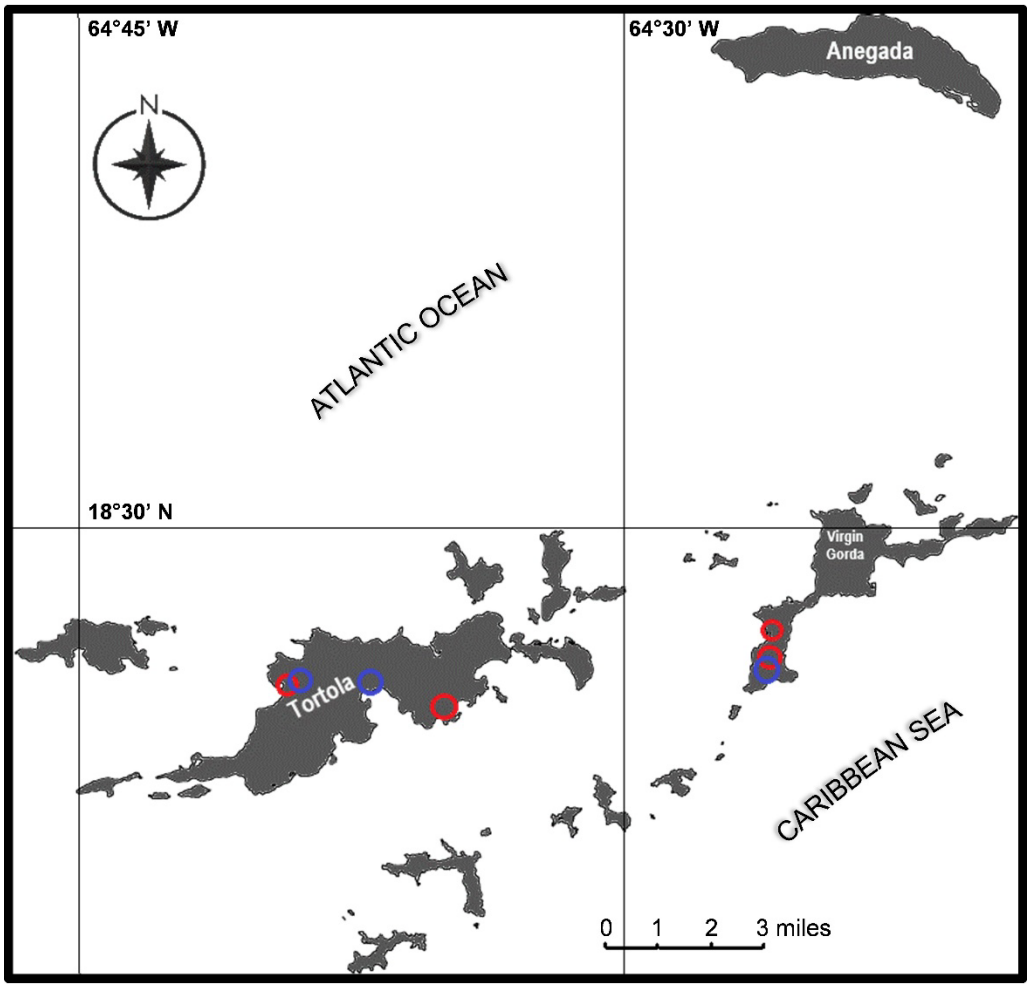

Figure 5- 1. Map of the study area and sites of *A. aegypti* larvae collection within the British Virgin Islands. The location of *Aedes aegypti* larvae collected from septic tanks (6 septic tanks within 4 different areas, red circles) and artificial containers containing freshwater (5 artificial containers within 3 different areas, blue circles) used in the present study are indicated. *A. aegypti* larvae were collected from urbanized sites on the islands of Tortola and Virgin Gorda.

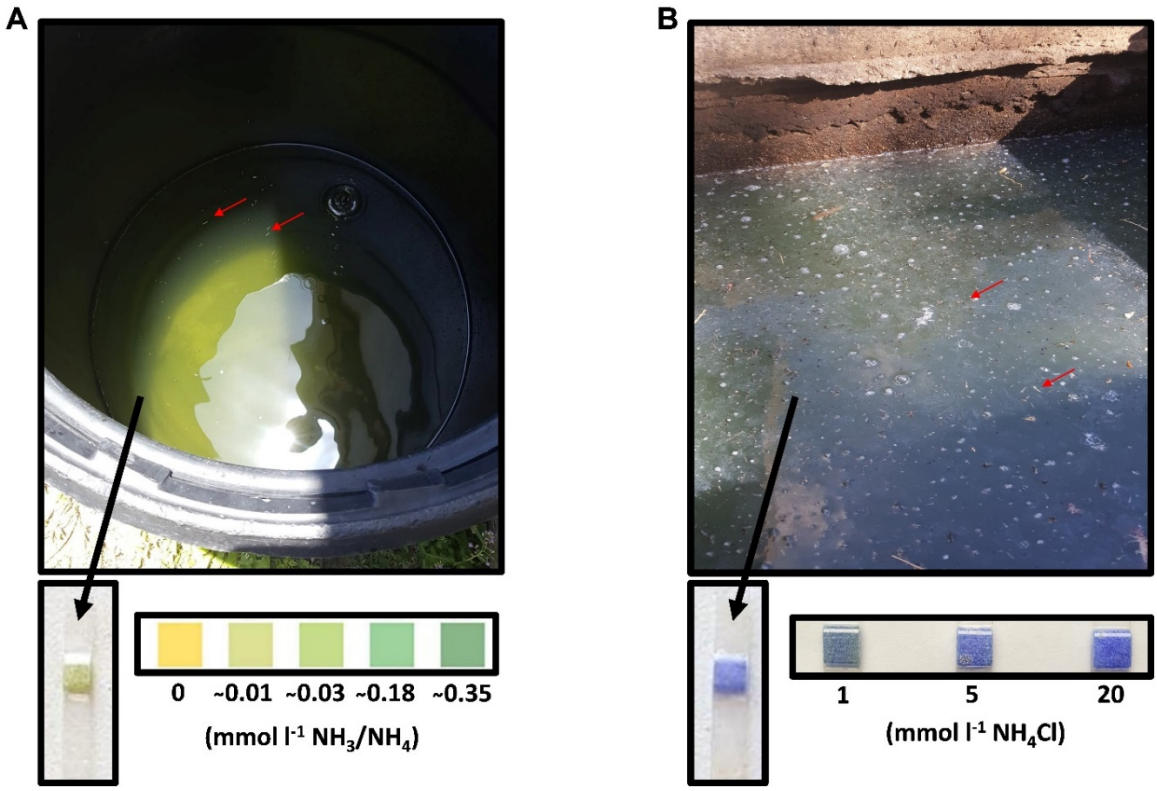

Figure 5- 2. Representative images of a freshwater container and a septic tank containing raw sewage water each with actively breeding *A. aegypti* used in the present study. (A) Barrel containing freshwater (FW) and (B) septic tank with raw sewage water each containing live *A. aegypti* larvae (indicated by red arrows). Representative ammonia (NH_3/NH_4^+) test strips (Tetra EasyStrips) from one FW site and one septic water site used to estimate ammonia levels are shown below each image (A and B) along with a control concentration gradient.

Table 5- 1. Concentration of inorganic ions, pH, osmolarity and total ammonia in raw sewage water collected from septic tanks containing developing *A. aegypti* larvae, pupae, and breeding adults. Values are shown as mean ± S.E.M. (n = 3 samples of raw sewage). Note: samples of freshwater were not analyzed here, however, freshwater [NH_4^+] and osmolarity measurements can be found in text (see Results).

Osmolarity (mOsm/L)	Total [NH_3/NH_4^+] (mmol/L)	NH_4^+ (mmol/L)	pH	Na^+ (mmol/L)	K^+ (mmol/L)	Cl^- (mmol/L)
29 ± 4.143	7.78 ± 1.217	4.57 ± 0.548	8.48 ± 0.134	4.25 ± 0.438	1.19 ± 0.108	8.24 ± 0.893

Haemolymph ion activities, body weight, and body moisture of larvae

Haemolymph ion activities and pH of wild collected and laboratory larvae reared in FW and septic water were measured using ISMEs (Fig. 5-3). A significant increase in haemolymph [NH_4^+] was observed in both wild collected and laboratory larvae reared in septic water compared to FW reared larvae (Fig. 5-3A,B). The pH of the haemolymph of wild collected septic-reared larvae was lower than FW reared larvae (Fig. 5-3A). There was no difference in haemolymph [Na^+] and [K^+] between FW and septic water reared larvae from wild collected or laboratory larvae (Fig. 5-3). Furthermore, mean body weight (in mg) and total body moisture (between 85-90% of total larval mass) of 4th instar laboratory *A. aegypti* larvae did not differ between FW and septic water treatments (Fig. 5-4).

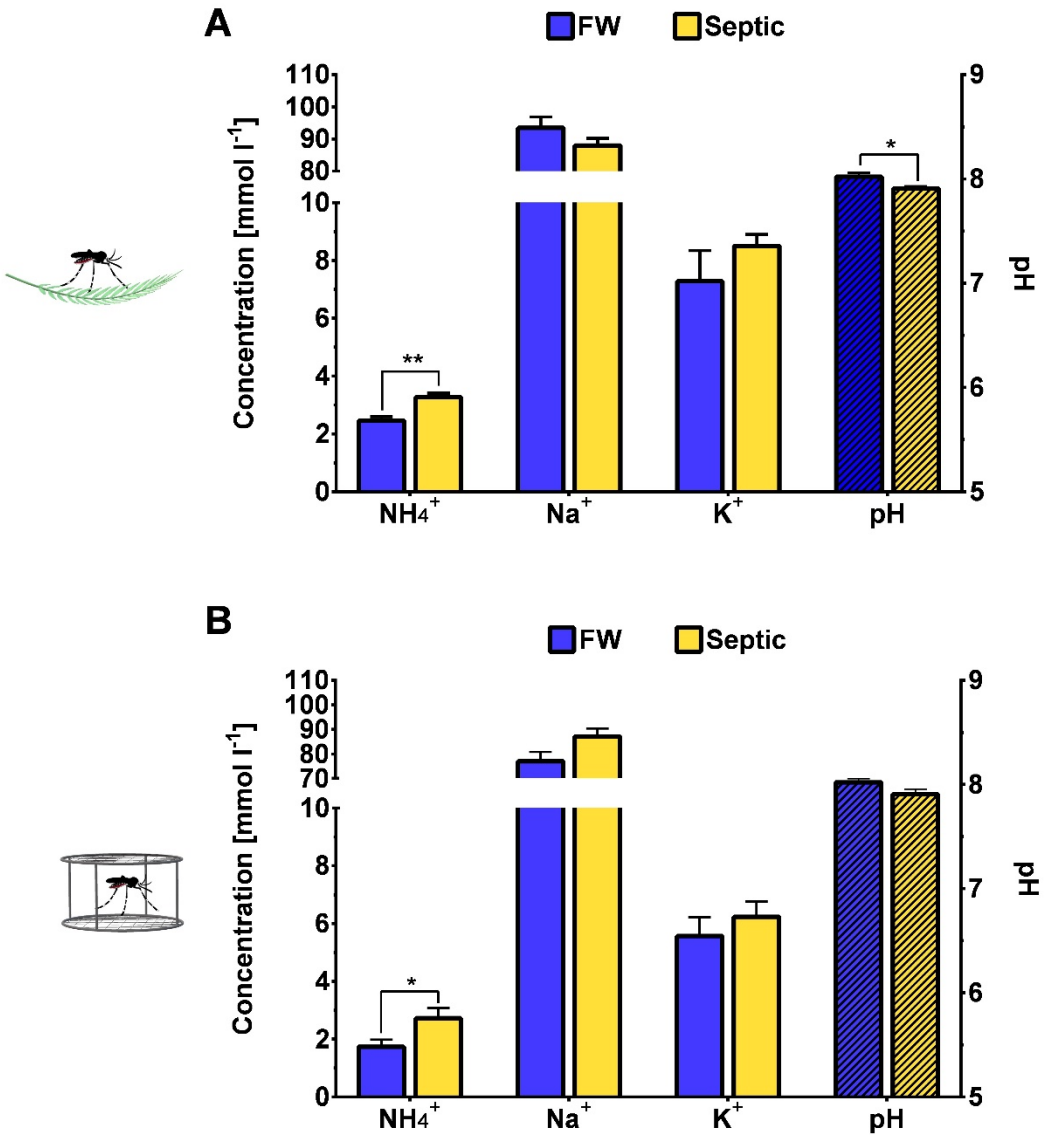

Figure 5- 3. Haemolymph ion and pH levels of wild-collected and laboratory *A. Aegypti* larvae reared in freshwater (FW) and septic water (Septic). Ammonium (NH_4^+), sodium (Na^+), potassium (K^+) and pH (dashed bars) levels in the haemolymph of (A) wild *A. aegypti* larvae (*n = 6-7* per group) and (B) laboratory *A. aegypti* larvae (*n = 15-17* per group) reared in FW or Septic. Data shown as mean ± S.E.M. Asterisks indicate statistical significance (* = $p < 0.05$; ** = $p < 0.005$) compared to FW control (*Unpaired, two-tailed t-test*; Adjusted *p* values shown; *Holm-Sidak* correction for multiple comparisons).

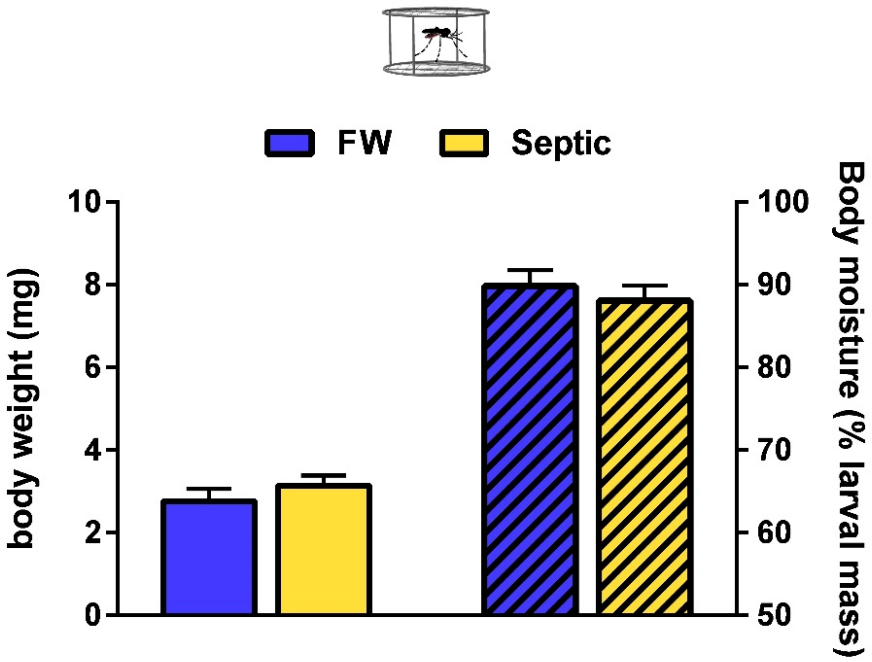

Figure 5- 4. Mean body weight and total body moisture (dashed bars) of laboratory *A. aegypti* larvae reared in freshwater (FW) or septic water (Septic). Data shown as mean ± S.E.M (*n = 9* for FW, *n = 9* for Septic). [*Unpaired, two-tailed t-test; p = 0.35* for body weight, *p = 0.51* for body moisture].

NH_4^+ flux at the anal papillae of FW- and Septic-reared larvae

NH_4^+ flux at the AP of FW and septic water reared larvae was measured using SIET (Fig. 5-5). Flux measurements for FW animals were recorded in a freshwater bath, and flux measurements for septic water collected animals were recorded in a septic water bath. In wild collected *A. aegypti* larvae, a mean absorption (5 ± 7.34 $pmol^{-2}$ s^{-1}; n=3 absorbing and n=1 secreting) of NH_4^+ at the AP of FW larvae, and a mean secretion (-18.5 ± 5.62 $pmol^{-2}$ s^{-1}; n=6 secreting) of NH_4^+ at the AP of septic larvae was measured, demonstrating significant differences in the magnitude and direction of NH_4^+ transport at the AP between groups (Fig. 5-5A). Similar observations of significant differences in NH_4^+ flux of laboratory *A. aegypti* larvae were seen, with mean NH_4^+ flux at the AP of FW larvae being close to zero (-0.9 ± 8.36 $pmol^{-2}$ s^{-1}; n=3 absorbing and n=2 secreting), and a net NH_4^+ secretion (-50.92 ± 12.55 $pmol^{-2}$ s^{-1}; n=5 secreting) at the AP of septic-reared larvae (Fig. 5-5B). NH_4^+ secretion in laboratory septic-reared larvae was approximately 2.75 times greater than NH_4^+ secretion in wild septic-reared larvae (*p = 0.0295;* Two-way ANOVA, Bonferroni's multiple comparisons test) (Fig. 5-5).

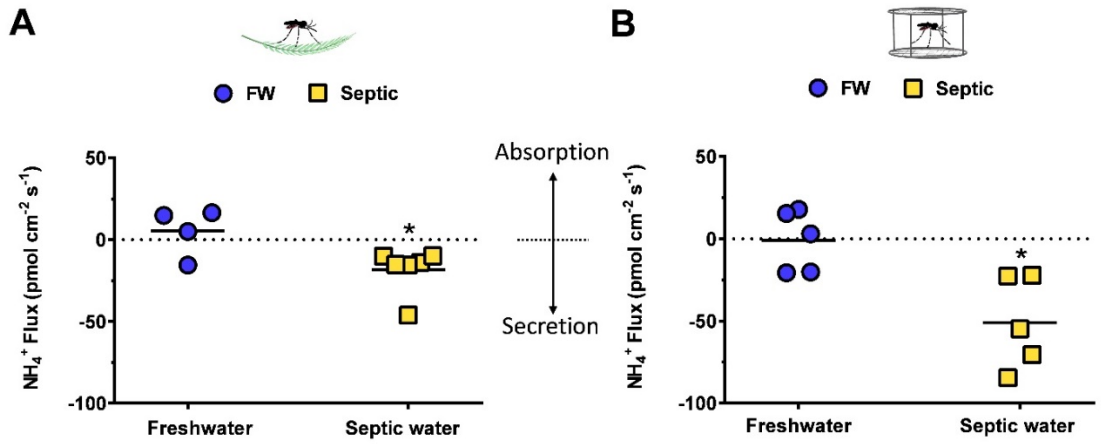

Figure 5- 5. Scanning ion-selective micro-electrode technique (SIET) measurements of NH_4^+ flux at the anal papillae of wild-collected and laboratory *A. aegypti* larvae reared in freshwater (FW) and septic water (Septic). (A) NH_4^+ flux at the anal papillae of wild *A. aegypti* larvae reared in FW or Septic ($n = 4$ for FW, $n = 6$ for Septic), and (B) NH_4^+ flux at the anal papillae of laboratory *A. aegypti* larvae reared in FW of Septic ($n = 5$ for FW and Septic), measured each in their respective freshwater or septic water baths. NH_4^+ flux for each individual animal is shown as a single point, with the mean flux for each group illustrated by a horizontal solid black line. Negative values indicate efflux, or excretion, and positive values indicate influx, or absorption from the external. Data shown as mean ± S.E.M. Asterisks indicate statistical significance (* = $p < 0.05$) compared to FW control (*Unpaired, two-tailed t-test*).

NH_4^+ activities, NH_4^+ transport rates, and fluid secretion rates of MT from FW- and Septic-reared larvae

The *in vitro* transepithelial fluid ion composition and secretion rates of the MT of wild collected and laboratory *A. aegypti* larvae reared in FW or septic water was examined (Fig. 5-6). The [NH_4^+] in the secreted fluid droplet did not differ between MT from wild collected FW or septic reared larvae (Fig. 5-6A), however, a significant increase in [NH_4^+] in the secreted fluid of MT from laboratory septic reared larvae compared to FW reared laboratory larvae MT was observed (Fig. 5-6B). Furthermore, the mean [NH_4^+] in the secreted fluid of MT from wild collected *A. aegypti* larvae was 23.25 ± 3.9 and 26.4 ± 4.1 mmol l^{-1} for FW and septic water wild larvae, respectively, whilst the mean [NH_4^+] in the secreted fluid of MT from laboratory *A. aegypti* larvae was significantly lower, 5.77 ± 0.5 and 11.55 ± 0.9 mmol l^{-1} for FW and septic water laboratory larvae, respectively ($p = 0.0057$ for FW colony vs. FW wild larvae; $p = 0.0355$ for Septic colony vs. Septic wild larvae, Two-way ANOVA, Bonferonni's multiple comparisons test) (Fig. 5-6A-B). There was no change in the secretion rates of fluid from the MTs of wild (Fig. 5-6C) and laboratory (Fig. 5-6D) larvae between FW and septic treatments, however, significant increases in the transport rates of [NH_4^+] within the secreted fluid by MT from laboratory (Fig. 5-6E) and wild collected (Fig. 5-6F) larvae was observed with septic water rearing compared to FW groups.

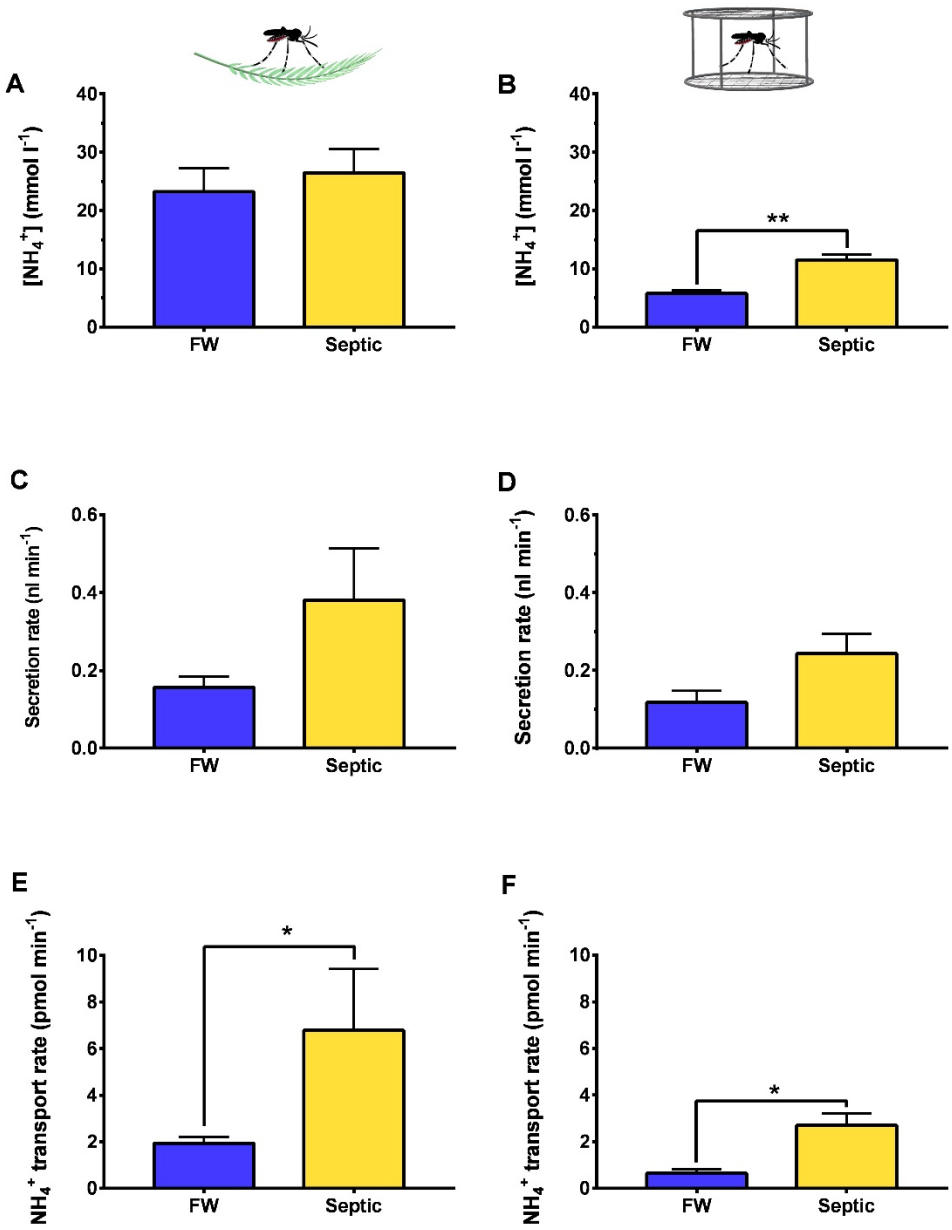

Figure 5- 6. Transepithelial fluid secretion rates, ammonium (NH_4^+) concentrations in the secreted fluid, and NH_4^+ transport rates of Malpighian tubules from wild-collected and laboratory *A. aegypti* larvae reared in freshwater (FW) or septic water (Septic). NH_4^+ concentrations in Malpighian tubule secreted fluid from (A) wild *A. aegypti* larvae and (B) laboratory *A. aegypti* larvae reared in FW and septic water. Transepithelial fluid secretion rate of the Malpighian tubules from (C) wild *A. aegypti* larvae and (D) laboratory *A. aegypti* larvae reared in FW and septic water. NH_4^+ transport rate by the Malpighian tubules from (E) wild *A. aegypti* larvae and (F) laboratory *A. aegypti* larvae reared in FW and septic water. Data shown as mean ± S.E.M (*n = 5-7* wild larvae, *n = 5* laboratory larvae). Asterisks indicate statistical significance (* = $p < 0.05$; ** = $p < 0.005$) compared to FW control (*Unpaired, two-tailed t-test*).

Ammonia transporter expression and localization in FW- and Septic-reared larvae

Relative protein abundance and immunolocalization of AeAmt1 in FW and septic water reared larvae was examined (Fig. 5-7). The AeAmt1 monomer (30 kDa) was detected in each organ. In wild collected larvae, AeAmt1 protein expression was only detected in the carcass, and not in the WG and AP of larvae, and no change in AeAmt1 abundance in the carcass was observed between FW and septic water rearing (Fig. 5-7A). On the other hand, immunohistochemistry did not detect AeAmt1 staining in the carcass but instead revealed AeAmt1 localization in transverse sections of the AP epithelium of FW and septic reared wild larvae (Fig. 5-7C,D), and in cross sections of the MT and RM epithelia where cytosolic staining in the principal cells and co-localization with VA at the apical membrane of the MT is observed (Fig. 5-7G,H). In laboratory larvae, AeAmt1 protein was detected in protein homogenates of the MT and AP, whereby rearing in septic water did not affect abundance in comparison to FW controls (Fig. 5-7B). AeAmt1 was not detected in the PMG and HG through Western blotting. However, immunohistochemistry revealed AeAmt1 localization in transverse sections of the epithelium of the rectum (the distal portion of the HG), where co-localization with VA occurs in septic-reared larvae (Fig. 5-7I,J), and AeAmt1 localization is also observed in AP cross sections (Fig. 5-7E,F).

AeAmt2 protein (55 kDa monomer) was detected in the carcass and AP of wild collected *A. aegypti* larvae, where AeAmt2 abundance was similar in FW and septic water reared larvae (Fig. 5-8A). AeAmt2 was not detected in the WG of wild larvae using Western blotting, however, immunohistochemistry revealed AeAmt2 localization in the epithelia of GC, MG, MT, and IL of FW and septic reared larvae (Fig. 5-8C-F). In all cases, an apical (lumen facing) localization of AeAmt2 was observed in wild collected larvae, with the exception of the MT where both apical and cytosolic staining in the principal cells is shown (Fig. 5-8E-F). Dashed arrows indicate co-localization of AeAmt2 with apical VA in the MT and GC (Fig. 5-8D,E). In laboratory larvae, AeAmt2 protein was detected in the MT and AP using Western blotting, whereby AeAmt2 significantly increased in the MT in response to

septic water rearing in comparison to FW controls (Fig. 5-8B). AeAmt2 was immunolocalized within all organs examined, including the epithelium of the AP (Fig. 5-8G,H), and the midgut (Fig. 5-8I,J). Localization in the CAR, which includes fat body, muscle, and cuticle (see Methods), was also observed. Similarly, to observations in wild larvae, an apical localization within the epithelia of organs comprising the alimentary canal, and the AP, was observed.

AeRh50 protein (48 kDa monomer) was detected in the carcass, WG, and AP of wild collected larvae, whereby AeRh50 protein abundance significantly decreased in the WG and AP of septic water reared larvae compared to FW controls (Fig. 5-9A). Rh protein immunostaining in transverse sections of the AP epithelium of larvae corresponded with findings from Western blotting, demonstrating a decrease in Rh immunostaining within the epithelium of AP of septic reared larvae in comparison to FW controls (Fig. 5-9C,D). On the other hand, whilst a significant decrease in Rh protein abundance in response to rearing in septic water using Western blotting was observed, an increase in Rh immunostaining in transverse sections of the MT and RM of septic reared larvae was also observed, compared to FW reared larvae (Fig. 5-9E,F). Additionally, an increase in NKA immunostaining in the RM of septic water reared larvae compared to FW reared larvae was also detected in these sections. In laboratory larvae, AeRh50 protein was detected in the epithelia of PMG, HG, MT and AP, whereby a significant increase in the MT in response to septic water rearing was observed (Fig. 5-9B). In all organs the Rh monomer (48 kDa) was detected, with the exception of the HG which displayed only a single band at 100 kDa, the presumed dimer form of the AeRh50 (Fig. 5-9B, right panel). Immunohistochemistry revealed AeRh50 localization in the MT and RM, where an apparent increase in Rh staining in the MT in septic water reared larvae compared to FW was observed corresponding to the change observed through Western blotting (Fig. 5-9G,H). Rh staining was also detected in the apical membrane of the MG epithelium (Fig. 5-9I,J). Similar to AeAmt2 localization, within each organ Rh

was localized to the apical membrane (lumen facing) of the epithelium, with the exception of the AP in which localization to a specific membrane could not be determined.

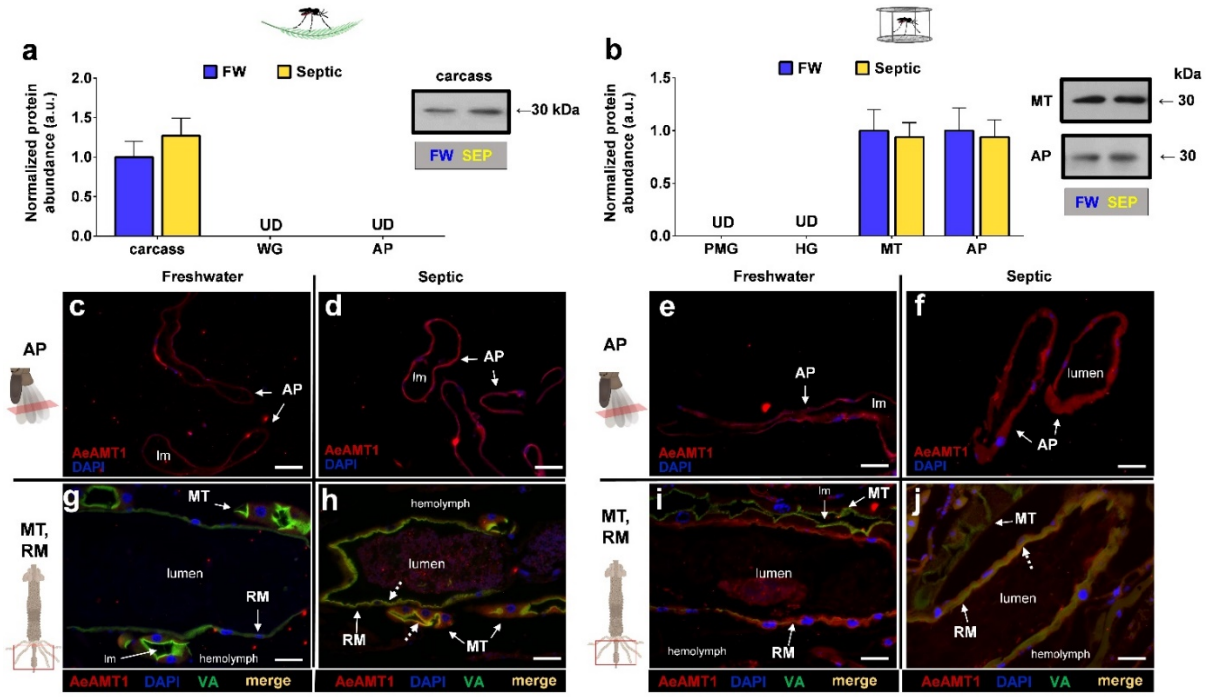

Figure 5- 7. AeAmt1 abundance and immunolocalization in the alimentary canal, anal papillae, and carcass of wild-collected and laboratory *A. aegypti* larvae reared in freshwater (FW) and septic water (Septic). (a) AeAmt1 abundance and representative Western blot (right panel) in the carcass of wild *A. aegypti* larvae *(n = 3).* (b) AeAmt1 abundance and representative Western blot (right panel) in the Malpighian tubules (MT) and anal papillae (AP) of laboratory *A. aegypti* larvae (*n = 3* FW, *n = 4* Septic*)*. The abundance of AeAmt1 protein was normalized to total protein (Coomassie protein stain, not shown), and Septic values are expressed relative to the control FW group (assigned a value of 1). Data shown as mean ± S.E.M. [*Unpaired, two-tailed t-test; $p < 0.05$]*. Representative transverse sections of anal papillae (AP) showing AeAmt1 (red) immunostaining from (c) wild FW-reared larvae, (d) wild Septic-reared larvae, (e) laboratory FW-reared larvae and (f) laboratory Septic-reared larvae. Nuclei are labelled by DAPI (blue) staining. Representative cross sections of the Malpighian tubules (MT) and rectum (RM) showing AeAmt1 (red) immunostaining from (g) wild FW-reared larvae, (h) wild Septic-reared larvae, (i) laboratory FW-reared larvae and (j) laboratory Septic-reared larvae. Nuclei are labelled by DAPI (blue) staining. Immunostaining of V_1 subunit of V-type H^+-ATPase (VA) is green (g-h, i-j). Co-localization of AeAmt1 with apical V_1 subunit of V-type H^+-ATPase is indicated (dashed arrows) in the MT and RM (merge, yellow). Control sections (primary antibodies omitted, not shown) were devoid of red and green staining. Illustrations of the alimentary canal and anal papillae of *A. aegypti* larvae to the left of each immunofluorescence image indicates the region of the cross or transverse section (red rectangles). Lumen, (lm); anal papillae (AP); rectum (RM). Scale bars: 50 µm (c-j).

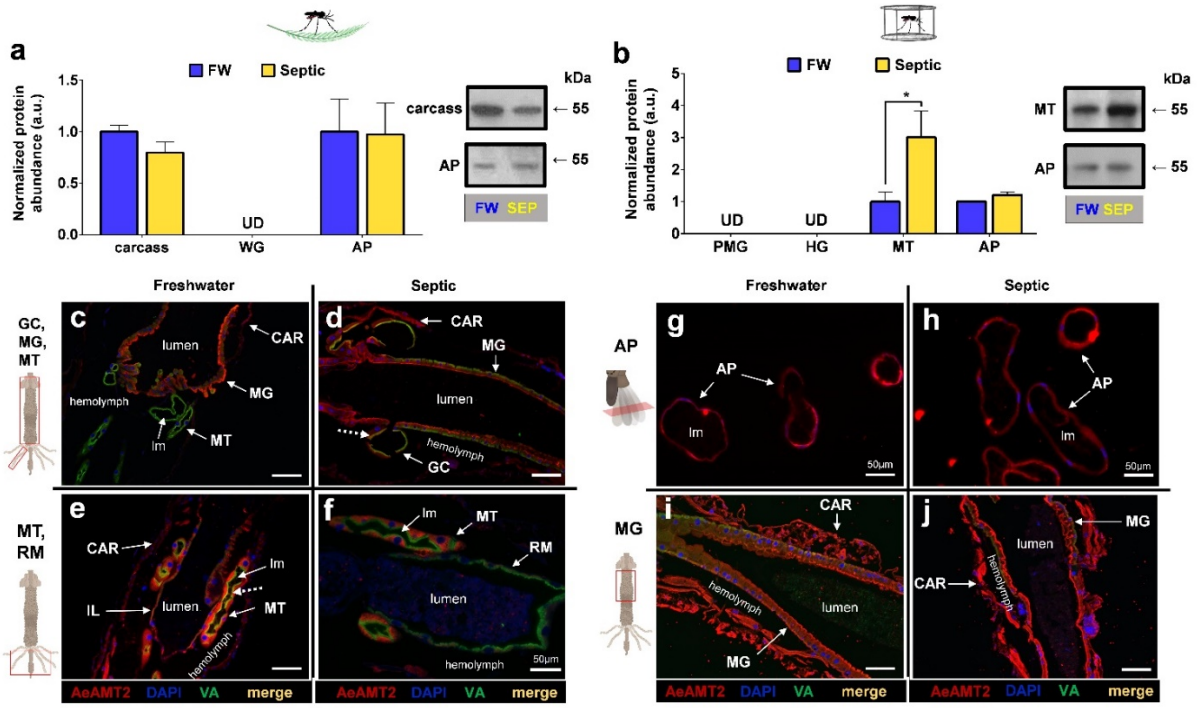

Figure 5- 8. AeAmt2 abundance and immunolocalization in the alimentary canal, anal papillae, and carcass of wild-collected and laboratory *A. aegypti* larvae reared in freshwater (FW) and septic water (Septic). (a) AeAmt2 abundance and representative Western blots (right panel) in the carcass and anal papillae (AP) of wild *A. aegypti* larvae *(n = 3).* (b) AeAmt2 abundance and representative Western blots (right panel) in the Malpighian tubules (MT) and anal papillae (AP) of laboratory *A. aegypti* larvae (*n = 3* FW, *n = 4* Septic*)*. The abundance of AeAmt2 protein was normalized to total protein (Coomassie protein stain, not shown), and Septic values are expressed relative to the control FW group (assigned a value of 1). Data shown as mean ± S.E.M. Asterisks indicate statistical significance (* = $p < 0.05$) compared to FW control (*Unpaired, two-tailed t-test*). Representative cross sections of the carcass (CAR), gastric caecae (GC), anterior and posterior midgut (MG) and Malpighian tubules (MT) and rectum (RM) showing AeAmt2 (red) immunostaining from (c-e) wild FW-reared larvae, (d-f) wild Septic-reared larvae. Representative cross sections of the anterior midgut (MG) and transverse sections of anal papillae (AP) showing AeAmt2 (red) immunostaining from (g-i) laboratory FW-reared larvae and (h-j) laboratory Septic-reared larvae. Nuclei are labelled by DAPI (blue) staining. Immunostaining of V_1 subunit of V-type H^+-ATPase (VA) is green (c-h). Co-localization of AeAmt2 with V_1 subunit of V-type H^+-ATPase is indicated (dashed arrows) (merge, yellow). Control sections (primary antibodies omitted, not shown) were devoid of red and green staining. Illustrations of the alimentary canal and anal papillae of *A. aegypti* larvae to the left of each immunofluorescence image indicates the region of the cross or transverse section (red rectangles). Lumen, (lm); carcass (CAR), gastric caecae (GC), midgut (MG), Malpighian tubule (MT), anal papillae (AP); rectum (RM). Scale bars: 100 µm, unless specified.

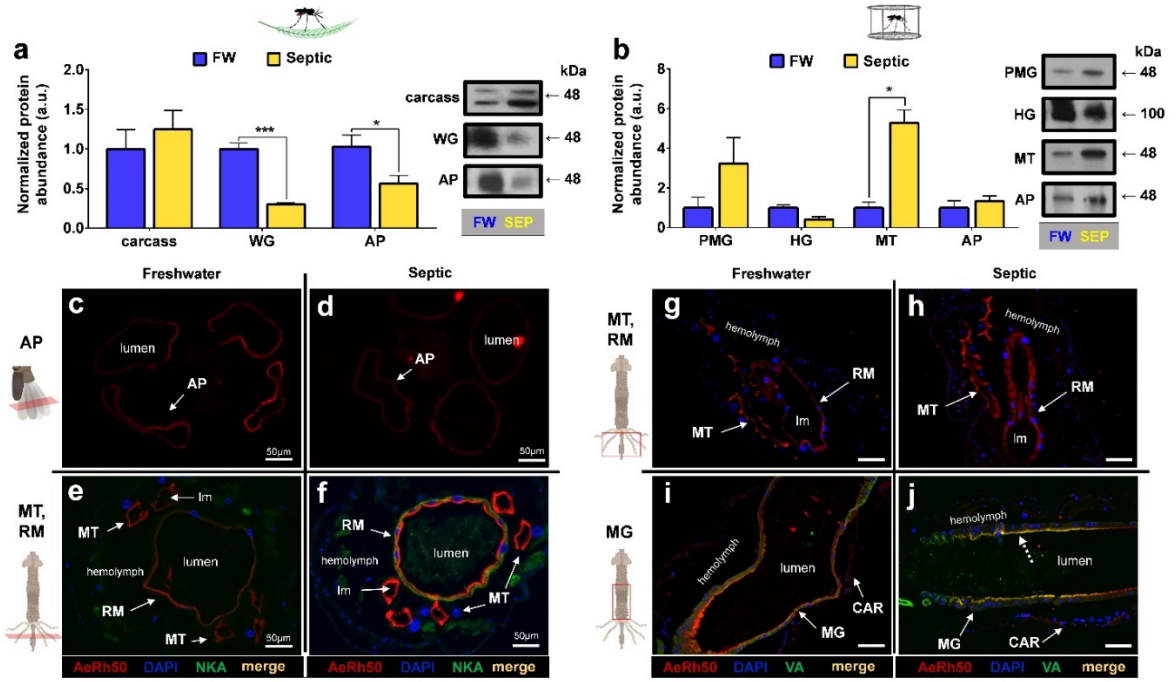

Figure 5- 9. Rh protein (AeRh50) abundance and immunolocalization in the alimentary canal, anal papillae, and carcass of wild-collected and laboratory *A. aegypti* larvae reared in freshwater (FW) and septic water (Septic). (a) AeRh50 abundance and representative Western blots (right panel) in the epidermis, whole gut (WG), and anal papillae (AP) of wild *A. aegypti* larvae *(n = 3).* (b) AeRh50 abundance and representative Western blots (right panel) in the posterior midgut (PMG), hindgut (HG), Malpighian tubules (MT) and anal papillae (AP) of laboratory *A. aegypti* larvae (*n = 3* FW, *n = 4* Septic*)*. The abundance of AeRh50 protein was normalized to total protein (Coomassie protein stain, not shown), and Septic values are expressed relative to the control FW group (assigned a value of 1). Data shown as mean ± S.E.M. Asterisks indicate statistical significance (* = $p < 0.05$; *** = $p < 0.001$) compared to FW control (*Unpaired, two-tailed t-test*). Representative transverse and cross sections of the anal papillae (AP), Malpighian tubules (MT) and rectum (RM) showing AeRh50 (red) immunostaining from (c-e) wild FW-reared larvae, (d-f) wild Septic-reared larvae. Representative cross sections of the posterior midgut (MG), Malpighian tubules, rectum (RM), and carcass (CAR) showing AeRh50 (red) immunostaining from (g-i) laboratory FW-reared larvae and (h-j) laboratory Septic-reared larvae. Nuclei are labelled by DAPI (blue) staining. Immunostaining of Na^+-K^+-ATPase (NKA) (e-f) and the V_1 subunit of V-type H^+-ATPase (VA) (i-j) are shown in green. Co-localization of AeRh50 with V_1 subunit of V-type H^+-ATPase is indicated (dashed arrows) (merge, yellow). Control sections (primary antibodies omitted, not shown) were devoid of red and green staining. Illustrations of the alimentary canal and anal papillae of *A. aegypti* larvae to the left of each immunofluorescence image indicates the region of the cross or transverse section (red rectangles). Lumen (lm), midgut (MG), Malpighian tubule (MT), anal papillae (AP); rectum (RM). Scale bars: 100 µm, unless specified.

NKA and VA immunostaining in the AP and RM of FW- and Septic-reared larvae

NKA and VA staining within the AP epithelium of wild collected *A. aegypti* larvae was examined (Fig. 5-10). Transverse sections of AP from FW and septic water reared larvae showed an increase in immunofluorescence in septic water reared larvae compared to FW groups (Fig. 5-10A,B). Similarly, compared to FW groups, an increase in VA staining in sections of AP from septic water-reared larvae was observed (Fig. 5-10E,F). Control slides incubated without primary antibody (NKA or VA antisera) did not show green immunofluorescence, and only nuclei were clearly stained with DAPI in these sections (in blue) (Fig 5-10E). A sample bright field image of a transverse section of AP corresponding to Fig. 5-10C is provided (Fig. 5-10F). In cross sections of the MT and RM from wild collected larvae, VA staining was localized to the apical membrane in both organs (Fig. 5-11) in both FW larvae (Fig. 5-11 A,C) and septic-reared larvae (Fig. 5-11 B,D). Co-localization with apical AeRh50 was observed in the MT (Fig. 5-11C) and RM (Fig 5-11D).

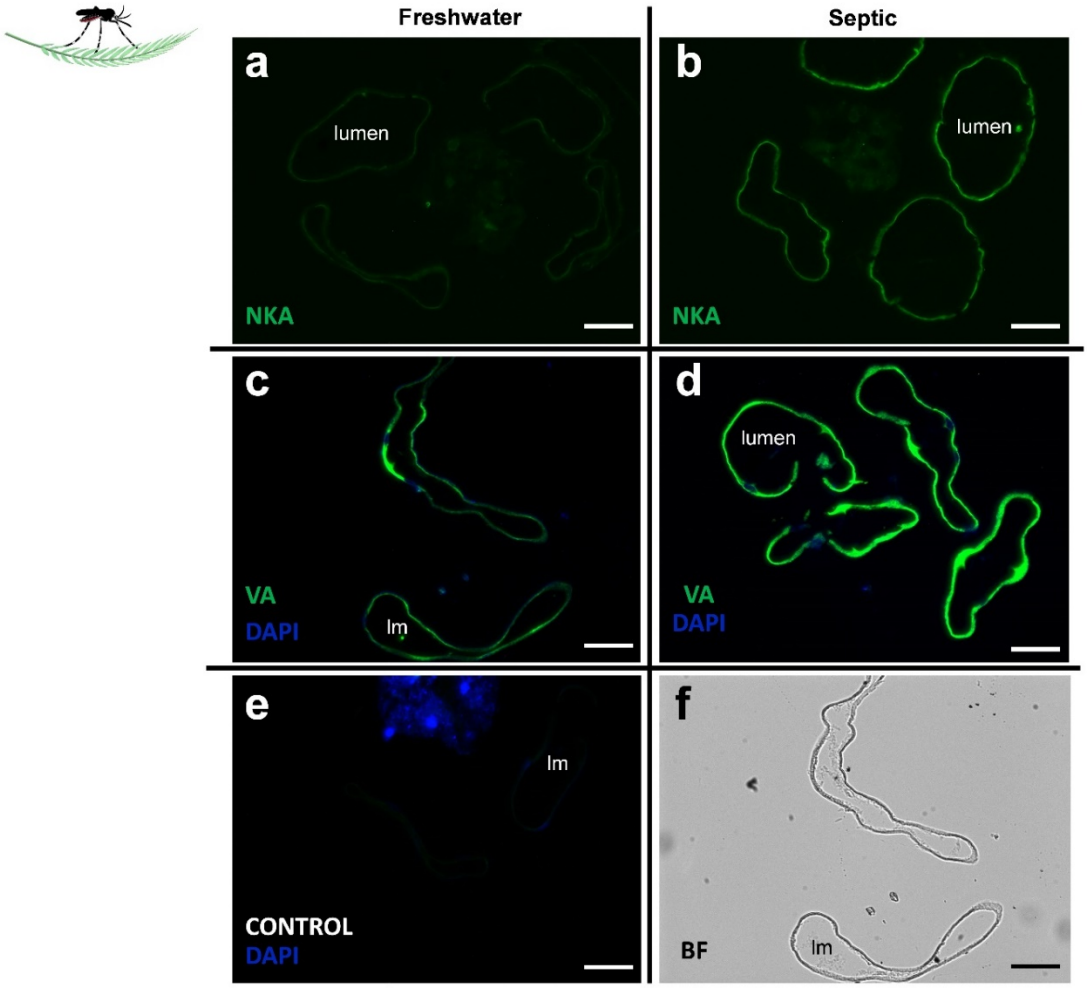

Figure 5- 10. Na^+-K^+-ATPase (NKA) and V-type H^+-ATPase (VA) immunolocalization in the anal papillae (AP) of wild-collected *A. aegypti* larvae reared in freshwater (FW) and septic water (Septic). NKA immunostaining (green) of representative transverse sections of the anal papillae from (a) FW-reared larvae and (B) Septic-reared larvae. VA immunostaining (green) of representative transverse sections of the anal papillae from (c) FW-reared larvae and (d) Septic-reared larvae. (e) Control sections of anal papillae (CONTROL, primary antibody omitted). DAPI staining of nuclei is in blue. (f) Representative bright field (BF) image of anal papillae (AP) transverse sections in C. Scale bars: 50 µm. Lumen (lm), anal papillae (AP).

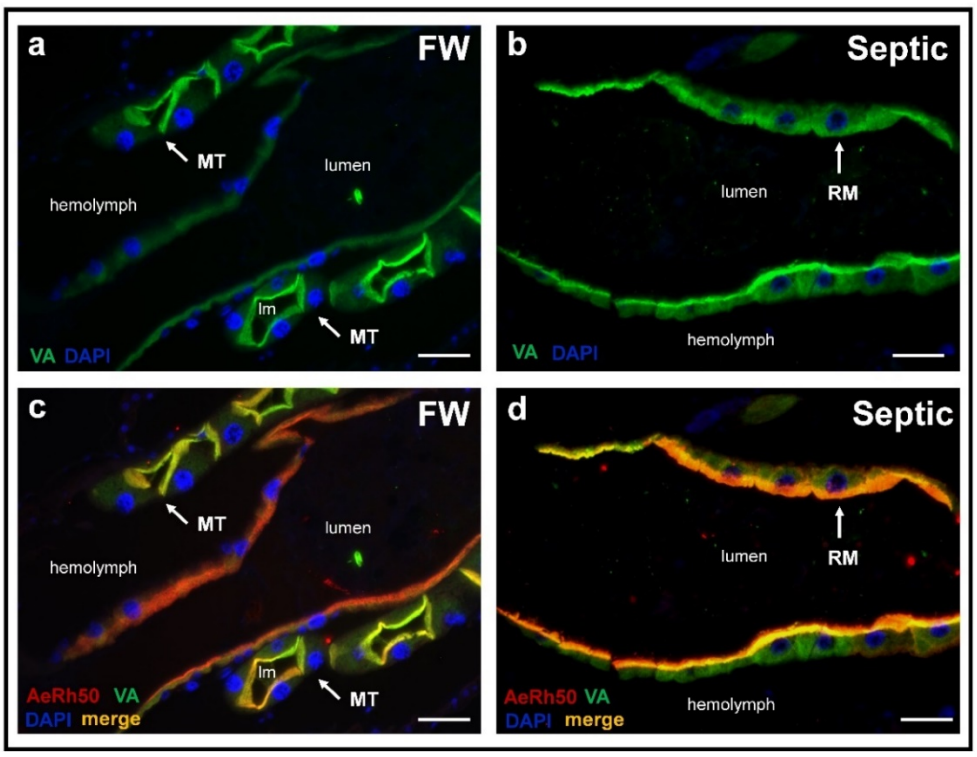

Figure 5- 11. V-type H^+-ATPase (VA) immunolocalization in the rectum (RM) of wild-collected *A. aegypti* larvae reared in freshwater (FW) and septic water (Septic). VA immunostaining (green) in representative paraffin-embedded cross sections of the (a) RM and Malpighian tubules (MT) from FW-reared wild A. aegypti larvae and (b) RM of septic-reared wild A. aegypti larvae. Nuclei are labelled with DAPI (blue). (c) cross section of MT and RM from (a) with apical AeRh50 staining (red) showing colocalization of with VA in MT (merge, yellow) in FW larvae and (d) cross section of RM corresponding to (b) showing co-localization (merge, yellow) of VA with apical AeRh50 staining (red) in septic larvae. Scale bars: 50 µm. Lumen (lm); rectum (RM), Malpighian tubule (MT).

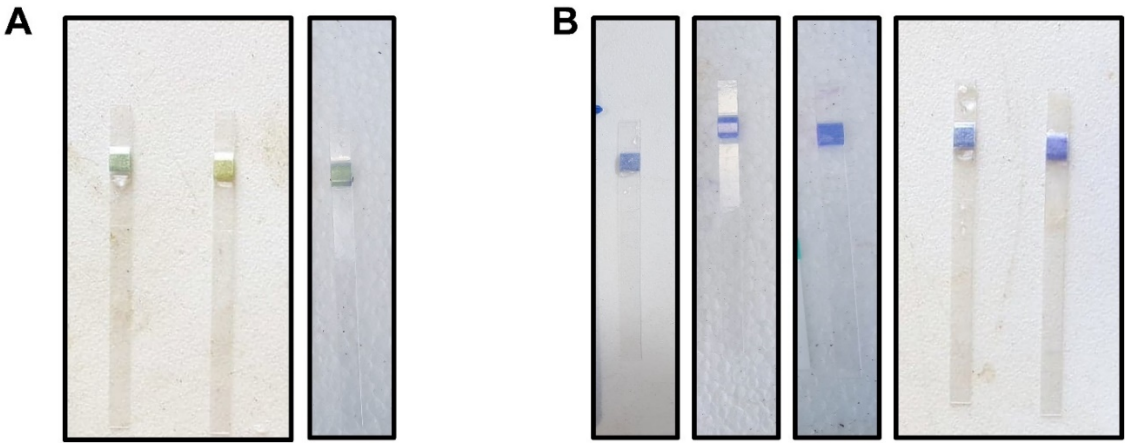

Figure 5-S 1. Images of ammonia (NH_3/NH_4^+) test strips (Tetra EasyStrips) used to estimate total ammonia levels in **(A)** freshwater sites and **(B)** septic water sites in which wild *A. aegypti* larvae were collected from and used in this study.

5.5 Discussion

Overview of Study and Collection Sites

Domestic septic tanks and sewage water systems are breeding sites of *A. aegypti* (Banerjee et al., 2015; Barrera et al., 2008; Burke et al., 2010; Chitolina et al., 2016; Hribar, 2007; Irving-Bell et al., 1987; Lam and Dharmaraj, 1982; Mackay et al., 2009). Physicochemical analyses of septic water report relatively high levels of free ammonia (Chitolina et al., 2016; Lam and Dharmaraj, 1982) and ammonium is the major toxic component of artificial sewage in the laboratory (Mitchell and Wood, 1984). With this in mind, the current study examined indicators of ammonia excretion physiology of wild *A. aegypti* larvae collected from septic water and freshwater in an effort to understand how larvae adjust their physiology to inhabit these high ammonia environments. *A. aegypti* from a laboratory colony were also reared in septic water and studied for comparison with the wild collected mosquitoes to validate previous laboratory studies on ammonia excretion physiology when larvae are faced with high external ammonia.

High [NH_4^+] and total ammonia levels similar to those reported from numerous other studies were measured from the septic tanks where mosquito larvae were collected in this study (Chitolina et al., 2016; Lam and Dharmaraj, 1982; Mitchell and Wood, 1984). The pH of the water in these septic tanks of ~8.5 is alkaline compared to that reported in other studies (~7.1 to 7.6) in similar systems in Puerto Rico and Paraná, Brazil (Burke et al., 2010; Chitolina et al., 2016). This finding may represent an additional challenge to mosquitoes inhabiting these septic tanks in the British Virgin Islands, as ammonia toxicity increases with increasing pH (pKa ~ 9.5) due to increases in the proportion of gaseous NH_3 which can readily permeate across biological membranes (Randall and Tsui, 2002; Weihrauch et al., 2012a). The mean osmolarity of septic water was approximately 10 times lower than that of *A. aegypti* haemolymph, and free [Na^+], [K^+], and [Cl^-] were also lower in the septic water compared to known levels in the haemolymph of larvae (Donini and O'Donnell, 2005; Edwards, 1982; Misyura et

al., 2017). This indicates that the larvae in these septic tanks are likely to face challenges to ion and water regulation, namely maintaining a hypertonic haemolymph compared to the FW, similar to those of larvae developing in FW but with the additional challenge of high ammonia toxicity.

Haemolymph Composition and [NH_4^+] Transport by Anal Papillae

The larvae collected from septic water had a higher haemolymph [NH_4^+] and lower pH than those collected from FW. These findings are analogous to results from laboratory studies where larvae reared in 5 mmol l^{-1} NH_4Cl (High Environmental Ammonia, HEA) had lower haemolymph pH compared to controls reared in FW (Chapter 4). Furthermore, larvae from the laboratory colony reared in septic water also had higher haemolymph [NH_4^+] compared with those reared in the field collected freshwater. Therefore, the effects of rearing wild and laboratory larvae in septic water and/or HEA on haemolymph pH and [NH_4^+] levels are consistent with one another. An elevation of haemolymph ammonia upon rearing in HEA conditions appears to be a common consequence amongst freshwater invertebrates, as well as in the body of some vertebrates (Clifford et al., 2015; Cruz et al., 2013; Martin et al., 2011; Quijada-Rodriguez et al., 2015). Evidently, this increase in haemolymph [NH_4^+] and [H^+] in septic water-reared larvae is not due to dehydration, nor do the larvae in septic water appear to be conserving extra water within intracellular spaces within the body since total body moisture of larvae was similar under septic water and FW rearing conditions. The elevated NH_4^+ levels in the haemolymph of mosquito larvae developing in septic water may be leading to acidification as a portion of the NH_4^+ dissociates into NH_3 and H^+ (Weiner and Verlander, 2017).

Previous work demonstrated that laboratory larvae reared in HEA secreted NH_4^+ from their anal papillae against an inwardly directed ammonium gradient (e.g. 2.5 mmol l^{-1} NH_4Cl in bath and ~ 1.4 mmol l^{-1} NH_4^+ in haemolymph) (Chapter 4). Here, larvae collected from septic tanks were also secreting NH_4^+ against an inwardly directed ammonia gradient from their anal papillae, as were laboratory larvae reared in septic water. Collectively these results indicate that active transport mechanisms

are facilitating NH_4^+ secretion from anal papillae in both laboratory and wild *A. aegypti* larvae. Since the anal papillae lumen is continuous with the haemocoel of the body (Clements, 1992), this secretion occurs almost directly from the haemolymph to the external environment and suggests that this is an important physiological strategy to combat the observed elevated haemolymph [NH_4^+] levels that these animals experience during development in septic water. Similar findings of increased body ammonia coupled with increased ammonia excretion rates during high external ammonia exposure has been reported in other aquatic freshwater invertebrates including *Caenorhabditis elegans* and *Schmidtea mediterranea* (Adlimoghaddam et al., 2015; Weihrauch et al., 2012b).

Laboratory larvae reared in FW (dechlorinated tap-water) secrete NH_4^+ from their anal papillae (Chasiotis et al., 2016; Donini and O'Donnell, 2005; Chapter 3; Chapter 2). Conversely, the majority of wild larvae developing in FW were absorbing NH_4^+ at the anal papillae as were the laboratory larvae reared in the FW collected from artificial containers in the British Virgin Islands. The reasons for this difference is not clear but is likely to be driven by either differences in the composition of the water (e.g. dechlorinated municipal tapwater versus field collected water), or the quantity and quality of available nitrogen rich food since the laboratory larvae either secrete NH_4^+ or absorb NH_4^+ depending on which water they have developed in. Consequently, ammonia absorption by the anal papillae may be a strategy to obtain nitrogen for the synthesis of proteins to support development and growth in a nitrogen deficient environment (Weihrauch, 2006; Weihrauch and Allen, 2018a). The results show clear differences between larvae developing in septic water or FW in terms of how their anal papillae are functioning in NH_4^+ transport and these differences are likely resulting from differences in the expression and/or activity of transport proteins as discussed below. A number of transport proteins have been studied and implicated in ammonia secretion by anal papillae of *A. aegypti* in the laboratory and a transport model with localization and function of transporters has been presented in numerous previous studies (Chasiotis et al., 2016; Chapter 3; Chapter 4; Chapter 2).

The anal papillae of septic water wild collected larvae had lower Rh protein abundance and Rh-like immunostaining intensity compared to FW collected larvae. These results were consistent with previous findings from laboratory larvae reared in HEA (Chapter 3). Since Rh proteins are thought to conduct gaseous NH_3 bidirectionally and are dependent on the P_{NH3} gradient across the biological membrane in which they are expressed, it was proposed that the decrease in Rh protein expression in response to HEA is a mechanism to limit NH_3 influx caused by an inwardly directed gradient in a high ammonia environment (Baday et al., 2015; Gruswitz et al., 2010; Kustu and Inwood, 2006). The immunostaining intensity of the primary active pumps, NKA and VA in the anal papillae epithelium of larvae collected from septic water was higher than larvae collected from FW, largely suggesting that the expression of these pumps are higher in the anal papillae of wild septic water collected larvae. These findings parallel that of a previous study on laboratory *A. aegypti* larvae reared in HEA, where VA activity was approximately 3 times higher in the anal papillae of these HEA larvae compared to control larvae reared in FW (Chapter 4). These results are also consistent with an actively driven secretion of NH_4^+ from the anal papillae in high ammonia water.

The expression of the putative ammonia transporters AeAmt1 and AeAmt2 has also previously been demonstrated in the anal papillae of laboratory *A. aegypti*. Here, while AeAmt1 could not be detected in protein homogenates of the AP of wild collected mosquitoes through Western blotting, AeAmt1-like immunostaining was evident and consistent with that reported for laboratory mosquitoes (Chasiotis et al., 2016). On the other hand, AeAmt2 expression in the AP of wild mosquitoes was detected with both western blotting and immunohistochemistry, and consistent with that reported for laboratory mosquitoes (Chapter 3). The expression and abundance of AeAmt1 and AeAmt2 in the AP of wild larvae was unaffected by development in septic water versus development in FW which suggests they have an important role in facilitating NH_4^+ secretion from the AP regardless of external ammonia levels. AeAmt1 protein abundance increases 48 hours after transferring laboratory larvae to

HEA and then returns to levels that are equal to controls after 7 days in HEA (Chapter 3). Therefore, in both wild and laboratory larvae AeAmt1 appears to be particularly important for NH_4^+ secretion by anal papillae. On the other hand, AeAmt2 protein abundance in the AP was shown to decrease in laboratory larvae transferred to HEA when this was assessed at 48 hours and 7 days after transfer to HEA (Chapter 3). Hence, in wild larvae, AeAmt2 appears to play a greater role in ammonia secretion by anal papillae than it does in the laboratory larvae when external levels of ammonia are high. Overall, our results with the wild larvae collected from septic water and FW in the British Virgin Islands largely support the ammonia transport models proposed by our previous work on laboratory reared *A. aegypti*. Furthermore, given the similarities of the results from septic water and laboratory HEA rearing we can conclude that ammonia is the major component of septic water and is the principal factor leading to our observations on alterations in ammonia excretory physiology of *A. aegypti* larvae.

Putative Ammonia Transporter Expression in the Gut and Malpighian tubules

Ammonia transporter expression and localization within the osmoregulatory and excretory organs of mosquitoes has presently only been examined in the blood-feeding adult female mosquito *Aedes albopictus* (*AalRh50*) whereby *AalRh50* is elevated in the gut following a blood meal (Wu et al., 2010a). In the present study we have mapped the expression and localization of AeRh50s, AeAmt1 and AeAmt2 in the gut and MT of wild and laboratory mosquitoes that developed in field collected FW and septic water.

Our previous studies on protein homogenates of anal papillae of laboratory *A. aegypti* larvae detected bands of ~ 30, ~55 and ~48 kDa for AeAmt1, AeAmt2 and AeRh50s, respectively (Chasiotis et al., 2016; Chapter 3; Chapter 2). Here, AeRh50 protein was detected as a ~48 kDa band in whole gut (including MTs) homogenates from wild larvae with lower abundance in the larvae collected from septic water compared with those from FW. Immunostaining of gut sections revealed qualitatively greater intensity of staining in the MT and rectum compared with other regions of the gut. Furthermore,

the intensity of AeRh50 immunostaining in the MTs and rectum appeared to be greater in the wild larvae that developed in septic water. It is possible that changes in AeRh50 abundance in other organs in the WG extracts (other than the MTs and rectum) are responsible for the observed decrease of protein abundance through Western blotting, particularly the midgut which is comparatively large. In homogenates of posterior midgut and MT of laboratory larvae that developed in field collected FW or septic water, AeRh50 protein was detected as a ~48 kDa band, whereas in the hindgut a band of ~ 100 kDa was detected which may be representative of dimers of AeRh50s. The Rh50 proteins are thought to function as homotrimers which would yield a band of ~ 150 kDa, thus the significance of the ~ 100 kDa band in the hindgut protein homogenates is unclear at this time (Lupo et al., 2007). Greater abundance of AeRh50 was detected in the MTs of larvae that developed in septic water relative to FW, but there was no difference in AeRh50 protein abundance in the hindgut (including rectum) between the two conditions. Furthermore, an apical localization of AeRh50 protein was found in the MT, RM and midgut epithelia.

In the MTs, AeRh50 is co-localized with apical VA which parallels the localization of AeRh50 with VA in the AP of *A. aegypti* larvae (Chapter 2). This suggests the possibility of an ammonia trapping mechanism in the MT for ammonia secretion in primary urine, as has been described in the AP (Chapter 2). An ammonia trapping mechanism has been proposed for ammonia secretion in the MT of *M. sexta* where an Rh protein would work in conjunction with VA (Weihrauch, 2006). AeAmt1 was detected as a ~ 30 kDa band in MT protein homogenates where it was localized to the cytosol of epithelial cells and expression was not affected by the water in which the larvae developed. AeAmt2 was detected as a ~ 55 kDa band in MT protein homogenates and expression was higher in MTs of laboratory larvae that developed in septic water. AeAmt2 was localized to the cytosol of MT epithelial cells. Since both AeAmts are expressed in MT epithelial cells they are likely to play a role in ammonia transport by the MTs but their apparent cytosolic localization makes it difficult to speculate how.

Consistent with the involvement of these transporters in ammonia transport, NH_4^+ was present in secreted fluid of MTs at concentrations ranging from ~ 5 to ~25 mmol l^{-1} depending on treatment when they were bathed in saline containing 2 mmol l^{-1} NH_4^+. These levels are much higher than those reported for *Drosophila* MTs which required bathing in 20 mmol l^{-1} NH_4^+ to reach similar concentrations in the secreted fluid (Browne and O'Donnell, 2013). This indicates that MTs of *A. aegypti* larve are better equipped to clear ammonia from the haemolymph and can do so against a gradient. Although fluid secretion rates of MTs from wild and laboratory mosquitoes were similar, the secreted fluid of MTs from wild larvae contained greater concentrations of NH_4^+ than those from laboratory larvae which was indicative of the higher rates of NH_4^+ transport in MTs of wild larvae. Furthermore, the MTs of larvae that developed in septic water had even higher NH_4^+ transport rates regardless of whether they were from wild or laboratory larvae. This increased NH_4^+ transport rate appeared to be driven by increased rates of fluid secretion that were almost double but not statistically different from those of MTs of larvae that developed in FW. It is likely that the observed increased expression of AeRh50s and AeAmt2 in the MTs of larvae that develop in septic water aid in transporting significantly more NH_4^+ over time to clear more NH_4^+ that accumulates in the haemolymph of these larvae.

The rectum (RM) of *A. aegypti* larvae is important for the reabsorption of Na^+, K^+ and Cl^- prior to the excretion of a dilute urine, and basolateral NKA is a key ion-motive pump in energizing ion reabsorption in aquatic dipterans (Jonusaite et al., 2013a; Patrick et al., 2006a). Although pinpointing the expression of VA in the RM of *A. aegypti* has proven challenging prior to this study, here we report that VA is on the apical side of the RM epithelium of FW and septic reared wild and laboratory *A. aegypti* larvae (Fig. 5-11) (Filippova et al., 1998; Patrick et al., 2006a). Relatively high levels of ammonia (~60 mmol l^{-1}) were measured in the rectal lumen of *M. sexta*, along with high mRNA expression of an Rh protein, RhMS in tissue homogenates of the rectum (Weihrauch, 2006). It was postulated that the function of NKA and RhMS is to confine ammonia within the rectal lumen for excretion;

however, the localization of RhMS protein in the rectal epithelium remains to be determined. In the RM of *A. aegypti* larvae AeRh50 proteins were localized to the apical side of the rectal epithelium and both AeRh50 and VA immunostaining intensity qualitatively increased in wild larvae developing in septic water. The arrangement of these transporters is the same as that presented here for the MTs and for the AP with AeRh50 colocalized with VA on the apical side of the epithelium. Therefore, the RM could sequester ammonia from the haemolymph through ammonia trapping while preventing the ammonia secreted into the primary urine by the MTs from being reabsorbed back into the haemolymph prior to excretion.

Conclusions

Aedes aegypti larvae were readily observed developing in septic tanks in the British Virgin Islands during both rainy and dry seasons. The ammonia levels in water collected from these septic tanks was ~ 8 mmol l^{-1}, levels that would kill most aquatic animals(Weihrauch et al., 2004; Weiner and Verlander, 2014; Wright, 1995b). In order to understand the underlying physiology that allows *A. aegypti* to inhabit this high ammonia refuge an examination of systemic physiological parameters, the ammonia excreting capacity, and the expression of ammonia transporters of larvae from septic tanks and freshwater was conducted. A comparison with laboratory sourced *A. aegypti* and previous laboratory studies conducted with high environmental ammonia (HEA) show that physiological differences between larvae developing in septic water versus freshwater are largely driven by the ammonia in septic water. Our results reveal a physiological triad of organs including the MT, rectum and anal papillae equipped to deal with the transport of ammonia for excretion. These organs are armed with ammonia transporting proteins and their expression can be adjusted by external ammonia levels leading to measurable differences in ammonia transport function which favours excretion. We therefore conclude that *Aedes aegypti* larvae possess inherent, inducible mechanisms for ammonia excretion in high

ammonia environments which, at least in part, permits them to inhabit and complete development in septic water.

5.6 References

Adlimoghaddam, A., Boeckstaens, M., Marini, A.-M., Treberg, J. R., Brassinga, A.-K. C. and Weihrauch, D. (2015). Ammonia excretion in *Caenorhabditis elegans*: mechanism and evidence of ammonia transport of the Rhesus protein CeRhr-1. *J. Exp. Biol.* **218**, 675–683.

Baday, S., Orabi, E. A., Wang, S., Lamoureux, G. and Bernèche, S. (2015). Mechanism of NH_4^+ Recruitment and NH_3 Transport in Rh Proteins. *Structure* **23**, 1550–1557.

Banerjee, S., Mohan, S., Saha, N., Mohanty, S. P., Saha, G. K. and Aditya, G. (2015). Pupal productivity & nutrient reserves of *Aedes* mosquitoes breeding in sewage drains & other habitats of Kolkata, India: Implications for habitat expansion & vector management. *Indian J. Med. Res.* **142**, 87–94.

Barrera, R., Amador, M., Diaz, A., Smith, J., Munoz-Jordan, J. L. and Rosario, Y. (2008). Unusual productivity of *Aedes aegypti* in septic tanks and its implications for dengue control. *Med. Vet. Entomol.* **22**, 62–69.

Bhatt, S., Gething, P. W., Brady, O. J., Messina, J. P., Farlow, A. W., Moyes, C. L., Drake, J. M., Brownstein, J. S., Hoen, A. G., Sankoh, O., et al. (2013). The global distribution and burden of dengue. *Nature* **496**, 504–507.

Browne, A. and O'Donnell, M. J. (2013). Ammonium secretion by Malpighian tubules of *Drosophila melanogaster*: Application of a novel ammonium-selective microelectrode. *J. Exp. Biol.* **216**, 3818–3827.

Burke, R. L., Barrera, R., Lewis, M., Kluchinsky, T. and Claborn, D. (2010). Septic tanks as larval habitats for the mosquitoes *Aedes aegypti* and *Culex quinquefasciatus* in Playa-Playita, Puerto Rico. *Med. Vet. Entomol.* **24**, 117–123.

Chasiotis, H. and Kelly, S. P. (2008). Occludin immunolocalization and protein expression in goldfish. *J. Exp. Biol.* **211**, 1524–1534.

Chasiotis, H., Ionescu, A., Misyura, L., Bui, P., Fazio, K., Wang, J., Patrick, M., Weihrauch, D. and Donini, A. (2016). An animal homolog of plant Mep/Amt transporters promotes ammonia excretion by the anal papillae of the disease vector mosquito *Aedes aegypti*. *J. Exp. Biol.* **219**, 1346–55.

Chitolina, R. F., Anjos, F. A., Lima, T. S., Castro, E. A. and Costa-Ribeiro, M. C. V. (2016). Raw sewage as breeding site to *Aedes (Stegomyia) aegypti* (Diptera, culicidae). *Acta Trop.* **164**, 290–296.

Clements, A. N. (1992). *The biology of mosquitoes, Vol. I; Development, nutrition and reproduction*. London: Elsevier.

Clifford, A. M., Goss, G. G. and Wilkie, M. P. (2015). Adaptations of a deep sea scavenger: High ammonia tolerance and active NH_4^+ excretion by the Pacific hagfish (Eptatretus stoutii). *Comp. Biochem. Physiol. -Part A Mol. Integr. Physiol.* **182**, 64–74.

Cruz, M. J., Sourial, M. M., Treberg, J. R., Fehsenfeld, S., Adlimoghaddam, A. and Weihrauch, D. (2013). Cutaneous nitrogen excretion in the African clawed frog *Xenopus laevis*: Effects of high environmental ammonia (HEA). *Aquat. Toxicol.* **136**–**137**, 1–12.

D'Silva, N. M., Patrick, M. L. and O'Donnell, M. J. (2017). Effects of rearing salinity on expression and function of ion-motive ATPases and ion transport across the gastric caecum of *Aedes aegypti* larvae . *J. Exp. Biol.* **220**, 3172–3180.

Donini, A. and O'Donnell, M. J. (2005). Analysis of Na^+, Cl^-, K^+, H^+ and NH_4^+ concentration gradients adjacent to the surface of anal papillae of the mosquito *Aedes aegypti*: application of

self-referencing ion-selective mi. *J. Exp. Biol.* **208**, 603–10.

Donini, A., Gaidhu, M. P., Strasberg, D. R. and O'donnell, M. J. (2007). Changing salinity induces alterations in haemolymph ion concentrations and Na^+ and Cl^- transport kinetics of the anal papillae in the larval mosquito, *Aedes aegypti*. *J. Exp. Biol.* **210**, 983–992.

Du, S., Liu, Y., Liu, J., Zhao, J., Champagne, C., Tong, L., Zhang, R., Zhang, F., Qin, C. F., Ma, P., et al. (2019). Aedes mosquitoes acquire and transmit Zika virus by breeding in contaminated aquatic environments. *Nat. Commun.* **10**, 1–11.

Durant, A. C. and Donini, A. (2018a). Ammonia excretion in an osmoregulatory syncytium is facilitated by AeAmt2, a novel ammonia transporter in *Aedes aegypti* larvae. *Front. Physiol.* **9**,.

Durant, A. C. and Donini, A. (2018b). Evidence that Rh proteins in the anal papillae of the freshwater mosquito *Aedes aegypti* are involved in the regulation of acid–base balance in elevated salt and ammonia environments . *J. Exp. Biol.* **221**, jeb186866.

Durant, A. C., Chasiotis, H., Misyura, L. and Donini, A. (2017). *Aedes aegypti* Rhesus glycoproteins contribute to ammonia excretion by larval anal papillae. *J. Exp. Biol.* **220**, 588–596.

Eaton, S. L., Roche, S. L., Llavero Hurtado, M., Oldknow, K. J., Farquharson, C., Gillingwater, T. H. and Wishart, T. M. (2013). Total protein analysis as a reliable loading control for quantitative fluorescent western blotting. *PLoS One* **8**, 1–9.

Edwards, H. a (1982). Ion concentration and activity in the haemolymph of *Aedes aegypti* larvae. *J. Exp. Biol.* **101**, 143–151.

Filippova, M., Ross, L. S. and Gill, S. S. (1998). Cloning of the V-ATPase B subunit cDNA from *Culex quinquefasciatus* and expression of the B and C subunits in mosquitoes. *Insect Mol. Biol.*

7, 223–232.

Gruswitz, F., Chaudhary, S., Ho, J. D., Schlessinger, A., Pezeshki, B., Ho, C.-M., Sali, A., Westhoff, C. M. and Stroud, R. M. (2010). Function of human Rh based on structure of RhCG at 2.1 A. *Proc. Natl. Acad. Sci.* **107**, 9638–9643.

Gubler, D. J. (1998). Resurgent vector-borne diseases as a global health problem. *Emerg. Infect. Dis.* **4**, 442–450.

Hribar, L. J. (2007). Larval habitats of potential mosquito vectors of West Nile virus in the Florida Keys. *J. Water Health* **5**, 97–100.

Irving-Bell, R. J., Okoli, E. I., Diyelong, D. Y., Lyimo, E. O. and Onyia, O. C. (1987). Septic tank mosquitoes: competition between species in central Nigeria. *Med. Vet. Entomol.* **1**, 243–250.

Jonusaite, S., Kelly, S. P. and Donini, A. (2013). Tissue-specific ionomotive enzyme activity and K^+ reabsorption reveal the rectum as an important ionoregulatory organ in larval *Chironomus riparius* exposed to varying salinity. *J. Exp. Biol.* **216**, 3637–3648.

Kustu, S. and Inwood, W. (2006). Biological gas channels for NH_3 and CO_2: evidence that Rh (Rhesus) proteins are CO_2 channels. *Transfus. Clin. Biol.* **13**, 103–110.

Lam, W. K. and Dharmaraj, D. (1982). A survey on mosquitoes breeding in septic tanks in several residential areas around Ipoh municipality. *Med. J. Malaysia* **37**, 114–123.

Luostarinen, S., Sanders, W., Kujawa-Roeleveld, K. and Zeeman, G. (2007). Effect of temperature on anaerobic treatment of black water in UASB-septic tank systems. *Bioresour. Technol.* **98**, 980–986.

Lupo, D., Li, X.-D., Durand, A., Tomizaki, T., Cherif-Zahar, B., Matassi, G., Merrick, M. and Winkler, F. K. (2007). The 1.3-A resolution structure of *Nitrosomonas europaea* Rh50 and

mechanistic implications for NH_3 transport by Rhesus family proteins. *Proc. Natl. Acad. Sci. U. S. A.* **104**, 19303–19308.

Mackay, A. J., Amador, M., Diaz, A., Smith, J. and Barrera, R. (2009). Dynamics of *Aedes aegypti* and *Culex quinquefasciatus* in septic tanks. *J. Am. Mosq. Control Assoc.* **25**, 409–416.

Martin, M., Fehsenfeld, S., Sourial, M. M. and Weihrauch, D. (2011). Effects of high environmental ammonia on branchial ammonia excretion rates and tissue Rh-protein mRNA expression levels in seawater acclimated Dungeness crab *Metacarcinus magister*. *Comp. Biochem. Physiol. - A Mol. Integr. Physiol.* **160**, 267–277.

Mazzalupo, S., Isoe, J., Belloni, V. and Scaraffia, P. Y. (2016). Effective disposal of nitrogen waste in blood-fed *Aedes aegypti* mosquitoes requires alanine aminotransferase. *FASEB J.* **30**, 111–120.

Misyura, L., Yerushalmi, G. Y. and Donini, A. (2017). A mosquito entomoglyceroporin, *Aedes aegypti* AQP5, participates in water transport across the Malpighian tubules of larvae . *J. Exp. Biol.* **220**, 3536–3544.

Mitchell, M. J. and Wood, R. J. (1984). Genetic variation in tolerance of ammonium chloride in *Aedes aegypti*. *Mosq. News* **44**, 498–501.

Nowghani, F., Chen, C. C., Jonusaite, S., Watson-Leung, T., Kelly, S. P. and Donini, A. (2019). Impact of salt-contaminated freshwater on osmoregulation and tracheal gill function in nymphs of the mayfly *Hexagenia rigida*. *Aquat. Toxicol.* **211**, 92–104.

Patrick, M. L., Aimanova, K., Sanders, H. R. and Gill, S. S. (2006). P-type Na^+/K^+-ATPase and V-type H^+-ATPase expression patterns in the osmoregulatory organs of larval and adult mosquito *Aedes aegypti*. *J. Exp. Biol.* **209**, 4638–51.

Pope, V. and Wood, R. J. (1981). Toleranace of *Aedes aegypti* larvae to synthetic sewage. *Mosq.*

News **41**, 732–736.

Quijada-Rodriguez, A. R., Treberg, J. R. and Weihrauch, D. (2015). Mechanism of ammonia excretion in the freshwater leech *Nephelopsis obscura*: characterization of a primitive Rh protein and effects of high environmental ammonia. *Am. J. Physiol. Regul. Integr. Comp. Physiol.* ajpregu.00482.2014.

Randall, D. J. and Tsui, T. K. N. (2002). Ammonia toxicity in fish.pdf. *Mar. Pollut. Bull.* **45**, 17–23.

Scaraffia, P. Y., Zhang, Q., Wysocki, V. H., Isoe, J. and Wells, M. A. (2006). Analysis of whole body ammonia metabolism in *Aedes aegypti* using [15N]-labeled compounds and mass spectrometry. *Insect Biochem. Mol. Biol.* **36**, 614–622.

Somers, G., Brown, J. E., Barrera, R. and Powell, J. R. (2011). Genetics and morphology of *Aedes aegypti* (Diptera: Culicidae) in septic tanks in Puerto Rico. *J. Med. Entomol.* **48**, 1095–1102.

Stagg, B. Y. A. P., Harrison, J. O. N. F. and Phillips, J. E. (1991). Acid-base variables in Malpighian tubule secretion and response to acidosis. *J. Exp. Biol.* **159**, 433–447.

Terpstra, P. M. J. (1999). Sustainable water usage systems: models for the sustainable utilization of domestic water in urban areas. *Wat. Sci. Tech.* **39**, 65–72.

Thomson, R. B., Thomson, J. M. and Phillips, J. E. (1988). NH_4^+ transport in acid-secreting insect epithelium. *Am. J. Physiol. - Regul. Integr. Comp. Physiol.* **254**,.

Verdouw, H., Van Echteld, C. J. A. and Dekkers, E. M. J. (1978). Ammonia determination based on indophenol formation with sodium salicylate. *Water Res.* **12**, 399–402.

Volkmann, A. and Peters, W. (1989a). Investigations on the midgut caeca of mosquito larvae-I. Fine structure. *Tissue Cell* **21**, 243–251.

Volkmann, A. and Peters, W. (1989b). Investigations on the midgut caeca of mosquito larvae-II. Functional aspects. *Tissue Cell* **21**, 253–261.

Weihrauch, D. (2006). Active ammonia absorption in the midgut of the Tobacco hornworm *Manduca sexta* L.: Transport studies and mRNA expression analysis of a Rhesus-like ammonia transporter. *Insect Biochem. Mol. Biol.* **36**, 808–821.

Weihrauch, D. and Allen, G. J. P. (2018a). Ammonia excretion in aquatic invertebrates: new insights and questions. *J. Exp. Biol.* **221**, jeb178673.

Weihrauch, D. and Allen, G. J. P. (2018b). Ammonia excretion in aquatic invertebrates: new insights and questions. *J. Exp. Biol.* **221**, 1–11.

Weihrauch, D., Morris, S. and Towle, D. W. (2004). Ammonia excretion in aquatic and terrestrial crabs. *J. Exp. Biol.* **207**, 4491–4504.

Weihrauch, D., Wilkie, M. P. and Walsh, P. J. (2009). Ammonia and urea transporters in gills of fish and aquatic crustaceans. *J. Exp. Biol.* **212**, 1716–1730.

Weihrauch, D., Donini, A. and O'Donnell, M. J. (2012a). Ammonia transport by terrestrial and aquatic insects. *J. Insect Physiol.* **58**, 473–487.

Weihrauch, D., Chan, a. C., Meyer, H., Doring, C., Sourial, M. and O'Donnell, M. J. (2012b). Ammonia excretion in the freshwater planarian *Schmidtea mediterranea*. *J. Exp. Biol.* **215**, 3242–3253.

Weiner, I. D. and Verlander, J. W. (2014). Ammonia transport in the kidney by Rhesus glycoproteins. *Am. J. Physiol. Renal Physiol.* **306**, F1107–F1120.

Weiner, I. D. and Verlander, J. W. (2017). Ammonia Transporters and Their Role in Acid-Base Balance. *Physiol. Rev.* **97**, 465–494.

Wilkerson, R. C., Linton, Y. M., Fonseca, D. M., Schultz, T. R., Price, D. C. and Strickman, D. A. (2015). Making mosquito taxonomy useful: A stable classification of tribe Aedini that balances utility with current knowledge of evolutionary relationships. *PLoS One* **10**, 1–26.

Wright, P. (1995a). Nitrogen excretion : three end products , many physiological roles. *J. Exp. Biol.* **281**, 273–281.

Wright, P. (1995b). Nitrogen excretion : three end products , many physiological roles. *J. Exp. Biol.* **281**, 273–281.

Wu, Y., Zheng, X., Zhang, M., He, A., Li, Z. and Zhan, X. (2010). Cloning and functional expression of Rh50-like glycoprotein, a putative ammonia channel, in *Aedes albopictus* mosquitoes. *J. Insect Physiol.* **56**, 1599–1610.

Zall, D. M., Fisher, D. and Garner, M. Q. (1956). Photometric determination of chlorides in water. *Anal. Chem.* **28**, 1665–1668.

Chapter Six

Malpighian tubules and hindgut of *Aedes aegypti*: Rh protein expression, transcriptomic analyses, and functional characterization of ammonia transport mechanisms

This chapter is not published at the time of this writing.

6.1 Summary

The role of the mosquito excretory organs (Malpighian tubules, MT and hindgut, HG) in ammonia transport as well as expression and function of the Rhesus (Rh protein) ammonia transporters within these organs was examined in *Aedes aegypti* larvae and adult females. Immunohistological examination revealed that the Rh proteins are co-localized with V-type H^+-ATPase (VA) to the apical membranes of MT and HG epithelia of both larvae and adult females. Of the two Rh transporter genes present in *A. aegypti*, *AeRh50-1* and *AeRh50-2*, we show using quantitative real-time PCR (qPCR) and an RNA *in-situ* hybridization (ISH) assay that *AeRh50-1* is the predominant Rh protein expressed in the excretory organs of larvae and adult females. Further assessment of AeRh50-1 function in larvae and adults using RNAi (i.e. dsRNA-mediated knockdown) revealed significantly decreased [NH_4^+] (mmol l^{-1}) levels in the secreted fluid of larval MT which does not affect overall NH_4^+ transport rates, as well as significantly decreased NH_4^+ flux rates across the HG (haemolymph to lumen) of adult females. We also employed RNAseq to identify the expression of ion transporters and enzymes within the rectum of larvae, of which limited information currently exists for this important osmoregulatory organ. Of the ammonia transporters in *A. aegypti*, *AeRh50-1* transcript is most abundant in the rectum thus validating our immunohistochemical and RNA ISH findings. In addition to enriched VA transcript (subunits A and d1) in the rectum, we also identified high Na^+-K^+-ATPase transcript (α subunit) expression which becomes significantly elevated in response to HEA, and we also found enriched carbonic anhydrase 9, inwardly rectifying K^+ channel *Kir2a*, and Na^+-coupled cation-chloride (Cl^-) co-transporter *CCC2* transcripts. Finally, the modulation in excretory organ function and/or Rh protein expression was examined in relation to high ammonia challenges, specifically (1) HEA rearing of larvae and (2) blood-feeding of adult females. NH_4^+ flux measurements using the scanning-ion selective electrode (SIET) technique revealed no significant differences in NH_4^+ transport across organs comprising the alimentary canal of larvae reared in HEA vs freshwater. Further, significantly increased VA

activity, but not NKA, was observed in the MT of HEA-reared larvae. Relatively high Rh protein immunostaining persists within the hindgut epithelium, as well as the ovary, of females at 24-48 hours post blood meal corresponding with previously demonstrated peak levels of ammonia formation. These data provide new insight into the role of the excretory organs in ammonia transport physiology and the contribution of Rh proteins in mediating ammonia movement across the epithelia of the MT and HG, and the first comprehensive examination of ion transporter and channel expression in the mosquito rectum.

6.2 Introduction

Ammonia (NH_3/NH_4^+) transport across biological membranes is a ubiquitous process in animals as a means of regulating and/or excreting nitrogen-containing compounds. Ammonia formation occurs principally from the catabolism of amino acids within all metabolically active cells (Ballantyne, 2001; Bender, 2012b), and animals are tasked with either excreting or recycling free ammonia (either as NH_3 or NH_4^+) to avert ammonia toxicity that can occur at the molecular, biochemical, and physiological levels (Martinelle and Häggström, 1993; Randall and Tsui, 2002; Weihrauch et al., 2012a). The need for ammonia regulatory and transport processes is constant due to routine protein turnover, ingestion of proteinaceous food, and periods of fasting or starvation. Many animals face specific challenges because of their life history, which necessitate the need for efficient ammonia detoxification and excretory pathways with the bulk of these pathways typically confined to organ systems involved in ion and water homeostasis (Biver et al., 2008; Ip and Chew, 2010; Weihrauch and O'Donnell, 2015; Weiner and Hamm, 2007) or gas-exchange (Adlimoghaddam et al., 2015; Cruz et al., 2013; Glover et al., 2013; Quijada-Rodriguez et al., 2015; Randall and Ip, 2006; Weihrauch et al., 2004). Insects, for example, constitute the largest class of animals on Earth in terms of species number and accordingly, have evolved specialized adaptations to suit the wide range of environments they inhabit. In particular, the holometabolous mosquitoes (Culicidae) undergo complete metamorphosis from the entirely aquatic-dwelling larval stages to the terrestrial adult forms (Clements, 1992). The aquatic larvae readily develop in osmotically stressful environments owing to specialized morphological, physiological, and behavioural adaptations. On the other hand, adult females of the majority of mosquito genera are anautogenous and therefore must ingest a protein-rich blood meal, one that is often three times their body weight, in order to complete each cycle of egg development (Nayar and Sauerman, 1975a; Nayar and Sauerman, 1975b; Zhou et al., 2004). Adding to the impressive capacity of female mosquitoes to cope with rapid overhydration, extreme metabolic demands in digesting protein, and other challenges related

to blood feeding, is the stark contrast in physiological requirements of the non-feeding phase which involve mechanisms aimed at conserving water and nutrients (Benoit and Denlinger, 2010; Bursell, 1967; Scaraffia et al., 2010).

Efficient ammonia transport and excretory processes are paramount to the success of larval and adult mosquitoes when faced with environmental and physiological challenges to ion and water homeostasis and nitrogen control. The larvae of the *Aedes aegypti* mosquito, for example, can inhabit polluted aquatic habitats that contain toxic levels of ammonia (Barrera et al., 2008; Burke et al., 2010; Chitolina et al., 2016; Chapter 5). The physiology of osmoregulation in *A. aegypti* larvae has been examined in some detail (Bradley, 1987; Clark, 2004; Clark et al., 2007; D'Silva et al., 2017; Donini et al., 2006; Patrick et al., 2006b), but the mechanisms underlying ammonia regulation and excretion have only recently received attention. Relatively high effluxes of ammonia were measured at the anal papillae (Donini and O'Donnell, 2005), which are a primary interface of larvae with the external environment and are specialized for active ion uptake from dilute freshwater (Del Duca et al., 2011; Stobbart, 1967). These structures possess a suite of ion transporters including the ion-motive enzymes Na^+-K^+-ATPase (NKA) and V-type H^+-ATPase (VA) (Bradley, 1987; Clements, 1992; Patrick et al., 2006b). Later, we demonstrated that the anal papillae express proteins from the AMT and Rh families of ammonia transporters; AeAmt1, AeAmt2, AeRh50-1, and AeRh50-2, each of which function in facilitating ammonia excretion from the haemolymph via this organ (Chasiotis et al., 2016; Chapter 3; Chapter 2). *A. aegypti* larvae field-collected from high ammonia septic tanks exhibited increased ATPase expression and NH_4^+ excretion rates at the anal papillae, but drastic changes in the function of the Malpighian tubules (MT) and hindgut (HG), both of which comprise the excretory system, and Rh protein expression within these organs was also observed (Chapter 5). These findings are intriguing as very little is known regarding the contribution of the MT, and the rectal segment of the hindgut, to the process of nitrogenous waste excretion in *A. aegypti* larvae (Bradley, 1987). The MT of *A. aegypti*

larvae secrete NH_4^+ at levels greatly exceeding haemolymph ammonia concentrations (Chapter 5), and this has also been demonstrated to occur within the MT of *Drosophila melanogaster* larvae (Browne and O'Donnell, 2013). High arginase activity measured in larval whole-body homogenates suggests that urea excretion is significant in these animals (Von Dungern and Briegel, 2001), but the excretion of ammonia as the primary nitrogenous waste is a phenomenon that is omnipresent among aquatic animals and requires further examination in *A. aegypti* larvae (Bursell, 1967).

Adult female *A. aegypti*, like many other blood-feeding animals, face high ammonia loads during blood meal digestion (Briegel, 1986; Pennington et al., 2003; Scaraffia et al., 2005; Scaraffia et al., 2006). Ammonia is the principal nitrogenous waste excreted by females during blood meal digestion, and a variety of mechanisms also exist for the removal of nitrogenous wastes as urea (Scaraffia et al., 2008). More recently, we demonstrated that an Amt protein, AeAmt1, in adult *A. aegypti* plays a functionally distinct role in sperm development and egg fertilization (Chapter 7). AeAmt2 protein is highly expressed within the chemosensory appendages (among other organs) which may be indicative of a function in ammonia sensing mechanisms underlying host-seeking behaviours, as has been demonstrated for the malaria vector mosquito *Anopheles gambiae* (Pitts et al., 2014; Ye et al., 2020). However, AeAmt2 function in these structures requires further investigation. Of great relevance to this current study is the finding that the transcript of an Rh protein in adult female *Aedes albopictus*, *AalRh50*, is highly expressed in the head and MT and blood-feeding significantly upregulates *AalRh50* expression in the fat body, midgut, and MT (Wu et al., 2010a). Prior to our work here, the expression, organ-specific localization, and the function of Rh proteins in adult *A. aegypti* was unknown.

The objectives of the current study were prompted by findings of altered Rh protein expression within the excretory organs of *A. aegypti* larvae developing in high ammonia habitats, coupled with the fact that there is currently little information as to the contribution of the excretory organs (i.e. MT and HG) to nitrogenous waste excretion in larval and adult *A. aegypti*. Three distinct regions; the ileum,

rectum, and anal canal comprise the hindgut of *A. aegypti*, all of which are lined with cuticle (Meredith and Phillips, 1973). It was hypothesized that the excretory organs are important sites for ammonia excretion, and underpinning this process is organ-specific Rh protein expression. This hypothesis was tested using a combination of RNAseq, RNA interference (i.e. RNAi), and electrophysiological approaches to measure biochemical and physiological endpoints in ammonia transport (i.e. absorption and secretion) by the excretory organs. The organ-specific transcript and protein expression of the Rh transporters (*AeRh50-1* and *AeRh50-2*) was also examined in the context of high environmental ammonia (for larvae) and nitrogen metabolism during blood meal digestion (for adult females).

6.3 Materials and Methods

Experimental animals

*Aedes aegypt*i (Liverpool strain) larvae and adult females were obtained from a laboratory colony at York University, Toronto, ON, Canada reared and maintained as previously described (Chapter 5). Fourth instar larvae and 7-10 days post-emergence females were used for all experiments in this study. For blood-feeding experiments, adult females were provided access to a 5% aqueous sucrose solution upon emergence, similar to control animals, in addition to a blood meal provided at 7 days post-emergence. For high environmental ammonia (HEA) rearing of larvae, eggs were first hatched in dechlorinated tap water (i.e. freshwater, FW) and equal densities of larvae were transferred to either 100ml containers of FW or 5 mmol l^{-1} NH_4Cl in dechlorinated tap water (i.e. HEA) at 2 days post hatching. Rearing water was refreshed every 2 days until larvae reached 4^{th} instar (approximately 7 days). Larvae were fed every other day until reaching 4^{th} instar and were starved for 24 hours prior to all experiments. For RNAseq studies, larvae were reared to 4^{th} instar in FW, and were then transferred to 250 ml of either 10 mmol l^{-1} NH_4Cl (HEA) or FW for 24 hours.

RNA isolation and purification for quantitative real-time PCR (qPCR) and RNA sequencing (RNAseq)

To examine AeRh50 expression in adult females using qPCR, biological samples (n = 6 for sugar fed, n = 3 for blood fed) each consisting of pooled midgut (MG), hindgut (HG), and Malpighian tubules (MT) tissue from 70-90 adult females were isolated in cold lysis buffer from the Purelink RNA mini kit (Ambion, Austin, TX). For RNAseq studies of the larval rectum, three biological replicates for both FW and HEA conditions consisted of pooled rectum tissues from 50 larvae per replicate isolated in cold lysis buffer. Samples were sonicated for 5s at 5W using an XL 2000 Ultrasonic Processor (Qsonica, LL, CT, USA). RNA was isolated using the Purelink RNA mini kit and was treated with the TURBO DNA-free^{TM} Kit (Applied Biosystems, Streetsville, Ontario, Canada) to remove genomic DNA. The concentration and purity of extracted RNA was determined using a NanoDrop 2000 spectrophotometer (Thermo Scientific), which yielded absorbance ratios (A_{260}/A_{280}) between 1.9-2.2. Total RNA for larval rectum samples were sent to Génome Quebec (Montreal, Quebec, Canada) for Illumina library preparation (see RNAseq). For qPCR analyses of adult female RNA samples, cDNA was prepared from isolated RNA samples (using 1 μg of RNA for all samples) using the iScript^{TM} cDNA Synthesis Kit (Bio-Rad, Mississauga, Ontario, Canada) following manufacturer recommendations.

qPCR, dsRNA synthesis and delivery, and immunohistochemistry of Rh protein expression

Primer sets for *AeRh50-1* and *AeRh50-2* were designed, validated, and utilized in previous studies (Chasiotis et al., 2016; Chapter 3). To determine the relative mRNA abundance of *AeRh50-1* and *AeRh50-2*, *AeAmt1,* and *AeAmt2* in adult female midgut, hindgut, and Malpighian tubules tissues, qPCR was performed using SsoFast^{TM} Evagreen® Supermix (Bio-Rad LaboratoriesCanada) Ltd. Mississauga, Ontario, Canada) according to the manufacturer's protocol. Primer sets for ribosomal protein 49 (*rp49*), 60s ribosomal protein S18 (*rpS18*), and ribosomal protein L8 (*rpL8*) genes were validated previously and determined to be suitable internal controls (Paluzzi et al., 2014; Durant and Donini, 2020). Reactions were carried out using the CFX96 real time PCR detection system (Bio-Rad), and undiluted cDNA for all tissue samples was used to assess *AeRh50-1* and *AeRh50-2* abundance, while

a 1/100 dilution of cDNA for all tissue samples was used for all three reference genes. Quantification of transcripts was determined according to the Pfaffl method (Pfaffl, 2004), using the geometric mean of the three reference genes for data normalization. Samples were run in duplicate, and a no-template negative control was used for each gene.

For *AeRh50-1* dsRNA synthesis, a 989 base pair fragment was amplified by reverse-transcription PCR (RT-PCR) using cDNA synthesized from purified anal papillae total RNA as previously detailed (Chapter 2). A 799 base pair DNA fragment of the control β-lactamase was amplified and ligated to pGEM-T vector (Promega, Madison, WI) (a kind gift from Jean Paul Paluzzi, York University, Canada) and the template was further amplified by PCR. The purified PCR products were used to generate dsRNA by in vitro transcription using the Promega T7 RiboMAX Express RNAi Kit (Promega). dsRNA delivery via ingestion in larvae (Chapter 2) and dsRNA injection of adult females (Chapter 7) has been outlined previously. Experiments were performed at 2 days post dsRNA treatment for both larvae and adults.

Immunolocalization of Rh protein in cross sections (5 μm thick) paraffin-embedded larvae and adult females was followed according to established protocols (Chasiotis and Kelly, 2008; Chasiotis et al., 2016; Chapter 5; Chapter 2). A custom-synthesized polyclonal antibody that was raised in rabbit against a synthetic peptide (CHHKDDAYWETPAES) corresponding to a 15-amino acid region of *AeRh50-1* (which was found to cross react with *AeRh50-2*) (GenScript USA Inc., Piscataway, New Jersey, USA) was used at a 6.44×10^{-03}μg μL^{-1} concentration. A mouse monoclonal anti-α5 antibody for NKA (Douglas Fambrough, Developmental Studies Hybridoma Bank, IA, USA) was used at a 1:10 dilution, and a guinea pig anti-VA antibody (kind gift from Dr. Weiczorek, University of Osnabruk, Germany) was used at a 1:5000 dilution. A sheep anti-mouse antibody conjugated to Cy2 and a goat anti-guinea pig antibody conjugated to AlexaFluor 647 (Jackson ImmunoResearch Laboratories, West Grove, PA, USA) at dilutions of 1:500 were used to visualize NKA and VA, respectively. To visualize

Rh protein, a goat anti-rabbit antibody conjugated to Alexa Fluor 594 (Jackson ImmunoResearch) at a dilution of 1:500 was utilized. Fluorescence microscopy images were taken using an Olympus IX71 inverted fluorescent microscope (Olympus Canada, Richmond Hill, ON, Canada) and CellSense 1.12 Digital Imaging software (Olympus Canada).

RNA in situ hybridization assay

Preparation of paraffin-embedded whole-body larvae and adult samples were carried out according to a previously established protocol (see Immunohistochemistry, above) which was slightly modified following the RNAscope® Assay instructions [Advanced Cell Diagnostics, Newark, CA, USA; (Wang *et al*., 2012)]. Fourth instar larvae and 10 day old, blood-fed (24 hours post blood meal) females were isolated and fixed for 24 hours at room temperature in 10% neutral-buffered formalin (NBF). Fixed larvae and adult samples were briefly washed in 1X phosphate-buffered saline (PBS) and were then dehydrated using a standard ethanol series followed by xylene. Fixed and dehydrated larvae and adult samples were then embedded in paraffin wax and cut into 5 µm thick sections using a microtome (Leica Microscopy Inc. RM 2125RT manual rotary, ON, Canada) and placed on Super-Frost® Plus slides (Fisher Scientific). Deparaffinization in xylene, tissue pre-treatment, *in situ* hybridization (ISH) with target probes, amplification steps, and chromogenic detection of *AeRh50-1* transcript in larval and adult *A. aegypti* sections were conducted according to the RNAscope® Assay protocol (Wang et al., 2012), with the exception that target retrieval was performed in a microwave at 50% power for 10 minutes. RNAscope® Assay proprietary RNA- specific probes hybridized to *AeRh50-1* transcript within larval and adult *A. aegypti* sections were run in parallel with positive (*A. aegypti* GAPDH) and negative controls to ensure interpretable results. Signals were visualized with bright field at 20X magnification using a Nikon Eclipse Ti fluorescence microscope (Neville, NY). Each single RNA transcript in cells appears as punctate dots of red chromogenic staining within each cell boundary.

Next generation sequencing (RNAseq), transcriptome mapping, and construction of heatmaps

Samples of total larval rectum RNA (see sections "Experimental Animals" and "RNA isolation and purification", above) from 4th instar larvae reared in FW or HEA were screened for quality control (Bioanalyser 2100). Six strand specific Illumina libraries (3 FW rectum and 3 HEA rectum samples) with paired-end 100 base pair reads were subsequently prepared using NovaSeq 6000 S2 PE100 (50 million reads) by Génome Quebec Innovation Center (Montreal, Quebec). Trimmomatic quality control trimming (usegalaxy.org) of all 100 base pair paired-reads was conducted as described previously (Goecks et al., 2010; Kolosov and O'Donnell, 2019) and were used for further analyses. The annotated *A. aegypti* transcriptome (AaegL5.2) was accessed from VectorBase (vectorbase.org) and the Salmon mapping software (version 0.14.1.2; usegalaxy.org) was used to map next-generation sequencing reads to this transcriptome. Heat maps of transcripts per million (TPM) values for identified transcripts of interest were averaged for three biological replicates of rectum samples for both FW and HEA conditions. To visualize the absolute TPM values of transcripts of interest in the rectum of FW and HEA larvae samples, heatmaps were constructed in GraphPad Prism version 7.00. Statistically significant differences in TPM values (differential expression) between FW and HEA samples were determined using the DESeq2 tool (usegalaxy.org). Mean normalised counts for each sample were averaged over all samples for FW and HEA (n = 3 for each condition). Log_2 fold-change (log_2FC) values and corresponding *P*-values of the change (Wald test, $P < 0.05$) for each gene were determined. Adjusted *P*-values (P_{adj}) for multiple testing (the false discovery rate, FDR) for each gene were determined using the Benjamini-Hochberg method. For the construction of heat maps in this study, transcript with the unadjusted *P*-value were considered differentially expressed.

ATPase enzyme assay for NKA and VA activity

To examine NKA and VA activity in the MT of larvae in response to HEA rearing, we utilized an enzyme assay which has been outlined previously in detail and has been adapted for insect larvae

tissues (Jonusaite et al., 2013b; Mccormick, 1993). This assay is dependent on the enzymatic coupling of NKA inhibitor ouabain (Sigma-Aldrich) or VA inhibitor bafilomycin (LC Laboratories, Woburn, MA, USA)- sensitive hydrolysis of adenosine triphosphate (ATP) with the oxidation of reduced nicotinamide adenine dinucleotide (NADH), with NADH disappearance being directly measured in a microplate spectrophotometer. Rectum samples from ~50 larvae per replicate (n = 3 replicates each for FW and HEA) were dissected under physiological saline (Donini et al., 2006) and pooled in 1.5 ml centrifuge tubes, flash-frozen in liquid nitrogen and stored at −80°C. Samples were later thawed on ice, and 100 µl of homogenizing buffer (four parts SEI, composed of 150 mmol l^{-1} sucrose, 10 mmol l^{-1} Na_2EDTA, 50 mmol l^{-1} imidazole, pH 7.3, and one-part SEID, composed of 0.5% deoxycholic acid in SEI) was added to each tube. Samples were sonicated on ice for 10 seconds at 5 W using an XL 2000 Ultrasonic Processor (Qsonica), and were then centrifuged at 10,000 g for 10 min at 4°C. The supernatants of each sample were transferred to 1.5 ml centrifuge tubes and stored at −80°C. The enzyme assay procedure was carried out exactly as described previously (Chapter 4; Jonusaite et al., 2013b).

Ramsay secretion assay and electrophysiology (ISME and SIET)

Analysis of luminal NH_4^+ concentrations and transport rates in the secreted fluid of the MT was conducted following established procedures for *A. aegypti* larvae (Chapter 5; Misyura et al., 2017). Briefly, the MT of larvae reared in FW or HEA for 7 days were carefully detached from the gut under physiological saline (Donini et al., 2006). Individual MT were transferred to 25 µl droplets of physiological saline submerged under paraffin oil, with the distal half of the tubule suspended in saline and the proximal half of the tubule wrapped around a fine metal pin adjacent to the saline droplet. After leaving the MT to secrete for 30-45 minutes, secreted fluid droplets were isolated under paraffin oil and analyzed for secretion rates (by calculating the volume of the droplet divided by secretion time) and [NH_4^+] (mmol l^{-1}) using the ion-selective micro-electrode (ISME) technique described elsewhere

((Chasiotis et al., 2016; Chapter 5; Chapter 2). An examination of NH_4^+ fluxes across the alimentary canal of *A. aegypti* larvae reared in FW or HEA, and along the adult female hindgut in response to *AeRh50-1* dsRNA injection was carried out using the scanning ion-selective electrode technique (SIET) (Donini and O'Donnell, 2005). Organs were mounted in a Sylgard-lined petri dish using bees-wax and submerged under larval (Donini et al., 2006) or adult (Paluzzi et al., 2014) physiological saline. NH_4^+ flux was measured using NH_4^+-selective electrodes (Browne and O'Donnell, 2013) whereby NH_4^+ voltage gradients were recorded over a 100 µm distance adjacent to each region of the gut. Each replicate indicated in the corresponding figure captions (Fig. 6-6 and Fig. 6-12) represents the average flux from 3 repeated measurements. Selected regions for NH_4^+ flux measurements within the ileum and rectum segments of the hindgut were kept consistent between each sample by moving the microelectrode in 1000 µm increments between target sites. Each plotted flux measurement consists of a sampling cycle which records a voltage reading at 2 µm from the target organ surface and then a second voltage recording 102 µm from the target organ surface, which is repeated four times and then converted to a voltage gradient by the Automated Scanning Electrode Technique software (ASET; Science Wares, East Falmouth, MA, USA) (Chasiotis et al., 2016). This sampling cycle also included a 4 second wait time and a 1 second sampling time for each voltage reading for each measurement at a single site.

Statistics

All data analysis and statistics were completed using the GraphPad Prism 7.0 software. Where applicable, data are presented as mean ± S.E.M. for the indicated sample size (*n)*, and this information along with the statistical test used is detailed in the figure caption. Differences in measurements were considered significant if $p < 0.05$.

6.4 Results

Rh mRNA and protein localization and *AeRh50-1* knockdown in the excretory organs of larvae

Rh protein immunostaining in cross sections through the rectum segment of the hindgut and five surrounding Malpighian tubules (MT) reveal an apical (i.e. lumen facing) localization of Rh proteins within these organs (Fig. 6-1). Rh immunofluorescence does not co-localize with basolaterally (i.e. haemolymph facing) expressed NKA (Fig. 6-1a) in the MT, but co-localization with apically expressed VA in the MT was observed (Fig. 6-1b-c). An apical localization of Rh protein immunostaining was also found within the ileum and rectum segments comprising the hindgut (Fig. 6-1c). A key limitation in the immunolocalization lies in the fact that the AeRh50-1 and AeRh50-2 protein are both detected by the AeRh50-1 custom antibody (Chapter 2). Therefore, an RNA *in-situ* hybridization (ISH) assay was utilized to discern the specific localization of *AeRh50-1* transcript and *AeRh50-2* transcript expression within cross sections of the larval MT and rectum (Fig. 6-2). Chromogenic dye staining of *AeRh50-1* mRNA was highly concentrated to the epithelium of the rectum (Fig. 6-2a), compared to *AeRh50-2* (Fig. 6-2b) and negative control staining (Fig. 6-2d). *AeRh50-1* mRNA staining in the MT, albeit punctate and much lower than positive control GAPDH (Fig. 6-2c), was also observed. In contrast, *AeRh50-2* mRNA staining was absent in the MT and comparable to negative control sections. With the use of the RNA ISH assay, it was also confirmed that both *AeRh50-1* and *AeRh50-2* mRNA is abundant within the anal papillae epithelium of larvae (Fig. 6-3). To assess the function for AeRh50-1 in NH_4^+ secretion within the MT, NH_4^+ transport rates by the MT were measured following dsRNA-mediated *AeRh50-1* knockdown (Fig. 6-4). While a significant decrease in the NH_4^+ concentration (mmol l^{-1}) of secreted fluid droplets was observed (Fig. 6-4a), this did not affect functional MT endpoints, namely secretion rates (nl min^{-1}, Fig. 6-4b) and overall NH_4^+ transport rates by the MT (pmol min^{-1}, Fig 6-4c).

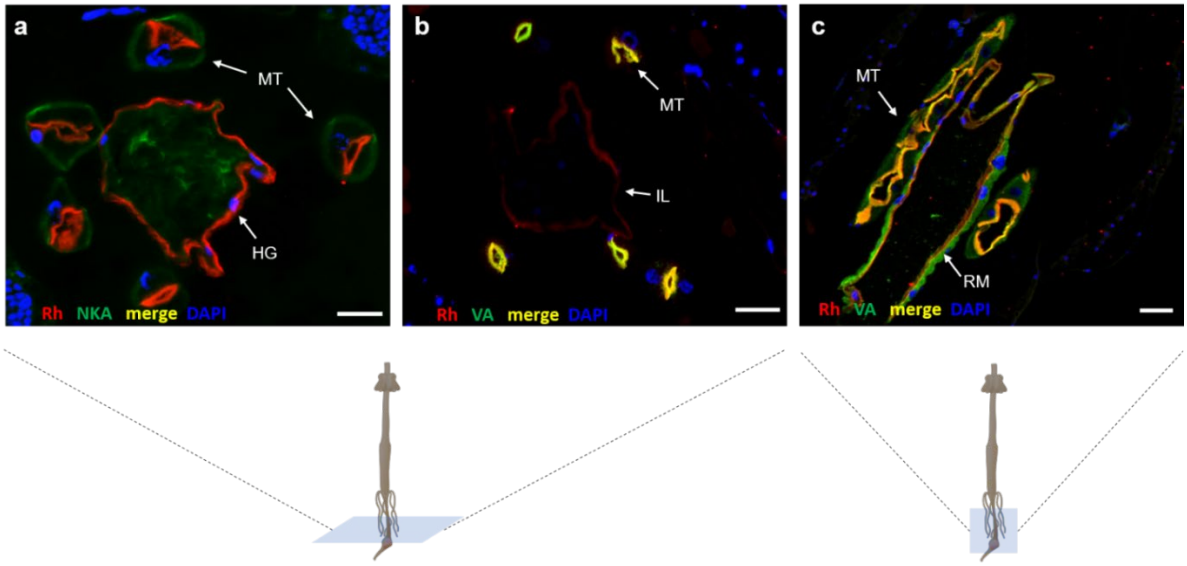

Figure 6- 1. Rh protein immunolocalization in paraffin-embedded cross sections of the Malpighian tubules (MT) and hindgut (HG) of *Aedes aegypti* larvae. (a) Rh protein (red) immunolocalization in a transverse section of MT and HG with basolateral-localized Na^+-K^+-ATPase (NKA; green) and nuclei (blue) staining. (b-c) Rh protein (red) immunolocalization in a transverse and longitudinal sections of MT and HG with apical-localized V-type H^+-ATPase (VA; green) and nuclei (blue) staining. Yellow immunostaining represents merged Rh protein (red) and NKA or VA (green) co-localization. Diagrams (bottom) of the larval digestive tract illustrate regions of transverse and longitudinal cross sections shown in panels a-c, respectively. Scale bars 50 µm. Illustrations of larval alimentary canal created by Dr. Chun Chih Chen.

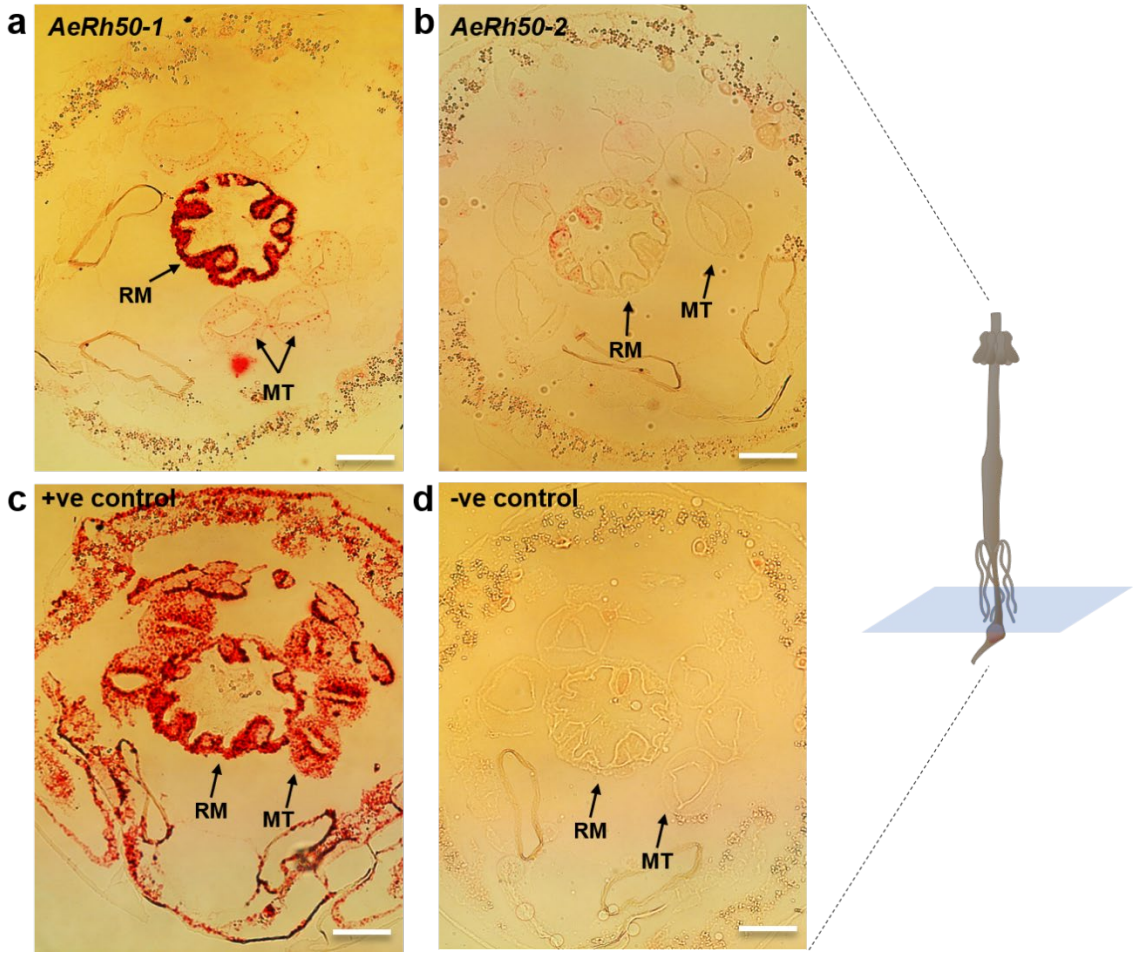

Figure 6- 2. Rh transporter (*AeRh50)* mRNA expression in transverse sections of excretory organs from *Aedes aegypti* larvae using an *in-situ* hybridization (ISH) assay. Chromogenic staining (red) of (a) *AeRh50-1* and (b) *AeRh50-2* mRNA expression in transverse sections of the five Malpighian tubules (MT) and rectum (RM) segment of the hindgut. Corresponding (c) positive (+ve) control (GAPDH) and (d) negative (-ve) control staining in the MT and RM are also shown. Diagram (right panel) of the larval digestive tract illustrates the region of transverse cross sections shown in panels a-d. Scale bars 50 µm. Illustrations of larval alimentary canal created by Dr. Chun Chih Chen.

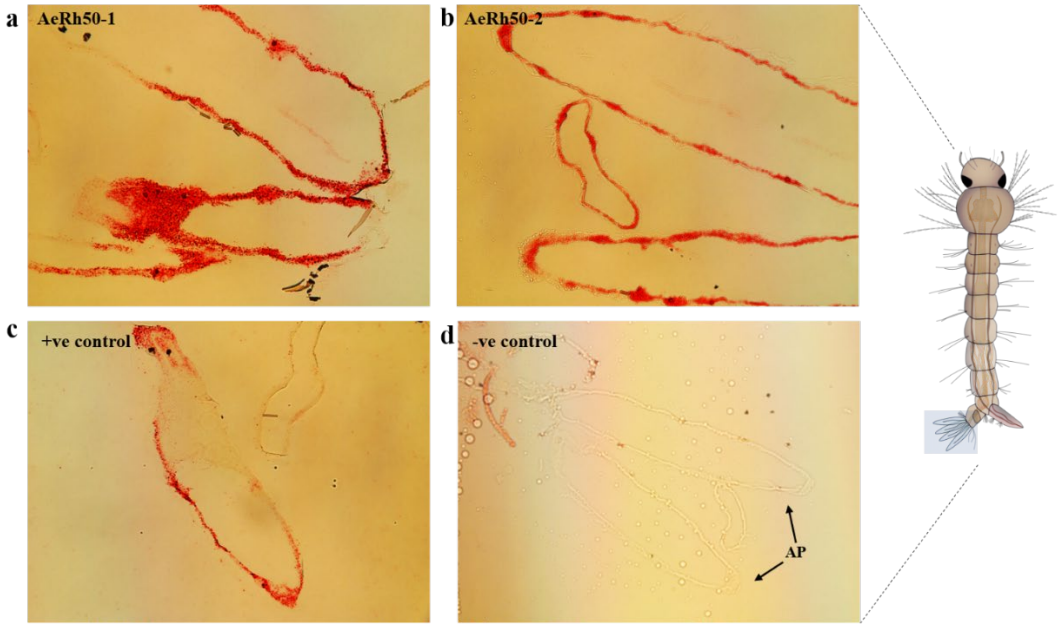

Figure 6- 3. *AeRh50* mRNA expression in longitudinal sections of anal papillae from *A. aegypti* larvae using an *in-situ* hybridization (ISH) assay. Chromogenic staining (red) of (a) *AeRh50-1* mRNA and (b) *AeRh50-2* mRNA localization in longitudinal anal papillae sections. (C) positive (+ve) control GAPDH and (D) negative (-ve) control staining in corresponding sections are also shown. Diagram (right panel) of the external anal papillae in larvae illustrates the region of longitudinal cross sections shown in panels a-d. Illustrations of larva created by Dr. Chun Chih Chen.

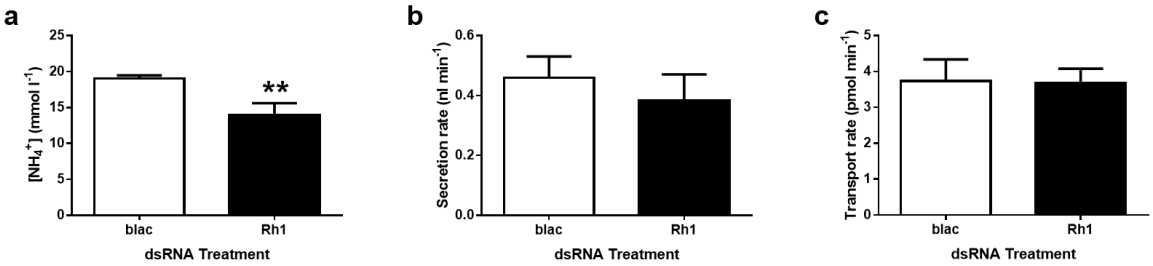

Figure 6- 4. Ammonium (NH_4^+) concentrations in the secreted fluid, transepithelial fluid secretion rates, and NH_4^+ transport rates of Malpighian tubules from *AeRh50-1-dsRNA* treated *Aedes aegypti* larvae. (a) NH_4^+ concentrations in Malpighian tubule secreted fluid, (b) transepithelial fluid secretion rate of the Malpighian tubules and (c) NH_4^+ transport rate by the Malpighian tubules from control *β-lac* dsRNA-treated larvae and *AeRh50-1* dsRNA-treated larvae at 48 hours post-dsRNA treatment. Data shown as mean ± S.E.M (n = 8-9 tubules from 4 animals for each group; Unpaired *Student's t-test*, *p = 0.0050*).

ATPase activity in the MT and NH_4+ transport across the alimentary canal of HEA-reared larvae

The activity of ion-motive pump VA, but not NKA, was significantly elevated in the MT of larvae reared in HEA (5 mM NH_4Cl) for 7 days compared to FW conditions (Fig 6-5). The NKA activity for FW-reared larvae was 0.046 ± 0.01 µmol ADP/mg protein/hour and for HEA-reared larvae was 0.063 ± 0.02 µmol ADP/mg protein/hour. The VA activity for FW-reared larvae was 0.043 ± 0.01 µmol ADP/mg protein/hour and for HEA-reared larvae was 0.13 ± 0.03 µmol ADP/mg protein/hour. An examination of NH_4^+ flux across all organs comprising the alimentary canal of HEA-reared and FW-reared larvae revealed significant NH_4^+ absorption from the gut lumen to the haemolymph at the proximal region of the gastric caeca from larvae reared in both conditions (Fig. 6-6). No significant difference in net NH_4^+ transport was observed along the alimentary canal of larvae reared in HEA for 7 days in comparison to FW-reared larvae. For both FW and HEA groups, NH_4^+ secretion from the haemolymph was measured at the MT (both proximal and distal regions), while NH_4^+ absorption was measured at the ileum and rectum segments of the hindgut (Fig. 6-6).

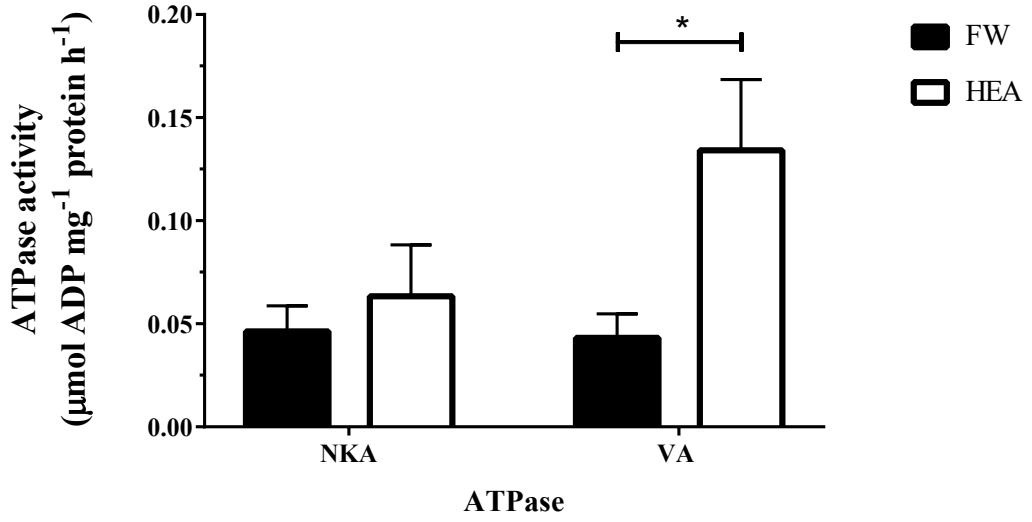

Figure 6- 5. Effect of high environmental ammonia (HEA) rearing on Na^+-K^+-ATPase (NKA) and V-type-H^+-ATPase (VA) activity in the Malpighian tubules (MT) of *Aedes aegypti* larvae. NKA and VA activity in the MT were measured at 7 days after 2nd instar larvae were reared in either dechlorinated tap water (FW) or HEA conditions (5 mM NH_4Cl). Data were analysed using a two-way ANOVA (Bonferroni's multiple comparisons test). Asterisk (*) signifies a significant difference (*p = 0.0448)*. All data are expressed as mean ± S.E.M (n = 3 for each treatment group).

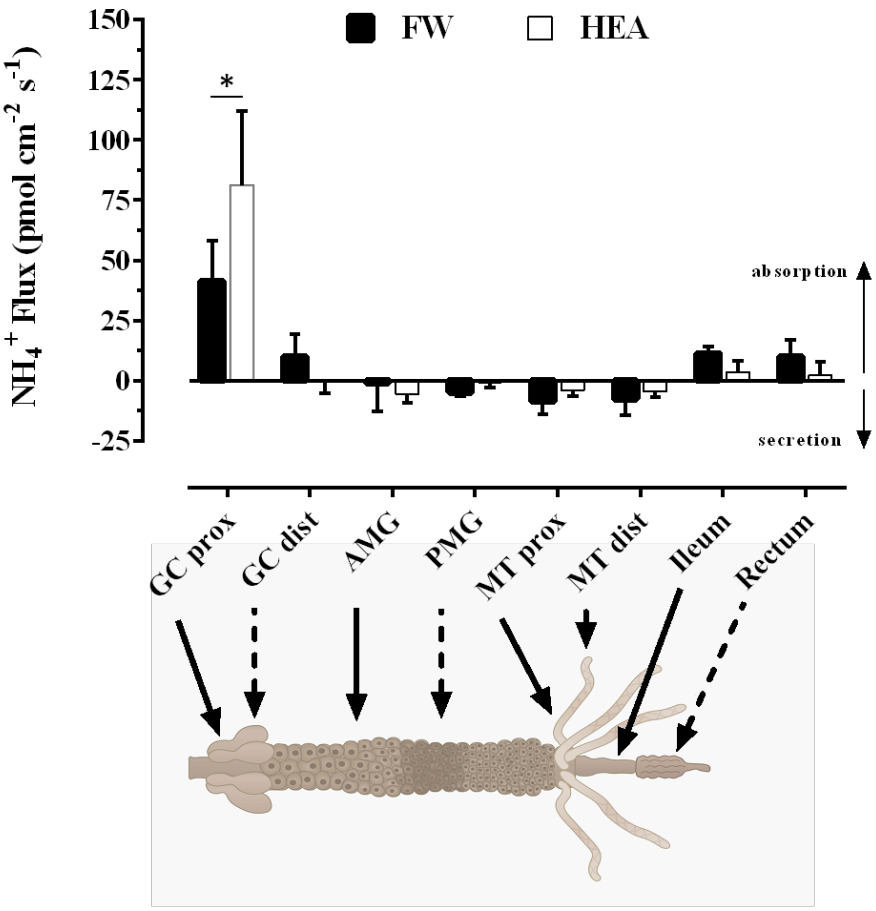

Figure 6- 6. The effect of high environmental ammonia (HEA) rearing conditions on NH_4^+ flux across organs of the alimentary canal of *Aedes aegypti* larvae measured using the scanning ion-selective electrode technique (SIET). Average NH_4^+ flux measurements across the gastric caecae (GC), anterior midgut (AMG), posterior midgut (PMG), Malpighian tubules (MT), and ileum and rectum segments of the hindgut are shown. Positive values signify NH_4^+ absorption from the gut lumen into the haemolymph, and negative values signify NH_4^+ secretion from the haemolymph to the gut lumen. Data are represented as mean ± S.E.M (n = 5 animals per rearing group). Asterisks denote statistically significant differences in NH_4^+ flux at the GC regions compared to all other organs (two-way ANOVA, Sidak's multiple comparisons test, $p < 0.05$). prox, proximal; dist, distal.

Expression of ammonia transporters and enzymes involved in nitrogen metabolism

Heatmaps of identified transcripts of interest in the rectum of 4th instar larvae acutely exposed to HEA conditions or control FW for 24 hours were constructed to visualize differences in expression (Fig. 6-7). All four ammonia transporters in *A. aegypti* are expressed in the rectum of larvae (Fig. 6-7a), with *AeRh50-1* having the highest transcript expression followed by *AeRh50-2*, *AeAmt1*, and *AeAmt2*, respectively. Acute HEA exposure (24 hours) did not significantly alter the transcript abundance of each gene in the rectum when compared to FW levels. Enzymes involved in key amino acid metabolism pathways for ammonia formation and/or sequestration were identified (Fig. 6-7b). Glutamine synthetase (GS, cytoplasmic and mitochondrial) together with glutamate synthase (GOGAT) comprising the GS/GOGAT pathway were expressed in the rectum. In HEA-exposed larvae, a significant decrease in glutamine synthetase (mitochondrial) expression occured. Glutamate dehydrogenase (GDH) transcript is enriched in the rectum in comparison to all other enzymes examined for glutamate metabolism, and GDH expression is unaltered upon exposure to HEA conditions. A mitochondrial glutamate carrier protein is also enriched in the rectum, whereby transcript expression significantly increases in HEA-exposed larvae. Other enzymes involved in ammonia metabolism in mosquitoes via glutamine and proline synthesis (alanine aminotransferase, glutamate oxaloacetate transaminase, and aspartate aminotransferase) were expressed in the rectum at levels higher than enzymes involved in purine metabolism, uric acid degradation, and urea formation; allantoicase, uricase, and arginase, respectively (Fig 6-7c).

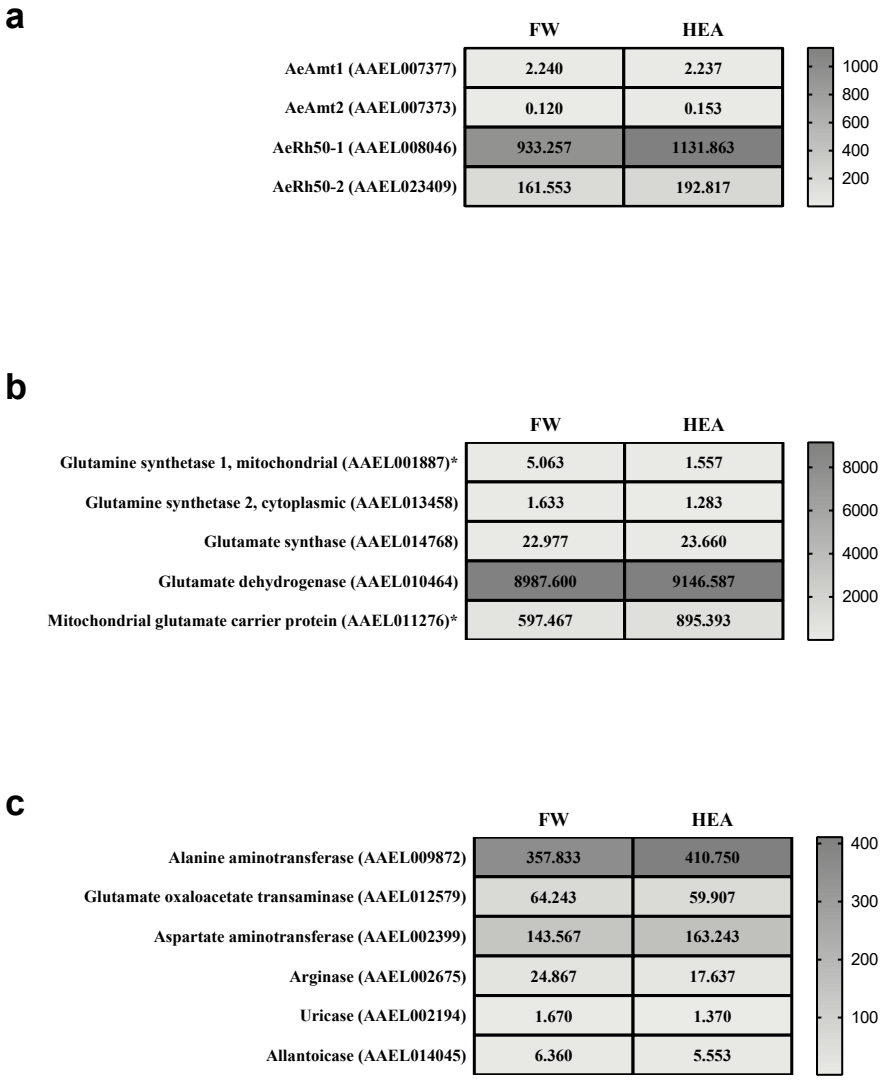

Figure 6- 7. Heatmaps of ammonia transporters, enzymes involved ammonia metabolism and urea formation in the rectum of *Aedes aegypti* larvae. Transcript expression using RNAseq methodology of identified transporters or enzymes in the rectum of 4th instar *A. aegypti* larvae exposed to freshwater (FW) or high environmental ammonia (HEA) conditions for 24 hours. Data in heatmaps are presented as average values (n = 3 biological replicates per treatment group) expressed in transcripts per kilobase million (TPM). Greyscale coloring is indicative of relative TPM values among all genes in each figure, with light grey being the least expressed and dark grey being the most abundantly expressed (scales shown on the right of each figure). (a) Ammonia transporters from the Amt and Rh families, (b) enzymes involved in glutamate formation or catabolism, and (c) enzymes involved in amino acid metabolism and urea formation, are shown. Transcript IDs and annotations (VectorBase) associated with each data value are provided. Asterisks (*) beside accession numbers signify a significant difference in transcript expression between FW and HEA groups (Differential expression (DE) analysis, $\log_2$ fold-change ($\log_2$FC), $p < 0.05$).

Expression of ion channels, exchangers, co-transporters, and ion-motive ATPases in the rectum

The rectum of larvae showed high levels of expression of various subunits of the ATPases NKA and VA compared to all other transcripts of interest analysed in the heatmap (Fig. 6-8), and the transcript of both subunits of the NKA were significantly elevated in the rectum of HEA-exposed larvae. Out of the genes of interest that were selected for analysis and shown in Figure 6-8, the transcripts of several ion transporters and enzymes were enriched in the rectum including carbonic anhydrase 9, sodium (Na^+)-coupled cation-chloride (Cl^-) co-transporter 2 (CCC2), and inwardly rectifying K^+ channels 2a and 2b (Kir2a, Kir2b), compared to the other transcripts of interest. Of the sodium (Na^+)-hydrogen (H^+) exchangers (NHE) expressed in the rectum, NHE8 was the most highly expressed in comparison to NHE 7,9 and NHE3 (Fig. 6-8).

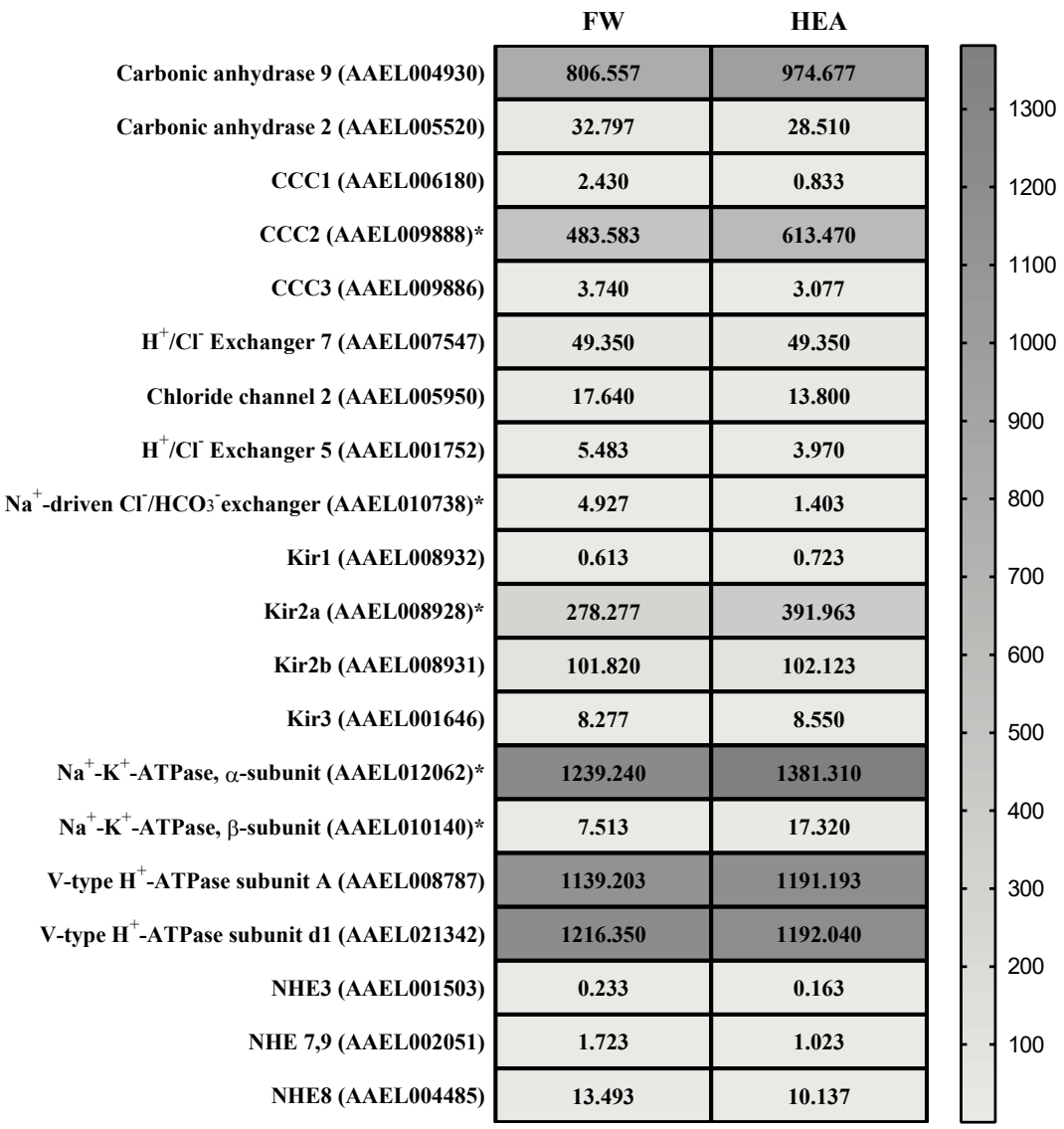

Figure 6- 8. Heatmaps of key ion transporter transcript expression in the rectum of *Aedes aegypti* larvae. Transcript expression using RNAseq methodology of identified transporters or enzymes in the rectum of 4th instar *A. aegypti* larvae exposed to freshwater (FW) or high environmental ammonia (HEA) conditions for 24 hours. Data in heatmaps are presented as average values (n = 3 biological replicates per treatment group) expressed in transcripts per kilobase million (TPM). Greyscale coloring is indicative of relative TPM values among all genes in each figure, with light grey being the least expressed and dark grey being the most abundantly expressed (scales shown on the right of each figure). Transcript IDs and annotations (VectorBase) associated with each data value are provided. CCC, sodium (Na^+)-coupled cation-chloride (Cl^-) co-transporter; Kir, inwardly rectifying K^+ channels; NHE, sodium (Na^+)-hydrogen (H^+) exchangers. Asterisks (*) beside accession numbers signify a significant difference in transcript expression between FW and HEA groups (Differential expression (DE) analysis, $\log_2$ fold-change ($\log_2$FC), $p < 0.05$).

Rh transporter mRNA and protein expression and localization in adult females

AeRh50-1 mRNA abundance was found to be highest in the hindgut of sugar-fed (i.e. non-blood fed) females, compared to levels in the midgut (MG) and the MT (Fig. 6-9a). At 24 hours post blood meal (PBM), a significant increase in *AeRh50-1* transcript abundance was observed within the MT compared to levels in sugar-fed (non-blood fed) females, whereas transcript abundance in the MG and HG did not change. The mRNA abundance of *AeRh50-2* is uniform among the MG, HG, and MT organs of sugar-fed females, and 24 hours PBM *AeRh50-2* levels are significantly elevated in the HG (Fig. 6-9b). Immunohistochemical assessment of Rh protein in cross sections through the abdomen of sugar-fed females revealed an apical localization of these transporters within the HG and MT which did not co-localize with basolateral NKA, as well as localization within the ovary (OV) (Fig. 6-10a). At 24 hours PBM (Fig. 6-10b) and 48 hours PBM (Fig. 6-10c-d), Rh protein immunostaining was present in the apical membrane of the hindgut, including the rectal pads (RP) within the rectum, as well as within cells of the OV, but was absent in the MT and the MG. Using RNA *in situ* hybridization, it was determined that *AeRh50-1* mRNA is highly localized within the ileum and rectum segments of the HG which is visible by the red chromogenic dye staining within these structures (Fig. 6-11a), similarly to positive control GAPDH staining in the ileum and rectal pads, specifically, but not the MT and MG (Fig. 6-11c). In contrast, *AeRh50-2* mRNA staining is notably absent in the HG and comparable to negative control staining (Fig. 6-11b,d). Chromogenic dye staining of both *AeRh50-1* and *AeRh50-2* mRNA appears to be present within cells of the OV, albeit to much lower levels in comparison to the positive control.

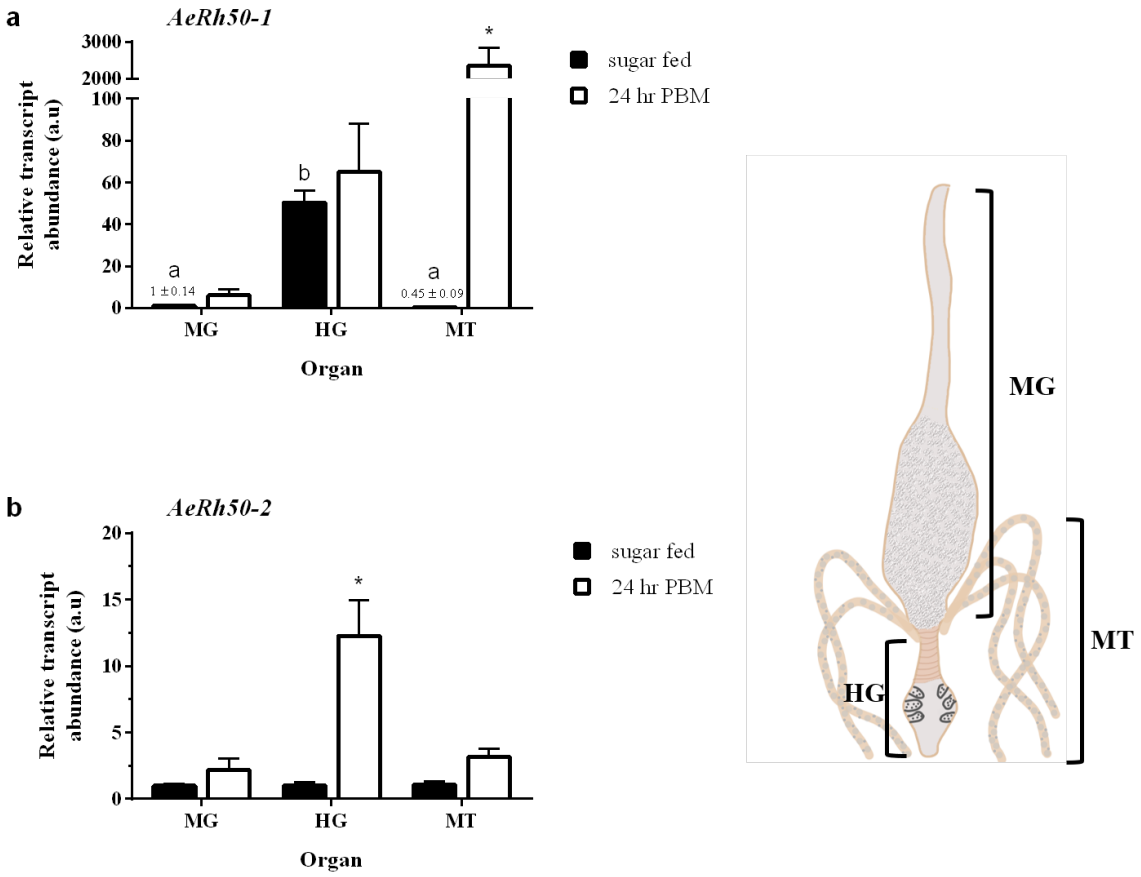

Figure 6- 9. Rh transporter mRNA expression in the midgut (MG), hindgut (HG), and Malpighian tubules (MT) of sugar-fed and blood-fed adult female *Aedes aegypti*. (a) AeRh50-1 relative transcript abundance and (b) AeRh50-2 relative transcript abundance in the MG, HG, and MT of sugar fed females or 24 hours post blood meal (PBM) females. Transcript levels for each gene was normalized to the geometric mean of three control reference genes (*rp49*, *rpS18*, *rpL8*), and are expressed relative to transcript levels in the midgut of that gene (for sugar fed values) or are expressed relative to sugar fed levels within each organ (for 24 hr PBM values). Data are expressed as mean ± S.E.M (n = 6 for sugar fed groups, n = 3 for blood fed groups). Letters denote a statistically significant difference between MG, HG, MT of sugar fed groups (One-way ANOVA, Tukey multiple comparisons test, $p < 0.0001$). Asterisks (*) denote a statistically significant difference between sugar fed and 24hr PBM values for each MG, HG, MT group (Mann Whitney test, $p < 0.05$).

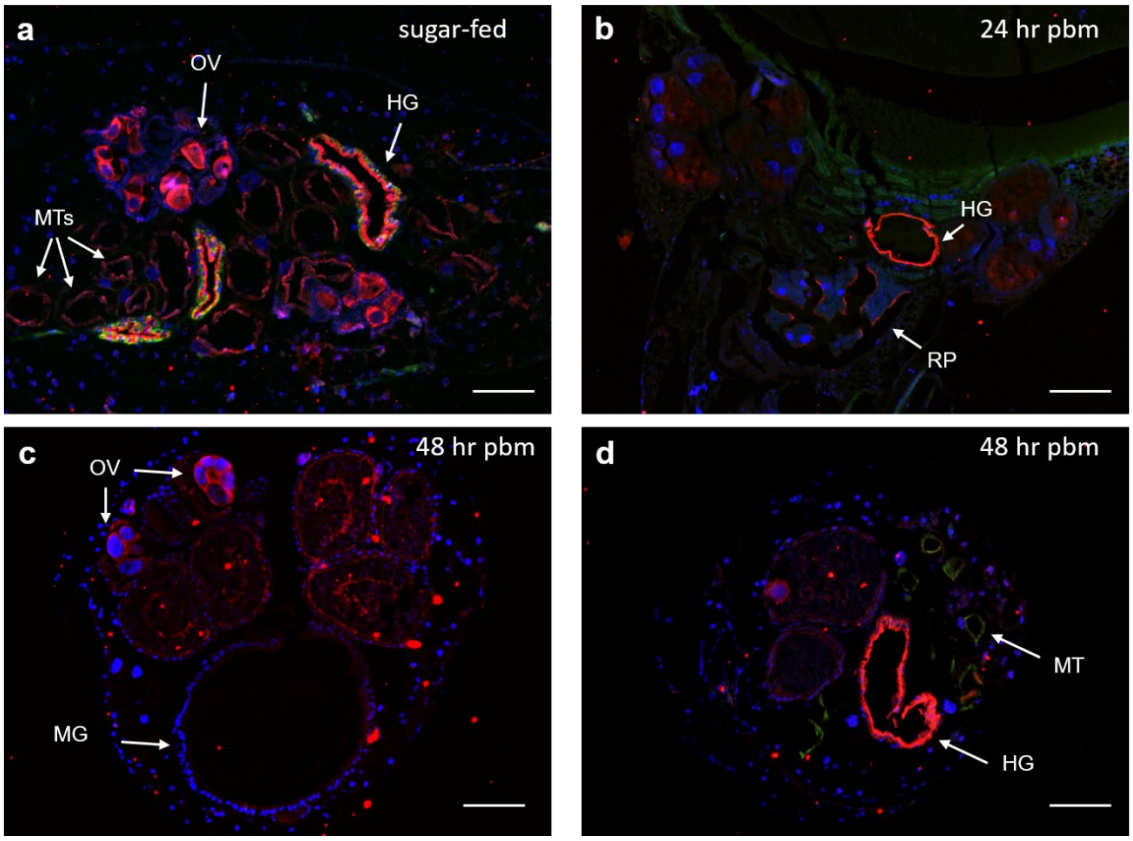

Figure 6- 10. **Rh protein immunolocalization in sugar fed and blood-fed adult female *A. aegypti***. (**a**) Rh protein (red), Na^+-K^+-ATPase (green), and nuclei (blue) immunostaining in paraffin-embedded longitudinal sections of sugar-fed females showing the Malpighian tubules (MT), ovary (OV), and hindgut (HG). (**b-d**) Rh protein (red), V-type H^+-ATPase (green), and nuclei (blue) immunostaining in transverse sections of females at 24 hr and 48 hr post blood meal (pbm), showing the ovary (OV), midgut (MG), HG with rectal pads (RP), and MT. Scale bars are 100 μm.

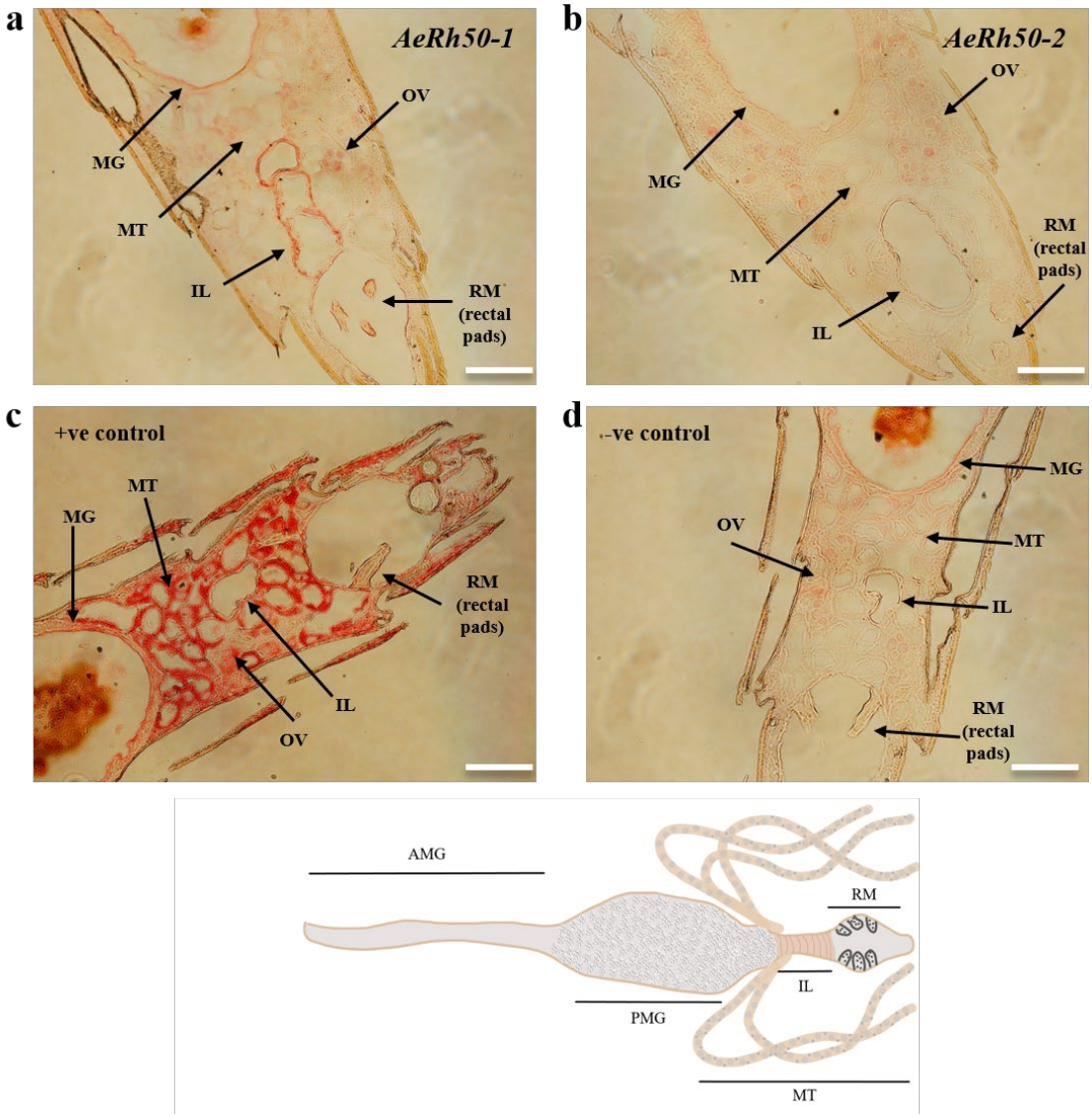

Figure 6- 11. Rh transporter (*AeRh50)* mRNA expression in transverse sections of excretory organs from blood fed female *A. aegypti* using an *in-situ* hybridization (ISH) assay. Chromogenic staining (red) of (a) *AeRh50-1* and (b) *AeRh50-2* mRNA expression in longitudinal sections of the midgut (MG), Malpighian tubules (MT), ovaries (OV), and ileum (IL) and rectum (RM; rectal pads, RP) segments of the hindgut. Corresponding (c) positive (+ve) control (GAPDH) and (d) negative (-ve) control staining in corresponding sections are also shown. Diagram (bottom panel) of the adult alimentary canal illustrates the organs within the longitudinal cross sections shown in panels a-d. Scale bars 100 µm.

NH_4^+ transport across the hindgut and the effects of *AeRh50-1* dsRNA injection

Regionalized NH_4^+ flux across the hindgut was measured using the scanning ion-selective electrode technique (SIET) at 2 days post-*AeRh50-1* dsRNA injection. For control adults, NH_4^+ secretion from the haemolymph into the gut lumen was found to occur at the upper and lower portions of the ileum, whereas the rectum was found to absorb NH_4^+ from the gut lumen into the haemolymph (Fig. 6-12). *AeRh50-1* dsRNA-injection caused a significant decrease in NH_4^+ secretion within the region of the lower ileum compared to the *β-lac* dsRNA-injected control groups. Furthermore, a reversal in NH_4^+ flux, from absorption (34.831 ± 28 pmol cm^{-2} s^{-1}) in the control group to secretion (-41.44 ± 28 pmol cm^{-2} s^{-1}) in the *AeRh50-1* dsRNA-injected group, occurred within the rectum.

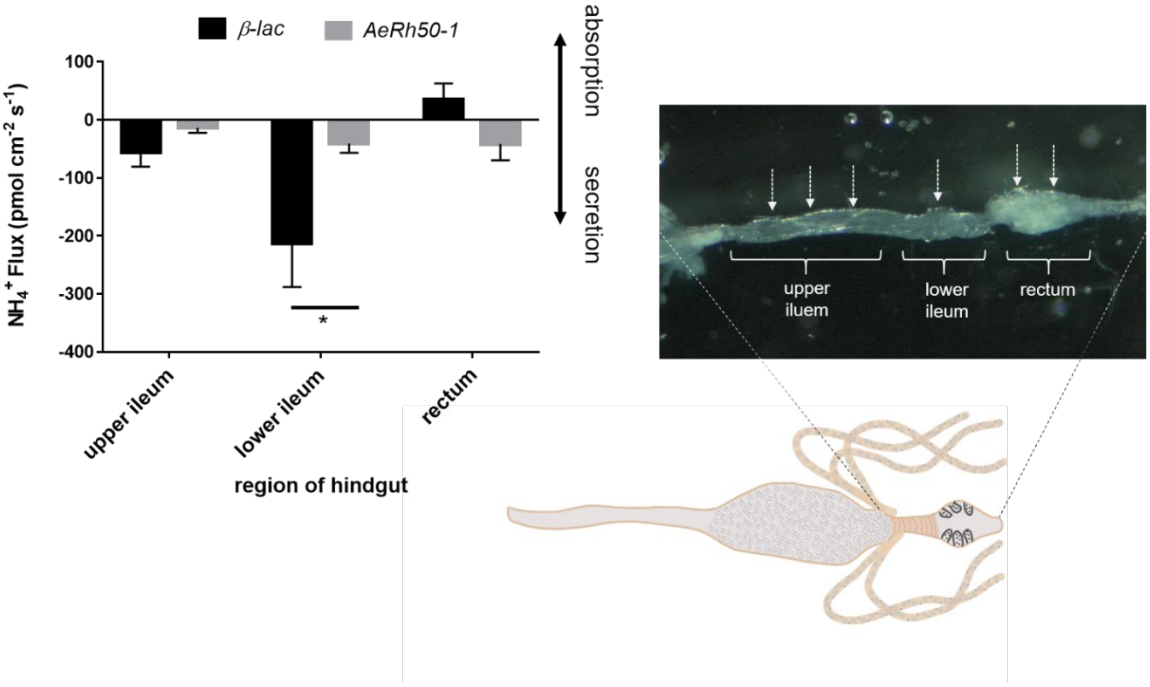

Figure 6- 12. Effect of dsRNA-mediated *AeRh50-1* knockdown on ammonium (NH_4^+) flux in the hindgut of adult female *A. aegypti*. Scanning ion-selective electrode technique (SIET) measurements of NH_4^+ flux measured at three regions of the hindgut (right panel: upper ileum, lower ileum, and rectum) from *AeRh50-1* and control *β-lac* dsRNA-injected adults. NH_4^+ flux measurements are shown as mean ± S.E.M (n = 4 animals per group). Asterisks signify statistically significant differences in regional flux measurements ($p = 0.0106$, Two-way ANOVA; Sidak's multiple comparisons test). Specific measurement sites in each region are indicated by the white dashed arrows.

6.5 Discussion

Overview

The current study considered the role of the MT and HG (i.e. the excretory system) in ammonia regulation and the contribution of the Rh protein ammonia transporters in facilitating ammonia movement across these osmoregulatory epithelia. The impact of HEA rearing of larvae and blood meal digestion of adult females was also examined in relation to MT and rectum function in ammonia transport and excretory processes. The blind-ended MT produce the primary urine through the transepithelial secretion of ions and the subsequent osmotic efflux of water, which is then emptied into the pyloric chamber at the junction of the posterior midgut and anterior hindgut (Bradley, 1987; Ramsay, 1951). The isosmotic (to the haemolymph) primary urine is modified in the rectum by the active resorption of ions, whereby a dilute urine is formed and subsequently eliminated via the anus (Ramsay, 1950). This study reveals the mRNA and protein expression of Rh transporter AeRh50-1 which is localized to the apical membranes of the MT and HG epithelia, and that injection of *AeRh50-1* dsRNA causes alterations in ammonia transport within these organs of both larval and adult *A. aegypti*. Furthermore, environmentally (i.e. HEA) induced changes in ion transporter, ion channel, and ion-motive ATPase mRNA expression in the larval rectum and physiologically (i.e. blood feeding) induced changes in Rh protein mRNA abundance in the HG of adult females points to the involvement of active and secondary active processes in driving ammonia movement across these organs. Overall, measurements of relatively high rates of ammonia secretion by the MT of larvae and high NH_4^+ efflux rates across the ileum segment of the HG (from haemolymph to lumen) of adult females implicates these organs as important sites for ammonia transport and excretion. Notably, this is the first study to examine gene expression in the mosquito rectum using next-generation sequencing tools in combination with electrophysiology, RNAi, microscopy, and molecular biology to examine novel molecular mechanisms of ion transport in relation to ammonia-transport physiology.

Functional significance of Rh protein expression in the MT and HG of larvae and the influence of HEA rearing conditions

Recently, we reported that the MT of field-collected and laboratory-reared *A. aegypti* larvae secrete NH_4^+, and that NH_4^+ transport rates become significantly elevated when larvae develop in high ammonia septic water in comparison to FW (Chapter 5). Furthermore, an examination of ammonia transporter expression in field-collected and laboratory-reared larvae revealed the expression of Rh protein within the epithelia of the MT and HG, and rearing in high ammonia septic water causes an increase in Rh protein immunostaining within these organs (Chapter 5). In the present study, we confirm that the Rh proteins are localized to the apical membrane of the MT of larvae through co-localization with apical VA and not basolateral NKA. Within the rectum, specifically, we have previously demonstrated that Rh protein expression is co-localized with VA to the apical membrane of field-collected larvae (Chapter 5), which is further verified in the present study with larvae from our laboratory colony. In an attempt to discern which AeRh50 transporter is expressed within these organs, which cannot be determined at the protein level due to the high amino acid sequence similarity of AeRh50-1 and AeRh50-2, we utilized an RNA *in-situ* hybridization assay to localize *AeRh50-1* and *AeRh50-2* transcript within the MT and HG. From this, it was demonstrated that AeRh50-1 is the predominant Rh protein expressed within the MT and HG epithelia, as opposed to AeRh50-2, because of the high levels of *AeRh50-1* mRNA expression detected within these organs. Consequently, the use of the RNA *in-situ* hybridization assay also validated our previous reports that both *AeRh50-1* and *AeRh50-2* are expressed within the anal papilla epithelium and both proteins function in facilitating ammonia excretion from these organs [Fig. 6-3; (Chapter 2)].

While the specific function of AeRh50-1 within the MT and HG of larvae requires further attention, we show *AeRh50-1* dsRNA treatment causes a significant reduction in $[NH_4^+]$ (mmol l^{-1}) in the secreted fluid droplets of the MT, an effect which is rapidly compensated for by the MT and does not affect overall NH_4^+ secretion rates. A more robust knockdown and/or an investigation of

compensatory mechanisms, including the involvement of AeRh50-2 and the AeAmts, is necessary. Nonetheless, substantial evidence from our work on Rh protein function in the anal papillae suggests that these ammonia transporters likely function in acid-base homeostasis in addition to ammonia regulation and excretion. AeRh50-1 protein knockdown within the anal papillae (and likely in other organs, in tandem) not only resulted in decreased NH_4^+ efflux rates, but also caused a decrease in haemolymph pH, an effect that was not observed with AeRh50-1 or AeAmt2 knockdown (Chapter 3; Chapter 2). Furthermore, larvae reared in moderate levels of salt (5 mmol l^{-1}) faced a significant decrease in haemolymph pH (i.e. acidification), and this corresponded with a 5-fold increase in Rh protein abundance within the anal papillae and elevated NH_4^+ excretion rates from this organ while the activities of NKA and VA did not change, AeAmt protein levels were unchanged or decreased, and the mRNA abundance of an NHE transporter, NHE3, also decreased (Chapter 4). While the role of the MT and HG in acid-base regulation is incomplete, the MT and rectum have been demonstrated to be important sites of acid excretion in *A. aegypti* larvae (Clark et al., 2007). It is very likely, based on our previous findings of AeRh50-1 function and alterations in haemolymph pH as a consequence of AeRh50-1 knockdown, that this transporter is involved in maintaining an acidic rectal lumen (Clark et al., 2007). The hindgut of the larval lepidopteran, *Manduca sexta*, expresses comparatively high mRNA levels of an Rh ammonia transporter (*RhMS*) and the high luminal ammonia concentration within the hindgut (~ 60 mmol l^{-1}) was 60 times greater than the ammonia content of other organs along the alimentary canal as well as haemolymph levels (Weihrauch, 2006). Furthermore, the movement of ammonia within the hindgut was directed towards the lumen from the haemolymph. Similarly, the rectal epithelium of locust, *Schistocerca gregaria*, was shown to be a significant site of ammonia secretion towards the lumen, irrespective of manipulations in luminal pH (Thomson et al., 1988). The role of NH_4^+ as a weak-acid equivalent in acid-base homeostasis has been noted in response to elevated CO_2-induced pH disturbances in some aquatic animals (reviewed in Weihrauch and Allen, 2018).

In the present study, we also measured a net NH_4^+ influx (lumen to haemolymph) at the ileum and rectum of larvae reared for 7 days in FW and HEA conditions. While this may seem counterintuitive, larvae were starved for 24 hours prior to SIET measurements and we have previously demonstrated that larvae tend to revert to ammonia absorption mechanisms at the anal papillae during periods of starvation or limited nutrient availability (Chapter 5). It is also worth noting that mean NH_4^+ flux measurements at the ileum and rectum (11.3 ± 2.8 and 10.1 ± 6.8 pmol cm^{-2} s^{-1}, respectively) are negligible in comparison to NH_4^+ flux measurements often observed at the anal papillae (~25-150 pmol cm^{-2} s^{-1}) (Chasiotis et al., 2016; Donini and O'Donnell, 2005; Chapter 2). In fact, based on the localization of AeRh50-1 and VA to the apical membranes of both the rectum and MT epithelia, we propose that an ammonia trapping mechanism exists in these organs as a means of significant ammonia secretion into the lumen from the haemolymph. This mechanism has been suggested or shown to occur across osmoregulatory organs of many animals whereby membrane acidification from the transport of H^+ coupled with NH_3 transport by Rh proteins leads to the formation of membrane impermeable NH_4^+ in the lumen or external media (Chasiotis et al., 2016; Quijada-Rodriguez et al., 2015; Weihrauch and O'Donnell, 2015; Weihrauch et al., 2012b; Wright and Wood, 2009). The significantly increased VA activity in the MT of larvae reared in HEA in this study further suggests that this ammonia-trapping mechanism may be important in ammonia secretion in the primary urine. A similar finding of increased VA activity within the anal papillae in response to HEA rearing lends further support to this proposed mechanism in the MT and the HG (Chapter 4). Altogether, these data implicate the MT and HG of larvae as important sites for ammonia regulation and possessing efficient ammonia transporting mechanisms. The contribution of the AeAmts also cannot be discounted, as these transporters were previously immunolocalized within the hindgut of larvae (Chapter 5).

Expression of ion transporters, ion channels, and enzymes involved in nitrogen metabolism in the larval rectum and the response to acute HEA exposure

The rectum of aquatic insect larvae is broadly acknowledged as a critical site for the selective reabsorption of ions, water, and nutrients for the maintenance of haemolymph ionic and osmotic composition (Bradley, 1987; Jonusaite et al., 2013a; Meredith and Phillips, 1973; Patrick et al., 2006b). However, limited information exists in terms of specific ion-transporting mechanisms within this organ. Furthermore, previous findings of high luminal ammonia concentrations in the hindgut of insect larvae and relatively high Rh transporter expression within rectal epithelia of insect larvae including findings from this current study (Weihrauch, 2006), suggest the presence of ion channels, ion transporters, and enzymes involved in ammonia metabolism and transport in the hindgut, which is currently unknown. Our RNAseq analysis of transcript expression in the rectum confirms the presence of a plethora of ion transporters and channels, ion-motive ATPases, and enzymes involved in ammonia formation and detoxification. The transcripts of all four ammonia transporters (*AeAmt1*, *AeAmt2*, *AeRh50-1*, and *AeRh50-2*) in *A. aegypti* are expressed in the rectum. *AeRh50-1* mRNA is the most highly abundant in comparison to the *AeRh50-2* and the AeAmts, supporting the present findings from our immunohistological and RNA *in situ* hybridization expression studies. Acute exposure of larvae to HEA conditions had little effect on ammonia transporter mRNA expression in the rectum, which may also support the observation that HEA rearing does not alter endpoints in NH_4^+ movement across the rectum measured by SIET. Nevertheless, when taken together with our immunohistochemical observations, AeRh50-1 expression within the hindgut strongly suggests that this protein plays a primary role in ammonia transport and the maintenance of high luminal ammonia levels.

Ammonia formation either as a metabolic waste product or as a nitrogen source that is recycled in animals generally occurs via one of two pathways: (1) glutamate dehydrogenase (GDH) which catalyzes the reversible reaction of glutamate formation from NH_4^+ and 2-oxoglutarate (i.e. α-ketoglutarate) and (2) glutamine synthetase (GS) and glutamate synthase (GOGAT) which either convert glutamate and ammonia to glutamine (via GS) or produce two glutamate molecules (via GOGAT)

(Merrick and Edwards, 1995). While the GDH pathway is regarded as the main route for glutamine and ammonia sequestration or formation in animal cells, increasing examples exist in insects demonstrating the GS/GOGAT as being the primary pathway for ammonia assimilation (Doverskog et al., 2000; Hirayama and Nakamura, 2002; Hirayama et al., 1997). The rectum of *A. aegypti* larvae is enriched with GDH transcript (8987.6 ± 245 transcripts per million, TPM in FW), approximately 400 to 5,000 times greater than GOGAT and GS levels, respectively. Therefore, it appears that GDH is the predominant pathway for ammonia formation in the rectum of larvae. The same may not be true for adult female *A. aegypti* during blood meal digestion, as GDH activity is shown to play a minor role in comparison to the GS/GOGAT (or GltS for glutamate synthase, alternatively) (Scaraffia et al., 2005; Scaraffia et al., 2006). The metabolism of amino acids other than glutamate, including proline and alanine, are important sources of ammonia production or ammonia assimilation in insects (Chamberlin and Phillips, 1983; Scaraffia et al., 2005; Scaraffia et al., 2006). We found that the transcripts of enzymes involved in many of these metabolic pathways were expressed in the rectum, including alanine aminotransferase which was highly enriched, glutamate oxaloacetate transaminase, and aspartate aminotransferase. Female *A. aegypti* are also capable of synthesizing urea through a metabolic pathway that involves the degradation of urea and the transcripts of at least two of the enzymes involved in this pathway are expressed in the larval rectum, uricase (i.e. urate oxidase) and allantoicase, albeit at comparatively lower levels than those involved in glutamate and proline metabolism (Scaraffia et al., 2008). The production of urea in insects is also attributed to the enzyme arginase, and transcripts of this enzyme were also identified within the rectum (Isoe and Scaraffia, 2013). While the specific composition of nitrogenous waste excretory products has not been examined in detail in *A. aegypti* larvae, specifically in relation to urea and uric acid excretion, ammonia as the predominant nitrogenous waste product is common among the majority of aquatic insects examined (O'Donnell and Donini, 2017).

Key ion transporters and channels, and enzymes that have well established roles in ion-transporting mechanisms in other osmoregulatory organs of larvae were also expressed in the rectum, consistent with its role in active ion resorption to form a dilute urine. Carbonic anhydrase 9 (CA9) transcript is enriched in the rectum, and pharmacological characterization of this enzyme in the anal papillae of larvae demonstrated its indirect involvement in ammonia excretory mechanisms within these organs (Chasiotis et al., 2016). In a previous study, immunostaining of CA9 along the alimentary canal of adult females revealed little to no expression in the hindgut, however, CA9 expression was not specifically examined in the rectum of larvae (Dixon et al., 2017). The transcripts of 3 genes encoding Na^+-dependent cation-chloride cotransporters (*CCC1* or *aeNKCC1*, *aeCCC2*, and *aeCCC3*) were expressed in the rectum. Of these, *aeCCC2* was found to be highly abundant in the rectum and significantly elevated upon acute HEA exposure (483.6 ± 37 TPM in FW and 613.47 ± 164 TPM in HEA). This finding supports previous evidence that *aeCCC2* is highly expressed in the adult hindgut in comparison to the MT where it may play an integral role in ion absorption, although the specific transport substrates are still unknown (Piermarini et al., 2017). Of the five genes encoding the inward-rectifying K^+ (Kir) channels in *A. aegypti*, the transcript of four of these genes (*AeKir1*, *AeKir2a*, *AeKir2b*, and *AeKir3*) were identified in the rectum. In the MT of adult female *A. aegypti*, AeKir1 and AeKir2b are abundantly expressed within the basolateral membrane of stellate cells and principal cells, respectively, where they generate a significant proportion of the basolateral membrane conductance which powers transepithelial K^+ secretion (Piermarini et al., 2013; Piermarini et al., 2015; Rouhier et al., 2014). Here we found that *AeKir2a* was most abundantly expressed in the rectum and transcript levels were significantly elevated in response to HEA (278.3 ± 11 in FW and 391.9 ± 67 in HEA). *AeKir2b* was also enriched within the rectum (101.8 ± 2.7 in FW and 102.1 ± 13 in HEA). Considering the important function of the rectum in selective K^+ reabsorption from the lumen in aquatic dipteran larvae (Bradley and Philips, 1977; Jonusaite et al., 2013b; Meredith and Phillips, 1973; Phillips, 1981) and the critical role of Kir channels in the transepithelial movement of K^+ in the MT, we posit that these ion channels

are highly involved in K^+ transport mechanisms in the larval rectum. Substantial evidence that ion-motive pumps, NKA and VA, are expressed within the rectal epithelia of aquatic insect larvae are further supported by our RNAseq analysis (Chapter 5; Jonusaite et al., 2013b; Patrick et al., 2006). NKA transcript (α subunit) is abundant in the rectum and increases (α and β subunits) in response to abrupt HEA exposure, and VA transcript (subunits A and d1) are found at similar expression levels but are unaltered in response to HEA exposure. Also identified at relatively lower transcript levels were transport mechanisms for chloride (H^+/Cl^- exchanger 7, H^+/Cl^- exchanger 5, and chloride channel 2,) bicarbonate (Na^+-driven Cl^-/HCO_3^- exchanger), and sodium-hydrogen exchangers (NHE3, NHE7/9, and NHE8). Altogether, these data provide novel insight into the specific ion transport mechanisms within the rectum that may be important for select ion movement, which is critical for the ability of larvae to inhabit dilute freshwater environments and aquatic habitats that contain toxic ammonia levels.

Rh protein expression in the hindgut of adult females facilitates NH_4^+ transport

Rh protein immunostaining was localized primarily to the apical membrane of the hindgut epithelium of sugar-fed and blood fed (24-48 hours PBM) adult females. Similarly to our findings from larvae, RNA in-situ hybridization and qPCR analyses revealed that AeRh50-1 is the primary Rh protein being expressed within this organ. Interestingly, our qPCR findings of elevated *AeRh50-1* mRNA expression in the MT at 24 hours post blood meal contradict immunohistochemical results which show Rh protein expression in the MT of sugar-fed females but is absent in the MT of blood-fed females and requires further investigation. Regardless, the enriched AeRh50-1 expression within the HG in comparison to other osmoregulatory organs is highly suggestive of a critical role in luminal ammonia secretion, similar to that proposed for larvae, as ammonia is the principal nitrogenous waste product in blood-fed adult female *A. aegypti* (Scaraffia et al., 2005). The high Rh protein expression in the HG of sugar-fed females is intriguing as the animals are devoid of dietary nitrogen prior to the ingestion of a blood meal, and in this regard the rectal lumen of herbivorous insects such as *Bombyx mori* possess

high ammonia concentrations secreted across the epithelium (Chamberlin and Phillips, 1983; Thomson et al., 1988; Weihrauch, 2006). Routine metabolic activities, such as regular protein turnover, are a significant source of endogenously produced ammonia in animal cells and it is likely that AeRh50-1 is important for facilitating ammonia secretion during all feeding (sugar and blood) states of the adult female. Indeed, comparatively (to larval HG) high levels of NH_4^+ efflux directed into the hindgut lumen was measured along the ileum and was significantly reduced following AeRh50-1 knockdown. This is in contrast to measurements of the larval ileum in which a net NH_4^+ absorption was measured, but at much lower rates (+11.3 ± 2.8 pmol cm^{-2} s^{-1} for larvae versus up to -213 ± 75 pmol cm^{-2} s^{-1} for adults). Notably, the ileum exhibits high Rh protein expression within the epithelium. The ileum is an actively contracting structure for the movement of gut contents and is comprised of a flattened epithelium which is enclosed by cuticle and bordered by inner circular muscles and outer longitudinal muscles (Christophers, 1960; Lajevardi and Paluzzi, 2020). The ileum is not considered to have a major function in osmoregulation (Phillips, 1981). However, the energetic demands related to its high contractile activity may result in significant levels of ammonia formation via amino acid catabolism within the musculature, necessitating mechanisms for ammonia transport into the lumen destined for excretion. Our observations of Rh protein expression in both larvae and adults demonstrate an apical localization that is almost always exclusively co-expressed with apical VA, further supporting the notion of ammonia trapping mechanisms as a means of confining NH_4^+ within the lumen (or external), often against a significant concentration gradient, for excretion. Similarly to larvae, the rectum of the adult female uptakes NH_4^+ into the haemolymph at relatively low flux rates, and AeRh50-1 dsRNA injection led to a trend towards a reversal in NH_4^+ flux to secretion at the rectum. Increasing examples of animals maintaining certain levels of ammonia systemically points towards the phenomenon of ammonia homeostasis which is likely of importance for some physiological processes (Hu and Tseng, 2017; Weihrauch and Allen, 2018a). The haemolymph NH_4^+ levels in larval and adult *A. aegypti* are upwards of 1 mmol l^{-1} (Chasiotis et al., 2016; Chapter 7), so the sugar-fed phase of adult females and a brief (24

hour) starvation period of larvae in the present study may explain the observations of NH_4^+ absorption at the rectum to maintain physiologically required levels of ammonia.

Conclusions

The current study has provided the groundwork for further study on ammonia transport within the excretory organs in both *A. aegypti* larvae and adult females. Findings from this work have implicated the MT and HG as key sites for ammonia transport and nitrogen regulation. Transcriptomic analyses of the larval rectum have revealed the presence of key ion channels, transporters, and enzymes involved in ion and water homeostasis, ammonia formation, and the formation of nitrogenous waste products. Collectively, these data also present the first molecular and physiological characterization of Rh protein expression and function within the excretory organs of *Aedes aegypti*, and our findings suggest that these transporters are important candidates in mediating ammonia transport across the epithelia of the MT and HG to be excreted. The expression of Rh protein, likely *AeRh50-1*, was also localized within ovarian cells of adult females and the role of these Rh proteins in egg maturation and more broadly, in reproduction, is worth pursuing. Incidentally, these preliminary findings further prompted us to examine the role of ammonia transporters (Amt and Rh proteins) in reproductive processes in adult *A. aegypti* (see Chapter 7).

6.6 References

Adlimoghaddam, A., Boeckstaens, M., Marini, A.-M., Treberg, J. R., Brassinga, A.-K. C. and Weihrauch, D. (2015). Ammonia excretion in *Caenorhabditis elegans*: mechanism and evidence of ammonia transport of the Rhesus protein CeRhr-1. *J. Exp. Biol.* **218**, 675–683.

Ballantyne, J. S. (2001). Amino acid metabolism. In *Nitrogen Excretion*, pp. 77–107. Academic Press.

Barrera, R., Amador, M., Diaz, A., Smith, J., Munoz-Jordan, J. L. and Rosario, Y. (2008). Unusual productivity of *Aedes aegypti* in septic tanks and its implications for dengue control. *Med. Vet. Entomol.* **22**, 62–69.

Bender, D. A. (2012). The metabolism of "surplus" amino acids. *Br. J. Nutr.* **108**, S113–S121.

Benoit, J. B. and Denlinger, D. L. (2010). Meeting the challenges of on-host and off-host water balance in blood-feeding arthropods. *J. Insect Physiol.* **56**, 1366–1376.

Biver, S., Belge, H., Bourgeois, S., Van Vooren, P., Nowik, M., Scohy, S., Houillier, P., Szpirer, J., Szpirer, C., Wagner, C. A., et al. (2008). A role for Rhesus factor Rhcg in renal ammonium excretion and male fertility. *Nature* **456**, 339–343.

Bradley, T. J. (1987). Physiology of osmoregulation in mosquitoes. *Annu. Rev. Entomol.* **32**, 439–462.

Bradley, T. J. and Philips, J. E. (1977). Regulation of rectal secretion in saline-water mosquito larvae living in waters of diverse ionic composition. *J. Exp. Biol.* **66**, 83 LP – 96.

Briegel, H. (1986). Protein catabolism and nitrogen partitioning during oogenesis in the mosquito *Aedes aegypti*. *J. Insect Physiol.* **32**, 455–462.

Browne, A. and O'Donnell, M. J. (2013). Ammonium secretion by Malpighian tubules of *Drosophila*

melanogaster: Application of a novel ammonium-selective microelectrode. *J. Exp. Biol.* **216**, 3818–3827.

Burke, R. L., Barrera, R., Lewis, M., Kluchinsky, T. and Claborn, D. (2010). Septic tanks as larval habitats for the mosquitoes *Aedes aegypti* and *Culex quinquefasciatus* in Playa-Playita, Puerto Rico. *Med. Vet. Entomol.* **24**, 117–123.

Bursell, E. (1967). The Excretion of Nitrogen in Insects. In (ed. Beament, J. W. L.), Treherne, J. E.), and Wigglesworth, V. B. B. T.-A. in I. P.), pp. 33–67. Academic Press.

Chamberlin, M. E. and Phillips, J. E. (1983). Oxidative metabolism in the locust rectum. *J. Comp. Physiol. B* **151**, 191–198.

Chasiotis, H. and Kelly, S. P. (2008). Occludin immunolocalization and protein expression in goldfish. *J. Exp. Biol.* **211**, 1524–1534.

Chasiotis, H., Ionescu, A., Misyura, L., Bui, P., Fazio, K., Wang, J., Patrick, M., Weihrauch, D. and Donini, A. (2016). An animal homolog of plant Mep/Amt transporters promotes ammonia excretion by the anal papillae of the disease vector mosquito *Aedes aegypti*. *J. Exp. Biol.* **219**, 1346–55.

Chitolina, R. F., Anjos, F. A., Lima, T. S., Castro, E. A. and Costa-Ribeiro, M. C. V. (2016). Raw sewage as breeding site to *Aedes (Stegomyia) aegypti* (Diptera, culicidae). *Acta Trop.* **164**, 290–296.

Christophers, R. (1960). *Aedes aegypti, the Yellow Fever Mosquito: Its Life History Bionomics and Structure.* London: Cambridge University Press.

Clark, T. M. (2004). pH tolerances and regulatory abilities of freshwater and euryhaline Aedine mosquito larvae. *J. Exp. Biol.* **207**, 2297–2304.

Clark, T. M., Vieira, M. A. L., Huegel, K. L., Flury, D. and Carper, M. (2007). Strategies for regulation of haemolymph pH in acidic and alkaline water by the larval mosquito *Aedes aegypti* (L.) (Diptera; Culicidae). *J. Exp. Biol.* **210**, 4359–4367.

Clements, A. N. (1992). *The biology of mosquitoes, Vol. I; Development, nutrition and reproduction*. London: Elsevier.

Cruz, M. J., Sourial, M. M., Treberg, J. R., Fehsenfeld, S., Adlimoghaddam, A. and Weihrauch, D. (2013). Cutaneous nitrogen excretion in the African clawed frog *Xenopus laevis*: Effects of high environmental ammonia (HEA). *Aquat. Toxicol.* **136**–**137**, 1–12.

D'Silva, N. M., Patrick, M. L. and O'Donnell, M. J. (2017). Effects of rearing salinity on expression and function of ion-motive ATPases and ion transport across the gastric caecum of *Aedes aegypti* larvae . *J. Exp. Biol.* **220**, 3172–3180.

Del Duca, O., Nasirian, A., Galperin, V. and Donini, A. (2011). Pharmacological characterisation of apical Na^+ and Cl^- transport mechanisms of the anal papillae in the larval mosquito *Aedes aegypti*. *J. Exp. Biol.* **214**, 3992–3999.

Dixon, D., Van Ekeris, L. and Linser, P. (2017). Characterization of carbonic anhydrase 9 in the alimentary canal of *Aedes aegypti* and its relationship to homologous mosquito carbonic anhydrases. *Int. J. Environ. Res. Public Health* **14**, 213.

Donini, A. and O'Donnell, M. J. (2005). Analysis of Na^+, Cl^-, K^+, H^+ and NH_4^+ concentration gradients adjacent to the surface of anal papillae of the mosquito *Aedes aegypti*: application of self-referencing ion-selective mi. *J. Exp. Biol.* **208**, 603–10.

Donini, A., Patrick, M. L., Bijelic, G., Christensen, R. J., Ianowski, J. P., Rheault, M. R. and O'Donnell, M. J. (2006). Secretion of water and ions by malpighian tubules of larval mosquitoes:

effects of diuretic factors, second messengers, and salinity. *Physiol. Biochem. Zool.* **79**, 645–55.

Doverskog, M., Jacobsson, U., Chapman, B. E., Kuchel, P. W. and Häggström, L. (2000). Determination of NADH-dependent glutamate synthase (GOGAT) in *Spodoptera frugiperda* (Sf9) insect cells by a selective 1H/15N NMR in vitro assay. *J. Biotechnol.* **79**, 87–97.

Durant, A. C. and Donini, A. (2018a). Ammonia excretion in an osmoregulatory syncytium is facilitated by AeAmt2, a novel ammonia transporter in *Aedes aegypti* larvae. *Front. Physiol.* **9**,.

Durant, A. C. and Donini, A. (2018b). Evidence that Rh proteins in the anal papillae of the freshwater mosquito *Aedes aegypti* are involved in the regulation of acid–base balance in elevated salt and ammonia environments . *J. Exp. Biol.* **221**, jeb186866.

Durant, A. C. and Donini, A. (2019). Development of *Aedes aegypti* (Diptera: Culicidae) mosquito larvae in high ammonia sewage in septic tanks causes alterations in ammonia excretion, ammonia transporter expression, and osmoregulation. *Sci. Rep.* **9**, 1–17.

Durant, A. C. and Donini, A. (2020). Ammonium transporter expression in sperm of the disease vector *Aedes aegypti* mosquito influences male fertility. *Proc. Natl. Acad. Sci.* **117**, 29712–29719.

Durant, A. C., Chasiotis, H., Misyura, L. and Donini, A. (2017). *Aedes aegypti* Rhesus glycoproteins contribute to ammonia excretion by larval anal papillae. *J. Exp. Biol.* **220**, 588–596.

Glover, C. N., Bucking, C. and Wood, C. M. (2013). The skin of fish as a transport epithelium: A review. *J. Comp. Physiol. B Biochem. Syst. Environ. Physiol.* **183**, 877–891.

Goecks, J., Nekrutenko, A., Taylor, J. and Galaxy Team, T. (2010). Galaxy: a comprehensive approach for supporting accessible, reproducible, and transparent computational research in the life sciences. *Genome Biol.* **11**, R86.

Hirayama, C., Konno, K. and Shinbo, H. (1997). The pathway of ammonia assimilation in the silkworm, *Bombyx mori*. *J. Insect Physiol.* **43**, 959–964.

Hirayama, C. and Nakamura, M. (2002). Regulation of glutamine metabolism during the development of *Bombyx mori* larvae. *Biochim. Biophys. Acta - Gen. Subj.* **1571**, 131–137.

Hu, M. and Tseng, Y.-C. (2017). Acid--base regulation and ammonia excretion in cephalopods: an ontogenetic overview. In *Acid-Base Balance and Nitrogen Excretion in Invertebrates: Mechanisms and Strategies in Various Invertebrate Groups with Considerations of Challenges Caused by Ocean Acidification* (ed. Weihrauch, D.) and O'Donnell, M.), pp. 275–298. Cham: Springer International Publishing.

Ip, Y. K. and Chew, S. F. (2010). Ammonia production, excretion, toxicity, and defense in fish: A review. *Front. Physiol.* **1 OCT**, 1–20.

Isoe, J. and Scaraffia, P. Y. (2013). Urea Synthesis and Excretion in *Aedes aegypti* Mosquitoes Are Regulated by a Unique Cross-Talk Mechanism. *PLoS One* **8**, e65393.

Jonusaite, S., Kelly, S. P. and Donini, A. (2013a). Tissue-specific ionomotive enzyme activity and K^+ reabsorption reveal the rectum as an important ionoregulatory organ in larval *Chironomus riparius* exposed to varying salinity. *J. Exp. Biol.* **216**, 3637–3648.

Jonusaite, S., Kelly, S. P. and Donini, A. (2013b). Tissue-specific ionomotive enzyme activity and K^+ reabsorption reveal the rectum as an important ionoregulatory organ in larval *Chironomus riparius* exposed to varying salinity. *J. Exp. Biol.* **216**, 3637–3648.

Kolosov, D. and O'Donnell, M. J. (2019). Malpighian tubules of caterpillars: blending RNAseq and physiology to reveal regional functional diversity and novel epithelial ion transport control mechanisms. *J. Exp. Biol.* **222**, jeb211623.

Lajevardi, A. and Paluzzi, J.-P. V (2020). Receptor characterization and functional activity of pyrokinins on the hindgut in the adult mosquito, *Aedes aegypti*. *Front. Physiol.* **11**,.

Martinelle, K. and Häggström, L. (1993). Mechanisms of ammonia and ammonium ion toxicity in animal cells: Transport across cell membranes. *J. Biotechnol.* **30**, 339–350.

Mccormick, S. D. (1993). Methods for non biopsy and measurement of Na^+, K^+-ATPase activity. *Can. J. Aquat. Sci.* **50**, 9–11.

Meredith, J. and Phillips, J. E. (1973). Rectal ultrastructure in salt- and freshwater mosquito larvae in relation to physiological state. *Zeitschrift fur Zellforsch. und mikroskopische Anat.* **138**, 1–22.

Merrick, M. J. and Edwards, R. A. (1995). Nitrogen control in bacteria. *Microbiol. Rev.* **59**, 604–622.

Misyura, L., Yerushalmi, G. Y. and Donini, A. (2017). A mosquito entomoglyceroporin, *Aedes aegypti* AQP5, participates in water transport across the Malpighian tubules of larvae . *J. Exp. Biol.* **220**, 3536–3544.

Nayar, J. K. and Sauerman, D. M. (1975a). The effects of nutrition on survival and fecundity in florida mosquitoes: Part 2. Utilization of a blood meal for survival. *J. Med. Entomol.* **12**, 99–103.

Nayar, J. K. and Sauerman, D. M. (1975b). The effects of nutrition on survival and fecundity in Florida mosquitoes Part 3. Utilization of blood and sugar for fecundity. *J. Med. Entomol.* **12**, 220–225.

O'Donnell, M. J. and Donini, A. (2017). Nitrogen excretion and metabolism in insects. In *Acid-Base Balance and Nitrogen Excretion in Invertebrates* (ed. Weihrauch, D.) and O'Donnell, M. J.), pp. 109–126. Springer International Publishing Switzerland.

Paluzzi, J. P., Vanderveken, M. and O'Donnell, M. J. (2014). The heterodimeric glycoprotein

hormone, GPA2/GPB5, regulates ion transport across the hindgut of the adult mosquito, *Aedes aegypti*. *PLoS One* **9**, e86386.

Patrick, M. L., Aimanova, K., Sanders, H. R. and Gill, S. S. (2006). P-type Na^+/K^+-ATPase and V-type H^+-ATPase expression patterns in the osmoregulatory organs of larval and adult mosquito *Aedes aegypti*. *J. Exp. Biol.* **209**, 4638–4651.

Pennington, J. E., Goldstrohm, D. A. and Wells, M. A. (2003). The role of haemolymph proline as a nitrogen sink during blood meal digestion by the mosquito *Aedes aegypti*. *J. Insect Physiol.* **49**, 115–121.

Pfaffl, M. (2004). Quantification strategies in real-time PCR. *A-Z Quant. PCR* 87–112.

Phillips, J. (1981). Comparative physiology of insect renal function. *Am. J. Physiol. Integr. Comp. Physiol.* **241**, R241–R257.

Piermarini, P. M., Rouhier, M. F., Schepel, M., Kosse, C. and Beyenbach, K. W. (2013). Cloning and functional characterization of inward-rectifying potassium (Kir) channels from Malpighian tubules of the mosquito *Aedes aegypti*. *Insect Biochem. Mol. Biol.* **43**, 75–90.

Piermarini, P. M., Dunemann, S. M., Rouhier, M. F., Calkins, T. L., Raphemot, R., Denton, J. S., Hine, R. M. and Beyenbach, K. W. (2015). Localization and role of inward rectifier K^+ channels in Malpighian tubules of the yellow fever mosquito *Aedes aegypti*. *Insect Biochem. Mol. Biol.* **67**, 59–73.

Piermarini, P. M., Akuma, D. C., Crow, J. C., Jamil, T. L., Kerkhoff, W. G., Viel, K. C. M. F. and Gillen, C. M. (2017). Differential expression of putative sodium-dependent cation-chloride cotransporters in *Aedes aegypti*. *Comp. Biochem. Physiol. -Part A Mol. Integr. Physiol.* **214**, 40–49.

Pitts, R. J., Derryberry, S. L., Pulous, F. E. and Zwiebel, L. J. (2014). Antennal-expressed ammonium transporters in the malaria vector mosquito *Anopheles gambiae*. *PLoS One* **9**,.

Quijada-Rodriguez, A. R., Treberg, J. R. and Weihrauch, D. (2015). Mechanism of ammonia excretion in the freshwater leech *Nephelopsis obscura*: characterization of a primitive Rh protein and effects of high environmental ammonia. *Am. J. Physiol. Regul. Integr. Comp. Physiol.* ajpregu.00482.2014.

Ramsay, J. A. (1950). Osmotic regulation in mosquito larvae. *J. Exp. Biol.* **27**, 145.

Ramsay, J. A. (1951). Osmotic regulation in mosquito larvae: the role of the Malpighian tubules. *J. Exp. Biol.* **28**, 62–73.

Randall, D. J. and Ip, Y. K. (2006). Ammonia as a respiratory gas in water and air-breathing fishes. *Respir. Physiol. Neurobiol.* **154**, 216–225.

Randall, D. J. and Tsui, T. K. N. (2002). Ammonia toxicity in fish.pdf. *Mar. Pollut. Bull.* **45**, 17–23.

Rouhier, M. F., Raphemot, R., Denton, J. S. and Piermarini, P. M. (2014). Pharmacological validation of an inward-rectifier potassium (Kir) channel as an insecticide target in the Yellow Fever Mosquito *Aedes aegypti*. *PLoS One* **9**, e100700.

Scaraffia, P. Y., Isoe, J., Murillo, A. and Wells, M. A. (2005). Ammonia metabolism in *Aedes aegypti*. *Insect Biochem. Mol. Biol.* **35**, 491–503.

Scaraffia, P. Y., Zhang, Q., Wysocki, V. H., Isoe, J. and Wells, M. A. (2006). Analysis of whole body ammonia metabolism in *Aedes aegypti* using [15N]-labeled compounds and mass spectrometry. *Insect Biochem. Mol. Biol.* **36**, 614–622.

Scaraffia, P. Y., Tan, G., Isoe, J., Wysocki, V. H., Wells, M. A. and Miesfeld, R. L. (2008). Discovery of an alternate metabolic pathway for urea synthesis in adult *Aedes aegypti* mosquitoes.

Proc. Natl. Acad. Sci. **105**, 518–523.

Scaraffia, P. Y., Zhang, Q., Thorson, K., Wysocki, V. H. and Miesfeld, R. L. (2010). Differential ammonia metabolism in *Aedes aegypti* fat body and midgut tissues. *J. Insect Physiol.* **56**, 1040–1049.

Stobbart, R. H. (1967). The effect of some anions and cations upon the fluxes and net uptake of chloride in the larva of *Aedes aegypti* (L.) and the nature of the uptake mechanisms for sodium and chloride. *J. Exp. Biol.* **47**, 35–57.

Thomson, R. B., Thomson, J. M. and Phillips, J. E. (1988). NH_4^+ transport in acid-secreting insect epithelium. *Am. J. Physiol. - Regul. Integr. Comp. Physiol.* **254**,.

Von Dungern, P. and Briegel, H. (2001). Protein catabolism in mosquitoes: Ureotely and uricotely in larval and imaginal *Aedes aegypti*. *J. Insect Physiol.* **47**, 131–141.

Wang, F., Flanagan, J., Su, N., Wang, L.-C., Bui, S., Nielson, A., Wu, X., Vo, H.-T., Ma, X.-J. and Luo, Y. (2012). A novel in situ RNA analysis platform for formalin-fixed,paraffin-embedded tissues. *J. Mol. Diagnostics* **14**, 22–29.

Weihrauch, D. (2006). Active ammonia absorption in the midgut of the Tobacco hornworm *Manduca sexta* L.: Transport studies and mRNA expression analysis of a Rhesus-like ammonia transporter. *Insect Biochem. Mol. Biol.* **36**, 808–821.

Weihrauch, D. and Allen, G. J. P. (2018). Ammonia excretion in aquatic invertebrates: new insights and questions. *J. Exp. Biol.* **221**, 1–11.

Weihrauch, D. and O'Donnell, M. J. (2015). Links between osmoregulation and nitrogen-excretion in insects and crustaceans. *Integr. Comp. Biol.* **55**, 816–829.

Weihrauch, D., Morris, S. and Towle, D. W. (2004). Ammonia excretion in aquatic and terrestrial

crabs. *J. Exp. Biol.* **207**, 4491–4504.

Weihrauch, D., Donini, A. and O'Donnell, M. J. (2012a). Ammonia transport by terrestrial and aquatic insects. *J. Insect Physiol.* **58**, 473–487.

Weihrauch, D., Chan, a. C., Meyer, H., Doring, C., Sourial, M. and O'Donnell, M. J. (2012b). Ammonia excretion in the freshwater planarian *Schmidtea mediterranea*. *J. Exp. Biol.* **215**, 3242–3253.

Weiner, I. D. and Hamm, L. L. (2007). Molecular mechanisms of renal ammonia transport. *Annu. Rev. Physiol.* **69**, 317–340.

Wright, P. A. and Wood, C. M. (2009). A new paradigm for ammonia excretion in aquatic animals: role of Rhesus (Rh) glycoproteins. *J. Exp. Biol.* **212**, 2303–12.

Wu, Y., Zheng, X., Zhang, M., He, A., Li, Z. and Zhan, X. (2010). Cloning and functional expression of Rh50-like glycoprotein, a putative ammonia channel, in *Aedes albopictus* mosquitoes. *J. Insect Physiol.* **56**, 1599–1610.

Ye, Z., Liu, F., Sun, H., Barker, M., Pitts, R. J. and Zwiebel, L. J. (2020). Heterogeneous expression of the ammonium transporter AgAmt in chemosensory appendages of the malaria vector, *Anopheles gambiae*. *Insect Biochem. Mol. Biol.* **120**,.

Zhou, G., Flowers, M., Friedrich, K., Horton, J., Pennington, J. and Wells, M. A. (2004). Metabolic fate of [14C]-labeled meal protein amino acids in *Aedes aegypti* mosquitoes. *J. Insect Physiol.* **50**, 337–349.

Chapter Seven

Ammonium transporter expression in sperm of the disease-vector *Aedes aegypti* mosquito influences male fertility

This chapter has been published and reproduced with permission:

Durant A.C., Donini A. (2020) Ammonium transporter expression in sperm of the disease-vector *Aedes aegypti* mosquito influences male fertility. *Proceedings of the National Academy of Sciences U.S.A.* 117(47) 29712-29719.

7.1 Summary

The ammonium transporter (AMT)/methylammonium permease (MEP)/Rhesus glycoprotein (Rh) family of ammonia (NH_3/NH_4^+) transporters have been identified in organisms from all domains of life. In animals, fundamental roles for AMT and Rh proteins in the specific transport of ammonia across biological membranes to mitigate ammonia toxicity and aiding in osmoregulation, acid-base balance, and excretion, has been well documented. Here, we observed enriched *Amt* (*AeAmt1*) mRNA levels within reproductive organs of the arboviral vector mosquito, *Aedes aegypti* prompting us to explore the role of AMTs in reproduction. We show that AeAmt1 is localized to sperm flagella during all stages of spermiogenesis and spermatogenesis in male testes. AeAmt1 expression in sperm flagella persists in spermatozoa that navigate the female reproductive tract following insemination and are stored within the spermathecae, as well as throughout sperm migration along the spermathecal ducts during ovulation to fertilize the descending egg. We demonstrate that RNAi-mediated AeAmt1 protein knockdown leads to significant reductions (~40%) of spermatozoa stored in seminal vesicles of males, resulting in decreased egg viability when these males inseminate non-mated females. We suggest that AeAmt1 function in spermatozoa is to protect against ammonia toxicity, based on our observations of high NH_4^+ levels in the densely packed spermathecae of mated females. The presence of AMT proteins, in addition to Rh proteins, across insect taxa may indicate a conserved function for AMTs in sperm viability and reproduction, in general.

7.2 Introduction

Ammonium transporters (AMT), methylammonium permeases (MEP), and Rhesus glycoproteins (Rh proteins) comprise a protein family with three clades, and homologues from each have been identified in virtually all domains of life (McDonald et al., 2012). AMT proteins were first identified in plants (Ninnemann et al., 1994) with the simultaneous discovery of MEP proteins in fungi (Marini et al., 1994), followed by Rh proteins in humans (Marini et al., 1997b). Ammonia (NH_3/ NH_4^+) is vital for growth in plants and microorganisms, and is retained in some animals for use as an osmolyte (Smith, 1936; Wood et al., 1995b), for buoyancy (Clarke et al., 1979; Seibel et al., 2004), and for those lacking sufficient dietary nitrogen(Weihrauch, 2006). In the majority of animals, however, ammonia is the toxic by-product of amino acid and nucleic acid metabolism and accordingly requires efficient mechanisms for its regulation, transport, and excretion (Ip and Chew, 2010; Randall and Tsui, 2002; Weiner and Verlander, 2017; Wright, 1995a). AMT, MEP, and Rh proteins are responsible for the selective movement of ammonia (NH_3) or ammonium (NH_4^+) across biological membranes, a process that all organisms require. Unlike their vertebrate, bacterial, and fungal counterparts which function as putative NH_3 gas channels (Khademi et al., 2004; Mayer et al., 2006; Soupene et al., 1998; Wu et al., 2010a; Zheng et al., 2004), a myriad of evidence suggests that plant AMT proteins and closely related members in some animals are functionally distinct and facilitate electrogenic ammonium (NH_4^+) transport (Ludewig et al., 2002; Mayer et al., 2006; McDonald and Ward, 2016b; Neuhäuser and Ludewig, 2014; Pitts et al., 2014). In contrast to vertebrates which only possess Rh proteins (Peng and Huang, 2006), many invertebrates are unique in that they express both AMT and Rh proteins, sometimes in the same cell (O'Donnell and Donini, 2017; Weihrauch and Allen, 2018b; Weihrauch and O'Donnell, 2015; Weihrauch et al., 2004; Weihrauch et al., 2012a). Among insects, the presence of both AMT and Rh proteins has been described in *Drosophila melanogaster* (Lecompte et al., 2019; Menuz et al., 2014) and mosquitoes that vector disease-causing pathogens, *Anopheles gambiae* (Pitts et al., 2014; Ye et al., 2020) and *Aedes aegypti* (Chasiotis et al., 2016; Chapter 3). It is unclear if, in

these instances, AMT and Rh proteins can functionally substitute for one another but, in the anal papillae of *A. aegypti* larvae, knockdown of either Amt or Rh proteins causes decreases in ammonia transport suggesting that they do not (Chasiotis et al., 2016; Chapter 3; Chapter 2). To date, studies on ammonia transporter (AMT and Rh) function in insects have focused on ammonia sensing and tasting in sensory structures (Delventhal et al., 2017; Menuz et al., 2014; Pitts et al., 2014; Ye et al., 2020), ammonia detoxification and acid-base balance in muscle, digestive, and excretory organs (Chapter 4; Wu et al., 2010), and ammonia excretion in a variety of organs involved in ion and water homeostasis (Chasiotis et al., 2016; Chapter 3; Chapter 2; Weihrauch, 2006; Weihrauch et al., 2012). *A. aegypti* is the primary vector for the transmission of human arboviral diseases Zika, yellow fever, chikungunya, and dengue virus which are of global health concern due to rapid increases in the geographical distribution of this species, presently at its highest ever (Kraemer et al., 2015; Leta et al., 2018). In light of the well documented evolution of insecticide resistance in mosquitoes (Hemingway et al., 2002; Smith et al., 2016; Vontas et al., 2012; Weill et al., 2003), more recent methods to control disease transmission such as the sterile insect technique (SIT) (Benedict and Robinson, 2003), trans-infection and sterilization of mosquitoes with the bacterium *Wolbachia* (Iturbe-Ormaetxe et al., 2011), and targeted genome editing rendering adult males sterile (Kandul et al., 2019) have proven effective. These methods take advantage of various aspects of mosquito reproductive biology, however, an understanding of male reproductive biology and the male contributions to female reproductive processes is still in its infancy (Degner and Harrington, 2016). Here, we describe the expression of an *A. aegypti* ammonium transporter (AeAmt1) in the sperm during all stages of spermatogenesis, spermiogenesis, and egg fertilization, which is critical for fertility.

7.3 Materials and Methods

Immunolocalization and western blotting of AeAmt1

For immunohistological studies, whole adult male and female *A. aegypti* (7-10 days post emergence) were fixed in Bouin's solution at room temperature overnight. Fixed animals were further processed (dehydrated), paraffin-embedded, and sectioned (5 μm thick) following an established protocol (Chasiotis and Kelly, 2008). Tissue sections were placed on VistaVision HistoBond adhesive microscope slides (VWR International, Mississauga, Ontario). Immunohistochemical localization of AeAmt1 was carried out using a 1:40 (7.46×10^{-04} μg μL^{-1}) dilution of a custom-made polyclonal antibody produced in rabbit, which has been outlined in detail (Chasiotis et al., 2016). For control slides, anti-AeAmt1 antibody was incubated with 20 × molar excess of immunogenic peptide for 1 hour at room temperature prior to application. To visualize the mitochondrial derivatives that are found along the entire length of the flagellum of isolated spermatozoa, seminal vesicles dissected from adult males were incubated in MitoTracker Red CMXRos at a 100nM dilution (Invitrogen, Carlsbad, CA, USA) in phosphate-buffered saline (PBS) for 2 hours at room temperature (Rocco et al., 2019). Seminal vesicles were then fixed in 4% paraformaldehyde for 2 hours and were then gently pressed onto a microscope slide using a coverslip to release the spermatozoa. Slides were mounted using ProLong Gold antifade reagent with DAPI (Life Technologies, Burlington, ON, Canada). Western blotting of AeAmt1 was carried out following a previously published protocol (Chasiotis et al., 2016). For assessment of AeAmt1 dsRNA-mediated protein knockdown (see below) in males, 3 biological replicates consisting of whole animal tissues from 10 males per replicate were processed. To examine AeAmt1 protein abundance in spermathecae from non-mated and mated females, isolated spermatheca (3 per animal) were pooled from 15-20 animals per replicate.

dsRNA synthesis and microinjection

AeAmt1 and control *β-lactamase* dsRNA was synthesized using the Promega T7 RiboMAX Express RNAi kit (Promega, WI, USA) following a published protocol (Chasiotis et al., 2016). Isolated male and female (2-3 days for males, and 5-7 days for females, post emergence) were briefly anaesthetized using CO_2. Males were injected with 150 nL (510 ng) and females were injected with 200 nL (680ng) of *AeAmt1* or control *β-lactamase* dsRNA diluted in PCR-grade water using a Nanojet III Programmable Nanoliter Injector (Drummond Scientific Company, Broomall, PA, USA). dsRNA was injected dorsally into the thorax of mosquitoes.

Sperm quantification and ammonium [NH_4^+] measurements in spermathecae

Sperm quantification in the paired seminal vesicles of male *A. aegypti* at 24 hours post dsRNA injection was performed following a published protocol, with minor modifications (Ponlawat and Harrington, 2007). The seminal vesicles were isolated from individual males, placed in 100 µl PBS, and were gently torn open using extra-fine forceps under a dissecting microscope (Carl Zeiss Canada, Toronto, ON) to release spermatozoa. An additional 10 µl PBS was used to rinse the forceps and the PBS with spermatozoa was mixed thoroughly using a P100 pipette. Immediately after mixing for each animal, five 1 µL droplets of the mixture were spotted onto a microscope slide, allowed to air dry, and were fixed with 70% ethanol. Slides were mounted using ProLong Gold antifade reagent with DAPI (Life Technologies, Burlington, ON, Canada) and nuclei of spermatozoa within each 1 µL droplet was imaged under 4× magnification using an Olympus IX81 inverted microscope (Olympus Canada, Richmond Hill, ON, Canada). The nuclei of spermatozoa in each 1 µL droplet were counted using ImageJ software (ImageJ ver.1.51J8, National Institutes of Health, USA), averaged across all 5 droplets for each animal, and multiplied by the dilution factor to determine total spermatozoa counts within the seminal vesicle. Free ammonium (NH_4^+) concentrations were measured using a liquid membrane ion-selective microelectrode that was constructed using a detailed protocol (Donini and O'Donnell, 2005).

The 3 spermathecae from female *A. aegypti* were isolated under physiological saline (Petzel et al., 1987), pooled together and transferred to a 0.5 µl droplet of saline submerged in hydrated paraffin oil, and carefully punctured with an extra-fine forcep to release contents into the droplet. Droplets were held in paraffin oil for no longer than 15 minutes before NH_4^+ measurements were made. Estimations of undiluted [NH_4^+] in spermathecae stated in the text were calculated by taking into account the volume of the spermathecae (60 µM diameter for the lateral lobes, 70 µM diameter for the large, median lobe), the dilution factor of the 3 spermathecae when punctured (in 0.5 µL physiological saline) and subtracting the background [NH_4^+] concentration in droplets of physiological saline submerged under paraffin oil (~0.538 mM).

Mating and egg-laying assays

Pupae of *A. aegypti* (Liverpool) were acquired from a colony reared in the Department of Biology, York University (Toronto, ON, Canada) and were used for all experiments (Chasiotis et al., 2016). Female *A. aegypti* of this colony were blood-fed twice weekly with sheep blood in Alsever's solution (Cedarlane Laboratories, Hornby, ON, Canada). Groups of male and female *A. aegypti* were separated at the pupal stage (identified by sexual dimorphisms in pupal size) and placed in BugDorm-5 insect boxes (MegaView Science Co, Taiwan) with 20% sucrose solution where the adults emerged. For experimental analyses of mated females, a 1:1 ratio of male and female pupae was collected and reared in the same insect boxes as described above. This study employed two different mating assays protocols; [**1**] *AeAmt1* dsRNA-knockdown males that were mated with non-mated females, and [**2**] AeAmt1 dsRNA-knockdown females that were mated with non-mated males prior to dsRNA injection. For protocol [**1**], dsRNA-injected males were placed with non-mated females (2:1 ratio of male:female per insect box) between 18-24 hours post dsRNA injection. After 24 hours, females were provided a blood meal. For protocol [**2**], mated females were separated from males and injected with dsRNA. After 48 hours, females were provided a blood meal. For both mating protocols [**1**] and [**2**], females

were given 20 minutes to blood feed and all blood-fed females were subsequently isolated individually in inverted 25 cm^2 cell culture flasks (Corning, NY, USA) containing 3mL of dH_2O from larvae rearing containers (to entice egg laying) lined with filter paper (Rocco et al., 2019). Laid eggs were collected after 4 days and were semi-desiccated for 48 hours and then counted. Spermathecae were dissected from females and viewed under a microscope to confirm insemination occurred, and any non-mated females were excluded from experimental analyses. Eggs were placed in 20 mL of dH2O with 0.5mL larval food (1:1 ratio of liver powder and inactive yeast) and hatchlings were counted after 48 hours.

Statistics

All statistical analyses were performed using the GraphPad Prism software, and the critical level was taken as $p = 0.05$. The appropriate statistical test used for each experimental analysis is indicated in the figure caption with corresponding *p-values*. Power analyses were performed on all datasets which yielded a minimum statistical power of 0.80 with the given sample sizes and variances of each group.

7.4 Results and Discussion

AeAmt1 is Expressed During All Stages of Spermatogenesis and Spermiogenesis

Previous characterizations of ammonia transporters (AMT and Rh proteins) in reproductive tissues in the context of male reproductive biology and fertility are scarce and come from vertebrate models (Biver et al., 2008; Lee et al., 2013). In the mosquito *Aedes albopictus*, Rh protein (*AalRh50*) transcript is expressed at modest levels in ovary tissue of adult females and is unaltered following blood feeding (Wu et al., 2010a). Given our previous characterizations of AMT proteins (AeAmt1 and AeAmt2) in *A. aegypti* larvae which are expressed in organs important for ion and water balance and digestion (Chasiotis et al., 2016; Chapter 3; Chapter 5), we speculated that AeAmt1 and AeAmt2 would play functionally similar roles in digestive and excretory organs in adults, particularly following ingestion of a protein-rich blood meal by females. To examine this hypothesis, we utilized

immunohistological techniques with previously validated AeAmt antibodies (Chasiotis et al., 2016; Chapter 3). To our surprise, our results demonstrate that AeAmt1 protein is immunolocalized almost exclusively to the reproductive organs of both male and mated, sugar-fed female *A. aegypti* (Fig. 7-1). In a longitudinal section of a mature testis follicle from male *A. aegypti*, AeAmt1 is expressed in primary spermatogonia (germ cells), primary spermatocytes, spermatids, and spermatozoa (Fig 7-1a). In early stages of spermatogenesis, AeAmt1 localizes to regions consistent with mitochondria found near the centriole which in later stages stretches alongside axial filament formation within the flagella (Engelmann, 2015). Live cell staining of mitochondrial derivatives that localize to the full length of the flagella of mature spermatozoa (Fig 7-1b, (Rocco et al., 2019)) shows a similar localization pattern to observed AeAmt1 staining along the length of the flagellum of a mature spermatozoa (Fig. 7-1c-d). Interestingly, AeAmt1 immunostaining appears to be absent within the centriole adjunct (Fig. 7-1d, red arrow), a structure located between the nuclei and flagella of spermatozoa and implicated in proper flagellar development (Rocco et al., 2019).

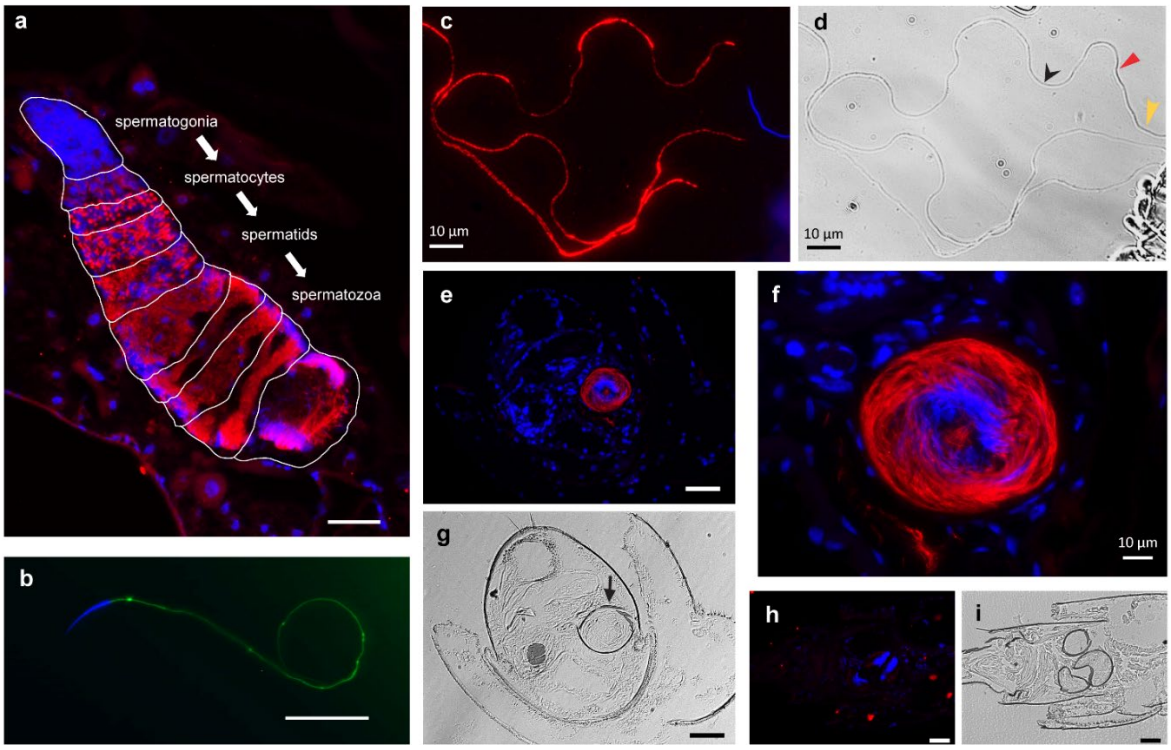

Figure 7- 1. AeAmt1 protein localization in male testes and spermatozoa stored within the spermathecae of female *Aedes aegypti*. (**a**) AeAmt1 (red) immunolocalization in a longitudinal section of a testis counterstained for nuclei (blue; DAPI). Zones of different stages of spermatogenesis, from primary spermatogonia (germ cells) to mature spermatozoa are indicated (white labels). (**b**) High magnification image of a single spermatozoa showing the nucleus (blue; DAPI) and the mitochondrial derivatives along the length of the flagellum (green; MitoTracker). (**c**) High magnification image of AeAmt1 (red) localization counterstained for nuclei (blue; DAPI) in mature spermatozoa isolated from the testis, and (**d**) corresponding brightfield image to panel **C** indicating the flagellum (black arrow), nucleus (yellow arrow), and region of the centriole adjunct (red arrow). (**e**) AeAmt1 (red) localization in a transverse section of spermathecae from mated female *A. aegypti* counterstained for nuclei (blue; DAPI), and (**f**) higher magnification image of AeAmt1 (red) and nuclei (blue; DAPI) immunolocalization in spermatozoa from a single spermatheca of mated female *A. aegypti* from panel **E**. (**g**) The corresponding bright field image to panel **E** indicating the sperm-filled spermatheca (black arrow). (**h**) Control slide (anti-AeAmt1 preincubated with 20x molar excess of AeAmt1-specific peptide) and (**i**) bright field image corresponding to (h). Scale bars are 50 µm, unless indicated otherwise.

In mated, sugar-fed females, AeAmt1 protein was immunolocalized to the spermathecae (Fig. 7-1e-g), and this immunostaining was absent when the AeAmt1 antibody was pre-absorbed with 20 × molar excess of AeAmt1 immunogenic peptide prior to application to tissue sections (Fig. 7-1h-i). High magnification images of spermathecae filled with spermatozoa reveal a similar flagellar-like AeAmt1 staining pattern as was observed in the mature spermatozoa within the male testis. The spermathecae are spherical reservoirs for spermatozoa in females, consisting of a cuticular lining surrounded by epithelial cells and glandular cells associated with the entrance of the spermathecal duct (Clements and Potter, 1967; Pascini et al., 2012). Our findings are consistent with those of other *Aedine* species in that only the largest, median spermatheca and one of the smaller lateral spermatheca are filled with sperm following copulation (Degner and Harrington, 2016; Oliva et al., 2013; Pascini et al., 2012). AeAmt1 immunostaining localized to the nurse cells of the previtellogenic egg chambers within the ovary of sugar-fed females was also observed [SI Appendix, Fig. 7-S1e-f (Valzania et al., 2019)]. AeAmt1 immunostaining is qualitatively absent in the midgut (MG) and Malpighian tubules (MT) (SI Appendix, Fig. 7-S1a-d), and the rectum (RM) epithelium and rectal pads (SI Appendix, Fig. 7-S1e-h) in contrast to AeAmt1 immunostaining of spermatozoa in recently inseminated female *A. aegypti* (SI Appendix, Fig. 7-S1e-h). *AeAmt1* mRNA levels corroborate these findings, whereby transcript levels are higher in the reproductive organs (RP) (combined with hindgut (HG) tissue to extract sufficient RNA for qPCR), relative to MG and MT levels (SI Appendix, Fig. 7-S2). *AeAmt1* mRNA is highest in fat body (FB) and carcass (CAR) tissues (SI Appendix, Fig. 7-S2), translating to only moderate AeAmt1 immunostaining in sections of fat body cells in comparison to the spermatozoa (SI Appendix, Fig. 7-S1f, yellow dashed arrow). We suggest that carcass tissues (muscle, nervous, and hypodermis) may also be enriched in AeAmt1 transcript, perhaps explaining the difference in transcript and protein levels but has yet to be examined. Alternatively, translation efficiency by specific cells can greatly influence the correlation between mRNA and protein levels, in part due to untranslated mRNA that remains in the cell (Maier et al., 2009). By comparison, *AeAmt2* mRNA is enriched in the HG, RP, and

FB (SI Appendix, Fig. 7-S2) and we have immunolocalized AeAmt2 within the MG, MT, ovary, HG (including rectal pads), and the fat body cells of sugar-fed, mated adult females (SI Appendix, Fig. 7-S3). From this, we postulate that AeAmt2 likely plays critical roles in ammonia detoxification and excretion during blood meal digestion, as this causes significantly elevated haemolymph [NH_4^+] within 48 hr post blood meal (SI Appendix, Fig. 7-S4) which corresponds to simultaneously elevated ammonia concentrations in the faeces (Scaraffia et al., 2005). Interestingly, *AeAmt2* mRNA and protein is also highly enriched in the antennae (SI Appendix, Fig. 7-S3a-d). In *Anopholes gambiae,* an ammonium transporter (*AgAmt*) sharing high sequence homology to *AeAmt2* (Chapter 3), is expressed in chemosensory appendages with evidence that *AgAmt* functions in critical host-seeking behaviors involving ammonia sensing (Pitts et al., 2014; Ye et al., 2020).

AeAmt1 Expression is Only Detected in Spermathecae from Mated Females Containing Sperm

In light of the finding that AeAmt1 is expressed in the flagella of mature spermatozoa and this expression persists during storage of spermatozoa within spermathecae, we predicted that spermathecae of non-mated females should lack AeAmt1 expression. Indeed, AeAmt1 immunostaining is absent in the spermathecae of non-mated females (Fig. 7-2a-b). Furthermore, Western blotting analysis confirmed these findings as AeAmt1 protein was not detected in spermathecae protein homogenate from non-mated females in contrast to AeAmt1 protein detected in the spermathecae of mated female *A. aegypti* (Fig. 7-2c). A single band at ~55 kDa was detected, the predicted monomer form (VectorBase), which is antibody-specific based on previous peptide-blocking analysis in other *A. aegypti* tissues (Chasiotis et al., 2016). In an effort to elucidate a functional role for AeAmt1 in spermatozoa during storage in spermathecae, ammonium (NH_4^+)-selective microelectrodes were used to measure the [NH_4^+] within the spermathecae of mated and non-mated female *A. aegypti*. Mated females exhibit significantly higher NH_4^+ levels released from spermathecae when punctured in a droplet of saline in comparison to non-mated females (Fig. 7-2d), and we estimate that non-diluted [NH_4^+] levels in intact

spermathecae is approximately 500mM for mated females and 300mM for non-mated females consistent with levels measured along the gastrointestinal tract (Terra and Regel, 1995) and within buoyancy organs (Seibel et al., 2004) of other invertebrates. Secretion of proteins by both male accessory glands and glandular cells of spermathecae are required for sperm viability during insemination and sperm storage in insects (Collins et al., 2006; den Boer et al., 2009), however, catabolism of these proteins would yield ammonia. These remarkably high levels in contrast to haemolymph [NH_4^+] (SI Appendix, Fig. 7-S4) suggest that, at least in spermathecae, AeAmt1 in spermatozoa is likely functioning to mitigate ammonia toxicity. This is particularly important considering female *A. aegypti* undergo a single mating event with one male and sperm are stored in spermathecae for the duration of the female's life (Clements and Potter, 1967; Degner and Harrington, 2016; Pascini et al., 2012). While it is unclear how the spermathecal cells mitigate the effects of high ammonia stored within the spermathecal reservoirs, the morphology of the spermathecae is such that the epithelial cells lie externally to the thick cuticle that lines the reservoirs, and the glandular cells are present on the surface of cuticle-lined spermathecal ducts (Clements and Potter, 1967; Pascini et al., 2012). This suggests that it is the cuticle that separates these cells from the high ammonia levels found within the spermathecae.

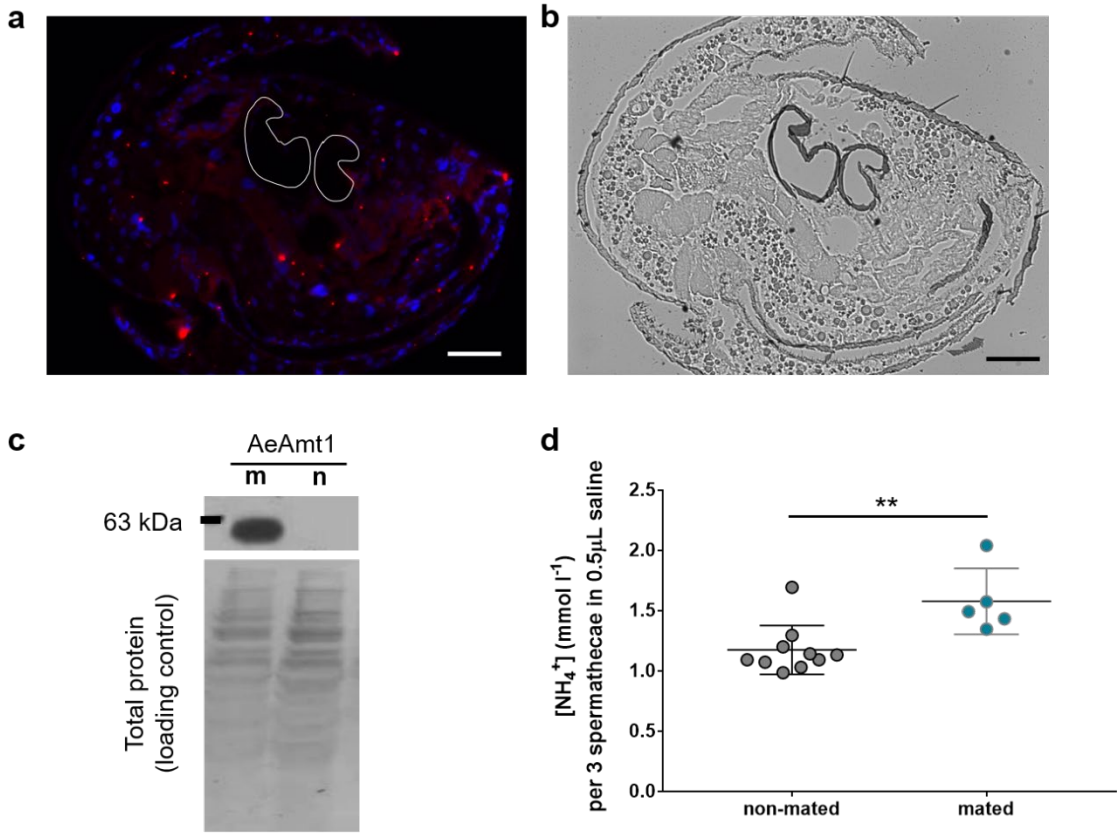

Figure 7- 2. Absence of AeAmt1 protein expression and localization in non-mated females, and ammonium (NH_4^+) content in spermathecae of non-mated and mated female *Aedes aegypti*. (A) AeAmt1 (red) immunolocalization is absent in longitudinal sections of spermathecae (white outlines) from non-mated females counterstained for nuclei (blue; DAPI). (B) Bright field image corresponding to (a). (C) AeAmt1 protein expression (top panel) in isolated spermathecae from mated (m) and non-mated (n) females, and Coomassie total protein staining (bottom panel) using Western blotting. (D) Diluted [NH_4^+] of pooled spermathecae (3 per animal) punctured in a 0.5 µL saline droplet from non-mated and mated female *A. aegypti* (*Mann-Whitney test*, $p = 0.0077$). Data shown at mean ± S.E.M. Scale bars are 50 µm. m, mated; n, non-mated.

During ovulation and oviposition in female *A. aegypti*, spermatozoa are released from the spermathecae and traverse the spermathecal ducts, and this release is highly coordinated with ovulation of the descending egg for successful egg fertilization (Degner and Harrington, 2016). At 48 hours post blood meal, we found that AeAmt1 shows continued expression in sperm flagella as they exit the spermathecae (Fig. 7-3a, b) and migrate through the spermathecal ducts (Fig. 7-3c). AeAmt1 immunostaining was also present in the follicular epithelium and within nurse cells surrounding the developing oocyte (SI Appendix, Fig. 7-S5), paralleling our observation of AeAmt1 localization in pre-vitellogenic egg chambers of sugar-fed females (SI Appendix, Fig. 7-S1e-f). The functional significance of AeAmt1 expression in the nurse cells of both pre-vitellogenic and vitellogenic (post blood meal) ovarian follicles is not yet known, however, the high metabolic activities of the nurse cells to meet energy and nutrient demands mirrors that of spermatozoa. In this regard, metabolic processes in sperm cells occur in part through oxidative phosphorylation whereby ammonia (NH_3/NH_4^+) formation occurs as a by-product and requires regulation, and ultimately excretion from the cell (Visconti, 2012). This putative function for AeAmt1 in facilitating ammonia excretion from these highly metabolically active cells is most plausible considering the similar localizations of AeAmt1 and the mitochondrial derivatives (the site of oxidative phosphorylation) to the sperm flagellum. Findings from a comparative study using a murine model reported the production of potentially inhibitory levels of ammonium resulting from amino acid metabolism during embryonic development (Gardner and Lane, 1993). Evidently, AeAmt1 likely has a critical function in protecting both spermatozoa and the developing oocyte against ammonia toxicity in reproductive organs in *A. aegypti*. Similarly, to sugar-fed females, AeAmt1 immunostaining within the midgut epithelium of females was not observed at 48-hour post blood meal (SI Appendix, Fig. 7-S5, white arrow in panel b).

Figure 7- 3. AeAmt1 protein localization in migrating spermatozoa within spermathecal ducts from blood fed (48 hr pbm) adult female *Aedes aegypti*. (a) AeAmt1 (red) immunolocalization in a longitudinal section of spermathecae (white outlines) counterstained for nuclei (DAPI, blue), (b) bright field image corresponding to panel (a), and (c) AeAmt1 (red) immunolocalization within spermathecal ducts containing migrating spermatozoa (white arrow) counterstained for nuclei (DAPI, blue) in a blood-fed female *A. aegypti*. All scale bars 50 μm.

AeAmt1 is Essential for Spermatozoa Viability and Male Fertility

Considering that AeAmt1 is highly expressed in spermatozoa during the entire course of development in males, insemination of females, and storage within spermathecae, we speculated that AeAmt1 plays an essential role in sperm viability. While information from insect models is certainly lacking, a Rh protein (*Rhcg*) in mice is highly expressed in the epididymis and late stage spermatids in the testes of males in which the epididymal luminal fluid is maintained acidic to immobilize sperm during maturation within this organ (Biver et al., 2008; Lee et al., 2013; Pastor-Soler et al., 2012). Consequently, *Rhcg* mutant mice exhibit decreased fertility. Here we employed RNA interference (RNAi) techniques whereby *AeAmt1-dsRNA* injection of males' results in significant decreases in AeAmt1 protein in whole-body tissues within 24 hours, which restores to normal levels within 36 hours (Fig. 7-4a-b). AeAmt1 protein knockdown at 24 hours causes significant reductions in mature spermatozoa counts in the seminal vesicle (Fig. 7-4c-d), a common storage unit for mature spermatozoa in male *A. aegypti* (Wandall, 1986). We speculated that reductions in the number of spermatozoa are due to viability (i.e. sperm death) rather than delays in spermatogenesis and spermiogenesis, as the latter processes occur over approximately 10 days in dipterans (Engelmann, 2015; Hannah-Alava, 1964). To examine if spermatozoa within the seminal vesicle were indeed dying or dead prior to when AeAmt1 protein is significantly decreased following dsRNA injection, we utilized a live/dead sperm viability assay. At 16 hours post-dsRNA injection, a higher proportion of cell death was observed in the AeAmt1 knockdown males and total sperm counts are significantly reduced within the seminal vesicle (SI Appendix, Fig. 7-S6), indicating that AeAmt1 knockdown begins earlier than 24-hour post-dsRNA treatment demonstrated through Western blotting.

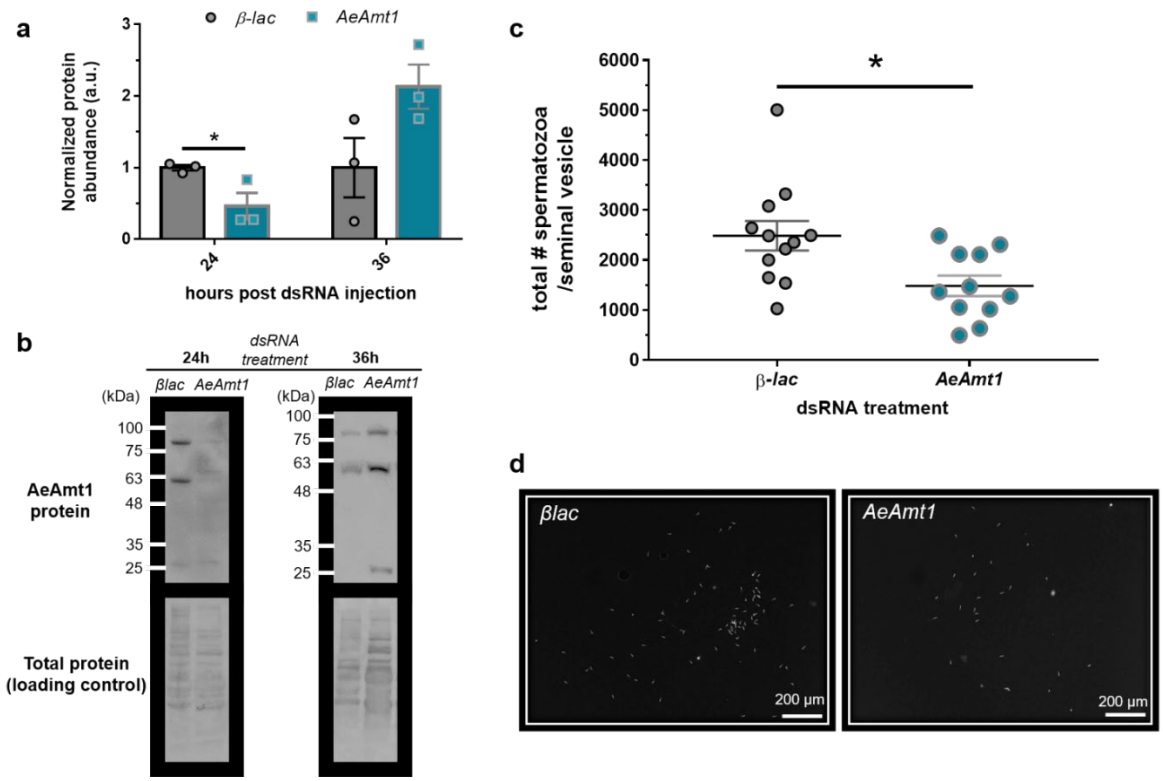

Figure 7- 4. Total spermatozoa in the seminal vesicle of male *Aedes aegypti* following RNAi (dsRNA)-mediated knockdown of AeAmt1. (**A**) AeAmt1 protein abundance in male *A. aegypti* at 24 h and 36 h post injection with *AeAmt1* (n = 3) or control *β-lactamase (β-lac;* n = 3*)* dsRNA (*p = 0.0467* for 24h, Unpaired *Student's t-test, two-tailed; p = 0.100* for 36h, *Mann Whitney* test*)*. (**B**) Representative Western blot images corresponding to (a) demonstrating AeAmt1 protein abundance (top panel) and Coomassie total protein staining (bottom panel) at 24 h and 36 h post *AeAmt1* and *β-lac* dsRNA injection. (**C**) Total spermatozoa number within the seminal vesicle of males at 24 h post *AeAmt1* and *β-lac* dsRNA injection (*p = 0.0073; Mann Whitney test). (***D***) Representative images of immunofluorescent nuclei (grayscale, DAPI) from fixed spermatozoa in a 1 µl droplet of phosphate buffered saline with from the seminal vesicles of *AeAmt1* and *β-lac* dsRNA-injected males at 24 h post injection. Data shown as mean ± S.E.M. (each point represents individual replicate values, panel C).

When non-mated females were inseminated by AeAmt1-knockdown males, significant reductions in the number of eggs laid (Fig. 7-5a), the number of larvae hatched (Fig. 7-5b), and ultimately the percentage of viable eggs laid per female (Fig. 7-5c) were observed. Although moderate levels of spermatozoa remain in the seminal vesicle following AeAmt1 protein knockdown at 24 hours post-injection, we cannot discount the possibilities that sperm death continues to occur prior to, during, and after mating and insemination of the female, or that physiological defects exist in these remaining sperm as a result of AeAmt1 knockdown, which would impact the ability of sperm to fertilize the egg. Mated female *A. aegypti* injected with *AeAmt1* dsRNA produce similar amounts of eggs and hatched larvae as control females, and no significant reduction in the percentage of hatched larvae per female was observed (SI Appendix, Fig. 7-S7a-c), which may be due to adequate amounts of spermatozoa surviving in the spermathecae following AeAmt1 knockdown. It should be noted that high proportions of male and female *A. aegypti* survive following *AeAmt1*-dsRNA injection, with gradual decreases in female survival post blood-feeding and decreases in the proportion of females that lay (viable) eggs occurring, and to a greater extent in AeAmt1 knockdown groups (SI Appendix, Fig. 7-S8).

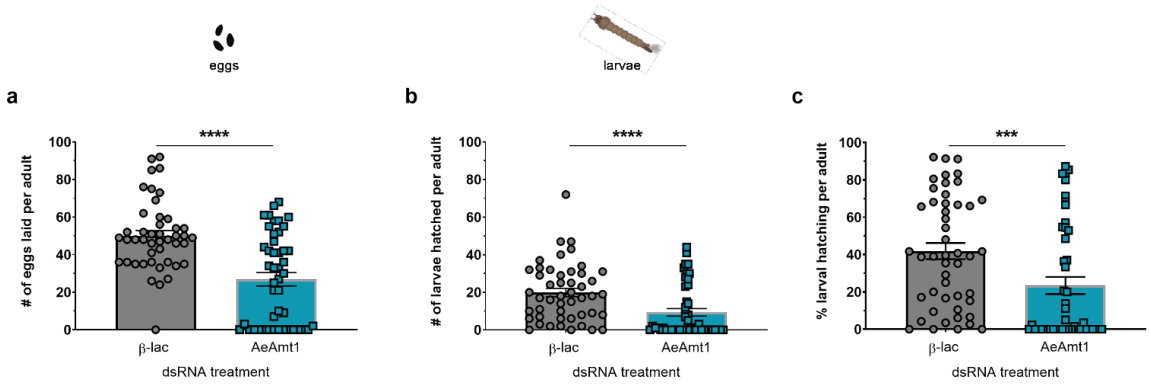

Figure 7- 5. Effects of *AeAmt1* protein knockdown in males on egg laying and larval hatching (egg viability) of mated female *Aedes aegypti*. (A) Number of eggs laid *($p < 0.0001$; Mann Whitney test)*, (B) number of larvae hatched *($p < 0.0001$; Mann Whitney test)*, and (C) percentage of larval hatching *($p = 0.0006$; Mann Whitney test)* by individual females mated with males that were injected with *AeAmt1* and *β-lac* dsRNA (n = 45 for β-lac; n = 46 for AeAmt1). Data shown as mean ± S.E.M. (each point represents individual replicate values).

Taken together, these multiple lines of evidence demonstrate that AeAmt1 expression in spermatozoa is important for sperm survival and successful egg fertilization in *A. aegypti*. AeAmt1 expression within the developing follicles of the ovaries merits further investigation because there was no effect on fertility when females were injected with *AeAmt1*-dsRNA and thus the functional role of AeAmt1 in this respect is unclear. While our findings provide an initial description of a member of the ammonia transporter (Amt/MEP/Rh) protein family that is localized within reproductive organs in a single mosquito genera, we posit that this feature may be conserved, at the very least across insect taxa, as a method of protecting sperm from ammonia toxicity as they navigate the reproductive tract. The use of spermathecae for sperm storage and maintenance of viability until fertilization is a general characteristic of insect reproductive biology, but also extends to other animal phyla including mollusks, annelids, nematodes, and some vertebrates (e.g. amphibians) (Hickman et al., 1984; Pascini and Martins, 2017). In this regard, prevention of the spermatozoa against ammonia toxicity is a challenge that likely many animals are tasked with and our current work highlights the importance of an AMT protein function in this aspect of insect reproduction. These findings also contribute to our understanding of *A. aegypti* reproductive biology, which is still in its infancy, but is of medical importance because of their frequent feeding on human hosts and their high vectorial capacity for arboviral pathogens. In this context, AeAmt1 protein expression during the early stages of sperm development, maturation, and later insemination and fertilization of the egg is necessary for male fertility and, more broadly, the reproductive fitness of *A. aegypti* which is significant in terms of the development of novel vector control methods.

7.5 References

Benedict, M. Q. and Robinson, A. S. (2003). The first releases of transgenic mosquitoes: An argument for the sterile insect technique. *Trends Parasitol.* **19**, 349–355.

Biver, S., Belge, H., Bourgeois, S., Van Vooren, P., Nowik, M., Scohy, S., Houillier, P., Szpirer, J., Szpirer, C., Wagner, C. A., et al. (2008). A role for Rhesus factor Rhcg in renal ammonium excretion and male fertility. *Nature* **456**, 339–343.

Chasiotis, H. and Kelly, S. P. (2008). Occludin immunolocalization and protein expression in goldfish. *J. Exp. Biol.* **211**, 1524–1534.

Chasiotis, H., Ionescu, A., Misyura, L., Bui, P., Fazio, K., Wang, J., Patrick, M., Weihrauch, D. and Donini, A. (2016). An animal homolog of plant Mep/Amt transporters promotes ammonia excretion by the anal papillae of the disease vector mosquito *Aedes aegypti*. *J. Exp. Biol.* **219**, 1346–55.

Clarke, M. R., Denton, E. J. and Gilpin-Brown, J. B. (1979). On the use of ammonium for buoyancy in squids. *J. Mar. Biol. Assoc. United Kingdom* **59**, 259–276.

Clements, A. N. and Potter, S. A. (1967). The fine structure of the spermathecae and their ducts in the mosquito *Aedes aegypti*. *J. Insect Physiol.* **13**, 1825–1836.

Collins, A. M., Caperna, T. J., Williams, V., Garrett, W. M. and Evans, J. D. (2006). Proteomic analyses of male contributions to honey bee sperm storage and mating. *Insect Mol. Biol.* **15**, 541–549.

Degner, E. C. and Harrington, L. C. (2016). A mosquito sperm's journey from male ejaculate to egg: Mechanisms, molecules, and methods for exploration. *Mol. Reprod. Dev.* **83**, 897–911.

Delventhal, R., Menuz, K., Joseph, R., Park, J., Sun, J. S. and Carlson, J. R. (2017). The taste response to ammonia in Drosophila. *Sci. Rep.* **7**, 1–12.

den Boer, S. P. A., Boomsma, J. J. and Baer, B. (2009). Honey bee males and queens use glandular secretions to enhance sperm viability before and after storage. *J. Insect Physiol.* **55**, 538–543.

Donini, A. and O'Donnell, M. J. (2005). Analysis of Na^+, Cl^-, K^+, H^+ and NH_4^+ concentration gradients adjacent to the surface of anal papillae of the mosquito *Aedes aegypti*: application of self-referencing ion-selective mi. *J. Exp. Biol.* **208**, 603–10.

Durant, A. C. and Donini, A. (2018a). Ammonia Excretion in an Osmoregulatory Syncytium Is Facilitated by AeAmt2, a Novel Ammonia Transporter in *Aedes aegypti* Larvae. *Front. Physiol.* **9**,.

Durant, A. C. and Donini, A. (2018b). Evidence that Rh proteins in the anal papillae of the freshwater mosquito *Aedes aegypti* are involved in the regulation of acid–base balance in elevated salt and ammonia environments . *J. Exp. Biol.* **221**, jeb186866.

Durant, A. C. and Donini, A. (2019). Development of *Aedes aegypti* (Diptera: Culicidae) mosquito larvae in high ammonia sewage in septic tanks causes alterations in ammonia excretion, ammonia transporter expression, and osmoregulation. *Sci. Rep.* **9**, 1–17.

Durant, A. C., Chasiotis, H., Misyura, L. and Donini, A. (2017). *Aedes aegypti* Rhesus glycoproteins contribute to ammonia excretion by larval anal papillae. *J. Exp. Biol.* **220**, 588–596.

Engelmann, F. (2015). *The Physiology of Insect Reproduction: International Series of Monographs in Pure and Applied Biology: Zoology*. Elsevier.

Gardner, D. K. and Lane, M. (1993). Amino acids and ammonium regulate mouse embryo development in culture. *Biol. Reprod.* **48**, 377–385.

Hannah-Alava, A. (1964). The brood-pattern of X-ray-induced mutational damage in the germ cells of *Drosophila melanogaster* males. *Mutat. Res. Mol. Mech. Mutagen.* **1**, 414–436.

Hemingway, J., Field, L. and Vontas, J. (2002). An overview of insecticide resistance. *Science (80-.).* **298**, 96–97.

Hickman, C. P., Roberts, L. S., Hickman, F. M. and Hickman, C. P. (1984). *Integrated principles of zoology*.

Ip, Y. K. and Chew, S. F. (2010). Ammonia production, excretion, toxicity, and defense in fish: A review. *Front. Physiol.* **1 OCT**, 1–20.

Iturbe-Ormaetxe, I., Walker, T. and O'Neill, S. L. (2011). Wolbachia and the biological control of mosquito-borne disease. *EMBO Rep.* **12**, 508–518.

Kandul, N. P., Liu, J., Sanchez C, H. M., Wu, S. L., Marshall, J. M. and Akbari, O. S. (2019). Transforming insect population control with precision guided sterile males with demonstration in flies. *Nat. Commun.* **10**, 1–12.

Khademi, S., O'Connell III, J., Remis, J., Robles-Colmenares, Y., Miercke, L. J. W. and Stroud, R. M. (2004). Mechanism of ammonia transport by Amt/MEP/Rh: Structure of AmtB at 1.35 angstroms. *Science (80-.).* **305**, 1587–1594.

Kraemer, M. U. G., Sinka, M. E., Duda, K. A., Mylne, A. Q. N., Shearer, F. M., Barker, C. M., Moore, C. G., Carvalho, R. G., Coelho, G. E., Van Bortel, W., et al. (2015). The global distribution of the arbovirus vectors *Aedes aegypti* and *Ae. Albopictus*. *Elife* **4**, 1–18.

Lecompte, M., Cattaert, D., Vincent, A., Birman, S. and Chérif-Zahar, B. (2019). Drosophila ammonium transporter Rh50 is required for integrity of larval muscles and neuromuscular system . *J. Comp. Neurol.* 1–14.

Lee, H.-W., Verlander, J. W., Handlogten, M. E., Han, K.-H., Cooke, P. S. and Weiner, I. D. (2013). Expression of the rhesus glycoproteins, ammonia transporter family members, RHCG and RHBG in male reproductive organs. *Reproduction* **146**, 283–296.

Leta, S., Beyene, T. J., De Clercq, E. M., Amenu, K., Kraemer, M. U. G. and Revie, C. W. (2018). Global risk mapping for major diseases transmitted by *Aedes aegypti* and *Aedes albopictus*. *Int. J. Infect. Dis.* **67**, 25–35.

Ludewig, U., Von Wiren, N. and Frommer, W. B. (2002). Uniport of NH_4^+ by the root hair plasma membrane ammonium transporter LeAMT1;1. *J. Biol. Chem.* **277**, 13548–13555.

Maier, T., Güell, M. and Serrano, L. (2009). Correlation of mRNA and protein in complex biological samples. *FEBS Lett.* **583**, 3966–3973.

Marini, A. M., Vissers, S., Urrestarazu, A. and Andre, B. (1994). Cloning and expression of the MEP1 gene encoding an ammonium transporter in *Saccharomyces cerevisiae*. *Embo J* **13**, 3456–3463.

Marini, A.-M., Urrestarazu, A., Beauwens, R. and André, B. (1997). The Rh (Rhesus) blood group polypeptides are related to NH_4^+ transporters. *Trends Biochem. Sci.* **22**, 460–461.

Mayer, M., Schaaf, G., Mouro, I., Lopez, C., Colin, Y., Neumann, P., Cartron, J.-P. and Ludewig, U. (2006). Different transport mechanisms in plant and human AMT/Rh-type ammonium transporters. *J. Gen. Physiol.* **127**, 133–144.

McDonald, T. R. and Ward, J. M. (2016). Evolution of electrogenic ammonium transporters (AMTs). *Front. Plant Sci.* **7**, 352.

McDonald, T. R., Dietrich, F. S. and Lutzoni, F. (2012). Multiple horizontal gene transfers of ammonium transporters/ammonia permeases from prokaryotes to eukaryotes: Toward a new functional and evolutionary classification. *Mol. Biol. Evol.* **29**, 51–60.

Menuz, K., Larter, N. K., Park, J. and Carlson, J. R. (2014). An RNA-Seq screen of the *Drosophila* antenna identifies a transporter necessary for ammonia detection. *PLoS Genet.* **10**,.

Neuhäuser, B. and Ludewig, U. (2014). Uncoupling of ionic currents from substrate transport in the plant ammonium transporter AtAMT1;2. *J. Biol. Chem.* **289**, 11650–11655.

Ninnemann, O., Jauniaux, J. C. and Frommer, W. B. (1994). Identification of a high affinity NH_4^+ transporter from plants. *EMBO J.* **13**, 3464–3471.

O'Donnell, M. J. and Donini, A. (2017). Nitrogen excretion and metabolism in insects. In *Acid-Base Balance and Nitrogen Excretion in Invertebrates* (ed. Weihrauch, D.) and O'Donnell, M. J.), pp. 109–126. Springer International Publishing Switzerland.

Oliva, C. F., Damiens, D., Vreysen, M. J. B., Lemperière, G. and Gilles, J. (2013). Reproductive strategies of *Aedes albopictus* (Diptera: Culicidae) and implications for the sterile insect technique. *PLoS One* **8**,.

Pascini, T. V. and Martins, G. F. (2017). The insect spermatheca: an overview. *Zoology* **121**, 56–71.

Pascini, T. V., Ramalho-Ortigão, M. and Martins, G. F. (2012). Morphological and morphometrical assessment of spermathecae of *Aedes aegypti* females. *Mem. Inst. Oswaldo Cruz* **107**, 705–712.

Pastor-Soler, N., Piétrement, C. and Breton, S. (2012). Role of Acid / Base transporters in the male reproductive tract and potential consequences of their malfunction role of Acid / Base transporters in the male reproductive tract and potential. 417–428.

Peng, J. and Huang, C. H. (2006). Rh proteins vs Amt proteins: an organismal and phylogenetic perspective on CO_2 and NH_3 gas channels. *Transfus. Clin. Biol.* **13**, 85–94.

Petzel, D. H., Berg, M. M. and Beyenbach, K. W. (1987). Hormone-controlled CAMP-mediated in yellow-fever mosquito. *Am. J. Physiol. Integr. Comp. Physiol.* **253**, R701–R711.

Pitts, R. J., Derryberry, S. L., Pulous, F. E. and Zwiebel, L. J. (2014). Antennal-expressed ammonium transporters in the malaria vector mosquito *Anopheles gambiae*. *PLoS One* **9**,.

Ponlawat, A. and Harrington (2007). Age and body size influence male sperm capacity of the Dengue vector *Aedes aegypti* (Diptera: Culicidae). *J. Med. Entomol.* **44**, 422–426.

Randall, D. J. and Tsui, T. K. N. (2002). Ammonia toxicity in fish.pdf. *Mar. Pollut. Bull.* **45**, 17–23.

Rocco, D. A., Garcia, A. S. G., Scudeler, E. L., Dos Santos, D. C., Nóbrega, R. H. and Paluzzi, J. P. V. (2019). Glycoprotein hormone receptor knockdown leads to reduced reproductive success in male Aedes aegypti. *Front. Physiol.* **10**, 1–11.

Scaraffia, P. Y., Isoe, J., Murillo, A. and Wells, M. A. (2005). Ammonia metabolism in *Aedes aegypti*. *Insect Biochem. Mol. Biol.* **35**, 491–503.

Seibel, B. A., Goffredi, S. K., Thuesen, E. V., Childress, J. J. and Robison, B. H. (2004). Ammonium content and buoyancy in midwater cephalopods. *J. Exp. Mar. Bio. Ecol.* **313**, 375–387.

Smith, H. W. (1936). The retention and physiological role of urea in the elasmobranchii. *Biol. Rev.* **11**, 49–82.

Smith, L. B., Kasai, S. and Scott, J. G. (2016). Pyrethroid resistance in *Aedes aegypti* and *Aedes albopictus*: Important mosquito vectors of human diseases. *Pestic. Biochem. Physiol.* **133**, 1–12.

Soupene, E., He, L., Yan, D. and Kustu, S. (1998). Ammonia acquisition in enteric bacteria: physiological role of the ammonium/methylammonium transport B (AmtB) protein. *Proc. Natl. Acad. Sci. U. S. A.* **95**, 7030–4.

Terra, W. R. and Regel, R. (1995). pH buffering in *Musca domestica* midguts. *Comp. Biochem. Physiol. -- Part A Physiol.* **112**, 559–564.

Valzania, L., Mattee, M. T., Strand, M. R. and Brown, M. R. (2019). Blood feeding activates the vitellogenic stage of oogenesis in the mosquito *Aedes aegypti* through inhibition of glycogen synthase kinase 3 by the insulin and TOR pathways. *Dev. Biol.* **454**, 85–95.

Visconti, P. E. (2012). Sperm bioenergetics in a Nutshell. *Biol. Reprod.* **87**, 1–4.

Vontas, J., Kioulos, E., Pavlidi, N., Morou, E., della Torre, A. and Ranson, H. (2012). Insecticide resistance in the major dengue vectors *Aedes albopictus* and *Aedes aegypti*. *Pestic. Biochem. Physiol.* **104**, 126–131.

Wandall, A. (1986). Ultrastructural organization of spermatocysts in the testes of *Aedes aegypti* (Diptera: Culicidae)1. *J. Med. Entomol.* **23**, 374–379.

Weihrauch, D. (2006). Active ammonia absorption in the midgut of the Tobacco hornworm *Manduca sexta* L.: Transport studies and mRNA expression analysis of a Rhesus-like ammonia transporter. *Insect Biochem. Mol. Biol.* **36**, 808–821.

Weihrauch, D. and Allen, G. J. P. (2018). Ammonia excretion in aquatic invertebrates: new insights and questions. *J. Exp. Biol.* **221**, jeb178673.

Weihrauch, D. and O'Donnell, M. J. (2015). Links between osmoregulation and nitrogen-excretion in insects and crustaceans. *Integr. Comp. Biol.* **55**, 816–829.

Weihrauch, D., Morris, S. and Towle, D. W. (2004). Ammonia excretion in aquatic and terrestrial crabs. *J. Exp. Biol.* **207**, 4491–4504.

Weihrauch, D., Donini, A. and O'Donnell, M. J. (2012). Ammonia transport by terrestrial and aquatic insects. *J. Insect Physiol.* **58**, 473–487.

Weill, M., Luffalla, G., Mogensen, K., Chandre, F., Berthomieu, A., Berticat, C., Pasteur, N., Philips, A., Fort, P. and Raymond, M. (2003). Insecticide resistance in mosquito vectors. *Nature* **423**, 136–137.

Weiner, I. D. and Verlander, J. W. (2017). Ammonia transporters and their role in acid-base balance. *Physiol. Rev.* **97**, 465–494.

Wood, C. F., Part, P. and Wright, P. A. (1995). Ammonia and urea metabolism in relation to gill function and acid-base balance in a marine elasmobranch, the spiny dogfish (*Squalus acanthias*). *J. Exp. Biol.* **198**, 1545–1558.

Wright, P. (1995). Nitrogen excretion : three end products , many physiological roles. *J. Exp. Biol.* **281**, 273–281.

Wu, Y., Zheng, X., Zhang, M., He, A., Li, Z. and Zhan, X. (2010). Cloning and functional expression of Rh50-like glycoprotein, a putative ammonia channel, in *Aedes albopictus* mosquitoes. *J. Insect Physiol.* **56**, 1599–1610.

Ye, Z., Liu, F., Sun, H., Barker, M., Pitts, R. J. and Zwiebel, L. J. (2020). Heterogeneous expression of the ammonium transporter AgAmt in chemosensory appendages of the malaria vector, *Anopheles gambiae*. *Insect Biochem. Mol. Biol.* **120**,.

Zheng, L., Kostrewa, D., Bernèche, S., Winkler, F. K. and Li, X.-D. (2004). The mechanism of ammonia transport based on the crystal structure of AmtB of *Escherichia coli*. *Proc. Natl. Acad. Sci. U. S. A.* **101**, 17090–5.

7.6 Supplementary Information (SI) Appendix: Figures

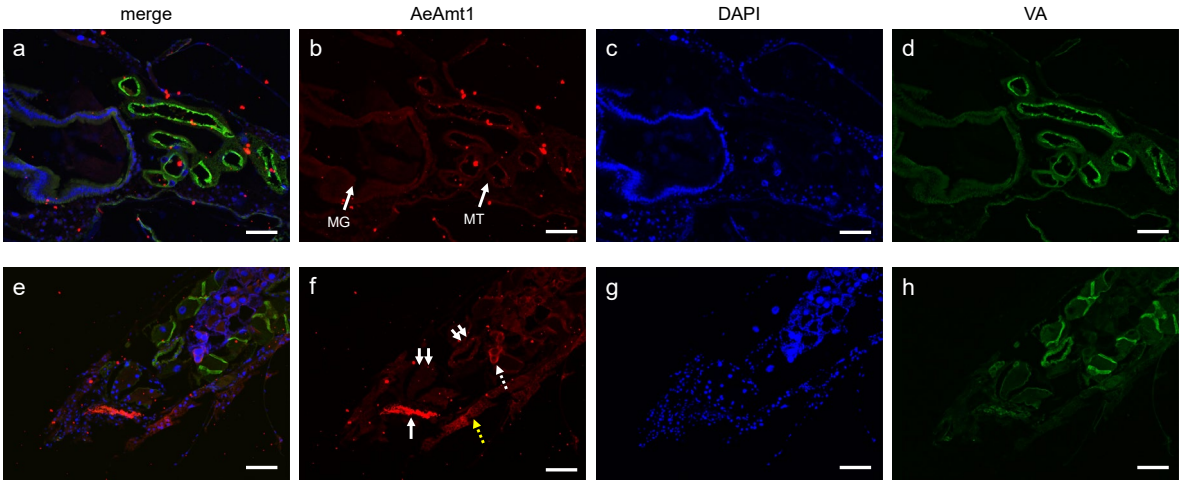

Figure 7S- 1. AeAmt1 protein localization in mated, sugar fed female *Aedes aegypti*. (a-d) Longitudinal section through midgut (MG) and Malpighian tubules (MT) (white arrows in b) showing AeAmt1 (red) immunolocalization counterstained for nuclei (blue; DAPI) and V-type-H^+ ATPase (VA; green). (**e-h**) Longitudinal section through distal regions of the Malpighian tubules, ovary (dashed white arrows), hindgut (double arrows), fat body (yellow dashed arrow), and sperm within the bursa inseminalis (solid white arrow) showing AeAmt1 (red) immunolocalization counterstained for nuclei (blue; DAPI) and VA (green). All scale bars are 100um.

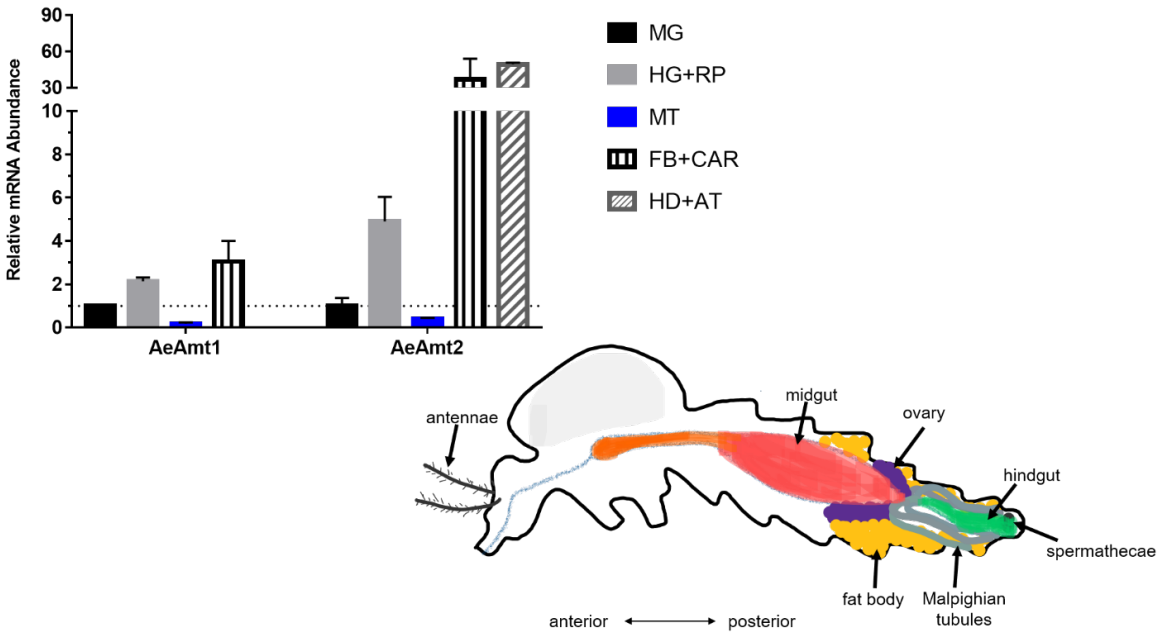

Figure 7S- 2. Organ expression profile of AeAmts in mated, sugar-fed adult female *Aedes aegypti.* *AeAmt1* and *AeAmt2* mRNA abundance in the midgut (MG), hindgut and reproductive organs (HG+RP), Malpighian tubules (MT), fat body and carcass (FB+CAR), and head and antennae (HD+AT; AeAmt2 only) of adult females. Each gene was normalized to the geometric mean of three control reference genes (*rp49*, *rpS18*, *rpL8*), and is expressed relative to transcript levels in the midgut of that gene (assigned a value of 1). Data are expressed as mean values ± S.E.M (n = 6 for MG, HG+RP, MT; n = 3 for FB+CAR, HD+AT).

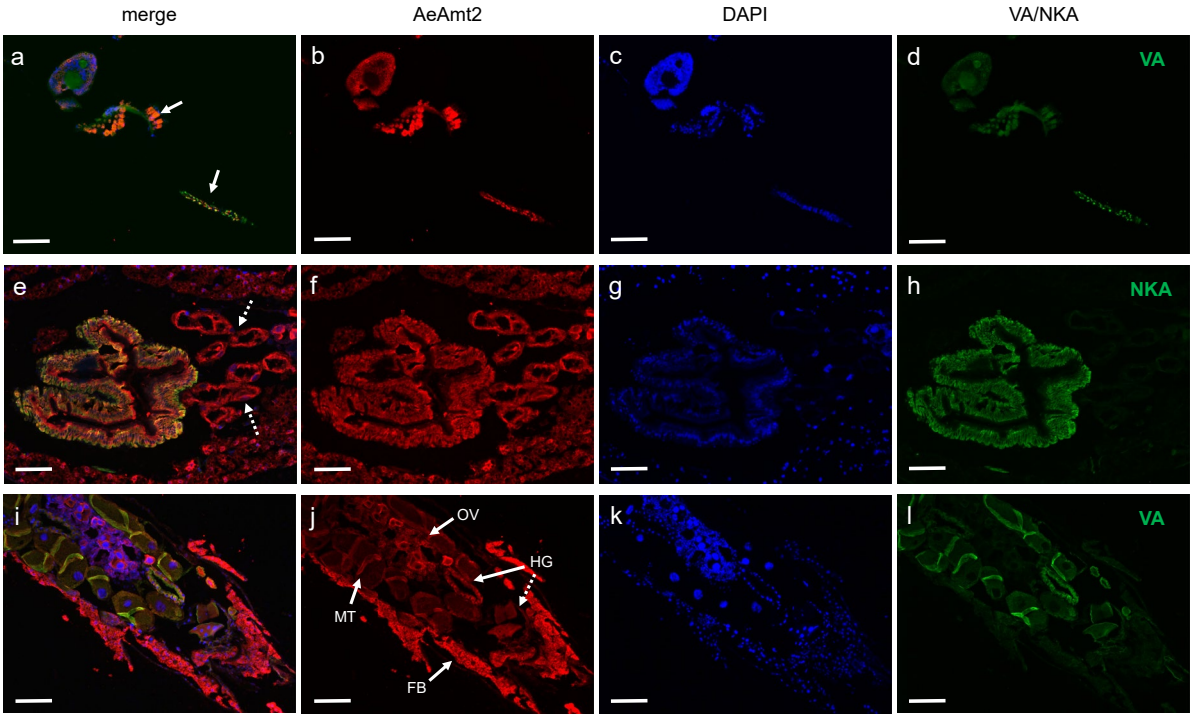

Figure 7S- 3. AeAmt2 protein localization in sugar-fed female *Aedes aegypti*. (a-d) Longitudinal section through antennae (white arrows in a) showing AeAmt2 (red) immunolocalization counterstained for nuclei (blue; DAPI) and V-type-H^+ ATPase (VA; green). (**e-h**) Longitudinal section through the midgut and proximal regions of the Malpighian tubules (dashed white arrows in e) showing AeAmt2 (red) immunolocalization counterstained for nuclei (blue; DAPI) and Na^+-K^+ ATPase (NKA; green). (**i-l**) Longitudinal section through distal regions of the Malpighian tubules (MT), ovary (OV), hindgut (HG; rectal pads, dashed arrow), and fat body (FB) showing AeAmt2 (red) immunolocalization counterstained for nuclei (blue; DAPI) and V-type-H^+ ATPase (VA; green). All scale bars are 100um.

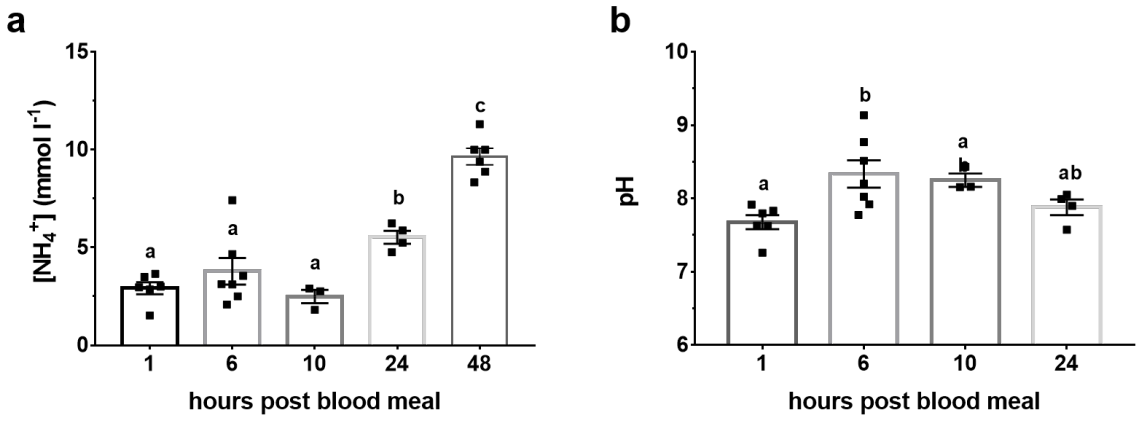

Figure 7S- 4. Haemolymph ammonium [NH_4^+] and pH of adult female *A. aegypti* following a blood meal. (a) haemolymph [NH_4^+] over 48 hrs and (**b**) haemolymph pH over 24 hours post blood meal (n=3-7 per time point). Data are expressed as mean values ± S.E.M. Different letters denote significant differences (One-way ANOVA, Tukey post-hoc test, $p < 0.05$).

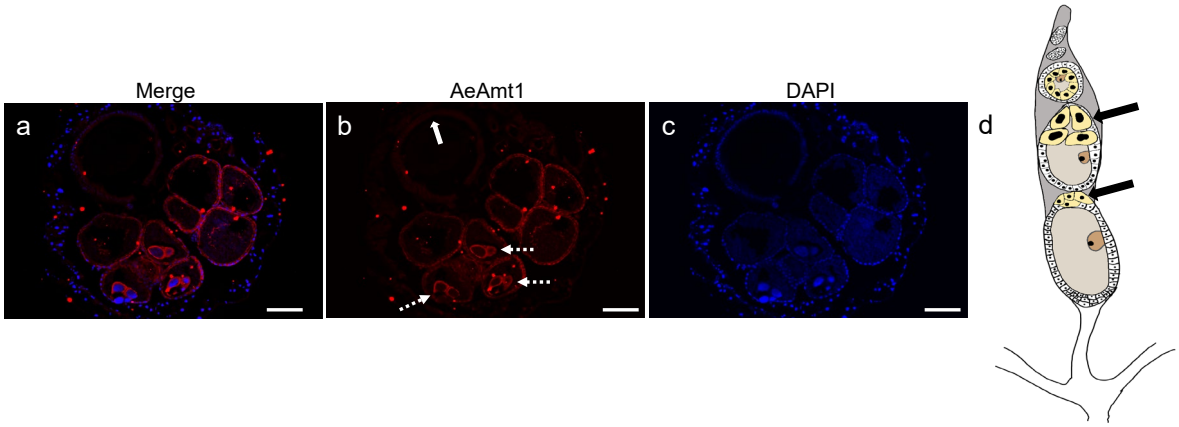

Figure 7S- 5. AeAmt1 protein localization in nurse cells of the developing follicle from blood fed (48 hr pbm) adult female *Aedes aegypti*. (a-c) AeAmt1 immunolocalization to the follicular epithelium and nurse cells (dashed arrows) of a transverse section through eight ovarioles each possessing follicles, and the midgut (white arrow, panel b) counterstained for nuclei (blue; DAPI). (d) Illustration highlighting the nurse cells (black arrows) and epithelial cells (white arrow) to which AeAmt1 immunolocalizes within a single ovariole possessing follicles at different stages of differentiation. All scale bars 100 µm.

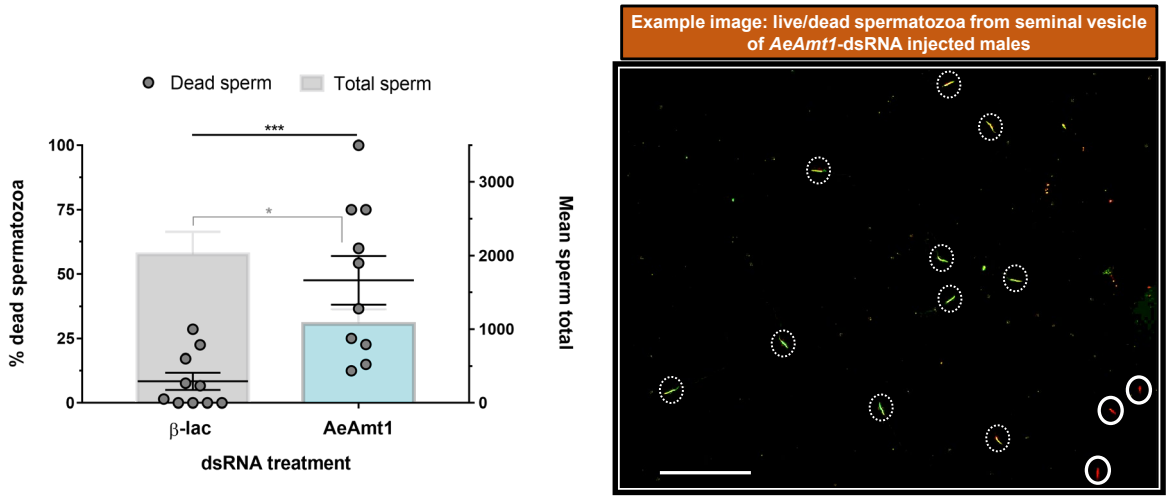

Figure 7S- 6. The proportion of dead or damaged spermatozoa (*p = 0.0007, Mann Whitney test*) and total sperm counts (*p = 0.0143; Unpaired t-test*) within the seminal vesicle of male *Aedes aegypti* at 16 hours following *AeAmt1* or control *β-lactamase* (*β-lac*) dsRNA injection. Representative merged fluorescence image (right panel) indicating live sperm cells (green nuclei, dashed circles) and membrane-compromised sperm cells (red nuclei, solid circles) isolated from the seminal vesicle of AeAmt1 dsRNA-injected males at 16 hours post-injection. Scale bar is 200 µm.

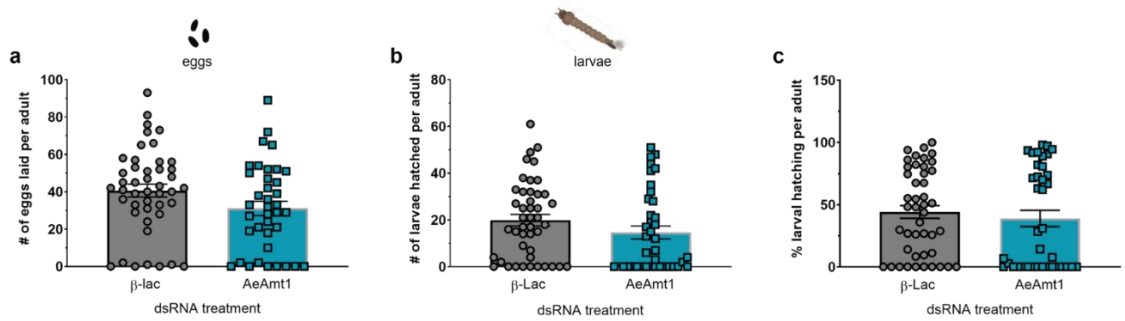

Figure 7S- 7. Effects of *AeAmt1* protein knockdown on egg laying and larval hatching (egg viability) of mated female *Aedes aegypti*. (A) Number of eggs laid *(p = 0.0656; Unpaired t-test),* (B) number of larvae hatched *(p = 0.1578; Unpaired t-test)*, and (C) percentage of larval hatching *(p = 0.4788; Mann Whitney test)* by individual females injected with *AeAmt1* and *β-lac* dsRNA (n = 45 for β-lac; n = 38 for AeAmt1). Data shown as mean ± S.E.M. (each point represents individual replicate values).

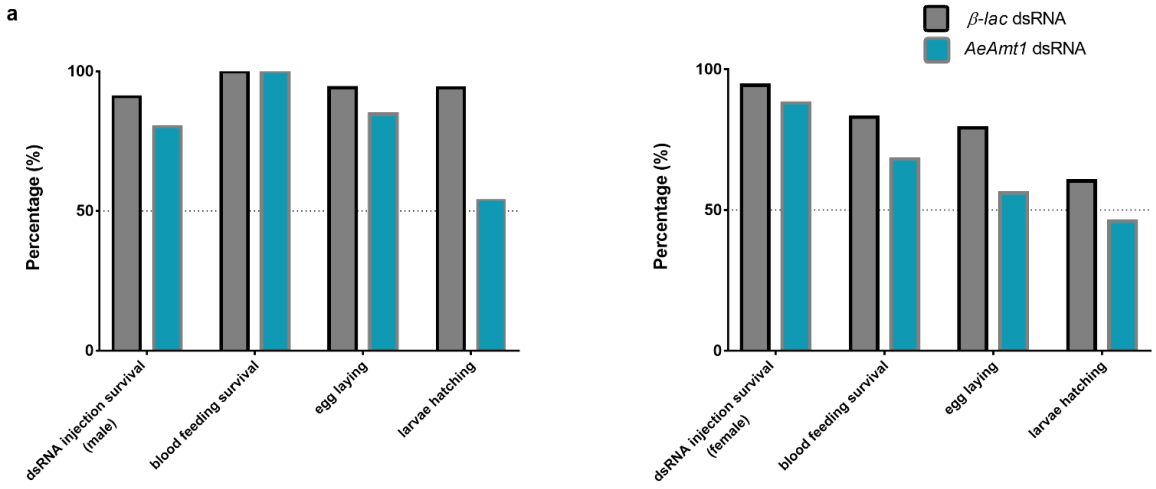

Figure 7S- 8. Female *Aedes aegypti* survival post *dsRNA* injection (males, left; females, right) and blood feeding, and the proportion of surviving females that laid viable eggs. Percentages of females that survived AeAmt1 or control *β-lac* dsRNA injection (dsRNA injection survival), and the percentage of females that survived up to 4 days post blood meal relative to the initial number injected with dsRNA (blood feeding survival). The percentage of females that laid eggs following dsRNA injection and a blood meal (proportion egg laying), and the percentage of females that laid eggs that resulted in hatched larvae after two days (proportion viable eggs/larval hatching) relative to the initial number of females injected with dsRNA is also shown.

7.7 Supplementary Information (SI) Appendix: Materials and Methods

Quantitative real-time PCR (qPCR) for AeAmt1 and AeAmt2 mRNA abundance

Biological samples (n = 3-6, as specified in figure legend) each consisting of pooled midgut (MG), hindgut and reproductive organs (HG+RP), Malpighian tubules (MT), fat body (FB), and head and antennae (HD+AT) tissue from 70-90 adult female *A. aegypti* per sample were isolated in cold lysis buffer from the Purelink RNA mini kit (Ambio, Austin, TX) and sonicated for 5s at 5W using an XL 2000 Ultrasonic Processor (Qsonica, LL, CT, USA). RNA was isolated using the Purelink RNA mini kit (Ambion, Austin, TX) and was treated with the TURBO DNA-free Kit (Applied Biosystems, Streetsville, Ontario, Canada) to remove genomic DNA. cDNA was prepared from isolated RNA samples (using 1 μg of RNA for all samples) using the iScript cDNA Synthesis Kit (Bio-Rad, Mississauga, Ontario, Canada) following manufacturer recommendations. The cDNA was stored at -20 ºC until subsequent use. To determine the relative mRNA abundance of *AeAmt1* and *AeAmt2* in adult female *A. aegypti* tissues, quantitative PCR (qPCR) was performed using SsoFast Evagreen Supermix (Bio-Rad Laboratories (Canada) Ltd. Mississauga, Ontario, Canada) according to the manufacturer's protocol, and the primers designed for each gene (Chasiotis et al., 2016; Chapter 3). Ribosomal protein 49, 60s ribosomal protein S18, and ribosomal protein L8 were used as internal controls. These reference genes were determined to be suitable as internal controls for adult female *Aedes aegypti* (Paluzzi et al., 2014), and primers were a kind gift from Dr. Jean Paul Paluzzi (York University). Reactions were carried out using the CFX96 real time PCR detection system (Bio-Rad). To confirm the presence of a single product after each reaction, a melting curve analysis was performed. For each gene of interest, a standard curve was generated to optimize reaction efficiency. Undiluted cDNA for all tissue samples was used to assess *AeAmt1* and *AeAmt2* mRNA abundance, while a 1/100 dilution of cDNA for all tissue samples was used throughout for all three reference genes. Quantification of transcripts was determined according to the Pfaffl method (Pfaffl, 2004), using the geometric mean of the three

reference genes for data normalization. Samples were run in duplicate, and a no-template negative control was used for each gene.

Immunohistochemistry for AeAmt2 protein localization

Immunohistochemistry of AeAmt2 in adult female *A. aegypti* organs was carried out following a previously published protocol (Chapter 3). A custom synthesized polyclonal antibody raised in rabbit against AeAmt2 was used at a dilution of 2.86×10^{-03} µg µL^{-1}. For AeAmt1 and AeAmt2 immunolocalization studies, a mouse monoclonal anti-α5 antibody for immunostaining of Na^+-K^+-ATPase (NKA; Douglas Fambrough, Developmental Studies Hybridoma Bank, IA, USA) as a basolateral membrane marker in the midgut epithelium was used at a 1:10 dilution. A guinea pig anti-V-type-H^+-ATPase (VA) (a kind gift from Dr. Weiczorek, University of Osnabruk, Germany) was used at a 1:15000 dilution as a marker in the antennae and the apical membrane of the Malpighian tubule epithelium. NKA and VA localization within the epithelia of A. aegypti organs has been previously established (Patrick et al., 2006a). To visualize AeAmt1 and AeAmt2, a goat anti-rabbit antibody conjugated to Alexa Fluor 594 was applied; to visualize NKA, a sheep anti-mouse antibody conjugated to Cy2 was applied; to visualize VA, a goat anti-guinea pig antibody conjugated to AlexaFluor 647 was applied. All secondary antibodies (Jackson ImmunoResearch Laboratories, West Grove, PA, USA) were used at 1:500 dilutions.

Haemolymph ammonium (NH_4^+) and pH levels using ion-selective microelectrodes (ISME)

Haemolymph droplets from adult female *A. aegypti* (7-10 days post emergence) were sampled at various intervals up to 48 hours post blood meal. For haemolymph collection, females were immobilized through brief exposure to CO_2 gas and were quickly submerged under hydrated paraffin oil. Using fine forceps, one hind leg was removed from the animal and gentle pressure was subsequently applied to the thorax to release a droplet of haemolymph from the opening where the leg was removed. Droplets from individual animals were kept under oil for no more than 15 minutes prior to ion activity

measurements using NH_4^+ and H^+ selective microelectrodes, constructed and calibrated as previously described (Chapter 5).

Live/dead spermatozoa assay

A Live/Dead Sperm Viability kit (Thermo Fischer Scientific, Waltham, MA, USA) was utilized to examine if sperm cell death was contributing to the observed lower sperm counts in the seminal vesicle following *dsRNA* mediated AeAmt1 knockdown compared to the *β-lac* dsRNA-injected control group. At 16 hours post-dsRNA injection, spermatozoa were carefully isolated from the seminal vesicle of male *A. aegypti* in 50 µL physiological saline containing 100 nM SYBER 14 dye (membrane-permeant nucleic acid stain for live cells). Samples were incubated at 36°C for 10 minutes, and propidium iodide (membrane-impermeant stain for membrane compromised cells) was added to each sample at a final concentration of 12 µM. Samples were incubated at 36°C for an additional 10 minutes, and 3 x 1 µL droplets of each sample were placed on a microscope slide and were covered immediately and gently with a coverslip. Slides were imaged using an inverted fluorescence microscope (Nikon Eclipse Ti-S, Nikon Instruments Inc., Minato, Japan) at 4 × magnification to capture the entire 1 µL droplet of spermatozoa in saline. A FITC filter set (excitation: 488, emission:519) was used to image SYBR 14 stained nuclei, and a Texas Red filter set (excitation: 560, emission:610) was used to image propidium iodide-stained cells. Each sample was collected and processed individually and imaged immediately upon being placed on the microscope slide. Fluorescence images for live and dead cell stains for each droplet were merged using ImageJ software (ImageJ ver.1.51J8, National Institutes of Health, USA). The total nuclei, number of live nuclei (green), and number of dead/damaged nuclei (red) in each 1 µL droplet were counted and were averaged among the 3 droplets per sample. Average total spermatozoa count in the seminal vesicle at 16 hours (from 3 droplets per animal) were calculated by multiplying the counted sperm by the dilution factor. The number of red (dead) and green (live) nuclei within the entire area of the image were quantified to obtain an averaged proportion (3 droplets per

animal, 10 animals per dsRNA group) of spermatozoa cell death, a reliable method that has been detailed previously (MacMillan et al., 2017).

7.8 Supplementary Information (SI) Appendix: References

Chasiotis, H., Ionescu, A., Misyura, L., Bui, P., Fazio, K., Wang, J., Patrick, M., Weihrauch, D. and Donini, A. (2016). An animal homolog of plant Mep/Amt transporters promotes ammonia excretion by the anal papillae of the disease vector mosquito *Aedes aegypti*. *J. Exp. Biol.* **219**, 1346–55.

Durant, A. C. and Donini, A. (2018). Ammonia Excretion in an Osmoregulatory Syncytium Is Facilitated by AeAmt2, a Novel Ammonia Transporter in *Aedes aegypti* Larvae. *Front. Physiol.* **9**,.

Durant, A. C. and Donini, A. (2019). Development of *Aedes aegypti* (Diptera: Culicidae) mosquito larvae in high ammonia sewage in septic tanks causes alterations in ammonia excretion, ammonia transporter expression, and osmoregulation. *Sci. Rep.* **9**, 1–17.

MacMillan, H. A., Yerushalmi, G. Y., Jonusaite, S., Kelly, S. P. and Donini, A. (2017). Thermal acclimation mitigates cold-induced paracellular leak from the Drosophila gut. *Sci. Rep.* **7**, 1–11.

Paluzzi, J. P., Vanderveken, M. and O'Donnell, M. J. (2014). The heterodimeric glycoprotein hormone, GPA2/GPB5, regulates ion transport across the hindgut of the adult mosquito, *Aedes aegypti*. *PLoS One* **9**, e86386.

Patrick, M. L., Aimanova, K., Sanders, H. R. and Gill, S. S. (2006). P-type Na^+/K^+-ATPase and V-type H^+-ATPase expression patterns in the osmoregulatory organs of larval and adult mosquito *Aedes aegypti*. *J. Exp. Biol.* **209**, 4638–51.

Pfaffl, M. (2004). Quantification strategies in real-time PCR. *A-Z Quant. PCR* 87–112.

Chapter Eight

Conclusions and future directions

8.1 Summary

At the beginning of this research, findings of ammonia transporter expression in the anal papillae of *A. aegypti* larvae combined with earlier evidence of ammonium (NH_4^+) excretion from these organs provided important insight into the mechanisms of ammonia excretion that exists in these mosquitoes (Chasiotis et al., 2016; Donini and O'Donnell, 2005). Decades of reports that *A. aegypti* larvae inhabit high ammonia sewage habitats, which would present significant challenges to the survival of many other aquatic animals, offered a particularly fruitful avenue of research in terms of how ammonia transport physiology translates into the ability of larvae to tolerate toxic levels of ammonia in the aquatic environment (Burke et al., 2010; Chitolina et al., 2016; Lam and Dharmaraj, 1982; Mackay et al., 2009). Furthermore, blood-feeding in adult *A. aegypti* females presents a substantial ammonia challenge (Scaraffia et al., 2005; Scaraffia et al., 2006), but nothing was known of the expression nor contribution of ammonia transporters to ammonia regulation and excretion in adults. Studies in this area from other mosquito species implicated Rh protein involvement in various osmoregulatory organs during the process of blood meal digestion, and that an Amt protein was involved in ammonia sensing related to host-seeking by adult female mosquitoes of a different species (Pitts et al., 2014; Wu et al., 2010a). It was evident that a detailed characterization of ammonia transporters (Amt and Rh proteins) at the molecular and functional levels in the *A. aegypti* aquatic larvae and blood-feeding adult, the principal vector of many arboviral diseases, was necessary. The compilation of studies presented in this dissertation provides a more profound understanding of the roles of ammonia transporter proteins in ammonia transport physiology and systemic ammonia regulatory processes in larval and adult *A. aegypti.* The major findings related to the aims of this research (as outlined in Chapter 1) are summarized below.

8.1.1 Amt and Rh proteins in A. aegypti: redundancies or functionally distinct roles in ammonia transport physiology?

Within the anal papillae, ammonium transporter AeAmt1 was previously shown to play an integral role in NH_4^+ excretion, a process that was also reliant on active ion transport machinery including the key ion-motive enzymes, V-type H^+-ATPase (VA) and Na^+-K^+-ATPase (NKA) (Chasiotis et al., 2016). A similar approach involving loss-of-function techniques (i.e. RNA interference) combined with electrophysiology was utilized to establish roles for the Rh proteins, AeRh50-1 and AeRh50-2 (Chapter 2), and the recently identified Amt protein, AeAmt2 (Chapter 3), which were each demonstrated to be important in facilitating NH_4^+ excretion at the anal papillae. What was surprising was the finding of significant decreases in AeAmt2 and Rh protein, and no change in AeAmt1 protein abundance, in response to long-term high environmental ammonia (HEA) exposure; an environmental challenge that was predicted to necessitate the greatest requirement for these transporters (Chapter 3). Of course, the findings begged the question as to whether redundancies in ammonia transport mechanisms exist within the *A. aegypti* mosquito, of which this species is one of only a few animal species demonstrated to express both Amt and Rh proteins. Even more intriguing was the observation that Rh protein abundance within the anal papillae increased 5-fold when larvae are reared in modest amounts of salt (5 mmol l^{-1} NaCl), which corresponded with elevated rates of NH_4^+ efflux and VA activity within the anal papillae, as well as overall decreased haemolymph [NH_4^+] (mmol l^{-1}) (Chapter 4). *Aedes aegypti* larvae can readily develop in brackish water (~150 mmol l^{-1} NaCl) (Akhter et al., 2017; Misyura et al., 2020; Ramasamy et al., 2011) and so the levels used in the current study likely do not present a significant challenge to larval development. Nevertheless, larvae reared in 5 mmol l^{-1} NaCl were faced with a decrease in haemolymph pH (i.e. acidification) (Chapter 4), and this may relate to the finding of haemolymph acidification that resulted from AeRh50-1 knockdown in the anal papillae (Chapter 2) whereby AeRh50-1 function is important for haemolymph pH maintenance and conversely, loss of AeRh50-1 function causes perturbations in haemolymph pH. Alterations in

haemolymph pH were not observed following AeAmt1, AeAmt2, or AeRh50-2 protein knockdown [Chapters 2-3; (Chasiotis et al., 2016)]. Collectively, these results were suggestive of an alternate role for AeRh50-1 in ammonia transport as a means of acid-base regulation in relation to the ionic composition of the external media. For instance, Rh proteins as gas channels for NH_3, and possibly CO_2, transport may be a detriment in the externally protruding anal papillae when larvae are in HEA due to the inwardly directed ammonia (NH_3/NH_4^+) gradient which is why a decrease in protein abundance was observed (Chapter 3), but they may be important in ridding NH_4^+ as an acid equivalent when larvae are reared in NaCl which increased Rh protein abundance (Chapter 4).

It was not until the close examination of Amt and Rh protein expression and function in adult *A. aegypti* that it became apparent that these transporters have distinct and highly specialized functions in a variety of physiological processes related to ammonia regulation, transport, and excretion. AeAmt1 is almost exclusively expressed within the spermatozoa during all stages of development in males and during storage within the spermathecae of females (Chapter 7). On the other hand, AeAmt2 is highly expressed in chemosensory appendages (e.g. the antennae) of females where it may play a role in ammonia-sensing (Chapter 7), similarly to the malaria vector mosquito, *Anopheles gambiae* (Pitts et al., 2014; Ye et al., 2020). AeAmt2 was also localized within the fat body cells, which is functionally analogous to the vertebrate liver and is an important organ for ammonia detoxification in *A. aegypti* females during blood meal digestion (Scaraffia et al., 2005). The Rh proteins, and AeRh50-1 in particular, are enriched within the excretory organs (Malpighian tubules, MT and rectum, RM) and may be important for ammonia secretion from the haemolymph and confinement within the MT and RM lumen, and ultimately ammonia excretion via these organs (Chapter 6). Based on findings from other mosquito species (Wu et al., 2010a), it was postulated that ammonia transporter function would be important within the midgut (Chapter 1), the primary site of blood meal digestion. However, based on the minimal (or lack of) Amt and Rh mRNA and protein expression within this organ up to 48 hours

post blood meal (Chapters 6 and 7), further examination of ammonia transport mechanisms within this organ may reveal the importance of alternate pathways.

8.1.2 Physiological plasticity of larvae to freshwater (FW) and high environmental ammonia (HEA) habitats

Findings from this research demonstrate that colony-strain (Liverpool) larvae alter ammonia transporter mRNA and protein abundances in the anal papillae in response to acute and long-term HEA exposure (Chapter 3). Changes in ion-motive NKA and VA activity within the anal papillae (Chapter 4) and the MT (Chapter 6) were also observed in response to rearing in HEA. These changes most likely occur, in part, to combat elevated haemolymph NH_4^+ levels and haemolymph acidification that the larvae often encounter when reared in HEA, probably due to the high drinking rates and ingestion of ammonia with food (Clark et al., 2007). Remarkably, an examination of wild *A. aegypti* larvae that were field-collected from either FW containers or high ammonia septic tanks yielded similar findings to colony larvae exposed to either FW or HEA (Chapters 3 and 4), mainly: (1) elevated haemolymph $[NH_4^+]$ (mmol l^{-1}) levels and decreased haemolymph pH of septic tank-collected larvae versus FW-collected larvae, (2) decreased Rh protein abundance within the anal papillae of septic tank-collected larvae versus FW-collected larvae, and (3) increased VA expression in anal papillae epithelia of septic tank-collected larvae versus FW-collected larvae (Chapter 5). Further evidence that larvae are capable of remodeling their physiology to acclimate to high ammonia sewage habitats comes from the findings that colony larvae hatched and reared in high ammonia sewage water from septic tanks not only thrived but also showed similar alterations in organ function and endpoints in ammonia regulation to wild *A. aegypti* larvae. For instance, similarly to wild larvae collected from septic tanks, colony larvae reared in septic water exhibited elevated haemolymph NH_4^+ levels as well as significantly increased NH_4^+ transport rates by the MT and enhanced NH_4^+ efflux rates at the anal papillae, compared to colony larvae reared in dilute natural freshwater (Chapter 5). This is an impressive feat physiologically,

considering that the laboratory larvae have been in the colony for many decades and are reared exclusively in distilled freshwater. These findings also partially highlight the mechanisms in larvae that confer their resilience to these harsh ammonia-rich environments that they now readily inhabit, consequently of which contributes to their year-round abundances and the prevalence of arboviral diseases.

8.1.3 A novel role for an Amt protein in sperm cells

In animals, ammonium transporter (Rh and Amt) function has been implicated in the most fundamental processes such as routine cellular protein turnover, amino acid catabolism aiding in metabolic processes, to much more peculiar strategies involving life in high ammonia environments. This research identified a novel role for an Amt protein specifically in the spermatozoa of *A. aegypti* (Chapter 7). AeAmt1 is almost exclusively localized to the spermatozoa of male *A. aegypti* relative to other cells and is highly expressed at all stages of spermatogenesis in the male testes and also evident in relation to egg fertilization in the female reproductive tract. This is the first instance of an ammonium transporter localized within sperm of any animal, offering a new realm of unconventional roles for this family of transporters which to date have primarily been localized within the epithelia of organs involved in digestion, excretion, ion-water homeostasis, and acid-base balance. RNAi-mediated protein knockdown of AeAmt1 in male *A. aegypti* causes significant perturbations in male fertility (decreased sperm counts) and egg viability (decreased proportions of hatched larvae) (Chapter 7). This is particularly significant in this monandrous mosquito species, in addition to many other insect taxa, which employs internal fertilization of eggs during reproduction following a single mating and insemination event with one male, and subsequent long-term sperm storage within the spermathecae (Degner and Harrington, 2016). These findings suggest that AeAmt1 functions in spermatozoa to mitigate ammonia toxicity that is produced both intracellularly and in the surrounding fluids, evidenced by the localization of AeAmt1 along the length of the spermatozoa flagellum corresponding to mitochondrial derivative expression, as well as the remarkably high NH_4^+ levels in the spermathecae fluid of female *A.*

aegypti. Indeed, a closer examination of the subcellular localization of AeAmt1 in relation to the mitochondria in other highly metabolically active cells may reveal that this transporter is involved in ammonia shuttling out of the mitochondria. This may be true for the nurse cells surrounding the developing oocyte in ovarian follicles during egg development, as AeAmt1 protein expression was also observed within these cells (Chapter 7). Evidently, the metabolic demands of oocyte maturation likely require efficient ammonia detoxification and transport mechanisms based on the observation that Rh proteins are also expressed within these ovarian cells in adult females (Chapter 6).

8.2 Future directions

The identification of ammonium transporter gene families [AMTs, MEPs, and Rh proteins; (Marini et al., 1994; Marini et al., 1997b; Ninnemann et al., 1994)] and the subsequent identification and characterization of ammonium transporters across all domains of life has transformed the ideology of simple, passive diffusion of ammonia within living organisms into what is now considered to be specific, highly regulated transport of this molecule across biological membranes. The present studies have greatly furthered our knowledge of systems-level ammonia transport mechanisms and the molecular physiology of ammonia transporters in larval and adult *A. aegypti* (Figure 8-1). This work has also provided important insight into the physiological mechanisms underpinning the tolerance of larvae to toxic levels of ammonia in the aquatic environments that they inhabit, a phenomenon that has been repeatedly documented but rarely investigated at the molecular and physiological levels. Insights into a novel role regarding ammonia transporter function in the spermatozoa of *A. aegypti* have also been provided.

To fully understand the specific functions of Amt and Rh proteins in *A. aegypti*, identification of the specific transport substrates of each protein is necessary. Phylogenetic analyses of ammonia transporters (AMT, MEP, and Rh proteins) show that invertebrate AMTs, including AeAmt1 and

AeAmt2, are most similar to the electrogenic plant AMTs in comparison to bacterial AMTs, fungal MEPs, and Rh proteins which may primarily mediate the electroneutral movement of ammonia (Chapter 3; Chasiotis et al., 2016). This research has laid the groundwork for these studies through cloning of the complete open reading frames of *AeAmt1* and *AeAmt2,* heterologous expression of AeAmt1 and AeAmt2 in *Xenopus laevis* oocytes, and the use of electrophysiology to examine the kinetics of ammonia (NH_3 and NH_4^+) transport (Appendix A1). While still incomplete, preliminary analyses of Michaelis-Menten kinetics of ammonia uptake point towards AeAmt1 and AeAmt2 having different transport substrates and/or different transport mechanisms (i.e. unidirectional versus bidirectional transport). An initial examination of NH_4^+ conductances of AeAmt-expressing oocytes revealed a higher inward conductance for AeAmt1-expressing oocytes in comparison to AeAmt2-expressing and control oocytes (Appendix A1). Continued work in this area would provide a more comprehensive understanding of the cell, tissue, and organ-specific roles of each ammonia transporter, particularly in the context of the environmental and physiological challenges related to ammonia. More broadly, knowledge of the specific transport substrate of each ammonia transporter may provide important insight into the cellular and/or organ-specific differences in expression that were observed in both larvae and adults.

The finding of enriched *AeAmt2* mRNA and protein within the antennae of adults deserves further investigation (Chapter 7). *AeAmt2* shows high sequence similarity with an Amt protein (*AgAmt*) from the mosquito *Anopheles gambiae*. *AgAmt* is abundant in the antennae of adults where it localizes to sensory neurons underlying ammonia sensitivity and modulates antennal sensitivity to ammonia and behavioral responses (Ye et al., 2020). Ammonia is a key human-derived volatile kairomone that is detected by hematophagous female mosquitoes, but the mechanisms underlying ammonia detection in the *A. aegypti* mosquito are largely unknown.

In summary, the ammonia transporters *AeAmt1*, *AeAmt2*, *AeRh50-1*, and *AeRh50-2* in *A. aegypti* participate in a variety of ammonia transport and excretory mechanisms, which generally occupies a dominant role in the physiology of nitrogen regulation in aquatic and blood-feeding animals. The primary osmoregulatory organs in larvae, the anal papillae, the Malpighian tubules, and the rectum, are also important sites of ammonia excretion which coincides with the highest expression of Amt and Rh proteins within these organs. The molecular physiology of Amt and Rh proteins points to critical functions in facilitating ammonia transport and excretion across the epithelia and an overall role in the systemic regulation of ammonia. Functionally distinct roles of Amt and Rh proteins in a variety of physiological processes in adult *A. aegypti* are revealed by findings from this research, including the maintenance of spermatozoa during development and ultimately successful egg fertilization (AeAmt1), ammonia secretion by the excretory organs (Rh proteins), and possibly ammonia detoxification in the fat body and ammonia sensing in the antennae (AeAmt2).

Figure 8- 1. Summary of the impacts of the present studies to society and the scientific community. The impact of this research is two-fold: (1) societal impacts related to vector control strategies, and (2) a mechanistic understanding of ammonia transport and excretion which permits larvae to tolerate high external ammonia and processes related to blood meal digestion and reproduction in adults.

8.3 References

Akhter, H., Misyura, L., Bui, P. and Donini, A. (2017). Salinity responsive aquaporins in the anal papillae of the larval mosquito, *Aedes aegypti*. *Comp. Biochem. Physiol. -Part A Mol. Integr. Physiol.* **203**, 144–151.

Burke, R. L., Barrera, R., Lewis, M., Kluchinsky, T. and Claborn, D. (2010). Septic tanks as larval habitats for the mosquitoes *Aedes aegypti* and *Culex quinquefasciatus* in Playa-Playita, Puerto Rico. *Med. Vet. Entomol.* **24**, 117–123.

Chasiotis, H., Ionescu, A., Misyura, L., Bui, P., Fazio, K., Wang, J., Patrick, M., Weihrauch, D. and Donini, A. (2016). An animal homolog of plant Mep/Amt transporters promotes ammonia excretion by the anal papillae of the disease vector mosquito *Aedes aegypti*. *J. Exp. Biol.* **219**, 1346–55.

Chitolina, R. F., Anjos, F. A., Lima, T. S., Castro, E. A. and Costa-Ribeiro, M. C. V. (2016). Raw sewage as breeding site to *Aedes (Stegomyia) aegypti* (Diptera, culicidae). *Acta Trop.* **164**, 290–296.

Clark, T. M., Vieira, M. A. L., Huegel, K. L., Flury, D. and Carper, M. (2007). Strategies for regulation of haemolymph pH in acidic and alkaline water by the larval mosquito *Aedes aegypti* (L.) (Diptera; Culicidae). *J. Exp. Biol.* **210**, 4359–4367.

Degner, E. C. and Harrington, L. C. (2016). A mosquito sperm's journey from male ejaculate to egg: Mechanisms, molecules, and methods for exploration. *Mol. Reprod. Dev.* **83**, 897–911.

Donini, A. and O'Donnell, M. J. (2005). Analysis of Na^+, Cl^-, K^+, H^+ and NH_4^+ concentration gradients adjacent to the surface of anal papillae of the mosquito *Aedes aegypti*: application of self-referencing ion-selective mi. *J. Exp. Biol.* **208**, 603–10.

Lam, W. K. and Dharmaraj, D. (1982). A survey on mosquitoes breeding in septic tanks in several residential areas around Ipoh municipality. *Med. J. Malaysia* **37**, 114–123.

Mackay, A. J., Amador, M., Diaz, A., Smith, J. and Barrera, R. (2009). Dynamics of *Aedes aegypti* and *Culex quinquefasciatus* in Septic Tanks. *J. Am. Mosq. Control Assoc.* **25**, 409–416.

Marini, A. M., Vissers, S., Urrestarazu, A. and Andre, B. (1994). Cloning and expression of the MEP1 gene encoding an ammonium transporter in *Saccharomyces cerevisiae*. *Embo J* **13**, 3456–3463.

Marini, A.-M., Urrestarazu, A., Beauwens, R. and André, B. (1997). The Rh (Rhesus) blood group polypeptides are related to NH_4^+ transporters. *Trends Biochem. Sci.* **22**, 460–461.

Misyura, L., Grieco Guardian, E., Durant, A. C. and Donini, A. (2020). A comparison of aquaporin expression in mosquito larvae (*Aedes aegypti*) that develop in hypo-osmotic freshwater and iso-osmotic brackish water. *PLoS One* **15**, e0234892.

Ninnemann, O., Jauniaux, J. C. and Frommer, W. B. (1994). Identification of a high affinity NH_4^+ transporter from plants. *EMBO J.* **13**, 3464–3471.

Pitts, R. J., Derryberry, S. L., Pulous, F. E. and Zwiebel, L. J. (2014). Antennal-expressed ammonium transporters in the malaria vector mosquito *Anopheles gambiae*. *PLoS One* **9**,.

Ramasamy, R., Surendran, S. N., Jude, P. J., Dharshini, S. and Vinobaba, M. (2011). Larval development of *Aedes aegypti* and *Aedes albopictus* in peri-urban brackish water and its implications for transmission of arboviral diseases. *PLoS Negl Trop Dis* **5**, e1369.

Scaraffia, P. Y., Isoe, J., Murillo, A. and Wells, M. A. (2005). Ammonia metabolism in *Aedes aegypti*. *Insect Biochem. Mol. Biol.* **35**, 491–503.

Scaraffia, P. Y., Zhang, Q., Wysocki, V. H., Isoe, J. and Wells, M. A. (2006). Analysis of whole

body ammonia metabolism in *Aedes aegypti* using [15N]-labeled compounds and mass spectrometry. *Insect Biochem. Mol. Biol.* **36**, 614–622.

Wu, Y., Zheng, X., Zhang, M., He, A., Li, Z. and Zhan, X. (2010). Cloning and functional expression of Rh50-like glycoprotein, a putative ammonia channel, in *Aedes albopictus* mosquitoes. *J. Insect Physiol.* **56**, 1599–1610.

Ye, Z., Liu, F., Sun, H., Barker, M., Pitts, R. J. and Zwiebel, L. J. (2020). Heterogeneous expression of the ammonium transporter AgAmt in chemosensory appendages of the malaria vector, *Anopheles gambiae*. *Insect Biochem. Mol. Biol.* **120**,.

Appendix A: Supplementary data

A.1: Functional characterization of ammonia transporters (Amts) from the mosquito, *Aedes aegypti*, using the Xenopus oocyte expression system, SIET analysis, and TEVC electrophysiology

A.1.1 Rationale

The initial descriptions of AMT/MEP/Rh proteins functioning as specific ammonia transporters led to the rapid identification of these proteins in organisms from all domains of life (see section 1.5.2). However, the specific transport substrates of these families of proteins are still up for debate, with evidence from x-ray crystallography studies suggesting that Rh proteins (Gruswitz et al., 2010; Li et al., 2007; Lupo et al., 2007) and some AMT proteins (Khademi et al., 2004; Soupene et al., 2002; Zheng et al., 2004) function as gas channels for NH_3 and even CO_2 in bacteria and animals. In contrast, it has been demonstrated that the AMT proteins in plants transport the charged ammonium ion, NH_4^+ for uptake from the environment (Loqué et al., 2009; Ludewig et al., 2002; Neuhäuser and Ludewig, 2014).

Knowledge of the specific transport substrates of the Amt and Rh proteins in *A. aegypti* would provide significant insight into the distinct roles these proteins play in ammonia transport within the cells, tissues, and organs in which they are expressed. Indeed, our current working model of transcellular ammonia transport across the anal papillae epithelium for excretion is limited by the lack of information on the specific substrate (NH_3 or NH_4^+) transported by the Rh/Amt proteins (Chapters 2 and 3; Chasiotis et al., 2016). The transport properties of the AeAmt proteins, AeAmt1 and AeAmt2, in *A. aegypti* are of particular interest because these transporters group closely with the electrogenic plant Amt proteins compared to their possibly electroneutral counterparts, the Rh and MEP proteins (Chapter 3; Chasiotis et al., 2019; Baday et al., 2015; Khademi et al, 20140; McDonald and Ward, 2016). However, recent evidence demonstrates that a bacterial Amt protein (*AmtB* from *Escherichia coli*) and an

ancestral Rh protein (*NeRh50* from *Nitrosomonas europaea*) recruit and deprotonate NH_4^+, and H^+ and gaseous NH_3 are carried separately across the membrane (Williamson et al., 2020). The goal of these studies was to explore this fundamental question in *A. aegypti* by examining the transport properties of the AeAmts using the *Xenopus* oocyte heterologous expression system in combination with the scanning ion-selective electrode technique (SIET) and two-electrode voltage clamp (TEVC) electrophysiology. Interestingly, the gene sequence of *AeAmt1* in *A. aegypti* is most similar to the *Amt* genes of plants relative to bacterial *Amt* and fungal *Mep* genes (Chasiotis et al., 2016). Based on this finding, it was hypothesized that AMT proteins AeAmt1 and AeAmt2 in *A. aegypti* would transport the ammonium ion, NH_4^+, across cell membranes.

A.1.2 Methodology

Generation of AeAmt1 and AeAmt2 cRNA for expression in *Xenopus* oocytes

The full nucleotide sequences of *AeAmt1* and *AeAmt2* were acquired from databases on VectorBase (www.vectorbase.org) and primers were designed to encompass the entire open reading frame (Table 1). Primer sets and a Q5 High-Fidelity DNA polymerase (New England Biolabs, Whitby, ON) were used to amplify the complete coding sequences of *AeAmt1* and *AeAmt2* using cDNA synthesized from isolated RNA from anal papillae tissue (for *AeAmt1*) and male antennal tissue (for *AeAmt2*). Amplicons for *AeAmt1* (1533 bp) and *AeAmt2* (1757 bp) were purified using a Monarch PCR purification kit (New England Biolabs, Whitby, ON), reamplified by RT-PCR using the *AeAmt1*/*Xba1* and *AeAmt2*/*Xba1* primers, and purified amplicons were cloned into a pGEM-T Easy sequencing vector. Miniprep samples (QIAprep Spin Miniprep Kit, Qiagen) were sequenced to verify base accuracy (The Center for Applied Genomics, SickKids, Toronto, ON). *AeAmt1* and *AeAmt2* constructs were excised using standard restriction enzyme digest and were subcloned into a pGEMHE *Xenopus* oocyte expression vector (a gift from Dr. Dirk Weihrauch). Plasmid DNA was linearized using restriction enzyme

digest (*NotI*), and capped RNA (cRNA) was synthesized by *in vitro* transcription using a HiScribe T7 ARCA mRNA kit (New England Biolabs, Whitby, ON).

Heterologous expression of AeAmts in *Xenopus* oocytes

For immunolocalization, Western blotting, and SIET experiments, stage IV-V oocytes from mature female *Xenopus laevis* (Xenopus 1, Dexter, MI, USA) were maintained in standard oocyte ringer's solution (OR2) containing (in mmol l^{-1}) 82.5 NaCl, 2.5 KCl, 1 $CaCl_2$, 1 $MgCl_2$, 1 Na_2HPO_4, 5 HEPES, pH 7.2 at 16°C. For TEVC experiments, stage IV-V defolliculated *Xenopus laevis* oocytes (Ecocyte Bioscience, Austin, TX) were maintained at 16°C in OR-3 media (Piermarini et al., 2009). Oocytes were injected with 18.4 ng of *AeAmt1* or *AeAmt2* cRNA, or nuclease-free water (sham) as a negative control. All oocyte experiments were conducted two days post-cRNA injection. To verify that Xenopus oocytes can translate AeAmt1 and AeAmt2 cRNA into protein, Western blotting of membrane fractions of oocytes was performed (described in Piermarini et al., 2009). Immunohistochemistry was also utilized to confirm AeAmt expression in the membrane of 5µm thick sections of paraffin-embedded oocytes following previously described protocols (Chasiotis et al., 2016; Chapter 3).

Scanning ion-selective electrode technique (SIET)

Ion-selective NH_4^+ and H^+ microelectrodes were constructed as previously described (Donini and O'Donnell, 2005). NH_4^+ and H^+ microelectrodes were calibrated in modified OR2 buffer (in mmol L^{-1}: CCl 85; $MgCl_2$ 1; Na_2HPO_4 1; $CaCl_2$ 1; HEPES 5, pH 7.2) with either 0.1, 1 and 10 mmol L^{-1} NH_4Cl (for NH_4^+ measurements) or standard hydrogen ion (pH) calibration buffer solutions (pH 4, 7, 10) for H^+ measurements. NH_4^+ and H^+ flux measurements from oocytes submerged in modified OR2 buffer (above) with 0.1, 0.5, 1, 5, or 10 mmol l^{-1} NH_4Cl were carried out according to an established protocol (Chasiotis et al., 2016). A different oocyte was used for each different NH_4Cl bath concentration, and each oocyte was acclimated to the bath media for 2 minutes prior to flux measurements.

Two-electrode voltage clamping (TEVC)

Whole-cell currents of oocytes were acquired using the OC-725 oocyte clamp (Warner Instruments), combined with a MiniDigi-1A data acquisition system (Molecular Devices) and AxoScope software (Molecular Devices) following an established protocol (Piermarini et al., 2009). Current-voltage (I-V) relationship plots of oocytes were acquired following a published protocol (Piermarini et al., 2007), and for membrane current (I_m) recordings the membrane voltage was clamped at a hyper-polarizing potential of 30 mV. All measurements from oocytes were recorded in a ND96 control bath (in mmol l-1: NaCl 96; NMDG-Cl 9; KCl 1; $MgCl_2$ 1; $CaCl_2$ 1.8; HEPES 5; pH = 7.2) or ND96 with 0.1, 0.5, 1, or 10 mmol l^{-1} NH_4Cl.

A.1.3 Results and Summary

Western blotting and immunohistochemical localization of AeAmt1 and AeAmt2 suggests that these proteins were functionally expressed in the oocyte membranes (Fig. A1 and Fig. A2). AeAmt1 and AeAmt2 immunolocalization within the membrane (indicated by white arrows) of paraffin-embedded sections of *AeAmt* cRNA-injected was apparent in comparison to H_2O-injected sham oocytes (Fig. A2). A 100 kDa protein band for AeAmt1 was detected in AeAmt1 cRNA injected oocytes but not in sham oocytes (Fig. A1, A) and a 55 kDa band corresponding to the monomer of AeAmt2 was detected in AeAmt2 cRNA-injected oocytes but not in sham oocytes (Fig. A1, B). Peptide block analysis through pre-absorption of AeAmt1 or AeAmt2 antibodies with immunogenic peptide (10x molar excess) revealed the specificity of these bands. Michaelis-Menten kinetics of NH_4^+ transport by AeAmt1 and AeAmt2 expressing oocytes exposed to increasing NH_4Cl bath concentrations showed a lower K_m and lower Jmax for AeAmt1 expressing oocytes compared to sham oocytes, and a higher K_m and higher J_{max} for AeAmt2 expressing oocytes (Fig. A3). This preliminary analysis suggests that AeAmt1 has a higher binding affinity for NH_4^+ (lower K_m) (Fig. A3, b) and AeAmt2 has a lower binding affinity for NH_4^+ (higher K_m) (Fig. A3, c) in comparison to sham measurements (Fig. A3,a). The lower J_{max} for

AeAmt1 expressing oocytes also indicates that this transporter becomes saturated at lower concentrations of NH_4Cl as a result of its higher binding affinity. Interestingly, the inward NH_4^+ flux measurements of AeAmt1 expressing oocytes were much lower at all bath concentrations of NH_4Cl compared to the sham and suggest that this transporter may be facilitating the outward movement of NH_4^+ from the inside of the cell to the external media. The whole-cell conductance measured using two-electrode voltage clamping was greatest for AeAmt1 expressing oocytes at low concentrations of NH_4Cl (0.1, 0.5, and 1 mmol l^{-1}), whereas the conductance of AeAmt2 expressing oocytes was similar to the sham (Fig. A4). These findings point towards the movement of charged NH_4^+ by AeAmt1, which are in agreement with the transport kinetics analysis of AeAmt1 using SIET. More studies are required to fully reveal the transport properties of AeAmt1 and AeAmt2. For example, an examination of Rh proteins in rainbow trout using similar methods demonstrated that ammonia transport by these proteins is heavily influenced by pH and led to the determination that they likely function as high capacity NH_3 gas channels that recruit and bind NH_4^+ (Nawata et al., 2010). If AeAmt1 is indeed an electrogenic transporter that moves NH_4^+, pH should have no effect on the transport kinetics of this protein. Previous findings that AeAmt2 protein abundance decreases in the anal papillae of *A. aegypti* larvae following long term high environmental ammonia (HEA) exposure (Chapter 3) seem to suggest that this protein relies on ammonia concentration gradient driven NH_4^+/NH_3 movement and is not an electrogenic, unidirectional NH_4^+ transporter. This may explain the findings of low NH_4^+ transport affinity coupled with low NH_4^+-induced conductance of AeAmt2 expressing oocytes.

Table A- 1. Primer sets used to amplify the complete coding sequences of *AeAmt1* (Genbank accession: XM_001652663) and *AeAmt2* (Genbank accession: XM_021844469) from *A. aegypti* tissues. The exact primers sets but also possessing the flanking *Xba1* restriction sites for cloning into the pGEMHE *Xenopus* oocyte expression vector are also shown.

Gene	Forward primer (5'-3')	Reverse Primer (5'-3')
AeAmt1	ATGGCTAACGCCACAGAAGC	GTGACACCAATGCAGAGC
AeAmt1/Xba1	TCTAGAATGGCTAACGCCACAGAAGC	TCTAGAGTGACACCAATGCAGAGC
AeAmt2	ATGGCCGATTCAAACTCAACG	CTTGTTGTGTGATCTCAATCAATCC
AeAmt2/Xba1	TCTAGAATGGCCGATTCAAACTCAACG	TCTAGACTTGTTGTGTGATCTCAATCAATCC

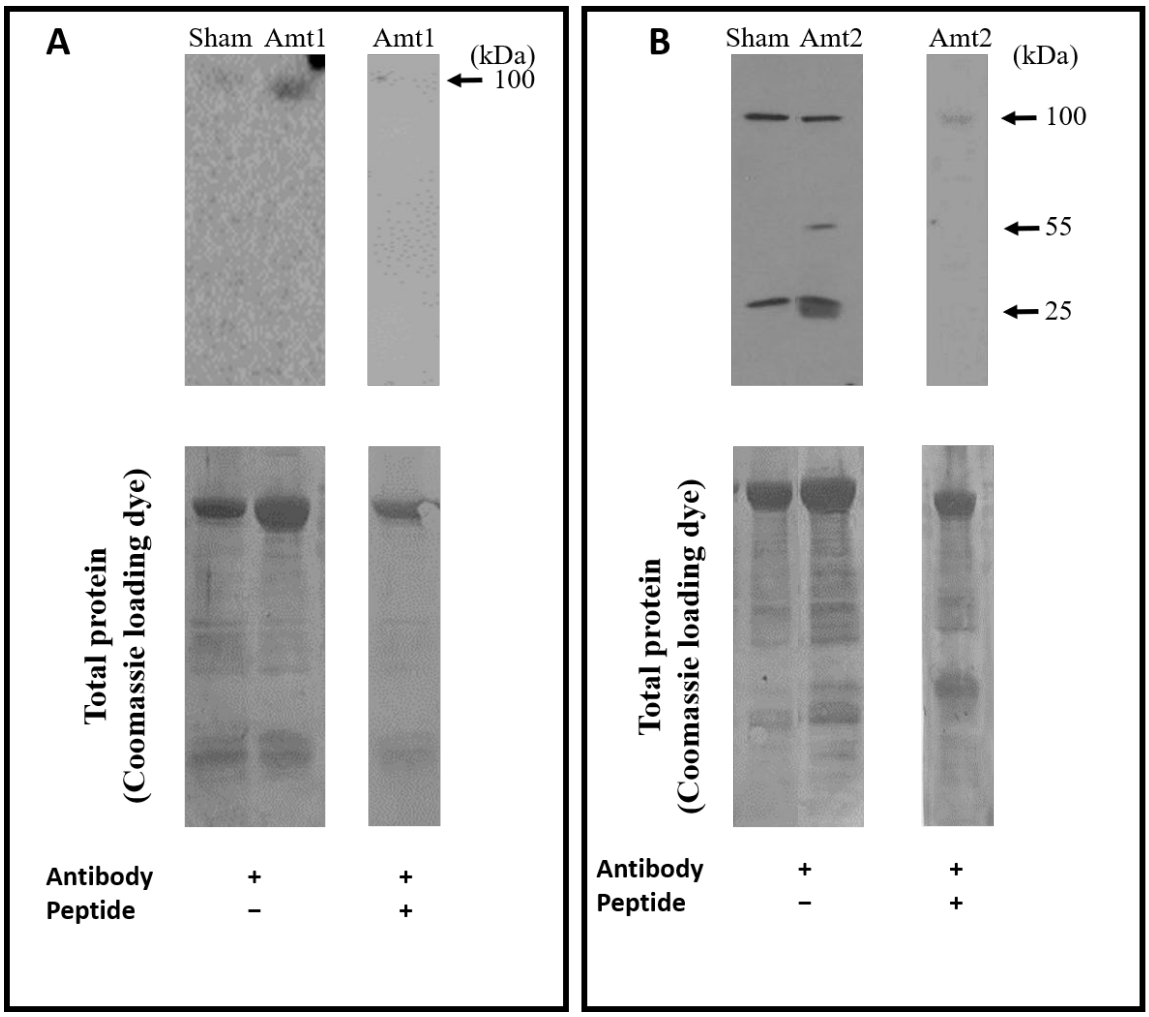

Figure A- 1. AeAmt protein expression in membrane fractions of cRNA or H_2O-injected (sham) *Xenopus laevis* oocytes. Representative western blots reveal **(a)** AeAmt1 (Amt1; dimer form, 100 kDa) and **(b)** AeAmt2 (Amt2; monomer form, 55kDa). All bands were blocked by pre-absorption of primary antibody with immunogenic peptide. Band specificity was determined through pre-absorption of antibody with the immunogenic peptide (as indicated). Bottom panels: Coomassie total protein staining was used as a loading control.

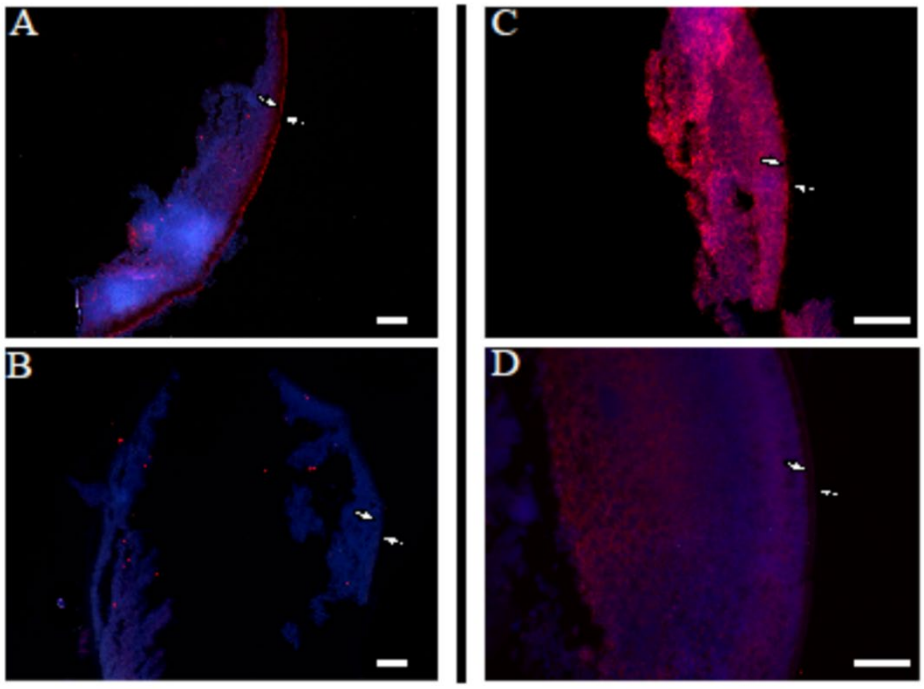

Figure A- 2. AeAmt immunostaining within membrane of paraffin-embedded sections of *Xenopus* oocytes at 2 days following cRNA-injection. Left panel: AeAmt1 (red) and nuclei (blue) staining in (a) *AeAmt1* cRNA-injected oocytes and (b) sham (H_2O-injected) oocyte membranes (white arrows). Right panel: AeAmt2 (red) and nuclei (blue) staining in (c) *AeAmt2* cRNA-injected oocytes and (d) sham (H_2O) injected oocyte membranes (white arrows). All scale bars are 50 µm.

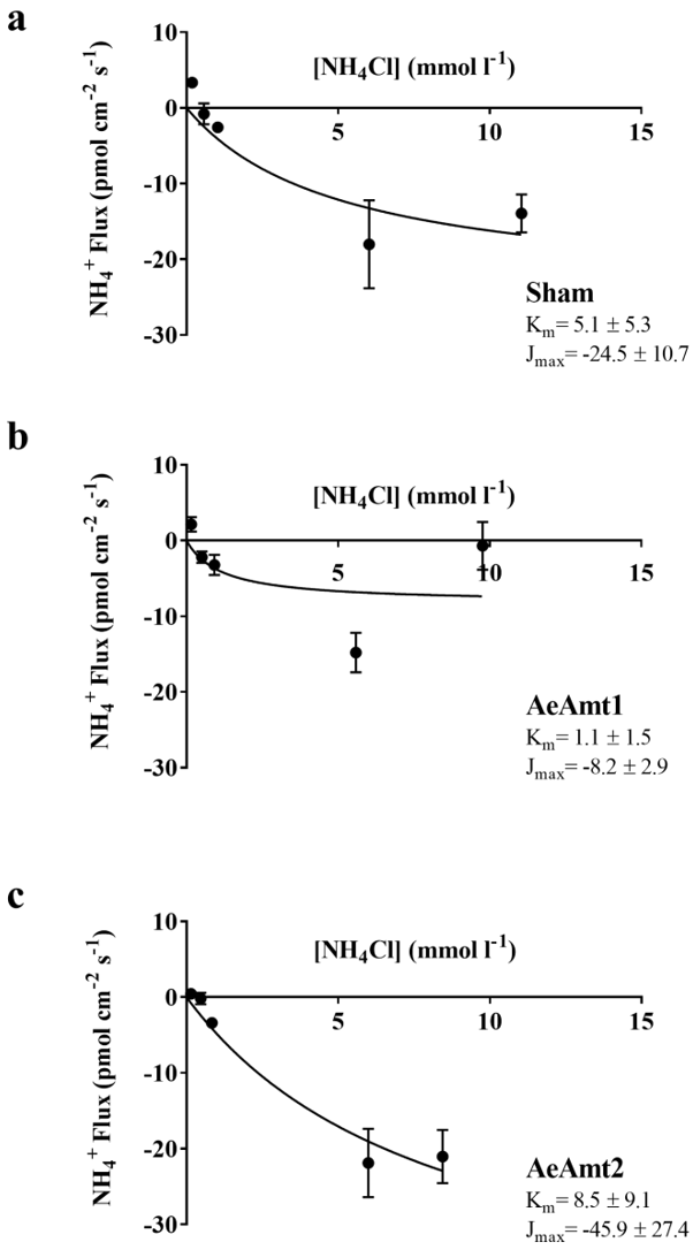

Figure A- 3. Kinetic analysis of NH_4^+ transport by AeAmt-expressing oocytes measured by the scanning ion-selective electrode technique (SIET). Michaelis-Mentin kinetics of NH_4^+ transport (in pmol cm^{-2} s^{-1}) from (a) sham (H_2O-injected) oocytes, (b) AeAmt2-expressing oocytes, and (c) AeAmt1-expressing oocytes over NH_4Cl concentrations of 0.1 to 10 mmol l^{-1}. K_m and J_{max} values are indicated under each graph. Data are means ± S.E.M (*N* = 7-8 oocytes for each treatment group at each concentration). Positive (+) fluxes indicate NH_4^+ secretion and negative (-) fluxes indicate NH_4^+ uptake by the oocytes.

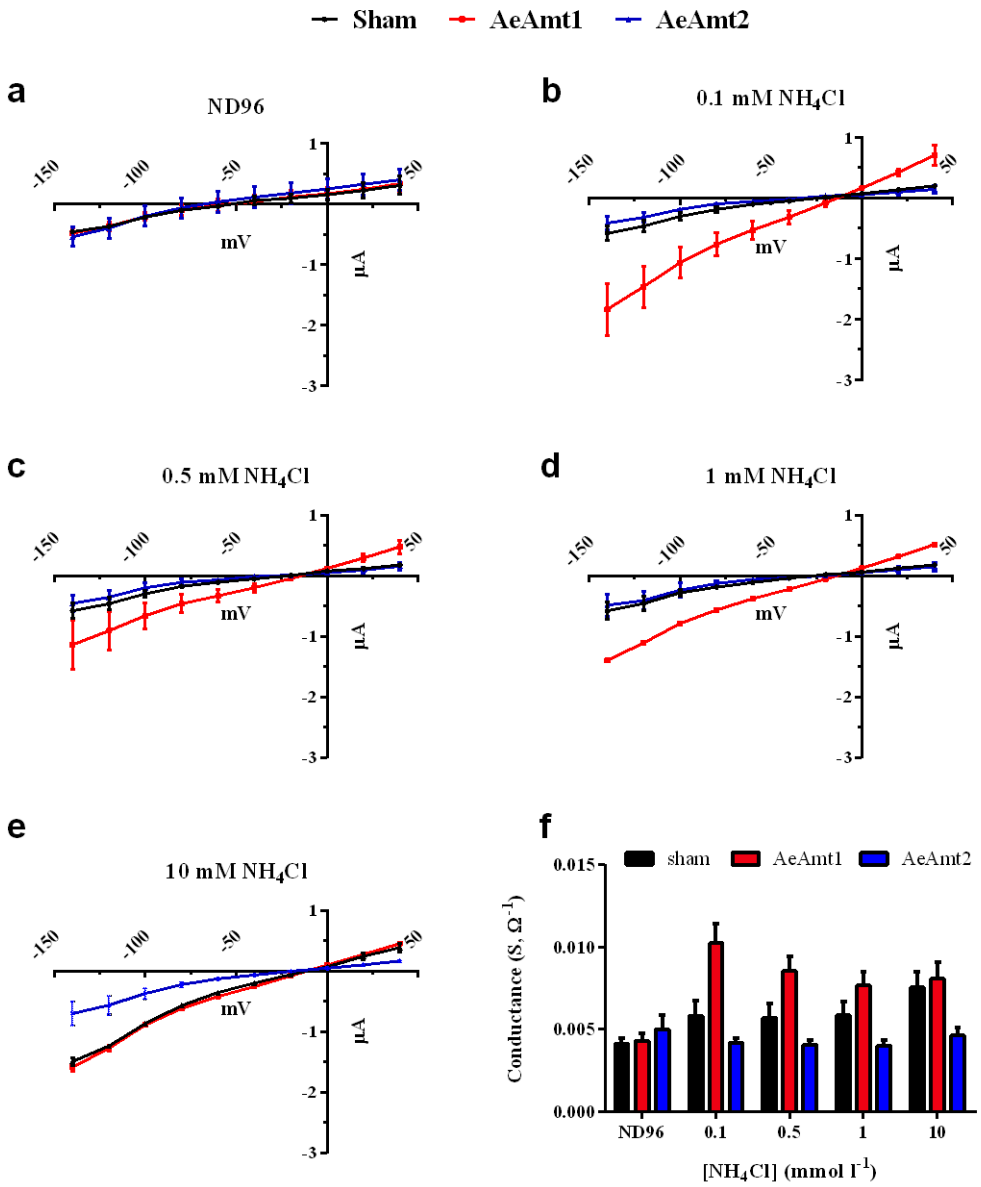

Figure A- 4. Current-voltage relationship for Sham and AeAmt-expressing *Xenopus* oocytes to increasing levels of NH_4Cl (0.1-10 mmol l^{-1}) using two-electrode voltage-clamp electrophysiology (TEVC). (a-e) I-V plots were generated by measuring ion-induced currents at increasing membrane holding potentials in control ND96 buffer and 0.1, 0.5, 1, and 10 mmol l^{-1} NH_4Cl in ND96 buffer. The slope of the current/voltage (Conductance, in Siemens) from each plot is graphed (panel f).

A.1.4 References

Chasiotis, H., Ionescu, A., Misyura, L., Bui, P., Fazio, K., Wang, J., Patrick, M., Weihrauch, D. and Donini, A. (2016). An animal homolog of plant Mep/Amt transporters promotes ammonia excretion by the anal papillae of the disease vector mosquito *Aedes aegypti*. *J. Exp. Biol.* **219**, 1346–55.

Gruswitz, F., Chaudhary, S., Ho, J. D., Schlessinger, A., Pezeshki, B., Ho, C.-M., Sali, A., Westhoff, C. M. and Stroud, R. M. (2010). Function of human Rh based on structure of RhCG at 2.1 A. *Proc. Natl. Acad. Sci.* **107**, 9638–9643.

Khademi, S., O'Connell III, J., Remis, J., Robles-Colmenares, Y., Miercke, L. J. W. and Stroud, R. M. (2004). Mechanism of ammonia transport by Amt/MEP/Rh: Structure of AmtB at 1.35 angstroms. *Science (80-.).* **305**, 1587–1594.

Li, X., Jayachandran, S., Nguyen, H.-H. T. and Chan, M. K. (2007). Structure of the *Nitrosomonas europaea* Rh protein. *Proc. Natl. Acad. Sci. U. S. A.* **104**, 19279–84.

Loqué, D., Mora, S. I., Andrade, S. L. A., Pantoja, O. and Frommer, W. B. (2009). Pore mutations in ammonium transporter AMT1 with increased electrogenic ammonium transport activity. *J. Biol. Chem.* **284**, 24988–24995.

Ludewig, U., Von Wiren, N. and Frommer, W. B. (2002). Uniport of NH_4^+ by the root hair plasma membrane ammonium transporter LeAMT1;1. *J. Biol. Chem.* **277**, 13548–13555.

Lupo, D., Li, X.-D., Durand, A., Tomizaki, T., Cherif-Zahar, B., Matassi, G., Merrick, M. and Winkler, F. K. (2007). The 1.3-A resolution structure of *Nitrosomonas europaea* Rh50 and mechanistic implications for NH_3 transport by Rhesus family proteins. *Proc. Natl. Acad. Sci. U. S. A.* **104**, 19303–19308.

Neuhäuser, B. and Ludewig, U. (2014). Uncoupling of ionic currents from substrate transport in the plant ammonium transporter AtAMT1;2. *J. Biol. Chem.* **289**, 11650–11655.

Soupene, E., Chu, T., Corbin, R. W., Hunt, D. F. and Kustu, S. (2002). Gas channels for NH3: Proteins from hyperthermophiles complement an Escherichia coli mutant. *J. Bacteriol.* **184**, 3396–3400.

Zheng, L., Kostrewa, D., Bernèche, S., Winkler, F. K. and Li, X.-D. (2004). The mechanism of ammonia transport based on the crystal structure of AmtB of *Escherichia coli*. *Proc. Natl. Acad. Sci. U. S. A.* **101**, 17090–5.